



Delft University of Technology

## Extracellular Polymeric Substances of Aerobic Granular Sludge Influences of Seawater

Chen, L.M.

**DOI**

[10.4233/uuid:8e290730-b412-4de8-bf07-741404e1bf28](https://doi.org/10.4233/uuid:8e290730-b412-4de8-bf07-741404e1bf28)

**Publication date**

2026

**Document Version**

Final published version

**Citation (APA)**

Chen, L. M. (2026). *Extracellular Polymeric Substances of Aerobic Granular Sludge: Influences of Seawater*. [Dissertation (TU Delft), Delft University of Technology]. <https://doi.org/10.4233/uuid:8e290730-b412-4de8-bf07-741404e1bf28>

**Important note**

To cite this publication, please use the final published version (if applicable).

Please check the document version above.

**Copyright**

Other than for strictly personal use, it is not permitted to download, forward or distribute the text or part of it, without the consent of the author(s) and/or copyright holder(s), unless the work is under an open content license such as Creative Commons.

**Takedown policy**

Please contact us and provide details if you believe this document breaches copyrights.  
We will remove access to the work immediately and investigate your claim.

# **Extracellular Polymeric Substances of Aerobic Granular Sludge**

Influences of Seawater

Le Min Chen

# **Extracellular Polymeric Substances of Aerobic Granular Sludge**

Influences of Seawater



# **Extracellular Polymeric Substances of Aerobic Granular Sludge**

Influences of Seawater

## **Dissertation**

for the purpose of obtaining the degree of doctor

at Delft University of Technology

by the authority of the Rector Magnificus, Prof. dr. ir. H. Bijl;

Chair of the Board for Doctorates

to be defended publicly on

Friday 30 January 2026 at 10:00 o'clock

by

**Le Min CHEN**

Master of Science in Life Science and Technology,

Delft University of Technology, The Netherlands,

Born in Delft, the Netherlands

This dissertation has been approved by the promotores

Composition of the doctoral committee:

Rector Magnificus	chairman
Prof. dr. ir. M.C.M. van Loosdrecht	Delft University of Technology, promotor
Dr. Y. Lin	Delft University of Technology, promotor
Dr. M. Pronk	Delft University of Technology, copromotor

Independent members:

Prof. dr. ir. M.H.M. Eppink	Delft University of Technology
Prof. dr. ir. I.Y. Smets	Katholieke Universiteit Leuven, Belgium
Prof. dr. D. Claessen	Universiteit Leiden
Dr. J.E. Flack	Delft University of Technology
Prof. dr. F. Hollmann	Delft University of Technology, reserve member



The research presented in this thesis was performed at the Environmental Biotechnology Section, Department of Biotechnology, Faculty of Applied Sciences, Delft University of Technology, The Netherlands. This research was financially supported by TKI Chemie 2017 (co-funded by Haskoning), from the Dutch Ministry of Economic Affairs and Climate Policy.

Keywords: Biofilm; Extracellular Polymeric Substances; Aerobic Granular Sludge; Seawater

Printed by: Proefschriftspecialist

Cover design by: Le Min Chen

ISBN: 978-94-6518-216-2

Copyright © 2026 by Le Min Chen

An electronic version of this dissertation is available at <https://repository.tudelft.nl>.

*For those with curious minds*

## Contents

Summary . . . . .	ix
Samenvatting . . . . .	xi
<b>1 Introduction . . . . .</b>	<b>1</b>
1.1 Biofilms in nature and technology . . . . .	3
1.2 Aerobic granular sludge . . . . .	4
1.3 Resource recovery from aerobic granular sludge . . . . .	6
1.4 Fundamental understanding of EPS components . . . . .	6
1.5 Scope and outline of the thesis . . . . .	9
References . . . . .	11
<b>2 Sialylation and sulfation of anionic glycoconjugates are common in the extracellular polymeric substances of both aerobic and anaerobic granular sludge . . . . .</b>	<b>15</b>
2.1 Introduction . . . . .	16
2.2 Material and Methods . . . . .	19
2.3 Results . . . . .	23
2.4 Discussion . . . . .	29
References . . . . .	33
<b>3 Anionic extracellular polymeric substances extracted from seawater-adapted aerobic granular sludge . . . . .</b>	<b>37</b>
3.1 Introduction . . . . .	39
3.2 Material and Methods . . . . .	40
3.3 Results . . . . .	46
3.4 Discussion . . . . .	54
References . . . . .	58
<b>4 Alterations of glycan composition in aerobic granular sludge during the adaptation to seawater conditions . . . . .</b>	<b>63</b>
4.1 Introduction . . . . .	65
4.2 Material and Methods . . . . .	66
4.3 Results . . . . .	69
4.4 Discussion . . . . .	76
4.5 Conclusions . . . . .	78
References . . . . .	79
<b>5 Extracellular polymeric substances in aerobic granular sludge under increasing salinity conditions . . . . .</b>	<b>83</b>
5.1 Introduction . . . . .	85
5.2 Material and Methods . . . . .	86
5.3 Results . . . . .	94

5.4 Discussion . . . . .	105
5.5 Conclusions . . . . .	110
References . . . . .	111
<b>6 Identification of a surface protein in the extracellular polymeric substances of seawater-adapted aerobic granular sludge . . . . .</b>	<b>117</b>
6.1 Introduction . . . . .	119
6.2 Material and Methods . . . . .	120
6.3 Results . . . . .	126
6.4 Discussion . . . . .	133
6.5 Conclusions . . . . .	138
References . . . . .	139
<b>7 Outlook . . . . .</b>	<b>145</b>
7.1 Towards the identification of the EPS components . . . . .	147
7.2 Influence of environmental conditions on EPS . . . . .	148
7.3 Resource recovery of EPS and its applications . . . . .	149
7.4 Limitations of this work . . . . .	150
References . . . . .	151
Acknowledgements . . . . .	154
Curriculum Vitae . . . . .	158
Scientific Contributions . . . . .	159



## Summary

The vast majority of bacteria in natural and engineered environments exist in the form of biofilms, where the bacteria are embedded in a self-produced matrix of diverse biopolymers known as extracellular polymeric substances (EPS). The EPS typically consists of lipids, polysaccharides, proteins, and extracellular DNA among other components. In particular in wastewater treatment technologies, EPS plays an important role. Over the last couple of decades, a wastewater treatment technology called aerobic granular sludge (AGS) has gained increasing attention due to its more efficient performance compared to conventional activated sludge systems. In AGS, microorganisms produce a dense EPS matrix that enables granule formation and stability. Moreover, the growing emphasis on a circular economy has led to the recovery of AGS-derived EPS as a valuable biopolymer, commercially known as Kaumera.

Despite decades of research, the detailed composition and function of individual EPS components in AGS, as well as their response to environmental conditions remains poorly understood. This thesis aims to characterize the EPS of AGS and to explore the influence of seawater salinity as an environmental stimulus.

Previous work indicated the presence of anionic glycoconjugates containing sulfated groups and nonulosonic acids (NulOs) in the EPS of full-scale anammox granules and AGS. These two modifications were further investigated in **Chapter 2**. Both the EPS of two anaerobic and aerobic granular sludges from full-scale systems were found to contain high molecular weight fractions dominant with NulOs, while the sulfated glycoconjugates were distributed across the molecular weight fractions. The similar distribution patterns indicate that these two modifications are common features of the EPS of anaerobic and aerobic granular sludges.

In **Chapter 3**, the potential of anionic glycoconjugates in a lab-scale seawater-adapted AGS as a raw material for producing heparin alternative was explored. The highest molecular weight fractions contained the majority of sulfated glycoconjugates and NulOs. Different molecular weight fractions showed binding with known proteins involved in sepsis and heparin chromatography, suggesting a potential application for the EPS and indicating that the utilization of seawater may be a strategy to enhance EPS production with specific properties.

This strategy was further evaluated in **Chapter 4**, which examined short-term (30-day) adaptation of lab-scale AGS to seawater salinity. Lectin microarray analysis revealed that glycan diversity on EPS glycoproteins increased during the adaptation phase and subsequently decreased once a stable state was reached. This indicates

that the EPS glycoproteins are actively being adapted by the community in response to environmental changes.

Building on these findings, **Chapter 5** investigated the long-term effects of stepwise increase in seawater salinity (0-4%) on the EPS composition of AGS and its microbial community structure. The charge density of the EPS was found to increase with 20% from 0-4% salinity, while the glycan diversity on the glycoproteins was reduced, but showed increased modifications of sialic acid and sulfated groups. Increasing salinity led to a community shift from a diverse mix to the dominance of a single "*Candidatus Accumulibacter*" species. While no glycoprotein pathways were detected, metaproteomic data indicated the presence of three putative glycoproteins produced by "*Ca. Accumulibacter*". These findings show that "*Ca. Accumulibacter*" dynamically adapts its EPS in response to salinity.

In **Chapter 6**, a dominant surface protein of 74.5 kDa was identified in the seawater-adapted AGS. The extracellular location of the protein was confirmed through immunofluorescence. Dense and large fiber structures were observed in a granule cross-section slice, suggesting a structural function of this protein in the EPS matrix of AGS.

Finally, in **Chapter 7** the main findings are summarized, an outlook is presented and the current bottlenecks in the EPS research are highlighted.

## Samenvatting

De overgrote meerderheid van bacteriën in natuurlijke en technische omgevingen bestaan in de vorm van biofilms, waarbij de bacteriën zijn ingebed in een zelfgeproduceerde matrix van diverse biopolymeren, bekend als extracellulaire polymerische substanties (EPS). De EPS bestaat doorgaans uit, onder anderen, lipiden, polysacchariden, eiwitten en extracellulair DNA. Met name binnen afvalwaterzuiveringstechnologieën speelt EPS een belangrijke rol. In de afgelopen decennia heeft een afvalwaterzuiveringstechnologie, genaamd aeroob korrelslib (AGS), steeds meer aandacht gekregen vanwege de efficiëntere prestaties in vergelijking met conventionele actief-slissenstelselen. In AGS produceren micro-organismen een dichte EPS-matrix die de vorming en stabiliteit van granulen mogelijk maakt. Bovendien heeft de groeiende nadruk op een circulaire economie geleid tot de terugwinning van EPS afkomstig van AGS als een waardevol biopolymeer, commercieel bekend als Kaumera.

Ondanks tientallen jaren aan onderzoek blijven de gedetailleerde samenstelling en functies van individuele EPS-componenten in AGS, evenals hun reacties op omgevingscondities, nog steeds slecht begrepen. Dit proefschrift heeft als doel de EPS van AGS te karakteriseren en de invloed van zeewaterzoutgehalte als omgevingsconditie te onderzoeken.

Eerder onderzoek wees op de aanwezigheid van anionische glycoconjugaten die gesulfateerde groepen en nonulosonische zuren (NulOs) bevatten in de EPS van grootschalige anammox-granulen en aeroob korrelslib. Deze twee modificaties werden verder onderzocht in **Hoofdstuk 2**. Zowel de EPS van twee anaërobe als aerobe korrelslibprocessen uit volleschaal bleken hoge molecuulgewichtfracties te bevatten die domineerden met NulOs, terwijl de gesulfateerde glycoconjugaten over de verschillende fracties waren verdeeld. De vergelijkbare verdelingspatronen duiden erop dat deze twee modificaties gemeenschappelijke kenmerken zijn van de EPS in zowel anaërobe als aerobe granulaire slissenstelselen.

In **Hoofdstuk 3** werd de potentie van anionische glycoconjugaten in een op laboratoriumschaal aan zeewater AGS onderzocht als grondstof voor de productie van een heparine-alternatief. De fracties met het hoogste molecuulgewicht bevatten het grootste deel van de gesulfateerde glycoconjugaten en NulOs. Verschillende molecuulgewichtfracties vertoonden binding met bekende eiwitten die van belang zijn bij sepsis en heparinechromatografie, wat wijst op een potentiële toepassing van de EPS. Dit suggereert dat het gebruik van zeewater een strategie kan zijn om de productie van EPS met bepaalde eigenschappen te bevorderen.

Deze strategie werd verder geëvalueerd in **Hoofdstuk 4**, waarin de kort termijn adaptatie (30 dagen) van laboratoriumschaal AGS aan zeewaterzoutgehalte werd onderzocht. Lectine-microarray-analyse toonde aan dat de glycaandiversiteit op EPS-glycoproteïnen toenam tijdens de adaptatiefase en vervolgens afnam zodra een stabiele toestand was bereikt. Dit geeft aan dat de EPS-glycoproteïnen actief worden aangepast door de gemeenschap als reactie op omgevingsveranderingen.

Voortbouwend op deze bevindingen onderzocht **Hoofdstuk 5** de langetermijneffecten van een stapsgewijze verhoging van het zeewaterzoutgehalte (0-4%) op de EPS-samenstelling van AGS en de microbiële gemeenschap. De ladingsdichtheid van de EPS bleek met 20% toe te nemen van 0-4% zoutgehalte, terwijl de glycaandiversiteit op de glycoproteïnen afnam, maar een toename liet zien van modificaties met sialzuur en gesulfateerde groepen. Toenemend zoutgehalte leidde tot een verschuiving van een diverse gemeenschap naar de dominantie van één enkele soort bacterie, "*Candidatus Accumulibacter*". Hoewel er geen routes voor de synthese van glycoproteïne werden gedetecteerd, toonde het metaproteoom de aanwezigheid van drie vermeende glycoproteïnen geproduceerd door "*Ca. Accumulibacter*". Deze bevindingen tonen aan dat "*Ca. Accumulibacter*" zijn EPS dynamisch aanpast in reactie op zoutgehalte.

In **Hoofdstuk 6** werd een dominante celoppervlakte-eiwit van 74,5 kDa geïdentificeerd in het zeewater AGS. De extracellulaire locatie van het eiwit werd bevestigd via immunofluorescentie. Dichte en grote vezelstructuren werden waargenomen in een dwarsdoorsnede van een granule, wat wijst op een structurele functie van dit eiwit in de EPS-matrix van AGS.

Tot slot worden in **Hoofdstuk 7** de belangrijkste bevindingen samengevat, wordt een toekomstperspectief gepresenteerd en worden de huidige knelpunten in het EPS-onderzoek belicht.

# Introduction





## 1.1 Biofilms in nature and technology

The earliest form of life on Earth is thought to have begun over 3500 million years ago with microorganisms living in communities called microbial mats (Nutman et al., 2016). These mats are considered an ancient form of biofilms, which are microbial communities enclosed in a matrix of self-produced extracellular polymeric substances (EPS) attached to surfaces and/or each other (Flemming et al., 2016). Over time, microbial mats are able to form distinct laminated structures called stromatolites, of which their fossils represent some of the oldest forms of life (Nutman et al., 2016). Because of their distinct structure and ancient origins, microbial mats have also become a key target in the search for extraterrestrial life on NASA's Mars missions (Farley et al., 2020; NASA, 2021). It is evident that these ancient biofilms not only represent the first ecosystems on Earth, but have also set the foundation for life of microbial communities through cooperation and adaptation.

Today, the vast majority of microorganisms are living in the form of biofilms. It has been estimated that approximately 40 – 80% of the cells on Earth exist as biofilms (Flemming and Wuertz, 2019). Biofilms are highly diverse, coming in different structures, and are ubiquitous in natural ecosystems, found in soils, marine biosphere and even in extreme environments, like hot springs and acid mines (Flemming and Wuertz, 2019), where individual microorganisms would not survive. In soils, microorganisms can adhere to the soil pores as films while contributing to ecological functions, such as nutrient recycling, degradation of organic matter and maintaining soil structure (Cai et al., 2019). In extreme environments such as hot springs, where temperatures can reach 70°C, biofilm formations have been observed (Boomer et al., 2009). These examples show how biofilms play essential roles in natural habitats, allowing microbial communities to survive and carry out critical ecological processes even under extreme environmental conditions.



Figure 1.1. Illustrative examples of biofilm systems. Biofilms can be problematic in household settings, such as in shower drains (left), investigated for their scientific roles, such as for NASA's Mars missions (middle), or cultivated for food purposes, such as for the production of kombucha (right). Illustrations drawn by D.J.T. Chen.

Given the biofilms' remarkable adaptability, it is no surprise that they impact human activities in both beneficial and harmful ways. Biofilms exhibit major challenges in both medical and industrial environments and are often referred to as biofouling (Flemming, 2020). In the medical field, they can grow on medical devices and implants, leading to serious infections, particularly when resistant to antibiotics (Sharma et al., 2019). In engineered systems, they can contribute to clogging and corrosion, causing increased maintenance costs, system failure and safety risks (Flemming, 2020). On the other hand, beneficial biofilms have been used for centuries in food production, such as in kombucha fermentation, carrying probiotic benefits to human health (Gong et al., 2021). Beyond food applications, biofilms used in biological wastewater treatment, including biofilms on the carriers, and biofilms without carriers, such as flocculant sludge and granular sludge are regarded as one of the most significant modern advancements, greatly improving sanitation and environment (Henze et al., 2008).

## 1.2 Aerobic granular sludge

Biological wastewater treatment is the largest biotechnological application in the world by volume (Mateo-Sagasta et al., 2015). This application relies on the activity of microorganisms in biofilms, removing organic pollutants from wastewater. Commonly, these biofilms can be grown as small flocs, also known as activated sludge, which is used in wastewater treatments globally (Wu et al., 2019). Recent advancements in improving the wastewater treatment process led to the development of aerobic granular sludge (AGS). Unlike the conventional activated sludge flocs, these microorganisms can grow in a compact and structured form of granules through the production of EPS. Compared to activated sludge, AGS exhibits excellent settling abilities and higher biomass retention, allowing a great reduction in energy costs and volumes of wastewater treatment facilities (Pronk et al., 2015). AGS is commercially implemented in the Nereda® technology by the Dutch engineering consultancy Haskoning and has been applied in over a hundred wastewater treatment plants (WWTPs) built worldwide and with continuing expansion (Haskoning, 2023). These plants treat a wide range of wastewaters, from municipal to industrial sources (Nancharaiah and Sarvajith, 2019), reflecting the adaptability of the AGS systems.

Microorganisms in AGS remove the contaminants from the wastewater by converting organic carbon, phosphate, and nitrogen into biomass. The treated wastewater is then discharged into natural water bodies. In particular, phosphate removal, known as enhanced biological phosphate removal (EBPR), is crucial to prevent eutrophication, which is the excessive growth of algae leading to oxygen depletion and ecosystem damage (Correll, 1998; Henze et al., 2008; Schindler et al., 2016). The EBPR process allows for the selection of phosphate accumulating

organisms (PAO) that dominate the AGS community (Henze et al., 2008). Under anaerobic conditions, PAO consume volatile fatty acids (VFA) and store them as intracellular storage polymers, while using energy from polyphosphate degradation. Subsequently, in the aerobic phase, these storage compounds are used for growth and replenishment of their phosphate reserves, resulting in net phosphate removal (Henze et al., 2008). Simultaneously, glycogen accumulating organisms (GAO) can also be selected, competing with PAO for VFA, but storing glycogen instead and not contributing to phosphate removal (Henze et al., 2008). The selection of PAO and GAO in AGS promotes the formation of stable, smooth, and dense granules (de Kreuk and van Loosdrecht, 2004), where the EPS plays a central role in stability (Nancharaiah and Sarvajith, 2019).

Building on this understanding of the AGS, emerging environmental challenges are reshaping wastewater treatment strategies. Rapid urbanization in combination with climate change has raised serious concerns about the global freshwater supply (Tully et al., 2019; Vörösmarty et al., 2000). One promising solution is the incorporation of seawater into urban water management (Zhang et al., 2023a). Especially in coastal cities, where over 40% of the world population resides, seawater can be used intentionally for toilet flushing or district cooling, thus reducing freshwater demand and saving energy (Zhang et al., 2023b). However, seawater may also enter wastewater systems unintentionally, often caused by infrastructures that are not designed to handle the increasing intrusion (de Almeida and Mostafavi, 2016). Whether intentionally or not, these shifts will result in a higher volume of seawater-based wastewater reaching wastewater treatment plants. Notably, AGS demonstrated good nutrient removal and granule stability under seawater conditions (de Graaff et al., 2020).

Despite the robustness and potential of the AGS technology, the underlying mechanisms of granule stability remain poorly understood, in particular the exact composition and the molecular structure of EPS matrix. As EPS plays a central role in the granule stability and formation (Nancharaiah and Sarvajith, 2019), an in-depth understanding of its composition and adaptive mechanisms is essential. The AGS, with EBPR performance, provides an excellent model to characterize those EPS and explore their adaptive response towards conditions, like seawater. This knowledge is crucial to obtain a better understanding of the granule stability, which ultimately could bring better control and engineering of biofilms in water processes.

### 1.3 Resource recovery from aerobic granular sludge

The sludge produced as by-product of wastewater treatment is expected to greatly increase in volume and mass due to the increasing population connected to sewage networks (Foladori et al., 2010). The treatment and disposal of sludge is a costly process, accounting for 25 – 65% of the total operating costs. In the Netherlands, the sludge is mostly being incinerated, but this is an expensive option and also raises public concern regarding the air quality (Mateo-Sagasta et al., 2015; Pérez-Elvira et al., 2006). With a strong drive toward a more circular economy (European Commission, 2015), recovering resources from sludge has gained much interest in the past decade (Kehrein et al., 2020). Especially with the rapid integration of the AGS technology, new opportunities in resource recovery arise due to the valuable properties linked to its EPS.

The EPS from Nereda® excess sludge is currently recovered as a biopolymer under the name of Kaumera, enabling a recovery of 30% from waste sludge, significantly lowering the costs for sludge incineration (STOWA, 2019). Two full-scale demonstration plants, in Epe and Zutphen (in the Netherlands), are currently being used for the production of Kaumera, and one mobile pilot plant (Kaumera, 2022, 2019).

The EPS extraction is based on a method inspired by the alginate extraction. It begins with a high-temperature alkaline extraction, followed by an acidic precipitation (Lin et al., 2010). The extracted EPS can reach up to 25 – 35% yield, of which the EPS mainly consists of 50 – 70% proteins and 25% polysaccharides and exhibiting excellent gel-forming ability with  $\text{Ca}^{2+}$  (Felz et al., 2016; STOWA, 2019). The recovered EPS from AGS can be used as a raw material for diverse applications. Its gel-forming ability and high phosphorus content make it attractive for the development of bio-stimulants, such as a seed coating or fertilizer (STOWA, 2019). The EPS also showed great flame-retardant properties, due to its self-extinguishing ability (Kim et al., 2020). Other potential applications include the use as an adsorption material, curing agent, or in composite materials (Feng et al., 2021). And potentially, the EPS could be used as a high-value raw material for the development of therapeutics due to its bio-active properties, such as anti-coagulation, antioxidant, anti-angiogenesis (Xue et al., 2019), and histone-binding activity (Tomás-Martínez et al., 2022).

### 1.4 Fundamental understanding of EPS components

With the strong drive in improving granular sludge technology processes and resource recovery from waste sludge, characterizing the EPS components is a fundamental basis (Seviour et al., 2019). Currently, many studies done on the EPS

composition of granular sludge mainly show general properties of the EPS, expressed as total polysaccharides, proteins, and yield (Feng et al., 2021). While these results show general trends for quick comparison, they make obtaining functional and structural understanding of the EPS challenging. Instead, identifying key EPS components, their function, and producers are essential.

Generally, EPS components in diverse biofilms could consist of various components, such as extracellular DNA, enzymes, and bacterial surface structures, for example, S-layer proteins and lipopolysaccharide. Together, the interaction between those individual EPS components allows for keeping the stability of the EPS matrix, playing key functions in cell-cell interaction and protection from harsh environments, amongst others (Flemming and Wingender, 2010). Currently, the major EPS components identified in granular sludge could be divided into proteins and glycans, which include sugars conjugated to another molecule, *i.e.* glycoconjugates, and free polysaccharides.

Several free polysaccharides have been identified in granular sludge communities enriched by specific granule-forming organisms. An acid-soluble polysaccharide was identified in a *Defluviicoccus* community (Pronk et al., 2017). A complex heteropolysaccharide named “granulan” was identified in a “*Candidatus Competibacter*” granular sludge enrichment (Seviour et al., 2011), showing species-specific EPS.

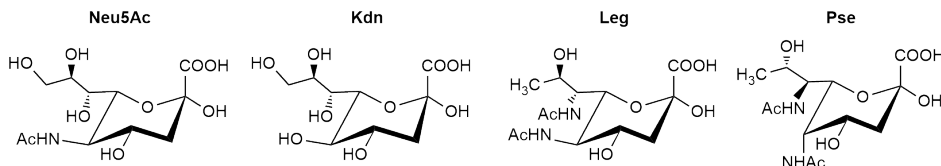


Figure 1.1. Structure of sialic acids and other nonulosonic acids (NulOs) covered in this thesis. Sialic acids such as neuraminic acid (Neu5Ac) and ketodeoxyribonolosonic acid (Kdn) are a subset of nonulosonic acids, such as legionaminic acid (Leg) and pseudaminic acid (Pse). All NulOs carry a negatively charged carboxylate group at C1. Linkages to other monosaccharides commonly occurs at the C2 hydroxyl group. Adapted from Varki et al., 2017b

On the other hand, glycoconjugates appear to be more common across granular sludges. They show great complexity due to the attached glycan, which can carry diverse modifications, including negatively charged sialic acids (Figure 1.1) and sulfated groups, similar to sulfated glycosaminoglycans (Figure 1.2). These modifications have been found in the EPS in AGS (Felz et al., 2020), anaerobic ammonium oxidizing (anammox) granules (Boleij et al., 2020), and anaerobic granular sludge (Bourven et al., 2015), suggesting a widespread function in granular biofilms. In particular, sialic acids, a subset of the nonulosonic acids (NulOs), have recently been characterized as part of glycoproteins in seawater-adapted AGS (de Graaff et al., 2019) and shown to be produced by the PAO “*Ca. Accumulibacter*”

## 1. Introduction

(Tomás-Martínez et al., 2021). More recently, lipopolysaccharides (LPS) have been identified as a hydrogel-forming component in AGS as a hydrogel forming component (Li et al., 2025), further expanding the glycoconjugate repertoire of granular sludge.

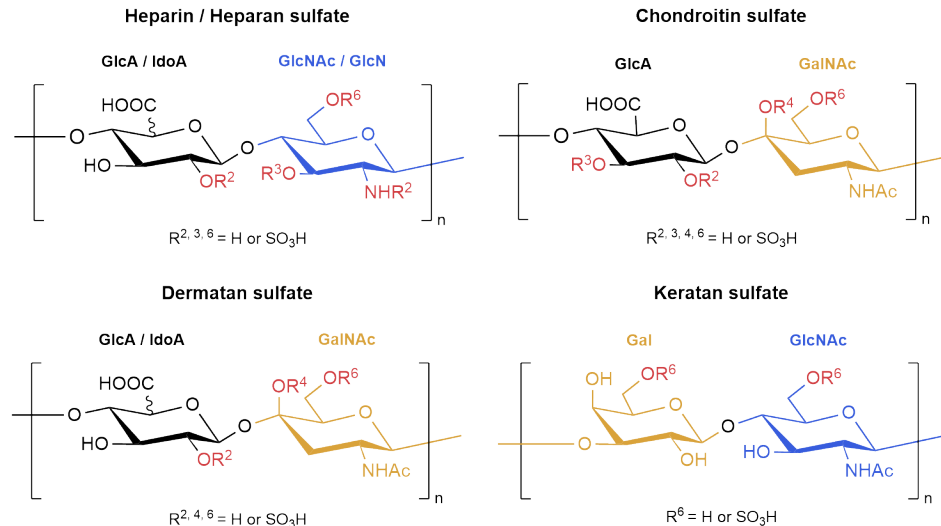


Figure 1.2. Structure of sulfated glycosaminoglycans (GAGs). Each sulfated GAGs consist of repeating disaccharides units: glucuronic acid (GlcA), L-iduronic acid (IdoA), N-acetyl glucosamine (GlcNAc), d-glucosamine (GlcN), N-acetyl-d-galactosamine (GalNAc) and galactose (Gal). Sulfate groups can be linked either to the hydroxyl group (O-sulfation) or amino groups (N-sulfation). Heparin (2.3 – 3 sulfates per disaccharide; 10% GlcA, 90% IdoA) and heparan sulfate (0.5 – 1 sulfates per disaccharide; 10 - 50% GlcA, 50 – 90% IdoA) contain both N- and O-linked sulfation. Chondroitin sulfate (0.1 – 1.3 sulfates per disaccharide) and dermatan sulfate (1-3 sulfates per disaccharide, IdoA >10%) are mainly O-sulfated. Keratan sulfate differs as it does not contain a carboxyl group and its sulfation occurs by O-sulfation, varying with the keratan sulfate type (Soares Da Costa et al., 2017). Adapted from Cohen & Merzendorfer (2019); Kang et al. (2018).

Proteins, either modified or unmodified, make up the largest fraction of the EPS (50 – 70%) and are believed to play a key structural role in granules. Although unmodified structural proteins have not yet been identified in the EPS of granules, an increasing number of studies report the presence of glycoproteins. For example, glycoproteins identified in anammox granules accounted for a large fraction of the EPS (Boleij et al., 2018) and were found distributed between anammox and other community members, indicating a role in adhesion (Wong et al., 2023). Similarly, glycoproteins were found in AGS dominated by ammonium oxidizing bacteria (Lin et al., 2018) and in anaerobic granular sludge (Bourven et al., 2015). More studies have shown the detailed glycan structure of those glycoproteins using mass spectrometry (Boleij et al., 2018; Pabst et al., 2022) and lectin microarray methods (Páez-Watson et al., 2024), demonstrating the potential of glycomic approaches to uncover new functional roles of EPS glycoproteins.

## 1.5 Scope and outline of the thesis

Despite the efforts made on EPS characterization, there are still fundamental questions that remain unanswered. For example, which components make up the EPS? How does the EPS composition change over different environmental conditions? How are the microorganisms producing the EPS, and can we understand their pathways? An in-depth understanding of the EPS composition could enable us to engineer specific EPS for targeted applications. To achieve this, detailed characterization of the EPS is essential. The aim of this thesis was to provide a better understanding of the EPS in AGS by characterizing EPS components and how environmental conditions, specifically seawater salinity, are influencing the EPS (Figure 1.3), which ultimately may contribute to better engineering of the biofilm, resource recovery, and the understanding of environmental biofilms in general. This thesis focuses specifically on the three following aspects of EPS:

1. The anionic glycoconjugates of EPS by evaluating the fractions to understand its prevalence across different granular sludges (Chapter 2) and the potential of some fractions for medical application (Chapter 3).
2. Effect of seawater on the EPS by studying the glycoprotein profiles in AGS cultivated at different salinity levels (Chapter 4) for composition, charge, and responses in the metaproteome (Chapter 5).
3. Identification of a dominant surface protein in seawater-adapted AGS (Chapter 6).

**Chapter 2** focuses on investigating how common anionic glycoconjugates, specifically sialic acids and sulfated groups, are in granular sludges. EPS from two full-scale AGS and AnGS reactors were fractionated and evaluated on the sialic acids and sulfated groups in each fraction.

**Chapter 3** describes the anionic-rich fractions from a lab-scale seawater-adapted AGS on the sialic acids and sulfated groups. A potential medical application as a replacement for heparin and its application as a column material was explored.

**Chapter 4** focusses on the presence and the changes in the glycoproteins of the EPS of seawater-adapted AGS, during a short period of adaptation from freshwater to seawater conditions.

**Chapter 5** investigated the fundamental questions raised in Chapters 3 and 4 on the composition and properties of EPS in AGS in response to stepwise increased salinity.

**Chapter 6** was focused on the identification of a surface protein in the EPS of seawater-adapted AGS by using proteomics. The surface protein was visualized *in-situ* by using immunofluorescence-FISH.

Finally, **Chapter 7** summarizes the main conclusions of this thesis and provides future research directions.

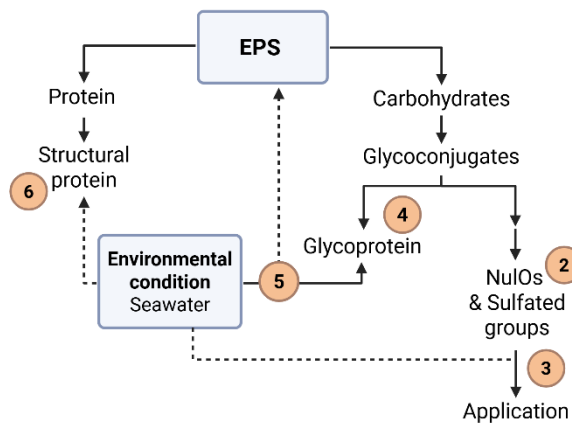


Figure 1.3. Schematic overview of the chapters (indicated by the numbers in the circles) presented in this thesis studying the EPS of AGS with the connection to seawater conditions.

## References

Boleij, M., Kleikamp, H., Pabst, M., Neu, T. R., van Loosdrecht, M. C. M., & Lin, Y. (2020). Decorating the Anammox House: Sialic Acids and Sulfated Glycosaminoglycans in the Extracellular Polymeric Substances of Anammox Granular Sludge. *Environmental Science & Technology*, acs.est.9b07207. <https://doi.org/10.1021/acs.est.9b07207>

Boleij, M., Pabst, M., Neu, T. R., Van Loosdrecht, M. C. M., & Lin, Y. (2018). Identification of Glycoproteins Isolated from Extracellular Polymeric Substances of Full-Scale Anammox Granular Sludge. *Environmental Science and Technology*, 52(22), 13127–13135. <https://doi.org/10.1021/acs.est.8b03180>

Boomer, S. M., Noll, K. L., Geesey, G. G., & Dutton, B. E. (2009). Formation of Multilayered Photosynthetic Biofilms in an Alkaline Thermal Spring in Yellowstone National Park, Wyoming. *Applied and Environmental Microbiology*, 75(8), 2464. <https://doi.org/10.1128/AEM.01802-08>

Bourven, I., Bachellerie, G., Costa, G., & Guibaud, G. (2015). Evidence of glycoproteins and sulphated proteoglycan-like presence in extracellular polymeric substance from anaerobic granular sludge. <https://dx.doi.org/10.1080/09593330.2015.1034186>, 36(19), 2428–2435. <https://doi.org/10.1080/09593330.2015.1034186>

Cai, P., Sun, X., Wu, Y., Gao, C., Mortimer, M., Holden, P. A., Redmile-Gordon, M., & Huang, Q. (2019). Soil biofilms: microbial interactions, challenges, and advanced techniques for ex-situ characterization. *Soil Ecology Letters*, 1(3–4), 85–93. <https://doi.org/10.1007/S42832-019-0017-7>/METRICS

Cohen, E., & Merzendorfer, H. (2019). *Extracellular sugar-based biopolymers matrices* (Vol. 12). Springer.

Correll, D. L. (1998). The Role of Phosphorus in the Eutrophication of Receiving Waters: A Review. *Journal of Environmental Quality*, 27(2), 261–266. <https://doi.org/10.2134/JEQ1998.00472425002700020004X>

de Almeida, B. A., & Mostafavi, A. (2016). Resilience of Infrastructure Systems to Sea-Level Rise in Coastal Areas: Impacts, Adaptation Measures, and Implementation Challenges. *Sustainability* 2016, Vol. 8, Page 1115, 8(11), 1115. <https://doi.org/10.3390/SU8111115>

de Graaff, D. R., Felz, S., Neu, T. R., Pronk, M., van Loosdrecht, M. C. M., & Lin, Y. (2019). Sialic acids in the extracellular polymeric substances of seawater-adapted aerobic granular sludge. *Water Research*, 343–351. <https://doi.org/10.1016/j.watres.2019.02.040>

de Graaff, D. R., van Loosdrecht, M. C. M., & Pronk, M. (2020). Biological phosphorus removal in seawater-adapted aerobic granular sludge. *Water Research*, 172, 115531. <https://doi.org/10.1016/j.watres.2020.115531>

de Kreuk, M. K., & van Loosdrecht, M. C. M. (2004). Selection of slow growing organisms as a means for improving aerobic granular sludge stability. *Water Science and Technology*, 49(11–12), 9–17. <https://doi.org/10.2166/wst.2004.0792>

European Commission. (2015). *Closing the loop - An EU action plan for the Circular Economy: Vol. COM(2015)*.

Farley, K. A., Williford, K. H., Stack, K. M., Bhartia, R., Chen, A., de la Torre, M., Hand, K., Goreva, Y., Herd, C. D. K., Hueso, R., Liu, Y., Maki, J. N., Martinez, G., Moeller, R. C., Nelessen, A., Newman, C. E., Nunes, D., Ponce, A., Spanovich, N., ... Wiens, R. C. (2020). Mars 2020 Mission Overview. *Space Science Reviews*, 216(8), 1–41. <https://doi.org/10.1007/S11214-020-00762-Y/TABLES/1>

Felz, S., Al-Zuhairy, S., Aarstad, O. A., van Loosdrecht, M. C. M., & Lin, Y. M. (2016). Extraction of structural extracellular polymeric substances from aerobic granular sludge. *Journal of Visualized Experiments*, 2016(115), 54534. <https://doi.org/10.3791/54534>

Felz, S., Neu, T. R., van Loosdrecht, M. C. M., & Lin, Y. (2020). Aerobic granular sludge contains Hyaluronic acid-like and sulfated glycosaminoglycans-like polymers. *Water Research*, 169. <https://doi.org/10.1016/j.watres.2019.115291>

Feng, C., Lotti, T., Canziani, R., Lin, Y., Tagliabue, C., & Malpei, F. (2021). Extracellular

## 1. Introduction

---

biopolymers recovered as raw biomaterials from waste granular sludge and potential applications: A critical review. In *Science of the Total Environment* (Vol. 753, p. 142051). Elsevier B.V. <https://doi.org/10.1016/j.scitotenv.2020.142051>

Flemming, H. C. (2020). Biofouling and me: My Stockholm syndrome with biofilms. *Water Research*, 173, 115576. <https://doi.org/10.1016/j.watres.2020.115576>

Flemming, H. C., & Wingender, J. (2010). The biofilm matrix. In *Nature Reviews Microbiology* (Vol. 8, Issue 9, pp. 623–633). Nature Publishing Group. <https://doi.org/10.1038/nrmicro2415>

Flemming, H. C., Wingender, J., Szewzyk, U., Steinberg, P., Rice, S. A., & Kjelleberg, S. (2016). Biofilms: An emergent form of bacterial life. In *Nature Reviews Microbiology* (Vol. 14, Issue 9, pp. 563–575). Nature Publishing Group. <https://doi.org/10.1038/nrmicro.2016.94>

Flemming, H. C., & Wuertz, S. (2019). Bacteria and archaea on Earth and their abundance in biofilms. *Nature Reviews Microbiology* 2019 17:4, 17(4), 247–260. <https://doi.org/10.1038/s41579-019-0158-9>

Foladori, P., Andreottola, G., & Ziglio, G. (2010). *Sludge Reduction Technologies in Wastewater Treatment Plants*. 380.

Gong, C., He, Y., Tang, Y., Hu, R., Lv, Y., Zhang, Q., Tardy, B. L., Richardson, J. J., He, Q., Guo, J., & Chi, Y. (2021). Biofilms in plant-based fermented foods: Formation mechanisms, benefits and drawbacks on quality and safety, and functionalization strategies. *Trends in Food Science & Technology*, 116, 940–953. <https://doi.org/10.1016/j.tifs.2021.08.026>

Haskoning. (2023). *Nereda changes wastewater treatment with the 100th plant* <https://nereda.haskoning.com/en/resource/s/news/2023/nereda-disrupts-the-world-of-wastewater-treatment-with-the-100th-plant>

Henze, M., van Loosdrecht, M. C. M., Ekama, G. A., & Brdjanovic, D. (2008). Biological Wastewater Treatment: Principles, Modelling and Design. *Biological Wastewater Treatment: Principles, Modelling and Design*. <https://doi.org/10.2166/9781780401867>

Kang, Z., Zhou, Z., Wang, Y., Huang, H., Du, G., & Chen, J. (2018). Bio-Based Strategies for Producing Glycosaminoglycans and Their Oligosaccharides. *Trends in Biotechnology*, 36(8), 806–818. <https://doi.org/10.1016/j.tibtech.2018.03.010>

Kaumera. (2019). *Raw materials plant Zutphen and Epe* <https://kaumera.com/en/technology/raw-materials-plant-zutphen-and-epe>

Kaumera. (2022). *Mobile Kaumera units moves to Portugal* <https://kaumera.com/en/news/mobile-kaumera-units-moves-portugal>

Kehrein, P., Van Loosdrecht, M., Osseweijer, P., Garfi, M., Dewulf, J., & Posada, J. (2020). A critical review of resource recovery from municipal wastewater treatment plants – market supply potentials, technologies and bottlenecks. *Environmental Science: Water Research & Technology*, 6(4), 877–910. <https://doi.org/10.1039/C9EW00905A>

Kim, N. K., Mao, N., Lin, R., Bhattacharyya, D., van Loosdrecht, M. C. M., & Lin, Y. (2020). Flame retardant property of flax fabrics coated by extracellular polymeric substances recovered from both activated sludge and aerobic granular sludge. *Water Research*, 170, 115344. <https://doi.org/10.1016/j.watres.2019.115344>

Li, J., Hao, X., van Loosdrecht, M. C. M., & Lin, Y. (2025). Understanding the ionic hydrogel-forming property of extracellular polymeric substances: Differences in lipopolysaccharides between flocculent and granular sludge. *Water Research*, 268, 122707. <https://doi.org/10.1016/j.watres.2024.122707>

Lin, Y., de Kreuk, M., van Loosdrecht, M. C. M., & Adin, A. (2010). Characterization of alginate-like exopolysaccharides isolated from aerobic granular sludge in pilot-plant. *Water Research*, 44(11), 3355–3364. <https://doi.org/10.1016/j.watres.2010.03.019>

Lin, Y., Reino, C., Carrera, J., Pérez, J., & van Loosdrecht, M. C. M. (2018). Glycosylated amyloid-like proteins in the structural extracellular polymers of aerobic granular sludge enriched with ammonium-oxidizing bacteria. *MicrobiologyOpen*, 7(6). <https://doi.org/10.1002/mbo3.616>

Mateo-Sagasta, J., Raschid-Sally, L., & Thebo, A. (2015). Global wastewater and sludge production, treatment and use. *Wastewater: Economic Asset in an Urbanizing World*, 15–38. [https://doi.org/10.1007/978-94-017-9545-6\\_2/FIGURES/7](https://doi.org/10.1007/978-94-017-9545-6_2/FIGURES/7)

Nancharaiah, Y. V., & Sarvajith, M. (2019). Aerobic granular sludge process: a fast growing biological treatment for sustainable wastewater treatment. In *Current Opinion in Environmental Science and Health* (Vol. 12, pp. 57–65). Elsevier B.V. <https://doi.org/10.1016/j.coesh.2019.09.011>

NASA. (2021). *Searching for Life in NASA's Perseverance Mars Samples*. <https://www.nasa.gov/solar-system/searching-for-life-in-nasas-perseverance-mars-samples>

Nutman, A. P., Bennett, V. C., Friend, C. R. L., Van Kranendonk, M. J., & Chivas, A. R. (2016). Rapid emergence of life shown by discovery of 3,700-million-year-old microbial structures. *Nature*, 537(7621), 535–538. <https://doi.org/10.1038/NATURE19355;TECHMETA=121,123,135;SUBJMETA=209,213,2151,414,704;KWRD=GEOCHEMISTRY, GEOLOGY, PALAEONTOLOGY>

Pabst, M., Grouzdev, D. S., Lawson, C. E., Kleikamp, H. B. C., de Ram, C., Louwen, R., Lin, Y. M., Lücker, S., van Loosdrecht, M. C. M., & Laureni, M. (2022). A general approach to explore prokaryotic protein glycosylation reveals the unique surface layer modulation of an anammox bacterium. *The ISME Journal*, 16(2), 346–357. <https://doi.org/10.1038/S41396-021-01073-Y>

Páez-Watson, T., Tomás-Martínez, S., de Wit, R., Keisham, S., Tateno, H., van Loosdrecht, M. C. M., & Lin, Y. (2024). Sweet Secrets: Exploring Novel Glycans and Glycoconjugates in the Extracellular Polymeric Substances of "Candidatus Accumulibacter." *ACS ES and T Water*, 4(8), 3391–3399. [https://doi.org/10.1021/ACSESTWATER.4C00247/ASSET/IMAGES/LARGE/EW4C00247\\_0005.JPG](https://doi.org/10.1021/ACSESTWATER.4C00247/ASSET/IMAGES/LARGE/EW4C00247_0005.JPG)

Pérez-Elvira, S. I., Nieto Diez, P., & Fdz-Polanco, F. (2006). Sludge minimisation technologies. *Reviews in Environmental Science and Biotechnology*, 5(4), 375–398. <https://doi.org/10.1007/S11157-005-5728-9/METRICS>

Pronk, M., de Kreuk, M. K., de Bruin, B., Kamminga, P., Kleerebezem, R., & van Loosdrecht, M. C. M. (2015). Full scale performance of the aerobic granular sludge process for sewage treatment. *Water Research*, 84, 207–217. <https://doi.org/10.1016/j.watres.2015.07.011>

Pronk, M., Neu, T. R., van Loosdrecht, M. C. M., & Lin, Y. M. (2017). The acid soluble extracellular polymeric substance of aerobic granular sludge dominated by *Defluviuscoccus* sp. *Water Research*, 122, 148–158. <https://doi.org/10.1016/j.watres.2017.05.068>

Schindler, D. W., Carpenter, S. R., Chapra, S. C., Hecky, R. E., & Orihel, D. M. (2016). Reducing phosphorus to curb lake eutrophication is a success. *Environmental Science and Technology*, 50(17), 8923–8929. [https://doi.org/10.1021/ACS.EST.6B02204/ASSET/IMAGES/LARGE/ES-2016-02204S\\_0002.JPG](https://doi.org/10.1021/ACS.EST.6B02204/ASSET/IMAGES/LARGE/ES-2016-02204S_0002.JPG)

Seviour, T., Derlon, N., Dueholm, M. S., Flemming, H.-C., Girbal-Neuhauser, E., Horn, H., Kjelleberg, S., van Loosdrecht, M. C. M., Lotti, T., Malpei, M. F., Nerenberg, R., Neu, T. R., Paul, E., Yu, H., & Lin, Y. (2019). Extracellular polymeric substances of biofilms: Suffering from an identity crisis. *Water Research*, 151, 1–7. <https://doi.org/10.1016/j.watres.2018.11.020>

Seviour, T. W., Lambert, L. K., Pijuan, M., & Yuan, Z. (2011). Selectively inducing the synthesis of a key structural exopolysaccharide in aerobic granules by enriching for *Candidatus "competibacter phosphatis"*. *Applied Microbiology and Biotechnology*, 92(6), 1297–1305. <https://doi.org/10.1007/s00253-011-3385-1>

Sharma, D., Misba, L., & Khan, A. U. (2019). Antibiotics versus biofilm: an emerging battleground in microbial communities. *Antimicrobial Resistance & Infection Control 2019*, 8(1), 8(1), 1–10. <https://doi.org/10.1186/S13756-019-0533-3>

Soares Da Costa, D., Reis, R. L., & Pashkuleva, I. (2017). Sulfation of Glycosaminoglycans and Its Implications in Human Health and Disorders. *Annual Review of Biomedical Engineering*, 19(Volume 19, 2017), 1–26. <https://doi.org/10.1146/ANNUREVBIOENG-071516-044610/1>

## 1. Introduction

---

STOWA. (2019). *Kaumera Nereda Gum - Samenvatting Naop Onderzoeken 2013-2018*. 1-34.

Tomás-Martínez, S., Chen, L. M., Pabst, M., Weissbrodt, D. G., van Loosdrecht, M. C. M., & Lin, Y. (2022). Enrichment and application of extracellular nonulosonic acids containing polymers of *Accumulibacter*. *Applied Microbiology and Biotechnology*, 1-11.

Tomás-Martínez, S., Kleikamp, H. B. C., Neu, T. R., Pabst, M., Weissbrodt, D. G., van Loosdrecht, M. C. M., & Lin, Y. (2021). Production of nonulosonic acids in the extracellular polymeric substances of "Candidatus *Accumulibacter phosphatis*". *Applied Microbiology and Biotechnology*, 105(8), 3327-3338. <https://doi.org/10.1007/s00253-021-11249-3>

Tully, K., Gedan, K., Epanchin-Niell, R., Strong, A., Bernhardt, E. S., Bendor, T., Mitchell, M., Kominoski, J., Jordan, T. E., Neubauer, S. C., & Weston, N. B. (2019). The Invisible Flood: The Chemistry, Ecology, and Social Implications of Coastal Saltwater Intrusion. *BioScience*, 69(5), 368-378. <https://doi.org/10.1093/BIOSCI/BIZ027>

Varki, A., Schnaar, R. L., & Schauer, R. (2017). *Sialic Acids and Other Nonulosonic Acids*. <https://doi.org/10.1101/GLYCOBIOLOGY.3E015>

Vörösmarty, C. J., Green, P., Salisbury, J., & Lammers, R. B. (2000). Global water resources: Vulnerability from climate change and population growth. *Science*, 289(5477), 284-288. [https://doi.org/10.1126/SCIENCE.289.5477.284/ASSET/8277DF2D-D298-4C85-88F2-B3A4F9CE0C3B/ASSETS/GRAPHIC/SE2508647003.JPG](https://doi.org/10.1126/SCIENCE.289.5477.284)

Wong, L. L., Lu, Y., Ho, J. C. S., Mugunthan, S., Law, Y., Conway, P., Kjelleberg, S., & Seviour, T. (2023). Surface-layer protein is a public-good matrix exopolymer for microbial community organisation in environmental anammox biofilms. *The ISME Journal* 2023 17:6, 17(6), 803-812. <https://doi.org/10.1038/s41396-023-01388-y>

Wu, L., Ning, D., Zhang, B., Li, Y., Zhang, P., Shan, X., Zhang, Q., Brown, M. R., Li, Z., Van Nostrand, J. D., Ling, F., Xiao, N., Zhang, Y., Vierheilig, J., Wells, G. F., Yang, Y., Deng, Y., Tu, Q., Wang, A., ... Consortium, G. W. M. (2019). Global diversity and biogeography of bacterial communities in wastewater treatment plants. *Nature Microbiology*, 4(7), 1183-1195. <https://doi.org/10.1038/s41564-019-0426-5>

Xue, W., Zeng, Q., Lin, S., Zan, F., Hao, T., Lin, Y., van Loosdrecht, M. C. M., & Chen, G. (2019). Recovery of high-value and scarce resources from biological wastewater treatment: Sulfated polysaccharides. *Water Research*, 163, 114889.

Zhang, Z., Liu, J., Xiao, C., & Chen, G. (2023a). Making waves: Enhancing sustainability and resilience in coastal cities through the incorporation of seawater into urban metabolism. *Water Research*, 242, 120140.

Zhang, Z., Sato, Y., Dai, J., Chui, H. kwong, Daigger, G., Van Loosdrecht, M. C. M., & Chen, G. (2023b). Flushing toilets and cooling spaces with seawater improve water-energy securities and achieve carbon mitigations in coastal cities. *Environmental Science & Technology*, 57(12), 5068-5078.

Sialylation and sulfation of anionic glycoconjugates are common in the extracellular polymeric substances of both aerobic and anaerobic granular sludge



## Abstract

Anaerobic and aerobic granular sludge processes are widely applied in wastewater treatment. In these systems, microorganisms grow in dense aggregates due to the production of extracellular polymeric substances (EPS). This study investigates the sialylation and sulfation of anionic glycoconjugates in anaerobic and aerobic granular sludges collected from full-scale wastewater treatment processes. Size exclusion chromatography revealed a wide molecular weight distribution (3.5 - >5,500 kDa) of the alkaline-extracted EPS. The high molecular weight fraction (>5,500 kDa), comprising 16.9 - 27.4% of the EPS, was dominant with glycoconjugates. Mass spectrometry analysis and quantification assays identified nonulosonic acids (NulOs, *e.g.* bacterial sialic acids) and sulfated groups contributing to the negative charge in all EPS fractions. NulOs were predominantly present in the high molecular weight fraction (47.2 - 84.3% of all detected NulOs), while sulfated glycoconjugates were distributed across the molecular weight fractions. Microorganisms, closely related to genera found in the granular sludge communities, contained genes responsible for NulOs and sulfate group synthesis or transfer. The similar distribution pattern of sialylation and sulfation of the anionic glycoconjugates in the EPS samples indicates that these two glycoconjugate modifications commonly occur in the EPS of aerobic and anaerobic granular sludges.

## Published as:

Chen, L. M., de Bruin, S., Pronk, M., Sousa, D. Z., van Loosdrecht, M. C. M., & Lin, Y. (2023). Sialylation and Sulfation of Anionic Glycoconjugates Are Common in the Extracellular Polymeric Substances of Both Aerobic and Anaerobic Granular Sludges. *Environmental Science and Technology*, 57(35), 13217–13225. [https://doi.org/https://doi.org/10.1021/acs.est.2c09586](https://doi.org/10.1021/acs.est.2c09586)

## 2.1 Introduction

Microbial granulation is often desired in wastewater treatment processes, as the higher sedimentation velocity of granular sludge allows the ease of biomass separation from treated water (van Lier et al., 2008; Pronk et al., 2015). Both aerobic and anaerobic microorganisms can granulate by immobilization in a matrix of self-excreted extracellular polymeric substances (EPS). In both processes, the technology inherently relies on the stability of the granules and the formation of EPS. The importance of negatively charged groups in the EPS for granule stability and for the adsorption of charged substances has been highlighted (Costa et al., 2018). Some studies have focused on negatively charged polysaccharides, for example bacterial alginate (Flemming & Wingender, 2010). However, negatively charged groups can also be found on the glycoconjugates linked to proteins and/or lipids in EPS, *e.g.*, sialic acids and sulfated groups.

Sialic acids are nine-carbon acidic monosaccharides that are mostly detected on the terminal of the glycoconjugate chain in the extracellular matrix of vertebrate cells or pathogenic bacteria (Varki et al., 2017). The most common sialic acids in animal tissue are N-acetyl neuraminic acid (NeuAc) and 2-keto-deoxynonulosonic acid (Kdn), whereas pseudaminic acid (Pse) and its stereoisomer legionaminic acid (Leg) seem to be exclusive bacterial sialic acids (Kleikamp et al., 2020; Morrison & Imperiali, 2014). These are all monosaccharides belonging to a subset of the family of nonulosonic acids (NulOs). Most literature reports on sialic acids have focused on their role in evolution and disease in vertebrates, or the interaction between host cells and pathogenic bacteria (Varki, Cummings, et al., 2017). Only very recently, the presence of NulOs in several non-pathogenic microorganisms has been described. NeuAc was found in a diversity of environmental samples and associated to non-pathogenic microbial species (Boleij et al., 2020; de Graaff et al., 2019; Kleikamp et al., 2020). Leg/Pse were predominant in an enrichment of the phosphate-accumulating organism, “*Candidatus Accumulibacter phosphatis*” (Tomás-Martínez et al., 2021). In S-layer glycoprotein of the Archaea *Halorubrum sp* PV6, Leg was detected and speculated to be important for cell-cell recognition (Zaretsky et al., 2018). It is therefore suggested that glycoconjugates containing these monosaccharides (glycoconjugates with sialylation) may play a role in microbial aggregates, where microbe-microbe interactions occur.

Sulfated groups have been well-studied in mucin and the proteoglycan component in the extracellular matrix of animals, especially in sulfated glycosaminoglycans (GAGs). Sulfated GAGs are highly negatively charged, linear polysaccharide chains, covalently linked to the protein core (Varki, Cummings, et al., 2017). They are involved in distinct functions such as keeping the structural integrity of the extracellular matrix, wound repairing and cell differentiation in eukaryotes. Like

2. Sialylation and sulfation of anionic glycoconjugates are common in the extracellular polymeric substances of both aerobic and anaerobic granular sludge

---

sialic acids, sulfated GAGs have been believed to be produced mostly by pathogenic bacteria. However, recently, the sulfated GAGs have been found in the capsule surround the microorganisms and the EPS between the microcolonies in aerobic and anammox granules (Boleij et al., 2020; Felz et al., 2020). In anaerobic granular sludge, sulfated proteoglycan-like compounds have been reported (Bourven et al., 2015).

Despite being carbohydrates, sialic acids and sulfated glycoconjugates cannot be detected by frequently used carbohydrate assay, which contributed to a so far underestimation of their occurrence, chemical structures, and location in the EPS (de Bruin et al., 2022; de Graaff et al., 2019; Felz et al., 2020; Masuko et al., 2005; Parc et al., 2014). Considering the significant importance of sialylated and sulfated glycoconjugates in the extracellular matrix of animals, further investigation is needed to see if they also are a common factor in the EPS of microbial aggregates beyond pathogenic microorganisms. Research on their chemical structure and secretion will shed light on their special functionality and evolutionary importance in the extracellular matrix of biofilm in general.

To investigate the presence of sialylated and sulfated glycoconjugates in the EPS of microbial aggregates and to develop specific methodologies to study them, both aerobic and anaerobic granular sludges were collected from full-scale wastewater bioreactors. The alkaline-extracted EPS of these granular sludges was first fractionated by size exclusion chromatography and the collected fractions were analyzed on the presence and diversity of the sialic acids and sulfated glycoconjugates. Genes encoding for known enzymes responsible for the synthesis or transfer of sialic acids and sulfate groups, respectively, were determined by genome database searches on the dominant microorganisms.

## 2.2 Material and Methods

### 2.2.1 Experimental set-up

The analysis of the anionic extracellular polymeric substances extracted from both aerobic and anaerobic granular sludge is summarized in Figure 2.1.

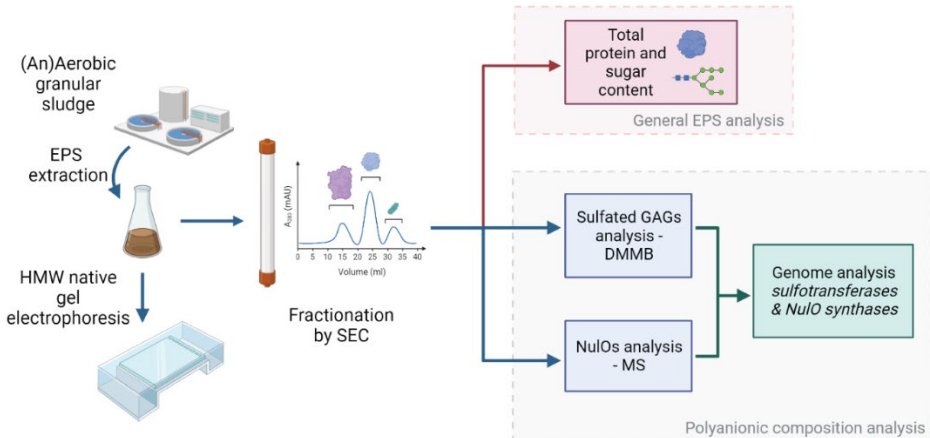


Figure 2.1. Schematic representation of the workflow of the analysis of the anionic extracellular polymeric substances. Abbreviations: EPS: extracellular polymeric substances, HMW: High molecular weight, SEC: Size exclusion chromatography, GAGs: glycosaminoglycans, DMMB: 1,9-dimethyl-methylene blue dye, NulOs: nonulosonic acids, MS: mass spectrometry.

### 2.2.2 Granular sludge and EPS extraction

The extraction of EPS from aerobic and anaerobic granules were both based on the alkaline-heat extraction method described in previous work (Felz et al., 2016; Pinel et al., 2020; Tomás-Martínez et al., 2022). Aerobic granular sludge was collected from two full-scale wastewater treatment plants (Epe and Zutphen) in the Netherlands, which are operated with the Nereda Technology. EPS was extracted by alkaline extraction as explained in detail by Bahgat et al., (2023) for the demonstration plants of Epe (sewage) and Zutphen (dairy). The extraction was performed between pH 9 – 11 by the addition of 25% KOH at 80°C. The EPS was precipitated afterwards by acidification with 30% HCl to pH 2 – 4. The acid-precipitated EPS was dialyzed to retain polymeric components with a 3.5 kDa molecular weight cut off dialysis bag (Snakeskin™, Thermo Fisher Scientific), frozen at -80°C, lyophilized, and stored at room temperature until further analysis.

Anaerobic granular sludge was collected from two full-scale anaerobic granular sludge wastewater treatment systems (treating papermill and brewery wastewaters). The EPS was extracted with an alkaline extraction as previously described by Pinel et al. (2020). In short, EPS was extracted by adding dried biomass

to 0.1 M NaOH at 80°C (10 g/L). The sample was stirred vigorously for 30 minutes, after which it was cooled and centrifuged at 3300  $\times g$  for 30 minutes. Supernatant was dialyzed, lyophilized and stored following the same procedure as the EPS from aerobic granular sludge. Detailed information regarding the wastewater treatment process and the type of wastewater is provided in the Supplementary Materials (Table S1).

### **2.2.3 Native agarose gel electrophoresis and staining with Coomassie blue and Alcian blue**

Native agarose gel electrophoresis was run on a submerged horizontal platform, with the wells positioned in the center of the gel. Lyophilized EPS samples were resolubilized in 50 mM Tris at 2 mg EPS/mL concentration for 1 hour at 30°C. Next, 10  $\mu$ L of the sample was loaded in the wells on a 0.8% agarose gel in 500 mM Tris/HCl, 160 mM boric acid, 1 M urea, pH 8.5. Electrophoresis was performed with a running buffer (90 mM Tris/HCl, 90 mM boric acid, pH 8.5) at 80 V for 90 min. Proteins carrying a net negative charge migrate toward the anode, whereas proteins carrying a positive charge migrate towards the cathode (Li & Arakawa, 2019). To determine if high molecular weight proteins could pass the gel, a high molecular weight marker was used as a ladder (high molecular weight – SDS Calibration kit, Cytiva, Marlborough, MA). The ladder was negatively charged due to the presence of sodium dodecyl sulfate (SDS). The sample position on the gel was revealed using Coomassie blue staining (SimplyBlue™ Safestain, Invitrogen, Waltham, MA) according to the manufacturer's instruction, and destained in water overnight. To identify the carboxyl groups R-COO<sup>-</sup> and the sulfated groups R-OSO<sub>3</sub><sup>-</sup>, staining with Alcian blue was performed at pH 2.5 and pH 1.0 respectively, as described by Boleij et al. (2020). The gel pictures were taken on a ChemiDoc MP imager (Bio-Rad, Hercules, CA).

### **2.2.4 EPS fractionation by size exclusion chromatography**

EPS samples (10 mg) were solubilized in demineralized water to a concentration of 10 mg EPS/mL and the pH was adjusted to 10 using NaOH. All solutions were centrifuged and filtered through a 0.45  $\mu$ m membrane filter before application to the column, to allow the samples to remain dissolved as much as possible.

Size exclusion chromatography (SEC) was performed using a Hiload 16/600 Superose 6 prepacked column (Cytiva Lifesciences, Marlborough, MA) fitted on a Gilson system containing a UV (280 nm) detector. Calibration of the column, upon which the elution volume was determined, was done using a Cytiva high molecular weight marker set (Cytiva Lifesciences, Marlborough, MA). This consisted of ovalbumin (44 kDa), conalbumin (75 kDa), aldolase (158 kDa), ferritin (440 kDa), thyroglobulin (669 kDa) and blue dextran (2,000 kDa). Blue dextran is usually included to determine the void volume, but Superose 6 has a very high fractionation

range (fractionation range  $M_r \sim 5$  kDa-5,000 kDa (globular proteins), exclusion limit  $M_r \sim 40,000$  kDa (globular proteins)), even blue dextran is retained in the column.

Fifteen mL of solubilized EPS samples were run through the column with a flow rate set to 1 mL/min, using a running buffer containing 0.15 M (NaCl) and 0.05 M (glycine) adjusted to pH 10 with NaOH. Five different fractions were chosen based on the retention times of the different proteins in the high molecular weight marker kit and the extrapolation of the calibration line. EPS fractions were subsequently dialyzed to remove excess salts with a 3.5 kDa molecular weight cut-off dialysis bag (Snakeskin™, ThermoFisher Scientific, Landsmeer), frozen at -80°C and lyophilized. The lyophilized samples were stored at room temperature until further analysis.

### 2.2.5 Characterization of EPS fractions

#### Total protein and carbohydrate contents in EPS fractions

Lyophilized EPS fractions were dissolved in 0.01 M NaOH to 0.5 mg/mL. The total protein content was determined by the BCA protein assay following the manufacturer's instruction with bovine serum albumin as a standard (Pierce™ BCA protein assay Kit, Thermo Scientific, USA). Protein absorbance was measured in duplicates at 562 nm using a multimode plate reader (TECAN Infinite M200 PRO, Männedorf, Switzerland). The total carbohydrate content of the EPS solutions, after 2.5 times dilution, was determined by the phenol sulfuric acid method with glucose as a standard (Dubois et al., 1956). The carbohydrate absorbance measurements were performed in cuvettes at 490 nm in duplicates with a VIS-spectrophotometer (HACH DR3900, Ames, IA).

#### Functional groups of EPS fractions

Functional group analysis was performed by Fourier Transform Infra-red (FT-IR) spectroscopy on a Spectrum 100 spectrometer (PerkinElmer, Shelton, CT). The spectra of the lyophilized samples were recorded at room temperature over a wavenumber range of 600 – 4000  $\text{cm}^{-1}$  with 16 accumulations and 4  $\text{cm}^{-1}$  resolution.

#### Sialic acid measurement with mass spectrometry

The NulOs measurement was performed according to the approach described by Kleikamp et al. (2020). In short, lyophilized EPS fractions were hydrolyzed by 2 M acetic acid for 2 hours at 80°C and dried with a SpeedVac concentrator. The released NulOs were labelled through the  $\alpha$ -keto acid using DMB (1,2-diamino-4,5-methylenedioxybenzene dihydrochloride) for 2.5 hours at 55°C and analyzed by reverse phase chromatography Orbitrap mass spectrometry (QE plus Orbitrap, ThermoFisher Scientific, Bleiswijk, Netherlands). Labelling with other sugars and sugar acids was found to give no DMB derivatives (Hara et al., 1986). To estimate the relative amounts of each type of NulOs, the peak area of 1  $\mu\text{g}$  of Kdn was used as a reference signal. The integrated peak areas in the mass spectrometry

chromatograms were calculated for each type of sialic acids in each EPS fraction. The peak area was used as a number proportional to the amount of NulOs. The relative amount of each type of sialic acids in each EPS fraction was presented as a ratio to the peak area of 1 µg of Kdn for comparison.

### **Sulfated glycosaminoglycan assay**

Detection and quantification of sulfated glycosaminoglycans was performed with the Blyscan sulfated glycosaminoglycan assay (Biocolor, Carrickfergus, UK, assay range is 0-50 µg/mL and the detection limit is 2.5 µg/mL), according to the manufacturer's instructions. Samples (2-5 mg) were digested with one mL of papain protein digestion solution at 65°C overnight (Sigma Aldrich, Zwijndrecht, Netherlands). The supernatant was recovered after centrifugation at 13000 ×g for 10 min. 50 µL of sample was then added to 1 mL of 1,9-dimethyl-methylene blue (DMMB) dye reagent. Sulfated GAGs-positive components bind and precipitate with DMMB at a low pH (measured pH in the DMMB solution was 1.7). The precipitate was subsequently isolated and resolubilized. The absorbance of the resolubilized solution at 656 nm (TECAN Infinite M200 PRO, Switzerland) indicated the amount of dye that formed a complex with the sulfated glycosaminoglycans. The standard that was included in the kit was bovine tracheal chondroitin 4-sulfate. Due to the low pH, the influence of intracellular components (*e.g.* DNA) is negligible (Zheng & Levenston, 2015). Lastly, the distribution of N-linked and O-linked sulfate in the samples was measured by performing nitrous acid cleavage as by the manufacturer's instructions prior to sulfated GAGs quantification.

#### **2.2.6 BLASTp (Protein Basic Local Search Alignment Tool) analysis for nonulosonic acid synthases and sulfotransferases**

To identify the 10 most dominant genera of the anaerobic granular sludge community, DNA from sludge samples was extracted using a PowerSoil DNA isolation kit (Qiagen Hilden, Germany) and the V3-V4 regions of the 16S rRNA gene sequenced with primers 341F and 806R (Kleikamp et al., 2022). DNA sequencing was performed at Novogene (Novogene Co., Ltd., China) using Illumina 51 NovaSeq platform. For aerobic granular sludge, the 10 most dominant genera of the community were selected from the study by Kleikamp et al. (2022). BLASTp from the NCBI website was used to identify the homologous enzymes for the biosynthesis of the NulOs and sulfotransferases in close relative organisms (Supplementary Materials Table S2) to the most abundant in the anaerobic granular sludge and aerobic granular sludge. The distinct reference protein sequences were taken from bacteria (*Campylobacter jejuni*, *Bacterioidetes thetaiotaomicron*) or archaea (*Halorubrum* sp PV6) known to produce these types of NulOs. Reference proteins for the NulO synthase of Neu5Ac (NeuB), legionaminic acid (LegI), pseudaminic acid (PseI) and 2-keto-3-deoxynulosonic acid (Kdn-9-phosphate) were used, with

corresponding GenBank accession numbers: ERP39285.1, AYD49523, CAL35431 and AA076821 (Wang et al., 2008; Zaretsky et al., 2018). The distinct reference proteins for sulfotransferases accession numbers: WP\_014336261, WP\_015887312 (Boleij et al., 2020). Matches with a hit below an *E*-value of 1E-20 were considered significant.

### 2.3 Results

The EPS was extracted from both anaerobic and aerobic granular sludges with a relatively significant amount, *i.e.* for the two types of anaerobic granular sludge-treating papermill and brewery wastewater; the extraction yield was  $43.3 \pm 5.5$  and  $58.4 \pm 0.6$  %VSS, respectively; for aerobic granular sludge, treating dairy and municipal wastewater, the yield was  $22.0 \pm 1.7$  and  $29.0 \pm 3.1$  %VSS, respectively.

#### 2.3.1 EPS native agarose gel electrophoresis and staining with Coomassie blue and Alcian blue

The extracted EPS were further analyzed by native agarose gel electrophoresis. Following Coomassie Blue staining (Figure 2.2A), it was observed that, for all EPS samples, a part of the proteins migrated towards the anode (indicative of negatively charged proteins). Another part of the EPS stayed within wells towards the anode, indicating that they may also carry a net negative charge. It is possible that the molecular weight of certain EPS polymers was too high to migrate through the gel (Serwer, 1983).

Alcian blue at pH 2.5 stains both carboxylic and sulfated glycoconjugates, whereas at pH 1.0 it stains only highly negatively charged components, *e.g.*, sulfated glycoconjugates (Boleij et al., 2020; Suvarna et al., 2019). For each EPS, the protein smear (Figure 2.2A) and the anionic glycoconjugates smear (Figure 2.2B and 2.2C) almost overlap with each other. In addition, regarding the part that stays within the well, the pattern stained with Alcian blue at pH 1.0 corresponds to the pattern stained with Coomassie Blue as well. All this information implies that the four EPS samples are all dominated by (glyco)proteins which have carboxylic and sulfated glycoconjugates.

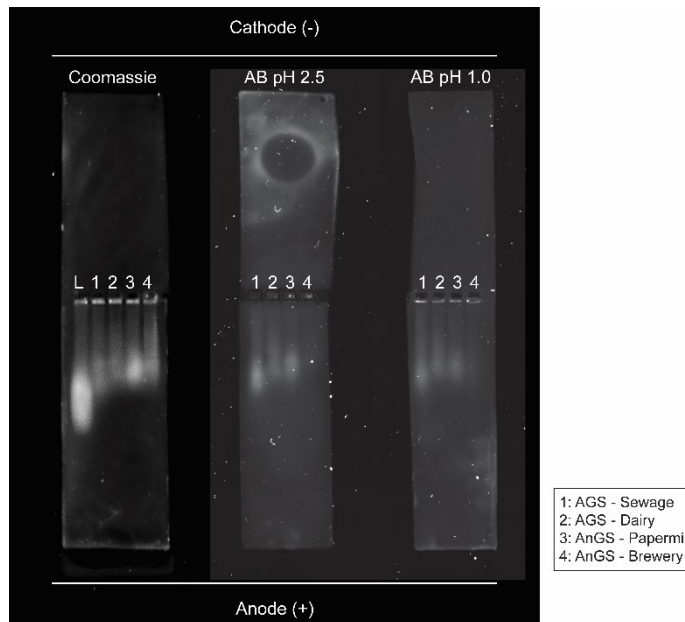


Figure 2.2. Native gel electrophoresis on agarose stained with Coomassie G-250 (A), with Alcian blue pH 2.5 (B) and pH 1.0 (C) with the crude EPS from aerobic granular sludge-Sewage (1), aerobic granular sludge-Dairy (2), anaerobic granular sludge-Papermill (3) and anaerobic granular sludge-Brewery (4) and ladder ranging from 53 to 220 kDa (L). The anode (+) is at the bottom of the gels and the cathode (-) is situated at the top.

### 2.3.2 EPS fractionation and molecular weight distribution

Native agarose gel electrophoresis indicated that the EPS samples are all dominated by (glyco)proteins and have high molecular weight fractions. To estimate their molecular weight distribution, size exclusion chromatography (SEC) was performed. The detection of proteins' signal at 280 nm was employed to obtain the chromatogram (Edelhoch, 1967). The chromatogram of the EPS samples does not show separate protein peaks, but a continuous curve with absorbance at 280 nm (Supplementary Materials Figure S1). It is noted that glycosylation of proteins leads to a continuous molecular weight distribution rather than a few specific molecular weights, because level of glycosylation and glycans length can vary for individual proteins (Heijenoort, 2001; Schäffer & Messner, 2017). This observation concurs with the glycosylation of proteins by carboxylic and sulfated glycoconjugates observed with the Alcian blue staining in section 2.3.1.

The EPS was separated into 5 fractions: 4 fractions in the apparent molecular weight range of 5 kDa to 5,500 kDa, and 1 fraction with an apparent molecular weight > 5,500 kDa. Overall, for each EPS, the mass of the five apparent molecular weight fractions varies (Table 2.1). Notably, the highest apparent molecular weight fraction (>5,500 kDa) was obtained for every EPS sample and its mass is 16-27% of the mass of the relevant EPS.

Table 2.1. Fractionation yields for different EPS used after lyophilization (% of fractionated EPS). The non-soluble fraction was not part of the fractionated samples. Samples marked with an asterisk (\*) are based on the extrapolation of the calibration line. Actual molecular weights measured would lie between ~2,000 – ~40,000 kDa.

Fraction #	Molecular weight range (kDa)	Aerobic granular sludge		Anaerobic granular sludge	
		Sewage	Dairy	Papermill	Brewery
1	>5,500*	18.8	27.4	17.5	16.9
2	738 – 5,500*	5.6	14.3	7.5	16.2
3	100 - 738	11.2	15.1	13.5	21.8
4	12 - 100	19.6	10.4	29.2	14.6
5	3.5-12	24.7	25.2	30.8	24.1
Non soluble fraction		18.0	7.6	2.4	6.5

### 2.3.3 Characterization of the EPS fractions

#### General EPS characterization – Carbohydrates/ Proteins ratio and functional group analysis

For the fractionated EPS samples, both carbohydrates and proteins were detected in each molecular weight fraction (Figure 2.3). The sugars to proteins ratio (PS/PN ratio) was significantly higher by 2.7 – 8.6-fold in the highest apparent molecular weight fraction compared to the average of the other fractions. In addition, as the molecular weight decreased, the PS/PN ratio decreased significantly. This indicated that the EPS fractions with apparent molecular weight >5,500 kDa (16.9 - 27.4% by weight of EPS) were probably dominated with glycosylated proteins, while the fractions with apparent molecular weight <5,500 kDa (63.1-81.0% by weight of EPS) were dominated with less or non-glycosylated proteins.

2. Sialylation and sulfation of anionic glycoconjugates are common in the extracellular polymeric substances of both aerobic and anaerobic granular sludge

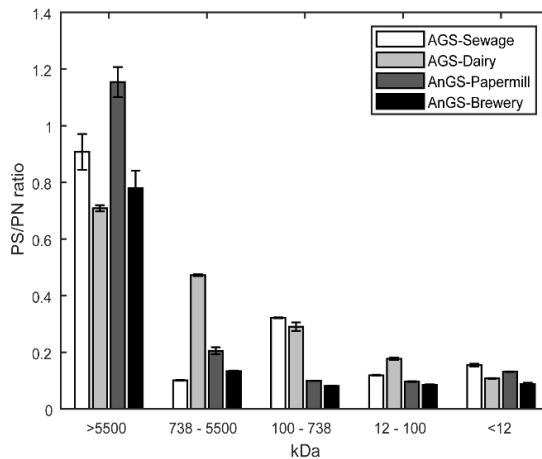


Figure 2.3. Carbohydrate to protein ratio over the different fractions in aerobic granular sludge-Sewage, aerobic granular sludge-Dairy, anaerobic granular sludge-Papermill and anaerobic granular sludge-Brewery. Carbohydrate content is expressed as glucose equivalents and proteins are expressed as BSA equivalents.

FT-IR spectra were recorded for different EPS fractions to check for the presence of functional groups, *e.g.* amide groups, C-O-C groups for carbohydrates (Supplementary Materials Figure S2). In addition to the peaks of proteins ( $1645\text{ cm}^{-1}$  and  $1536\text{ cm}^{-1}$ ) and carbohydrates ( $1078\text{ cm}^{-1}$ ), two other peaks, which indicate the presence of sialic acids ( $1730\text{ cm}^{-1}$ ) and sulfated esters ( $1230\text{ cm}^{-1}$ ) were observed as well.

### Nonulosonic acids

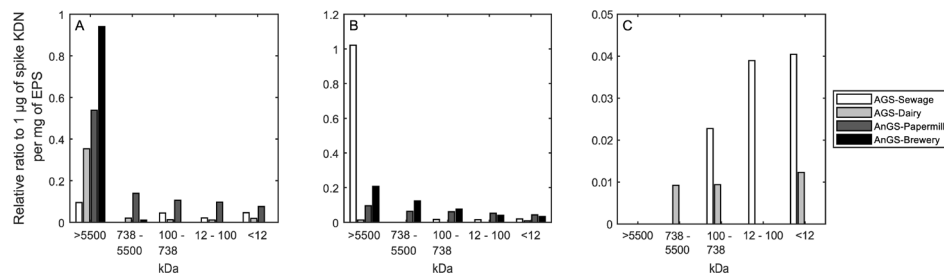


Figure 2.4. Nonulosonic acids detected in each fraction by MS. The detected NulOs, Leg2Ac/Pse2Ac (A), Kdn (B) and NeuAc (C) are expressed as relative ratio of area to spike 1  $\mu\text{g}$  of Kdn per mg EPS in each fraction in aerobic granular sludge-Sewage, aerobic granular sludge-Dairy, anaerobic granular sludge-Brewery, anaerobic granular sludge-Papermill

To investigate if sialic acids or other types of NulOs are widespread in different EPS fractions, mass spectrometry analysis was performed. As shown in Figure 2.4, each EPS fraction was sialylated, with diverse types of NulOs and in different amounts. In

total, there were 3 types of NulOs detected: bacterial sialic acids (legionaminic acid (Leg) and/or its stereoisomer pseudaminic acid (Pse)), deaminated neuraminic acid (Kdn) and N-acetylneuraminic acid (NeuAc). The most predominant NulO is PseAc2/LegAc2. The highest apparent molecular weight fraction ( $>5,500$  kDa) had the highest amount of PseAc2/LegAc2. Especially for the EPS of the two anaerobic granular sludge, PseAc2/LegAc2 were present to a great extent, 75.5% (brewery) and 99.5% (papermill) of their total amount were located at this fraction. In comparison, the EPS of aerobic granular sludge had slightly lower amount than that of anaerobic granular sludge; about 60.9% (sewage) and 91.3% (dairy) of the total PseAc2/LegAc2 were found in these fractions. The second abundant NulO detected was Kdn, except for the EPS from aerobic granular sludge treating dairy wastewater, which had a low amount of Kdn compared to the other EPS. The distribution trend was the same as PseAc2/LegAc2: the highest signal of Kdn was located at the highest apparent molecular weight fraction ( $>5,500$  kDa). Especially for the EPS from aerobic granular sludge (sewage), 95.2% of the detected Kdn was at this fraction. In contrast, the relative amount of NeuAc was on average 16-fold lower than the other two types of NulOs. Only the two aerobic granular sludge EPS had NeuAc which is mainly located at the lower apparent molecular weight fractions ( $<5,500$  kDa).

### Sulfated glycosaminoglycans

As FT-IR results indicated the possible presence of sulfate esters, the detection and quantification of sulfate esters such as sulfated glycosaminoglycans was performed. Unlike the profile of NulOs, the presence of sulfated GAGs was widely spread across all samples and sample fractions, with no clear trend (Figure 2.5). The amount ranged from  $7.2 \pm 0.1$  to  $93.7 \pm 5.7$   $\mu\text{g}$  sulfated GAGs / mg EPS. On average across the molecular weight range, the total sulfated GAGs content in aerobic granular sludge EPS was  $64.2 \pm 2.2$   $\mu\text{g}$  sulfated GAGs / mg EPS and  $55.3 \pm 1.9$   $\mu\text{g}$  sulfated GAGs / mg EPS, for granular sludge from sewage and dairy, respectively. In the anaerobic granular sludge EPS,  $42.1 \pm 1.6$   $\mu\text{g}$  sulfated GAGs / mg EPS and  $15.4 \pm 0.9$   $\mu\text{g}$  sulfated GAGs / mg EPS, for granular sludge from papermill and brewery, respectively. In addition to sulfated GAGs, O-linked sulfated GAGs and N-linked sulfated GAGs were determined separately. In the case of aerobic granular sludge, the average weighted percentage of O-linked sulfated GAGs were found to be  $46.1 \pm 8.6\%$  and  $36.6 \pm 7.0\%$  in the fractions, for sewage and dairy, respectively. While for anaerobic granular sludge,  $29.4 \pm 5.8\%$  and  $31.9 \pm 8.2\%$  O-linked sulfated GAGs were found for papermill and brewery, respectively. Overall, the percentage of O-linked sulfated GAGs was lower than the N-linked sulfated GAGs.

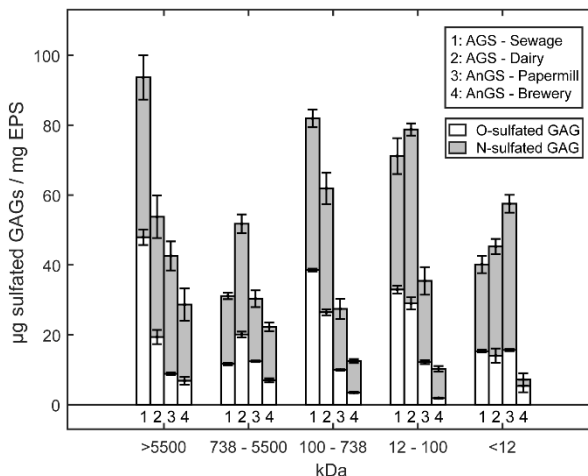


Figure 2.5. Sulfated glycosaminoglycan concentration ( $\mu\text{g sulfated GAGs / mg EPS}$ ) of O-linked sulfated GAGs (white) or N-linked sulfated GAGs (grey) detected in each fraction in aerobic granular sludge-Sewage, aerobic granular sludge-Dairy, anaerobic granular sludge-Papermill, anaerobic granular sludge-Brewery.

### 2.3.4 Genome analysis of sulfotransferases and nonulosonic acid synthases

To further evaluate the production potential of NulOs and sulfated polymers, BLASTp was performed with key proteins for the formation of these compounds on representative organisms of the top ten most abundant genera in the microbiome of aerobic granular sludge and anaerobic granular sludge (Figure 2.6). Sulfotransferases, the enzyme which transfers sulfo groups onto polysaccharides, and NulO synthases, the enzyme responsible for the condensation of a 6-carbon sugar with the 3-carbon phosphoenolpyruvate to generate the 9-carbon Leg, Pse, Neu5Ac and Kdn, were used as a reference. Most of the genomes from the mined microorganisms contain homologous genes for the NulO biosynthesis of either Neu5Ac, Leg or Pse, implying that these organisms can synthesize NulOs. Hits that matched with the selected NulO synthases were mainly annotated as pseudaminic acid synthase or N-acetylneuraminic acid synthase in the community of aerobic granular sludge and anaerobic granular sludge. A few hits were found for genes annotated with N, N'-diacetyllegionaminic acid synthase (LegI). Differentiation between Neu5Ac and Kdn synthases cannot be made due to the way the genes are annotated in the database.

Hits for the sulfotransferases were less abundant. Only few organisms related to representative organisms in the anaerobic granular sludge and aerobic granular sludge microbiome showed positive hits for sulfotransferases. However, when lowering the threshold for the BLASTp search to 5E-2, more organisms showed hits with genes annotated with sulfotransferases. This suggests that the genes encoding

for sulfotransferases might have a more distant relation to the reference protein than what is reported for NulOs.

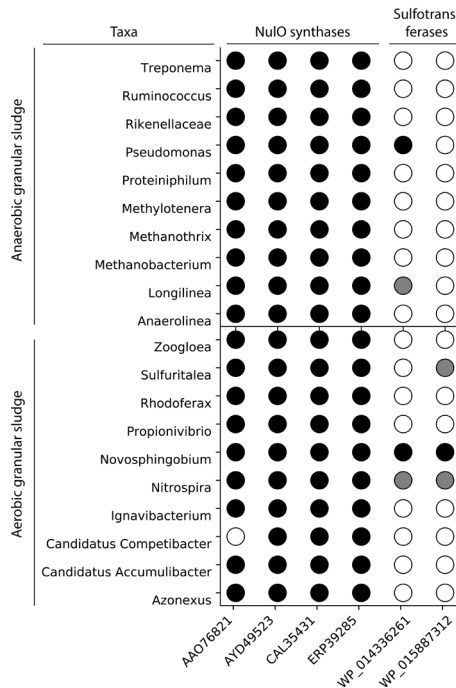


Figure 2.6. BLASTp analysis of sulfotransferases and the nonulosonic acid synthases over the top 10 most abundant genera in the microbial community of anaerobic granular sludge and aerobic granular sludge. Hits are indicated as a black circle, when the BLASTp analysis showed a match with an *E*-value lower than 1E-20. No hits are indicated as a white circle. Lowering the threshold to 5E-2 revealed more distant hits for sulfotransferases, indicated as a grey circle.

## 2.4 Discussion

### 2.4.1 Sialylation and sulfation of anionic glycoconjugates are common in the extracellular polymeric substances of both aerobic and anaerobic granular sludge

In the current research, the EPS of anaerobic and aerobic granular sludge collected from two different types of wastewater treatment systems was extracted. The sialylation and sulfation of anionic glycoconjugates in the EPS were investigated. Three types of NulOs were detected, with significant differences in their amount and location: both bacterial sialic acids (PseAc2/LegAc2) and Kdn were much more abundant than NeuAc (with the relative amount almost 30 times of NeuAc); the majority of both PseAc2/LegAc2 and Kdn were located in the highest molecular weight fraction, while NeuAc was only present in the lower molecular weight fractions of the EPS recovered from aerobic granular sludge. Different from NulOs, the sulfated GAGs were equally distributed over every molecular weight fraction.

## 2. Sialylation and sulfation of anionic glycoconjugates are common in the extracellular polymeric substances of both aerobic and anaerobic granular sludge

---

The presence of sulfated glycosaminoglycans and NulOs in aerobic granular sludge, anaerobic granular sludge and anammox granular sludge was reported recently (Boleij et al., 2020; Bourven et al., 2015; de Graaff et al., 2019; Felz et al., 2020). Each study focused on either one specific glycoconjugates or one specific sludge. In comparison, in the current research, granular sludges from different waste streams, enriched with different microbial communities (*e.g.*, aerobic and anaerobic microorganisms) and operated under different conditions (*e.g.*, temperature and pH) were investigated. The EPS extraction methods were not identical for the different sludge samples: although both extraction methods are based on harsh alkaline extraction, they varied in scale (*i.e.*, full-scale and lab-scale extraction), the type of the base (*i.e.*, KOH and NaOH), and the subsequent recovery of the solubilized EPS (acidic precipitation and dialysis). Despite of all these differences, it was still observed that NulOs and sulfated groups were present in the EPS samples with similar trends in their abundance and their location at different molecular weight fraction.

Based on the current work and the previous report, the conclusion can be drawn that sialylation and sulfation of anionic glycoconjugates are widely distributed in the extracellular polymeric substances of granular sludge and could be a common phenomenon in environmental biofilms in general. This provides the support that the function of sialylated and sulfated glycoconjugates produced by the microorganisms is not just limited to being a camouflage to avoid the detection of the host immune system, as suggested for pathogenic bacteria, but could be involved in structural components of the granule.

One could speculate on potential functions of sialylated and sulfated glycoconjugates by looking at the role of analogous compounds in animal tissue. Glycosaminoglycans are well-defined polyanionic compounds in the extracellular matrix of animals. These high molecular weight compounds are found widely distributed in the connective tissue, creating a highly porous and hydrophilic hydrogel structure (Alberts et al., 2002). Furthermore, sialic acids have also been well described in vertebrate cells and are involved in hydration, protein stabilization and cell-cell interactions, due to their negative charge (Varki, 2017). The mass of the highest molecular weight fraction (>5,500 kDa) comprised of 16-27% of the total EPS and was the most glycosylated fraction with a measured carbohydrate content of 35 - 58%. Interestingly, a similar characterization was reported for mucin. Mucins are space-filling large molecular weight glycoproteins (20 - 20,000 kDa) with 50-90% carbohydrate content. The mucin glycoproteins may be sialylated and/or sulfated (Brown & Hollingsworth, 2013; Rose & Voynow, 2006). The carbohydrate part are largely involved in the mucin properties, such as hydration, binding of ions and water, and protease inhibitors (Brown & Hollingsworth, 2013). It can be speculated that the function of the highest molecular

weight EPS fraction might be similar. The exact role of these glycoconjugates inside the extracellular matrix of environmental biofilm is an interesting topic for future investigation.

#### 2.4.2 Separation and enrichment of the sialylated and sulfated glycoconjugates by size exclusion chromatography with high molecular weight column

The separation and enrichment of glycoconjugates of the extracted EPS aids in further analysis regarding the exact linkage of monomers and chemical structure of these glycoconjugates. This is necessary for a better understanding of the function and production of glycoconjugates in biofilm. Since most sialic acids are on the highest molecular weight fraction ( $> 5,500$  kDa), which is heavily glycosylated and sulfated, enrichment can be achieved at the same time of separation. In this respect, applying a SEC column which can separate large molecular weight polymers is necessary and important. It is noted that, most fractionation studies done with microbial EPS seldom consider protein glycosylation and use columns that can separate molecules up to 670 kDa (Garnier et al., 2006; Ni et al., 2009; Simon et al., 2009). Frequently, the fraction with molecular weight  $> 2,000$  kDa is not analyzed since it exceeds the void volume of the column. If the result of the current research is considered, ignoring this fraction leads to the loss of almost 1/3 of the extracted EPS, not to mention the consequence that most of sialylated EPS could never be collected and studied.

High molecular mass biopolymers (molecular weight  $> 2,000$  kDa) are common in nature and are found for instance in the extracellular matrix of vertebrates. Aggrecan, a highly glycosylated and sulfated proteoglycan in articular cartilage, can have molecular mass up to 2,000 kDa (Athanasios et al., 2017). It has been speculated in literature that bacterial EPS is chemically similar to mucin (Morales-García et al., 2019). Mucin, which is both a sialylated and sulfated glycoprotein complex has a molecular mass of 20 – 20,000 kDa (Brown & Hollingsworth, 2013; Rose & Voynow, 2006). Sialylated and/or sulfated glycoconjugates can tremendously increase the molecular mass of proteins.

#### 2.4.3 Bottlenecks in the study of sialylated and sulfated glycoconjugates in the EPS

Although in the current research, by chemical analysis, both sialylated and sulfated glycoconjugates are found widely spread in all the EPS samples, in the genome analysis of sulfotransferases, very few microorganisms from the most abundant ones in both aerobic granular sludge and anaerobic granular sludge showed positive hits for sulfated glycosaminoglycan sulfotransferases. The reason could be that sulfotransferases were searched in close relatives which do not have this specific gene. Analyzing the metagenome of these samples would improve the estimation of the sulfated glycoconjugates production potential. However, analysis of

## 2. Sialylation and sulfation of anionic glycoconjugates are common in the extracellular polymeric substances of both aerobic and anaerobic granular sludge

---

glycoconjugates production from metagenome data is not trivial. This is due to the fact that metabolic pathways of sulfated GAGs production in bacteria are not well known. The known reference sulfotransferases may not be the enzymes involved in the formation of sulfated glycoconjugates in the EPS. Thus, knowing the exact chemical structure of the sulfated glycoconjugates can aid in finding sulfated polymer production pathways. At present, the methodologies used to study the sulfated glycoconjugates in EPS depend on dye-spectrometric methods, *i.e.*, visualization by Alcian blue staining and heparin red staining, and quantification by DMMB staining (Boleij et al., 2020; Bourven et al., 2015; Felz et al., 2020; Liu et al., 2021). These methods are useful for indicating the presence of sulfated GAGs or other sulfated polymers but have difficulty in distinguishing between different types of sulfated polymers. Sensitive methods, *e.g.*, MS/MS or liquid chromatography (LC)-fluorescence and LC-mass spectrometry (MS), could be used to distinguish between the types of sulfated polymers (Kubaski et al., 2017). As the wide range of molecular size and type of EPS may increase the complexity, the separation of different molecular weight EPS fractions could help with decreasing the complexity and thereby improving the identification of the sulfation patterns.

Separating the EPS by SEC would also help to further determine the exact molecular location of bacterial sialic acids and Kdn. Determine the saccharide sequence that the sialic acids are attached to would reveal more information about the structure-function relationship to understand their role in the EPS. Unfortunately, no sequencing tool such as that existing in proteomics or genomics is available to date for glycoconjugates, since glycoconjugates are far more complex and diverse than proteins and nucleic acids (Merritt et al., 2013). In addition, the diversity of NulOs types and modification increase the complexity even more. Altogether, studying NulOs from an environmental sample is challenging. Therefore, to better understand the production and diversity of NulOs in EPS, lectin array or glycoengineering methods can provide novel insights (Ma et al., 2020).

## Supplementary Materials

The Supplementary Materials of the chapters can be found at DOI 10.1021/acs.est.2c09586.

## References

Alberts, B., Johnson, A., Lewis, J., Raff, M., Roberts, K., & Walter, P. (2002). *The Extracellular Matrix of Animals*.

Athanasiosi, K. A., Darling, E. M., Hu, J. C., DuRaine, G. D., & Reddi, A. H. (2017). *Articular Cartilage*. <https://doi.org/10.1201/B14183>

Bahgat, N. T., Wilfert, P., Korving, L., & van Loosdrecht, M. (2023). Integrated resource recovery from aerobic granular sludge plants. *Water Research*, 234, 119819. <https://doi.org/10.1016/J.WATRES.2023.119819>

Boleij, M., Kleikamp, H., Pabst, M., Neu, T. R., van Loosdrecht, M. C. M., & Lin, Y. (2020). Decorating the Anammox House: Sialic Acids and Sulfated Glycosaminoglycans in the Extracellular Polymeric Substances of Anammox Granular Sludge. *Environmental Science & Technology*, acs.est.9b07207. <https://doi.org/10.1021/acs.est.9b07207>

Bourven, I., Bachellerie, G., Costa, G., & Guibaud, G. (2015). Evidence of glycoproteins and sulphated proteoglycan-like presence in extracellular polymeric substance from anaerobic granular sludge. <Http://Dx.Doi.Org/10.1080/09593330.2015.1034186>, 36(19), 2428–2435. <https://doi.org/10.1080/09593330.2015.1034186>

Brown, R. B., & Hollingsworth, M. A. (2013). Mucin family of glycoproteins. In *Encyclopedia of Biological Chemistry: Second Edition* (pp. 200–204). Elsevier Inc. <https://doi.org/10.1016/B978-0-12-378630-2.00670-8>

Costa, O. Y. A., Raaijmakers, J. M., & Kuramae, E. E. (2018). Microbial extracellular polymeric substances: Ecological function and impact on soil aggregation. *Frontiers in Microbiology*, 9(JUL), 1636. <https://doi.org/10.3389/FMICB.2018.01636> /BIBTEX

de Bruin, S., Vasquez-Cardenas, D., Sarbu, S. M., Meysman, F. J. R., Sousa, D. Z., van Loosdrecht, M. C. M., & Lin, Y. (2022). Sulfated glycosaminoglycan-like polymers are present in an acidophilic biofilm from a sulfidic cave. *Science of the Total Environment*, 829, 154472. <https://doi.org/10.1016/J.SCITOTENV.2022.154472>

de Graaff, D. R., Felz, S., Neu, T. R., Pronk, M., van Loosdrecht, M. C. M., & Lin, Y. (2019). Sialic acids in the extracellular polymeric substances of seawater-adapted aerobic granular sludge. *Water Research*, 343–351. <https://doi.org/10.1016/j.watres.2019.02.040>

Dubois, M., Gilles, K. A., Hamilton, J. K., Rebers, P. A., & Smith, F. (1956). Colorimetric Method for Determination of Sugars and Related Substances. *Analytical Chemistry*, 28(3), 350–356. [https://doi.org/10.1021/AC60111A017/ASSET/AC60111A017.FP.PNG\\_V03](https://doi.org/10.1021/AC60111A017/ASSET/AC60111A017.FP.PNG_V03)

Edelhoch, H. (1967). Spectroscopic Determination of Tryptophan and Tyrosine in Proteins. *Biochemistry*, 6(7), 1948–1954. [https://doi.org/10.1021/BI00859A010/ASSET/BI00859A010.FP.PNG\\_V03](https://doi.org/10.1021/BI00859A010/ASSET/BI00859A010.FP.PNG_V03)

Felz, S., Al-Zuhairy, S., Aarstad, O. A., van Loosdrecht, M. C. M., & Lin, Y. M. (2016). Extraction of structural extracellular polymeric substances from aerobic granular sludge. *Journal of Visualized Experiments*, 2016(115), 54534. <https://doi.org/10.3791/54534>

Felz, S., Neu, T. R., van Loosdrecht, M. C. M., & Lin, Y. (2020). Aerobic granular sludge contains Hyaluronic acid-like and sulfated glycosaminoglycans-like polymers. *Water Research*, 169. <https://doi.org/10.1016/j.watres.2019.115291>

Flemming, H. C., & Wingender, J. (2010). The biofilm matrix. In *Nature Reviews Microbiology* (Vol. 8, Issue 9, pp. 623–633). Nature Publishing Group. <https://doi.org/10.1038/nrmicro2415>

Garnier, C., Gorner, T., Guinot-Thomas, P., Chappe, P., & de Donato, P. (2006). Exopolymeric production by bacterial strains isolated from activated sludge of paper industry. *Water Research*, 40(16), 3115–3122. <https://doi.org/10.1016/J.WATRES.2006.06.005>

Hara, S., Yamaguchi, M., Takemori, Y., Nakamura, M., & Ohkura, Y. (1986). Highly sensitive determination of N-acetyl- and N-glycolylneuraminic acids in human serum and urine and rat serum by reversed-phase liquid chromatography with fluorescence detection. *Journal of Chromatography B*:

2. Sialylation and sulfation of anionic glycoconjugates are common in the extracellular polymeric substances of both aerobic and anaerobic granular sludge

---

*Biomedical Sciences and Applications*, 377(C), 111–119. [https://doi.org/10.1016/S0378-4347\(00\)80766-5](https://doi.org/10.1016/S0378-4347(00)80766-5)

Heijnen, J. van. (2001). Formation of the glycan chains in the synthesis of bacterial peptidoglycan. *Glycobiology*, 11(3), 25R–36R. <https://doi.org/10.1093/GLYCOB/11.3.25R>

Kleikamp, H. B. C., Grouzdev, D., Schaasberg, P., van Valderen, R., van der Zwaan, R., van de Wijgaart, R., Lin, Y., Abbas, B., Pronk, M., van Loosdrecht, M. C. M., & Pabst, M. (2022). Comparative metaproteomics demonstrates different views on the complex granular sludge microbiome. *BioRxiv*, 2022.03.07.483319. <https://doi.org/10.1101/2022.03.07.483319>

Kleikamp, H. B. C., Lin, Y. M., McMillan, D. G. G., Geelhoed, J. S., Naus-Wiezer, S. N. H., Van Baarlen, P., Saha, C., Louwen, R., Sorokin, D. Y., Van Loosdrecht, M. C. M., & Pabst, M. (2020). Tackling the chemical diversity of microbial nonulosonic acids—a universal large-scale survey approach. In *Chemical Science* (Vol. 11, Issue 11, pp. 3074–3080). Royal Society of Chemistry. <https://doi.org/10.1039/c9sc06406k>

Kubaski, F., Osago, H., Mason, R. W., Yamaguchi, S., Kobayashi, H., Tsuchiya, M., Orii, T., & Tomatsu, S. (2017). Glycosaminoglycans detection methods: Applications of mass spectrometry. *Molecular Genetics and Metabolism*, 120(1–2), 67–77. <https://doi.org/10.1016/J.YMGME.2016.09.005>

Li, C., & Arakawa, T. (2019). Agarose native gel electrophoresis of proteins. *International Journal of Biological Macromolecules*, 140, 668–671. <https://doi.org/10.1016/J.IJBIOMAC.2019.08.066>

Liu, J., Zhang, Z., Xue, W., Siriweera, W. B., Chen, G., & Wu, D. (2021). Anaerobic digestion of saline waste activated sludge and recovering raw sulfated polysaccharides. *Bioresource Technology*, 335, 125255. <https://doi.org/10.1016/J.BIOTECH.2021.125255>

Ma, B., Guan, X., Li, Y., Shang, S., Li, J., & Tan, Z. (2020). Protein Glycoengineering: An Approach for Improving Protein Properties. *Frontiers in Chemistry*, 8, 622. <https://doi.org/10.3389/FCHEM.2020.00622>

Masuko, T., Minami, A., Iwasaki, N., Majima, T., Nishimura, S. I., & Lee, Y. C. (2005). Carbohydrate analysis by a phenol-sulfuric acid method in microplate format. *Analytical Biochemistry*, 339(1), 69–72. <https://doi.org/10.1016/J.AB.2004.12.001>

Merritt, J. H., Ollis, A. A., Fisher, A. C., & Delisa, M. P. (2013). Glycans-by-design: engineering bacteria for the biosynthesis of complex glycans and glycoconjugates. *Biotechnology and Bioengineering*, 110(6), 1550–1564. <https://doi.org/10.1002/BIT.24885>

Morales-García, A. L., Bailey, R. G., Jana, S., & Burgess, J. G. (2019). The role of polymers in cross-kingdom bioadhesion. *Philosophical Transactions of the Royal Society B*, 374(1784). <https://doi.org/10.1098/RSTB.2019.0192>

Morrison, M. J., & Imperiali, B. (2014). The Renaissance of Bacilosamine and Its Derivatives: Pathway Characterization and Implications in Pathogenicity. *Biochemistry*, 53(4), 624. <https://doi.org/10.1021/BI401546R>

Ni, B. J., Fang, F., Xie, W. M., Sun, M., Sheng, G. P., Li, W. H., & Yu, H. Q. (2009). Characterization of extracellular polymeric substances produced by mixed microorganisms in activated sludge with gel-permeating chromatography, excitation–emission matrix fluorescence spectroscopy measurement and kinetic modeling. *Water Research*, 43(5), 1350–1358. <https://doi.org/10.1016/J.WATRES.2008.12.004>

Parc, A. Le, Lee, H., Chen, K., Barile, D., Parc, A. Le, Lee, H., Chen, K., & Barile, D. (2014). Rapid Quantification of Functional Carbohydrates in Food Products. *Food and Nutrition Sciences*, 5(1), 71–78. <https://doi.org/10.4236/FNS.2014.51010>

Pinel, I. S. M., Kleikamp, H. B. C., Pabst, M., Vrouwenvelder, J. S., van Loosdrecht, M. C. M., & Lin, Y. (2020). Sialic Acids: An Important Family of Carbohydrates Overlooked in Environmental Biofilms. *Applied Sciences* 2020, Vol. 10, Page 7694, 10(21), 7694. <https://doi.org/10.3390/APP10217694>

Pronk, M., de Kreuk, M. K., de Bruin, B., Kamminga, P., Kleerebezem, R., & van Loosdrecht, M. C. M. (2015). Full scale performance of the aerobic granular sludge

process for sewage treatment. *Water Research*, 84, 207–217. <https://doi.org/10.1016/j.watres.2015.07.011>

Rose, M. C., & Voynow, J. A. (2006). Respiratory tract mucin genes and mucin glycoproteins in health and disease. *Physiological Reviews*, 86(1), 245–278. <https://doi.org/10.1152/PHYSREV.00010.2005/ASSET/IMAGES/LARGE/Z9J0010623871006.jpeg>

Schäffer, C., & Messner, P. (2017). Emerging facets of prokaryotic glycosylation. *FEMS Microbiology Reviews*, 41(1), 49. <https://doi.org/10.1093/FEMSRE/FUW036>

Serwer, P. (1983). Agarose gels: Properties and use for electrophoresis. *ELECTROPHORESIS*, 4(6), 375–382. <https://doi.org/10.1002/ELPS.1150040602>

Simon, S., Païro, B., Villain, M., D'Abzac, P., Hullebusch, E. Van, Lens, P., & Guibaud, G. (2009). Evaluation of size exclusion chromatography (SEC) for the characterization of extracellular polymeric substances (EPS) in anaerobic granular sludges. *Bioresource Technology*, 100(24), 6258–6268. <https://doi.org/10.1016/j.biortech.2009.07.013>

Suvarna, S. K., Layton, C., & Bancroft, J. D. (2019). Bancroft's THEORY and TECHNIQUES of HISTOLOGICAL PRACTICE. *Analisis Standar Pelayanan Minimal Pada Instalasi Rawat Jalan Di RSUD Kota Semarang*, 3, 557.

Tomás-Martínez, S., Chen, L. M., Pabst, M., Weissbrodt, D. G., van Loosdrecht, M. C. M., & Lin, Y. (2022). Enrichment and application of extracellular nonulosonic acids containing polymers of *Accumulibacter*. *Applied Microbiology and Biotechnology*, 1–11.

Tomás-Martínez, S., Kleikamp, H. B. C., Neu, T. R., Pabst, M., Weissbrodt, D. G., van Loosdrecht, M. C. M., & Lin, Y. (2021). Production of nonulosonic acids in the extracellular polymeric substances of "Candidatus Accumulibacter phosphatis." *Applied Microbiology and Biotechnology*, 105(8), 3327–3338. <https://doi.org/10.1007/s00253-021-11249-3>

van Lier, J. B., Mahmoud, N., & Zeeman, G. (2008). Anaerobic biological wastewater treatment. In M. Henze, M. van Loosdrecht, G. A. Ekama, & D. Brdjanovic (Eds.), *Biological wastewater treatment* (2008th ed., pp. 415–457). IWA publishing.

Varki, A. (2017). Biological roles of glycans. *Glycobiology*, 27(1), 3–49. <https://doi.org/10.1093/GLYCOB/CWW086>

Varki, A., Cummings, R. D., Esko, J. D., Stanley, P., Hart, G. W., Aebi, M., Darvill, A. G., Kinoshita, T., Packer, N. H., Prestegard, J. H., Schnaar, R. L., & Seeberger, P. H. (2017). Essentials of Glycobiology. *Cold Spring Harbor (NY)*, 823.

Wang, L., Lu, Z., Allen, K. N., Mariano, P. S., & Dunaway-Mariano, D. (2008). Human Symbiont *Bacteroides thetaiotaomicron* Synthesizes 2-Keto-3-Deoxy-D-Glycero-D-Galacto-Nononic Acid (KDN). *Chemistry and Biology*, 15(9), 893–897. <https://doi.org/10.1016/j.chembiol.2008.08.005>

Zaretsky, M., Roine, E., & Eichler, J. (2018). Sialic acid-like sugars in archaea: Legionaminic acid biosynthesis in the halophile *Halorubrum* sp. PV6. *Frontiers in Microbiology*, 9(SEP), 2133. [https://doi.org/10.3389/FMICB.2018.02133/BIBTEX](https://doi.org/10.3389/FMICB.2018.02133)

Zheng, C. H., & Levenston, M. E. (2015). Fact versus artifact: Avoiding erroneous estimates of sulfated glycosaminoglycan content using the dimethylmethyle blue colorimetric assay for tissue-engineered constructs. *European Cells and Materials*, 29, 224–236. <https://doi.org/10.22203/eCM.v029a17>



Anionic extracellular polymeric  
substances extracted from  
seawater-adapted aerobic  
granular sludge

3

## Abstract

Anionic polymers, such as heparin, have been widely applied in the chemical and medical fields, particularly for binding proteins (*e.g.*, fibroblast growth factor 2 (FGF-2) and histones). However, the current animal-based production of heparin brings great risks, including resource shortages and product contamination. Recently, anionic compounds, nonulosonic acids (NulOs), and sulfated glycoconjugates were discovered in the extracellular polymeric substances (EPS) of aerobic granular sludge (AGS). Given the prevalence of anionic polymers, in marine biofilms, it was hypothesized that the EPS from AGS grown under seawater condition could serve as a raw material for producing the alternatives to heparin. This study aimed to isolate and enrich the anionic fractions of EPS and evaluate their potential application in the chemical and medical fields. The AGS was grown in a lab-scale reactor fed with acetate, under the seawater condition (35 g/L sea salt). The EPS was extracted with an alkaline solution at 80°C and fractionated by size exclusion chromatography. Its protein binding capacity was evaluated by native gel electrophoresis. It was found that the two highest molecular weight fractions (438- > 14,320 kDa) were enriched with NulO and sulfate-containing glycoconjugates. The enriched fractions can strongly bind the two histones involved in sepsis and a model protein used for purification by heparin-column. These findings demonstrated possibilities for the application of the extracted EPS and open up a novel strategy for resource recovery.

## Published as:

Chen, L. M., Beck, P., van Ede, J., Pronk, M., van Loosdrecht, M. C. M., & Lin, Y. (2024). Anionic extracellular polymeric substances extracted from seawater-adapted aerobic granular sludge. *Applied Microbiology and Biotechnology*, 108(1), 144. <https://doi.org/10.1007/s00253-023-12954-x>

### 3.1 Introduction

Heparin is the most negatively charged natural polymer, belonging to the family of glycosaminoglycans. Due to the strong anionic charge on its molecular chain, it can bind specific proteins, growth factors, and regulate their diffusion (Varki et al., 2017a). Currently, animal-derived heparin is used as a pharmaceutical drug (*e.g.* sepsis treatment drug and anticoagulant agent), as the component of the endothelial cell culture media to help the binding of growth factors (*e.g.* Endothelial Growth Factor (VEGF) and Fibroblast Growth Factor (FGF)), and as packing material for columns in affinity chromatography for proteins purification (Nolin Bolten et al., 2018; Wildhagen et al., 2014). As heparin is currently derived from animal sources, significant resource shortages and product contaminations may happen, resulting in an unpredictable supply (McCarthy et al., 2020; Nolin Bolten et al., 2018). It is important to search for sustainable and reliable alternatives for heparin. It has been reported that some algae and bacteria living in the marine environment produce sulfated glycoconjugates (Collicec-Jouault et al., 2012). Sulfated polysaccharides extracted from marine organisms are used as gelling agents in the food and pharmaceutical industries, because of their distinct properties. Moreover, due to their bioactive properties (*e.g.* anticancer, anti-inflammatory, and anticoagulant), sulfated polysaccharides from marine organisms have become a source of interest for the development of heparin alternatives and new materials (Collicec-Jouault et al., 2012; Delbarre-Ladrat et al., 2014; Lee and Ho, 2022; Xue et al., 2019).

Biopolymers carrying anionic charges have been found in biofilms such as aerobic granular sludge (AGS) as well (Chen et al., 2023; de Graaff et al., 2019; Felz et al., 2020). The AGS technology is increasingly used as an efficient wastewater treatment technology (Nancharaiah and Sarvajith, 2019; Pronk et al., 2015). This biotechnological process is based on a microbial community forming granules by a self-produced biofilm matrix using extracellular polymeric substances (EPS). The EPS matrix consists of numerous macromolecular compounds, such as (glyco)lipids, (glyco)proteins and polysaccharides (Felz et al., 2016; Seviour et al., 2019). Negatively charged glycoconjugates are shown to play an important role in the formation and stabilization of the complex EPS structure, through bridging with multivalent cations (Flemming and Wingender, 2010).

One type of strongly negatively charged components in the EPS are nonulosonic acids (NulOs). NulOs are 9-carbon acidic monosaccharides usually reported as part of the glycoconjugates in eukaryotes or pathogenic bacteria (Varki et al., 2017b). Within the NulOs family, neuraminic acid (NeuAc) and its derivatives are well studied, especially in relation to the interaction between pathogens and human cells. Other forms of NulOs such as pseudaminic acid and legionaminic acid are found on lipopolysaccharides produced by pathogenic bacteria (Angata and Varki, 2002).

Only recently it has been shown that the NulOs are widespread in non-pathogenic microbial aggregates, such as seawater-adapted AGS, enriched cultures of "*Candidatus Accumulibacter phosphatis*" and anammox granular sludge (Boleij et al., 2020; de Graaff et al., 2019; Kleikamp et al., 2020; Tomás-Martínez et al., 2021). These polymers enriched with NulOs were shown to have interaction with positive charged histones, suggesting a source for sepsis treatment drugs (Tomás-Martínez et al., 2022). Sulfated glycoconjugates are another type of strongly negatively charged compounds that were recently reported in the EPS of various granular sludge systems including AGS (Boleij et al., 2020; Bourven et al., 2015; Felz et al., 2020). Sulfated glycoconjugates, especially sulfated glycosaminoglycans in the extracellular matrix of animals are well studied (Bedini et al., 2019).

Based on the recent research, the EPS of AGS contains anionic glycoconjugates with NulOs and sulfated groups. Thus, it may have great potential to be a sustainable resource for the production of biomaterials for various biotechnological applications. With the AGS system, it is possible to use microbial communities instead of pure cultures and to adjust the operational conditions of the reactor to stimulate the production of the EPS. Therefore, the AGS system may become a new platform to produce biopolymers and provide novel strategies for resource recovery.

Expanding on the recent findings of anionic glycoconjugates in AGS, the aim of the current research was to evaluate the anionic properties of the EPS from seawater-adapted AGS. We are specifically focusing on NulOs and sulfated glycoconjugates and explore the potential application in the medical field (*e.g.* raw material for sepsis treatment drugs) and chemical field (*e.g.* column material for proteins purification). The extracted EPS was fractionated by size exclusion chromatography to obtain fractions containing different apparent molecular weight. The EPS and the derived fractions were characterized for the presence of anionic compounds by measuring the content of NulOs and sulfated glycoconjugates. Finally, the potential applications of the extracted EPS were evaluated by using a protein binding assay.

### **3.2 Material and Methods**

#### **3.2.1 Reactor operation and biomass microbial community analysis**

##### **Reactor operation**

Seawater-adapted aerobic granular sludge was cultivated in a 2.8 L bubble column with an internal diameter of 6.25 cm as a sequencing batch reactor (SBR) adapted from de Graaff et al. (2019). The reactor was inoculated with sludge collected from a lab-scale reactor with glycerol as the carbon source under freshwater condition (Elahinik et al., 2022). The room temperature was controlled at 20°C and the pH was controlled at pH  $7.3 \pm 0.1$  by dosing 1.0 M NaOH or 1.0 M HCl. The DO was controlled

by a mixture of nitrogen gas and air at 0% and 80% saturation during the anaerobic and aerobic phases, respectively.

Reactor cycles consisted of 5 min settling, 5 min effluent withdrawal, 5 min N<sub>2</sub> sparging, 5 min of feeding, 50 min N<sub>2</sub> gas sparging (anaerobic phase) and 110 min of aeration (aerobic phase). Artificial seawater (Instant Ocean® Sea Salt, Instant Ocean) was gradually introduced by incrementally increasing the seawater concentration with 10 g/L Instant Ocean® Sea Salt each week, while maintaining complete anaerobic acetate removal. After the final concentration of 35 g/L Instant Ocean® Sea Salt was reached, the average sludge retention time (SRT) was kept at 14 days. Granules were sampled for EPS extraction and microbial community analysis after 12 days of exposure to 35 g/L Instant Ocean® Sea Salt.

The feed of 1.5 L per cycle consisted of 1.2 L artificial seawater (final concentration 35 g/L Instant Ocean® Sea Salt), 150 mL of medium A and 150 mL of medium B. Medium A was composed of 8506 mg/L of sodium acetate trihydrate. Medium B contained 2200 mg/L of NH<sub>4</sub>Cl, 340 mg/L of K<sub>2</sub>HPO<sub>4</sub>, 270 mg/L of KH<sub>2</sub>PO<sub>4</sub>, 70 mg/L of allylthiourea to inhibit nitrification and 10 mL/L of trace elements solution similar to Vishniac & Santer (1957). The trace element solution contained 4.99 g/L FeSO<sub>4</sub>.7H<sub>2</sub>O, 2.2 g/L ZnSO<sub>4</sub>.7H<sub>2</sub>O, 7.33 g/L CaCl<sub>2</sub>.2H<sub>2</sub>O, 4.32 g/L MnSO<sub>4</sub>.H<sub>2</sub>O, 2.18 g/L Na<sub>2</sub>MoO<sub>4</sub>.2H<sub>2</sub>O, 1.57 g/L CuSO<sub>4</sub>.5H<sub>2</sub>O, 1.61 g/L CoCl<sub>2</sub>.6H<sub>2</sub>O and 50 g/L EDTA. The combination of these feed streams led to influent concentrations of 400 mg/L COD, 57.6 mg/L NH<sub>4</sub>-N and 12.2 mg/L PO<sub>4</sub>-P. To monitor the performance of the reactor, samples were taken at certain interval and filtered through a 0.22 µm PVDF filter. Acetate concentration was measured through high performance liquid chromatography on the Vanquish HPLC system (Thermo Scientific, Waltham, USA) at 50°C (0.75 mL/min) with 1.5 mM phosphoric acid as eluent and Aminex HPC-87H (Bio-Rad, California, USA) as a column. Phosphate and ammonia concentration were measured by using a Thermo Fisher Gallery Discrete Analyzer (Thermo Fisher Scientific, Waltham, USA). Visualization of the granules was performed by using a stereo zoom microscope (M205 FA, Leica Microsystems, Germany). The images of the granules were captured, processed and exported in “.jpg” format with Qwin image analysis software (V3.5.1, Leica Microsystems, Germany).

The organic and ash fractions of the biomass were determined according to the standard methods (APHA, 1998), after washing the granules three times with five times of its volume with demi-water. For EPS extraction and characterization, the washed granules were lyophilized immediately and stored at room temperature.

#### **Microbial community analysis by fluorescent in-situ hybridization (FISH)**

The granules were collected from the reactor at the end of the aerobic phase. The handling, fixation and staining of FISH samples was performed as described in

Bassin et al. (2011). The PA0mix combination (PA0462, PA0651, and PA0846) was used for visualizing polyphosphate accumulating organisms (PAO) (Crocetti et al., 2000). The GAOmix (GAOQ431 and GAOQ989) (GAOmix) was used for visualizing glycogen accumulating organisms (GAO) (Crocetti et al., 2000). Probes targeting the clade I and clade II of Accumulibacter (Acc444-I and Acc444-II) were used for visualizing the clades of Accumulibacter (Flowers et al., 2009). EUBmix (EUB338, EUB338-II and EUB338- III) was used for staining all bacteria (Amann et al., 1990; Daims et al., 1999). Images were taken with a Zeiss Axio Imager M2 microscope equipped with the fluorescent light source X-Cite Xylis 720L. The image acquisition was performed with the Zeiss Axiocam 705 mono camera. The images were processed and exported in ".tif" format with the Zeiss microscopy software (ZEN version 3.3).

### **3.2.2 EPS extraction from aerobic granular sludge and characterization**

#### **EPS extraction**

Lyophilized granules were extracted in 0.1 M NaOH (1% VS w/v) for 30 min at 80°C while stirring at 400 rpm. The solution was cooled down and centrifuged at 4000  $\times$  g for 20 min at 4°C. The supernatant was collected and subsequently dialyzed against demi-water overnight in dialysis tubing with a molecular weight cut-off 3.5 kDa MWCO (Snakeskin™, ThermoFisher Scientific, Landsmeer). The dialyzed EPS solution was lyophilized and stored at room temperature until further analysis.

#### **EPS fractionation by size-exclusion chromatography**

Forty mg lyophilized EPS was solubilized in eight ml of running buffer containing 0.15 M NaCl, 0.05 M glycine-NaOH (pH 10) with gentle stirring overnight. The pH was adjusted to 10 using NaOH. All solutions were filtered through a 0.45  $\mu$ m membrane filter before application to the column, to allow the samples to remain dissolved as much as possible.

Size exclusion chromatography (SEC) was performed using a Hiload 16/600 Superose 6 prepacked column (Cytiva Lifesciences, Marlborough, MA) fitted on a Bio-Rad system containing a UV detector. Superose 6 column has a high fractionation range (fractionation range Mr  $\sim$  5 kDa - 5,000 kDa (globular proteins) with an exclusion limit of Mr  $\sim$  40,000 kDa (globular proteins). Calibration of the column, upon which the elution volume was determined, was done using a Cytiva HMW marker set (Cytiva Lifesciences, Marlborough, MA). This set consists of ovalbumin (44 kDa), conalbumin (75 kDa), aldolase (158 kDa), ferritin (440 kDa) and thyroglobulin (669 kDa). The molecular weight of the fractions of the sample was determined based on the calibration line. Molecular weights higher than the standards were calculated by linear extrapolation of the calibration line.

EPS fractions were collected based on the chromatogram (280 nm) of the elution. They were subsequently dialyzed against demi water with a 3.5 kDa MWCO dialysis bag, frozen at -80°C and lyophilized. The lyophilized samples were stored at room temperature until further analysis.

### Native agarose gel staining with Coomassie Blue and Alcian Blue

Native agarose gel electrophoresis was run on a submerged horizontal platform, with the wells positioned in the center of the gel. Lyophilized EPS samples were resolubilized in 50 mM Tris at 2.5 mg EPS/mL concentration for 1 hour at 30°C. Next, 10  $\mu$ L of the sample was loaded in the wells on a 0.8% agarose gel in 500 mM Tris/HCl, 160 mM boric acid, 1 M urea, pH 8.5. Electrophoresis was performed with a running buffer (90 mM Tris/HCl, 90 mM boric acid, pH 8.5) at 80 V for 90 min. Proteins carrying a net negative charge migrate toward the anode, whereas proteins carrying a positive charge migrate towards the cathode. To determine if high molecular weight proteins could pass the gel, a high molecular weight marker was used as a ladder (HMW – SDS Calibration kit, Cytiva, Marlborough, MA). The ladder was negatively charged due to the presence of sodium dodecyl sulfate (SDS). The proteins in the EPS were revealed using Coomassie blue staining (SimplyBlue™ Safestain, Invitrogen, Waltham, MA) according to the manufacturer's instruction, and destained overnight. To visualize glycoconjugates containing the carboxyl groups R-COO<sup>-</sup> and the sulfated groups R-OSO<sup>3-</sup>, staining with Alcian Blue was performed at pH 2.5 and pH 1.0 respectively, as described by Boleij et al. (2020). Other negatively charged groups, *e.g.* phosphate groups, are hardly stained since they are unable to bind as strong as carboxyl and sulfate groups with Alcian Blue under low salt conditions done in this study (Scott and Dorling, 1965). The gel pictures were taken on a ChemiDoc MP imager (Bio-Rad, Hercules, CA).

### Functional group analysis by Fourier-Transform Infrared Spectroscopy

Functional group analysis was performed by Fourier Transform Infra-red (FTIR) spectroscopy on a Spectrum 100 spectrometer (PerkinElmer, Shelton, CT). The spectra of the lyophilized samples were recorded at room temperature over a wavenumber range of 600 – 4000  $\text{cm}^{-1}$  with 16 accumulations and 4  $\text{cm}^{-1}$  resolution.

### Sulfated glycoconjugates assay

Detection and quantification of sulfated glycoconjugates was performed with the Blyscan sulfated glycosaminoglycan (sulfated GAGs) assay (Biocolor, Carrickfergus, UK), according to the manufacturer's instructions. Samples (2-5 mg) were digested with one mL of papain protein digestion solution at 65°C for 3 hours at 300 rpm (Sigma Aldrich, Zwijndrecht, Netherlands). The supernatant was recovered after centrifugation at 10.000 x g for 10 min. 50  $\mu$ L of sample was then added to 1 mL of DMMB dye reagent. Sulfated GAGs positive components bind and precipitate with the dye, which are subsequently isolated and resolubilized. The concentration of

sulfated GAGs was measured with a multimode plate reader at 656 nm (TECAN Infinite M200 PRO, Switzerland) as chondroitin sulfate equivalents. Lastly, the distribution of N-linked and O-linked sulfate in the samples was measured by performing nitrous acid cleavage as by the manufacturer's instructions prior to sulfated GAGs quantification.

#### **Nonulosonic acids analysis with mass spectroscopy**

The NulOs measurement was done according to the approach described by Kleikamp et al. (2020) with small modifications. Lyophilized EPS fractions were hydrolyzed by 2 M acetic acid for 2 hours at 80°C and dried with a Speed Vac concentrator. The released NulOs were labelled using a final concentration of 7 mM DMB (1,2-diamino-4,5-methylenedioxybenzene dihydrochloride) for 2.5 hours at 50°C.

The LC-MS analysis was performed on a Q Exactive™ Focus Hybrid Quadrupole-Orbitrap™ Mass Spectrometer (Thermo Scientific, Bleiswijk, Netherlands) coupled to an Acquity M-Class Ultra Performance Liquid Chromatograph (Waters, Milford, MA). The chromatographic separations were performed with a 1.0 x 100 mm C18 1.7 µm column (Acquity UPLC® BEH) at a constant flow rate of 40 µL/min. Solvent A consisted of 0.1% formic acid in MS-grade H2O and solvent B of 0.1% formic acid in MS-grade acetonitrile. A linear gradient from 2.5% B to 35% B was applied over 10 min, followed by a linear gradient up to 65% B over another 2.5 minutes. Each sample was analysed in duplicate followed by two blanks.

Electrospray ionization was performed in positive ionisation mode and MS1 analysis was executed at a 35K resolution, an AGC target of 2.0E5 and a maximum injection time of 50 ms. Continuous fragmentation of small mass segments was performed in 5.0 Da steps from 340–530 Da (isolation window of 5.5 m/z). Fragmentation was performed using a normalized collision energy of 26. For MS2 analysis a 17.5K resolution, a AGC target of 2.0E5 and a maximum IT of 50 ms was used. The number of micro scans was set to 1. Raw data were analysed using XCalibur 4.1 (Thermo Fisher Scientific, Germany) and Matlab R2022a (MathWorks). The mass spectrometer was calibrated using the Pierce™ LTQ ESI positive ion calibration solution (Thermo Fisher Scientific, Germany).

Semi-quantitative estimation of the relative amounts of each type of NulOs was done by using the peak area of spiked 10 pmol of Kdn as a reference signal. The integrated peak areas in the mass spectrometry chromatograms were calculated for each type of NulOs in each EPS fraction. The peak area was used as a parameter proportional to the amount of NulOs. The relative amount of each type of NulOs in each EPS fraction was presented as a ratio to the peak area of 1 µg of Kdn for comparison.

### 3.2.3 EPS binding potential with cationic proteins

To study the binding potential of EPS and its fractions with cationic proteins, the interactions between EPS and three known cationic proteins, histone H2A, H2B and fibroblast growth factor 2 (FGF-2) were evaluated according to Zlatina et al. (2017) with modifications. Solutions of EPS were prepared in 50 mM Tris at a concentration of 2.5 mg/mL. Five  $\mu$ g of a cationic protein was incubated with 10  $\mu$ g from the EPS solution to a final concentration of 50 mM Tris at 30°C, 300 rpm for 1 hour. One  $\mu$ L of glycerol was added to the sample, vortexed and spun down briefly. The entire sample was loaded on a horizontal 0.8% agarose gel (500 mM Tris/HCl, 160 mM boric acid, 1 M urea, pH 8.5), with the wells positioned in the middle of the gel. The electrophoresis was performed at 80V for 90 min with a running buffer (90 mM Tris/HCl, 90 mM boric acid, pH 8.5). Staining was performed with Coomassie Blue G-250 (SimplyBlue™ Safestain, Invitrogen, Waltham, MA) according to the manufacturer's instruction. In parallel, as a comparison to the EPS, the solutions of heparin (from porcine intestinal mucosa, Sigma Aldrich) and cationic protein-heparin samples with the same concentrations as described above were prepared accordingly.

### 3.3 Results

#### 3.3.1 Reactor operation and EPS extraction

After stable granulation and complete acetate and phosphate removal was achieved (Figure 3.1), the EPS was extracted from the granules. The reactor operation and behavior was similar to previously reported AGS experiments (de Graaff et al., 2019). The yield of the EPS extracted was  $640 \pm 42$  mg VS EPS / g VS granules. The microbial community consisted, according to FISH staining, mainly phosphate accumulating organisms (PAO), specifically “*Candidatus Accumulibacter phosphatis* sp.” were the dominant microorganisms present, together with small amounts of glycogen accumulating organisms (GAO) (Figure 3.2).

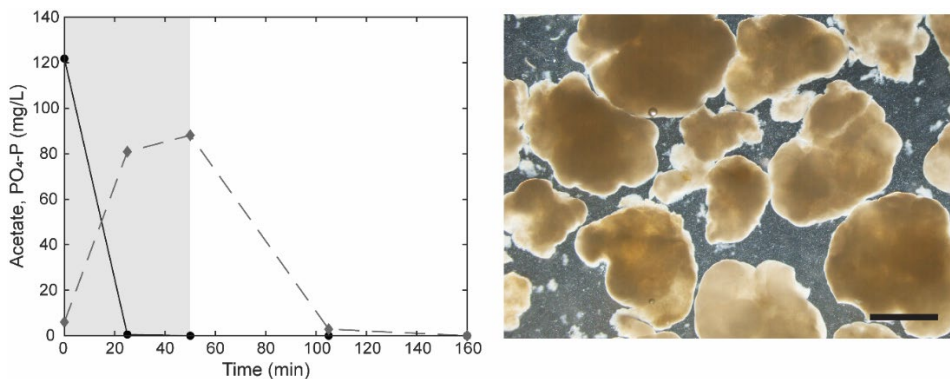


Figure 3.1. Profile of acetate (●) and phosphate (◆) in the seawater-adapted AGS reactor (left). The shaded area indicates the anaerobic phase. Granules grown at 35 g/L Instant Ocean® Sea Salt with a scale bar representing 1 mm visualized through stereo imaging (right).

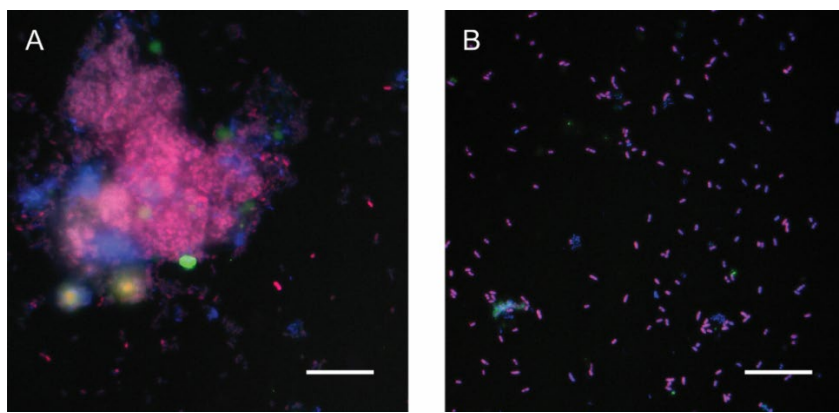


Figure 3.2. Fluorescent in-situ hybridization of seawater-adapted AGS. A: Eubacteria (blue), GAO (green), PAO (red). B: Eubacteria (blue), Acc I (red) and Acc II (green). Overlapping probes of blue and red results in a magenta color. Overlapping green and blue result in a turquoise color. The scale bar represents 20  $\mu\text{m}$  for both A and B.

### 3.3.2 EPS fractionation and characterization

#### EPS fractionation and functional groups

The extracted EPS was fractionated by size exclusion chromatography to obtain fractions containing different apparent molecular weight (aMW). Five fractions with aMW ranging from <12 kDa to more than 14,320 kDa were collected (Table 3.1). There was no clear difference in the amount of mass among these five fractions. Specifically, fractions F1 and F2 were collected at the beginning of the chromatogram (Supplementary Materials Figure S1); both had a high aMW and low absorbance at 280 nm, their mass in total contributed to almost 40% of the extracted EPS. Judging from the chromatogram, F1 and F2 might be proteins which are heavily glycosylated.

Table 3.1. Fractionation yields of the total eluted EPS through size exclusion chromatography and the corresponding apparent MW (aMW). The calibration is based on globular proteins and thus the molecular weight range is here expressed in aMW. The fractions are collected based on the eluted peaks at 280 nm of the chromatogram (Supplementary Materials Figure S1). The fractions marked with an asterisk (\*) are based on extrapolation of the calibration line.

Fraction #	aMW range (kDa)	Weight percentage of EPS (%)
F1	2815 – >14,320 *	20
F2	439 – 2815	19
F3	68 – 439	19
F4	12 – 68	26
F5	<12 *	16

To investigate the differences among the obtained fractions, FT-IR spectroscopy was used to analyze the functional groups. The spectrum of each fraction is shown in Figure 3.3. The relative intensity ratio between the typical band of carbohydrates (C-O-C stretching at  $\sim 1030\text{ cm}^{-1}$ ) and the typical band of proteins (N-H bending at  $\sim 1630\text{ cm}^{-1}$ ) was much higher in the spectrum of F1 and F2 than in the spectrum of F3 and F4, suggesting that the glycoconjugates content is decreasing while the protein content is increasing as the molecular weight decreases from F1 to F4 (Tomás-Martínez et al., 2022). The spectrum of F5 was significantly different from the other fractions, the N-H bending of proteins downshift to  $\sim 1620\text{ cm}^{-1}$ , while the band of carbohydrates split into two bands at  $1068\text{ cm}^{-1}$  and  $978\text{ cm}^{-1}$ , indicating the appearance of furan ring in the glycoconjugates (Zou et al., 2019).

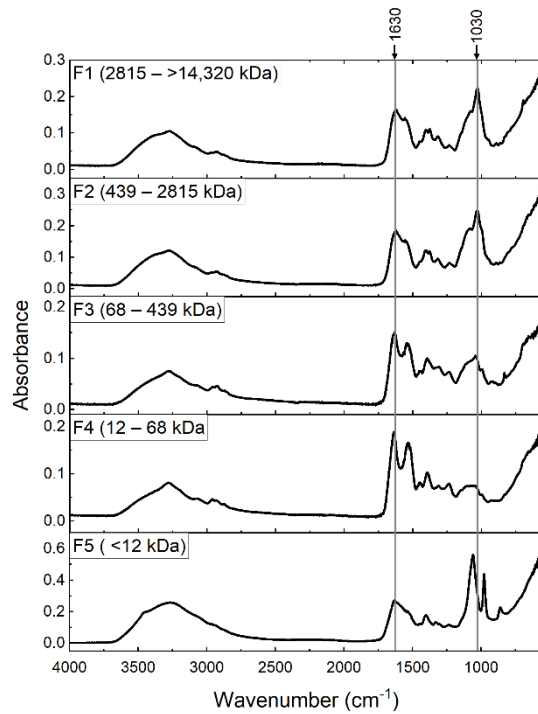


Figure 3.3. FT-IR spectrum of fractionated EPS. The gray lines indicate the wavenumbers  $1630\text{ cm}^{-1}$  (-NH bending) and  $1030\text{ cm}^{-1}$  (C-O-C stretching).

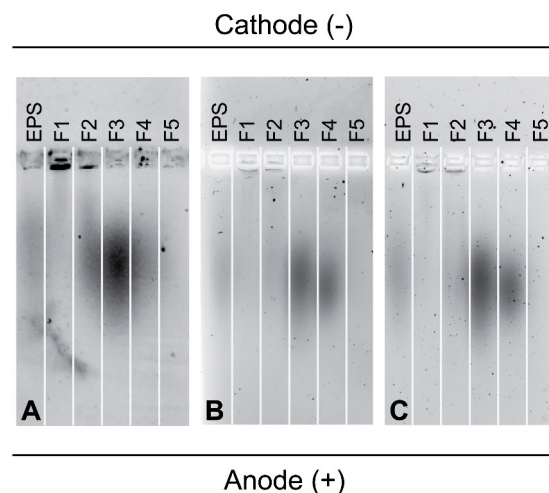


Figure 3.4. Native gel electrophoresis on agarose stained with Coomassie Blue (A), Alcian Blue pH 2.5 (B), and Alcian Blue pH 1.0 (C) with 10 µg of unfractionated EPS (EPS), and the different molecular weight fractions F1 (2815 - >14,320 kDa), F2 (439 - 2815 kDa), F3 (68 - 439 kDa), F4 (12 - 68 kDa) and F5 (<12 kDa).

To further characterize the EPS fractions on the possible types of acidic glycoconjugates, native agarose gel stained with Coomassie Blue (proteins), Alcian Blue at pH 2.5 (strongly acidic R-COO<sup>-</sup> and R-OSO<sup>3-</sup>) and 1.0 (R-OSO<sup>3-</sup>) was performed (Figure 3.4). Firstly, Coomassie blue staining showed that the EPS migrated towards the anode as a light smear (Figure 3.4A), indicating an overall negative charge on the extracted EPS. A large proportion of F1 and F2 were retained within the well towards the anode, implying that both F1 and F2 are negatively charged. Probably, due to their high molecular weight and/or the overall low negative charge density, it was difficult for these two fractions to migrate further in the gel. In comparison, both F3 and F4 migrated towards the anode as an intense smear without being retained in the well. Likely, due to their lower molecular weight, the negative charge density is sufficient for the molecules to migrate. Secondly, both F1 and F2 in the well were stained with Alcian Blue at both pH 2.5 and 1.0, indicating the presence of glycoconjugates containing both R-COO<sup>-</sup> and R-OSO<sup>3-</sup> groups. In comparison, both F3 and F4 were stained as a smear with Alcian Blue at both pH 2.5 and 1.0, implying the glycoconjugates which contained R-COO<sup>-</sup> and R-OSO<sup>3-</sup> groups have a range of chain length (Figure 3.4B and C). In contrast, F5 did not react with any of the dyes. Probably, because the agarose gel has large pore size (Stellwagen, 2009), F5 which has the molecular weight of <12 kDa could not be retained in the gel.

### Distribution of sulfated glycoconjugates and NulOs in the EPS fractions

Sulfated glycoconjugates and the carboxylic groups of NulOs confer negative charges to the EPS. To confirm the presence and the types of sulfated glycoconjugates and NulOs, the extracted EPS and the fractions were analyzed by DMMB assay for sulfated glycoconjugates and mass spectrometry for NulOs, respectively.

Quantification of sulfated glycoconjugates by DMMB assay has been reported to be more sensitive and reliable than Alcian Blue (De Jong et al., 1994; Zheng and Levenston, 2015). As shown in Figure 3.5, the amount of sulfated glycoconjugates (chondroitin-4-sulfate equivalent) in F1 and F2 was increased by 2-fold in comparison to that of the unfractionated EPS. The amount in F3 and F4 was much lower, and F5 showed negligible amounts of sulfated glycoconjugates. These results correspond well to the Alcian Blue staining for R- $\text{OSO}_3^-$  (pH 1.0). Apparently, the fractionation with SEC allowed to obtain fractions which are highly enriched with sulfated glycoconjugates. F1 and F2, which were the two fractions with the highest molecular weights, contained the majority of the total sulfated glycoconjugates.

In addition, it was possible to differentiate the two types of sulfated glycoconjugates, N-sulfation and O-sulfation, by performing nitrous acid pretreatment. N-sulfated glycoconjugates were found to be between 52% to 66% of the total sulfated glycoconjugates in the EPS and the fractions. This suggests that the N-sulfated glycoconjugates are relatively predominant.

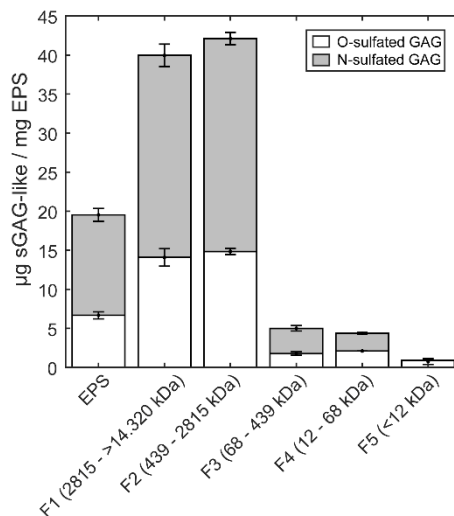


Figure 3.5. The content of sulfated glycosaminoglycans in the EPS and its fractions ( $\mu\text{g}$  sulfated GAG-like / mg EPS) with chondroitin-4-sulfate as reference. White: O-linked sulfated GAGs (white); Gray: N-linked sulfated GAGs.

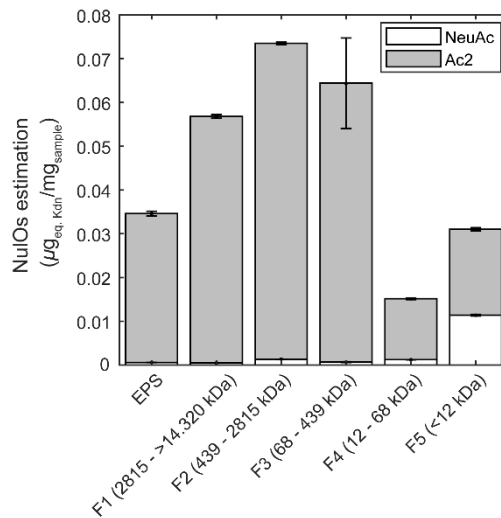
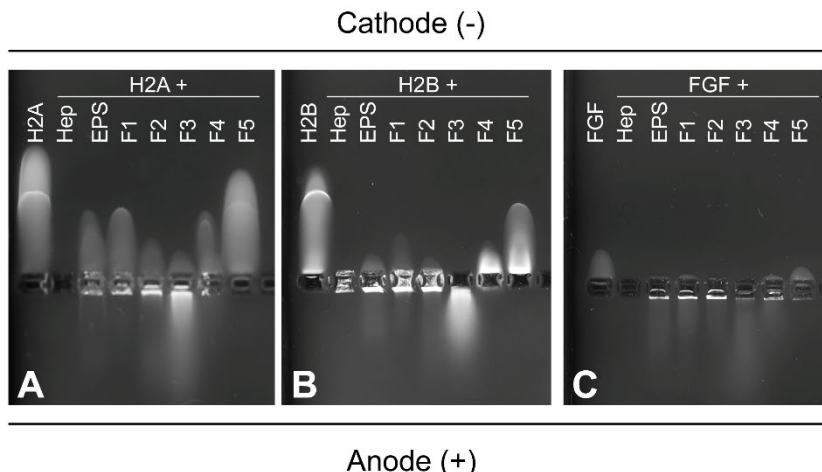


Figure 3.6. Relative quantification of nonulosonic acids in the extracted EPS and each fraction (F1-F5) based on the relative area signal of a spiked standard of Kdn. Correlating the spiked signal of Kdn with the signal of the detected nonulosonic acids species gives a relative estimation of the EPS and the fractions. The different nonulosonic acids found are NeuAc (white) and double acetylated variant (Ac2), PseAc2 or LegAc2 (gray).

To identify the types of nonulosonic acids (NulOs) and estimate their relative amounts in the EPS and its fractions, derivatization with DMB and mass spectrometry was used (Figure 3.6) (Tomás-Martínez et al., 2022). The analysis showed that the EPS and all fractions contain predominantly double acetylated NulO, likely the bacterial NulOs pseudaminic or legionaminic acid (PseAc<sub>2</sub> or LegAc<sub>2</sub>), which cannot be distinguished as they have the same molecular mass. However, other types of double acetylated NulOs could not be ruled out. Trace amounts of NeuAc were detected in the EPS across F1-F4, while a higher amount was detected in F5. Thus, NulOs were found in all fractions, with F1-F3 containing higher amount of NulOs than the original EPS and the other fractions.

### 3.3.3 Histone and FGF binding assay



Anode (+)

Figure 3.7. Protein binding assay. Histone H2A (A), H2B (B) and FGF (C) (5 µg) were incubated with heparin (Hep), EPS and the fractions (10 µg) and stained with Coomassie Blue. F1 (2815 - >14,320 kDa), F2 (439 - 2815 kDa), F3 (68 - 439 kDa), F4 (12 - 68 kDa) and F5 (<12 kDa).

Negatively charged polymers, such as heparin or polysialic acids, can be used to bind cationic proteins due to their high concentration of anionic groups. These polymers have been used for binding histones as the treatment of sepsis and as a column material for proteins purification (Ke et al., 1992; Nicolin Bolten et al., 2018; Seeger and Rinas, 1996). To explore the potential of the extracted EPS and the fractions for these applications, histones (H2A and H2B, which are the most abundant histones causing sepsis (Urban et al., 2009)) and the model protein FGF-2 binding tests were performed (Nicolin Bolten et al., 2018). These three cationic proteins were incubated with EPS and its fractions and their migration characteristics before and after incubation were compared (Figure 3.7). Cationic proteins migrate towards the cathode due to their positive charge. Upon interacting with the EPS, which is anionic, the charge will be neutralized resulting in a reduction of the migration towards the cathode.

Heparin is the most negatively charged natural polymer. After being incubated with the three proteins, the migration of all of them was completely stopped. Since heparin is a polysaccharide, when it binds with proteins, it may prevent Coomassie Blue staining of the proteins (Zlatina et al., 2017), thus leaving an empty spot on the gel. To compare, the EPS and the fractions demonstrated binding capacity to the three proteins, but was not as good as that of heparin. It was observed that after incubation with the EPS, the migration of H2A, H2B and FGF-2 towards the cathode was indeed reduced, indicating that there was interaction between the EPS and the proteins. The charge neutralization effect of EPS appeared to be stronger for H2B

than for H2A, judging from the length of the smear towards the cathode after the incubation. Probably the binding mechanism is not the same, and/or due to the difference of the cationic property between these two histones. In comparison, the migration of FGF-2 was completely stopped after incubation with the EPS. Likely, since FGF-2 itself already has relatively weak cationic property, binding with the anionic EPS can completely neutralize the charge.

Regarding the fractions, the tendency of their binding capacity to the three cationic proteins is similar: In general, all the five fractions can reduce the migration of the proteins by neutralizing the charge. Their binding capacity was increased from F1 to F3, but decreased from F4 to F5. F1 had roughly the same effect as the EPS, while F2 decreased the migration, and F3 almost stopped the migration of the proteins. It is interesting to see that the two higher aMW fractions (F1 and F2), which have significantly higher amount of sulfated glycoconjugates and the similar amount of NulOs as F3, did not neutralize the charge of the proteins as well as F3. Probably, besides the anionic sulfated glycoconjugates and NulOs in the EPS, other factors such as polymer conformation, molecular weight and other anionic groups might also be involved in protein-EPS interaction.

### 3.4 Discussion

#### 3.4.1 Sulfate and NulOs containing glycoconjugates are enriched in the high MW fractions of EPS extracted from seawater adapted AGS

Finding animal-free sources for the production of anionic polymers is of great interest for both medical and chemical applications (Delbarre-Ladrat et al., 2014; Nicolin Bolten et al., 2018). Producing anionic polymer by using bioreactors can be one sustainable alternative. In this study, the anionic polymers were successfully extracted from seawater-adapted aerobic granular sludge, and enriched by size exclusion chromatography fractionation. EPS fractions with aMW ranging from 68 - 14,320 kDa were enriched with sulfated glycoconjugates and/or NulOs containing glycoconjugates. They displayed application potential as a raw material in pharmaceutical and chemical field.

The presence of anionic polymers with sulfated groups and NulOs have been reported in granular sludge (Boleij et al., 2020; Bourven et al., 2015; Felz et al., 2020; Tomás-Martínez et al., 2022). The amount of sulfated glycoconjugates (chondroitin sulfate equivalent) in anammox EPS was around 6.9% and in aerobic granular sludge EPS was around 8.7% (Boleij et al., 2020; Felz et al., 2020). In the current research, it was found that the amount of sulfated glycoconjugates was about 2.0% of the extracted EPS, which is relatively lower than that was reported in literature. However, the molecular weight of the EPS fractions reported here are much higher in comparison to the literature value, *i.e.* >439 kDa in this research versus 12 kDa for anammox EPS (Boleij et al., 2020) and 10 - 50 kDa for fresh water aerobic granular sludge EPS (estimated from the elution time reported in the Supplementary Materials of Felz et al., 2020). Regarding NulOs containing glycoconjugates, the EPS fractions from a "*Ca. Accumulibacter phosphatis*" enriched culture might resemble more closely to what is found in this study (Tomás-Martínez et al., 2022). The high molecular weight fractions (5,500 - >15,000 kDa) reported by Tomás-Martínez et al. contained the majority of NulOs. However, it is unknown if those fractions have sulfated conjugates or not. Although a few factors might cause those differences, such as the microbial communities, the EPS extraction, separation methods and the operational conditions, it is expected that cultivation in seawater might contribute to the formation of EPS rich in anionic groups such as NulOs and sulfated groups.

Seawater environments have been shown in stimulating the production of glycoconjugates with anionic properties containing sulfated and carboxylic groups (*e.g.* NulOs) (Decho and Gutierrez, 2017). There are indications that marine bacteria possess NulOs production genes (Lewis et al., 2009; McDonald and Boyd, 2021). In addition, marine bacteria *Pseudomonas* and *Alteromonas* have been found to produce sulfated polysaccharides for protection and adhesion. The average

molecular weight of those polysaccharides are 330 kDa and 1000 kDa, respectively (Collicec-Jouault et al., 2012; Matsuda et al., 2003; Raguenes et al., 1996). Likely, microorganisms produce specific glycoconjugates to adapt to seawater condition. On the other hand, high molecular weight glycoconjugates produced under non-saline condition have been reported as well. For instance, capsular polysialic acid from *E. coli*K-235 can reach up to 1,000 kDa (Colley et al., 2014; Rohr & Troy, 1980). Whether seawater has an impact on the production of high molecular weight glycoconjugates containing both NulOs and sulfated groups should be a topic for further investigation.

#### 3.4.2 Binding with cationic proteins reveals potential applications for EPS extracted from seawater-adapted AGS

Anionic polymers have broad applications, *e.g.* heparin, a highly negatively charged biopolymer extracted from animal mucosa, can be used for medical treatment such as sepsis (Wildhagen et al., 2014) and for chemical applications such as column material for protein separation (Nicolin Bolten et al., 2018). In the current research, the extracted EPS and its fractions displayed binding capacity to histones H2A and H2B and FGF-2, which are model proteins related to these applications. This indicates that the EPS, especially the higher MW fractions, have great potential to be used as raw material for pharmaceutical and chemical applications.

Among the EPS fractions, F1, F2 and F3 bind the model proteins much stronger than F4 and F5. The most apparent difference is that F1-F3 are both heavily sulfated and contain more NulOs, which suggests that both of these two types of glycoconjugates are crucial for the binding of cationic proteins. Other factors such as molecular weight and charge density influence the binding capacity as well. In fact, it is reported that particular patterns of sulfation on the glycan chain and the linkage influences the binding strength of heparan sulfate with FGF and histones (Lindahl and Li, 2009; Meara et al., 2020; Mulloy, 2005). A decrease in molecular weight from a sulfated glycosaminoglycan analog show increased binding affinity to growth factors (Esposito et al., 2022). The chain length of polysialic acid affects the binding with histone (Zlatina et al., 2017). In addition, other anionic groups such as phosphate may play a role as well. Further research is needed to determine the exact mechanism of protein-EPS interaction, in order to manipulate the bioprocess towards producing anionic polymers which have higher binding capacity.

There are limited reports about the interaction between the anionic EPS and cationic proteins. Comparing to a recent study which looked into the interaction between histones and EPS fractions recovered from "*Ca. Accumulibacter phosphatis*" enriched culture, it was found that if the same ratio between the histone and EPS fraction is applied, the binding capacity of the EPS fractions recovered from seawater-adapted aerobic granular sludge, in this study, is higher (judging from the

length of the migration smear of histone-EPS complex) (Tomás-Martínez et al., 2022). This might be because the EPS fractions in the current study contain both sulfated and NulOs glycoconjugates. Moreover, the binding ability to both histones and FGF-2 protein of the EPS fractions in this research clearly displayed that the EPS recovered from seawater-adapted AGS is not only an attractive raw material in the medical field but also has the potential to be applied as a column material in the chemical field (Nicolin Bolten et al., 2018). It is worth pointing out that, different from animal-based biomolecules, microbial polymers can be produced in strictly controlled environments. This can reduce the variations in the quality of the product and contaminations with generally lower production costs (Sutherland, 1998).

### **3.4.3 Challenges in the characterization of glycoconjugates in EPS**

To produce EPS with specific application potential, studies are needed to elucidate their exact molecular structure, which is important to understand their function and identify the regulation pathways. The structural diversity of glycans and the unavailability of well-defined glycoconjugates standards make the in-depth EPS characterization challenging (Schäffer and Messner, 2017). In addition, glycan structures cannot be directly translated into a genetic template. External factors such as nutrient availability and environmental conditions can modify the structures as well (Varki et al., 2017a). Glycan structures and modifications (*e.g.* sulfate and NulOs) may vary depending on the environmental conditions (Poli et al., 2010; Schäffer and Messner, 2017). These structural variations can play a critical role in the bioactivity related to their applications. By studying the changes in EPS composition coupled with omics techniques under different environmental conditions, it might be possible to gain better understanding of the factors regulating their production and chemical structures. This information can ultimately contribute to an improved control of the EPS production in the bioreactor.

To understand which components of the EPS contribute to the protein binding ability, the structure of the EPS components needs to be revealed. For the glycoconjugates, specific labelling methods, such as microarrays, can be employed by targeting functional groups (Seviour et al., 2019). Additionally, a combination of separation methods, such as size exclusion chromatography, coupling with mass spectrometry may enable the structural elucidation of individual components (Zamfir et al., 2011). Finally, when the purified anionic glycoconjugates are obtained, protein-ligand studies are necessary to understand the specificity and affinity, and ultimately, clinical tests are required for evaluating the possible application in the medical field.

In summary, the current study has demonstrated that the EPS extracted from seawater-adapted AGS contain anionic polymers rich in NulOs and sulfated

glycoconjugates. The majority of these two glycoconjugates are located at the higher molecular weight EPS fractions. The binding of the EPS and its fractions with cationic histones and FGF-2 protein suggests their potential application as a raw material in pharmaceutical and chemical fields. EPS extracted from seawater-adapted AGS can be a valuable source for the recovery of biomolecules with interesting properties.

### Supplementary Materials

The Supplementary Materials of this chapter can be found at DOI 10.1007/s00253-023-12954-x

## References

Amann, R. I., Binder, B. J., Olson, R. J., Chisholm, S. W., Devereux, R., & Stahl, D. A. (1990). Combination of 16S rRNA-targeted oligonucleotide probes with flow cytometry for analyzing mixed microbial populations. *Applied and Environmental Microbiology*, 56(6), 1919–1925. <https://doi.org/10.1128/AEM.56.6.1919-1925.1990>

Angata, T., & Varki, A. (2002). Chemical diversity in the sialic acids and related  $\alpha$ -keto acids: An evolutionary perspective. *Chemical Reviews*, 102(2), 439–469. <https://doi.org/10.1021/cr000407m>

APHA. (1998). Standard methods for the examination of water and wastewater (20th ed.). American Public Health Association, American Water Works Association, Water Environment Federation, Washington, D.C., 1998.

Bassin, J. P., Pronk, M., Muyzer, G., Kleerebezem, R., Dezotti, M., & van Loosdrecht, M. C. M. (2011). Effect of elevated salt concentrations on the aerobic granular sludge process: Linking microbial activity with microbial community structure. *Applied and Environmental Microbiology*, 77(22), 7942–7953. <https://doi.org/10.1128/AEM.05016-11>

Bedini, E., Corsaro, M. M., Fernández-Mayoralas, A., & Iadonisi, A. (2019). Chondroitin, Dermatan, Heparan, and Keratan Sulfate: Structure and Functions. 187–233. [https://doi.org/10.1007/978-3-030-12919-4\\_5](https://doi.org/10.1007/978-3-030-12919-4_5)

Boleij, M., Kleikamp, H., Pabst, M., Neu, T. R., van Loosdrecht, M. C. M., & Lin, Y. (2020). Decorating the Anammox House: Sialic Acids and Sulfated Glycosaminoglycans in the Extracellular Polymeric Substances of Anammox Granular Sludge. *Environmental Science & Technology*, acs.est.9b07207. <https://doi.org/10.1021/acs.est.9b07207>

Bourven, I., Bachellerie, G., Costa, G., & Guibaud, G. (2015). Evidence of glycoproteins and sulphated proteoglycan-like presence in extracellular polymeric substance from anaerobic granular sludge. <Http://Dx.Doi.Org/10.1080/09593330.2015.1034186>, 36(19), 2428–2435. <https://doi.org/10.1080/09593330.2015.1034186>

Chen, L. M., de Bruin, S., Pronk, M., Sousa, D. Z., van Loosdrecht, M. C. M., & Lin, Y. (2023). Sialylation and Sulfation of Anionic Glycoconjugates Are Common in the Extracellular Polymeric Substances of Both Aerobic and Anaerobic Granular Sludges. *Environmental Science and Technology*, 57(35), 13217–13225. <https://doi.org/https://doi.org/10.1021/acse.est.2c09586>

Collicec-Jouault, S., Bavington, C., & Delbarre-Ladrat, C. (2012). Heparin-like entities from marine organisms. *Handbook of Experimental Pharmacology*, 207(207), 423–449. [https://doi.org/10.1007/978-3-642-23056-1\\_19](https://doi.org/10.1007/978-3-642-23056-1_19)

Crocetti, G. R., Hugenholtz, P., Bond, P. L., Schuler, A., Keller, J., Jenkins, D., & Blackall, L. L. (2000). Identification of polyphosphate-accumulating organisms and design of 16S rRNA-directed probes for their detection and quantitation. *Applied and Environmental Microbiology*, 66(3), 1175–1182. <https://doi.org/10.1128/AEM.66.3.1175-1182.2000>

Daims, H., Brühl, A., Amann, R., Schleifer, K. H., & Wagner, M. (1999). The Domain-specific Probe EUB338 is Insufficient for the Detection of all Bacteria: Development and Evaluation of a more Comprehensive Probe Set. *Systematic and Applied Microbiology*, 22(3), 434–444. [https://doi.org/10.1016/S0723-2020\(99\)80053-8](https://doi.org/10.1016/S0723-2020(99)80053-8)

de Graaff, D. R., Felz, S., Neu, T. R., Pronk, M., van Loosdrecht, M. C. M., & Lin, Y. (2019). Sialic acids in the extracellular polymeric substances of seawater-adapted aerobic granular sludge. *Water Research*, 343–351. <https://doi.org/10.1016/j.watres.2019.02.040>

De Jong, J. G. N., Heijs, W. M. J., & Wevers, R. A. (1994). Mucopolysaccharides screening: Dimethylmethylene blue versus Alcian blue. *Annals of Clinical Biochemistry*, 31(3), 267–271. <https://doi.org/10.1177/000456329403100309>

Decho, A. W., & Gutierrez, T. (2017). Microbial extracellular polymeric substances (EPSs) in ocean systems. *Frontiers in Microbiology*, 8(MAY), 922. <https://doi.org/10.3389/fmicb.2017.00922>

Delbarre-Ladrat, C., Sinquin, C., Lebellenger, L., Zykwińska, A., & Colliec-Jouault, S. (2014). Exopolysaccharides produced by marine bacteria and their applications as glycosaminoglycan-like molecules. *Frontiers in Chemistry*, 2(OCT), 85. <https://doi.org/10.3389/FCHEM.2014.00085>

Elahinik, A., Haarsma, M., Abbas, B., Pabst, M., Xevgenos, D., van Loosdrecht, M. C. M., & Pronk, M. (2022). Glycerol conversion by aerobic granular sludge. *Water Research*, 227, 119340. <https://doi.org/10.1016/J.WATRES.2022.119340>

Esposito, F., Vessella, G., Sinquin, C., Traboni, S., Iadonisi, A., Colliec-Jouault, S., Zykwińska, A., & Bedini, E. (2022). Glycosaminoglycan-like sulfated polysaccharides from *Vibrio diabolicus* bacterium: Semi-synthesis and characterization. *Carbohydrate Polymers*, 283, 119054. <https://doi.org/10.1016/J.CARBPOL.2021.119054>

Felz, S., Al-Zuhairy, S., Aarstad, O. A., van Loosdrecht, M. C. M., & Lin, Y. M. (2016). Extraction of structural extracellular polymeric substances from aerobic granular sludge. *Journal of Visualized Experiments*, 2016(115), 54534. <https://doi.org/10.3791/54534>

Felz, S., Neu, T. R., van Loosdrecht, M. C. M., & Lin, Y. (2020). Aerobic granular sludge contains Hyaluronic acid-like and sulfated glycosaminoglycans-like polymers. *Water Research*, 169. <https://doi.org/10.1016/j.watres.2019.115291>

Flemming, H. C., & Wingender, J. (2010). The biofilm matrix. In *Nature Reviews Microbiology* (Vol. 8, Issue 9, pp. 623–633). Nature Publishing Group. <https://doi.org/10.1038/nrmicro2415>

Flowers, J. J., He, S., Yilmaz, S., Noguera, D. R., & McMahon, K. D. (2009). Denitrification capabilities of two biological phosphorus removal sludges dominated by different 'Candidatus Accumulibacter' clades. *Environmental Microbiology Reports*, 1(6), 583–588. <https://doi.org/10.1111/j.1758-2229.2009.00090.X>

Ke, Y., Wilkinson, M. C., Fernig, D. G., Smith, J. A., Rudland, P. S., & Barraclough, R. (1992). A rapid procedure for production of human basic fibroblast growth factor in *Escherichia coli* cells. *Biochimica et Biophysica Acta (BBA)-Gene Structure and Expression*, 1131(3), 307–310.

Kleikamp, H. B. C., Lin, Y. M., McMillan, D. G. G., Geelhoed, J. S., Naus-Wiezer, S. N. H., Van Baarlen, P., Saha, C., Louwen, R., Sorokin, D. Y., Van Loosdrecht, M. C. M., & Pabst, M. (2020). Tackling the chemical diversity of microbial nonulosonic acids—a universal large-scale survey approach. In *Chemical Science* (Vol. 11, Issue 11, pp. 3074–3080). Royal Society of Chemistry. <https://doi.org/10.1039/c9sc06406k>

Lee, W. K., & Ho, C. L. (2022). Ecological and evolutionary diversification of sulphated polysaccharides in diverse photosynthetic lineages: A review. *Carbohydrate Polymers*, 277, 118764. <https://doi.org/10.1016/J.CARBPOL.2021.118764>

Lewis, A. L., Desa, N., Hansen, E. E., Knirel, Y. A., Gordon, J. I., Gagneux, P., Nizet, V., & Varki, A. (2009). Innovations in host and microbial sialic acid biosynthesis revealed by phylogenomic prediction of nonulosonic acid structure. *Proceedings of the National Academy of Sciences of the United States of America*, 106(32), 13552–13557. <https://doi.org/10.1073/pnas.0902431106>

Lindahl, U., & Li, J. ping. (2009). Chapter 3 Interactions Between Heparan Sulfate and Proteins—Design and Functional Implications. *International Review of Cell and Molecular Biology*, 276(C), 105–159. [https://doi.org/10.1016/S1937-6448\(09\)76003-4](https://doi.org/10.1016/S1937-6448(09)76003-4)

Matsuda, M., Yamori, T., Naitoh, M., & Okutani, K. (2003). Structural revision of sulfated polysaccharide B-1 isolated from a marine *Pseudomonas* species and its cytotoxic activity against human cancer cell lines. *Marine Biotechnology*, 5(1), 13–19. <https://doi.org/10.1007/S10126-002-0046-5/METRICS>

McCarthy, C. P., Vaduganathan, M., Solomon, E., Sakhija, R., Piazza, G., Bhatt, D. L., Connors, J. M., & Patel, N. K. (2020). Running thin: implications of a heparin shortage. *The Lancet*, 395(10223), 534–536. [https://doi.org/10.1016/S0140-6736\(19\)33135-6](https://doi.org/10.1016/S0140-6736(19)33135-6)

McDonald, N. D., & Boyd, E. F. (2021). Structural and Biosynthetic Diversity of Nonulosonic Acids (Nulos) That Decorate Surface Structures in Bacteria. *Trends in*

### 3. Anionic extracellular polymeric substances extracted from seawater-adapted aerobic granular sludge

Microbiology, 29(2), 142. <https://doi.org/10.1016/J.TIM.2020.08.002>

Meara, C. H. O., Coupland, L. A., Kordbacheh, F., Quah, B. J. C., Chang, C. W., Simon Davis, D. A., Bezos, A., Browne, A. M., Freeman, C., Hammill, D. J., Chopra, P., Pipa, G., Madge, P. D., Gallant, E., Segovis, C., Dulhunty, A. F., Arnolda, L. F., Mitchell, I., Khachigian, L. M., ... Parish, C. R. (2020). Neutralizing the pathological effects of extracellular histones with small polyanions. *Nature Communications* 2020 11:1, 11(1), 1-17. <https://doi.org/10.1038/s41467-020-20231-y>

Mulloy, B. (2005). The specificity of interactions between proteins and sulfated polysaccharides. *Anais Da Academia Brasileira de Ciencias*, 77(4), 651-664.

Nanchariah, Y. V., & Sarvajith, M. (2019). Aerobic granular sludge process: a fast growing biological treatment for sustainable wastewater treatment. In *Current Opinion in Environmental Science and Health* (Vol. 12, pp. 57-65). Elsevier B.V. <https://doi.org/10.1016/j.coesh.2019.09.011>

Nicolin Bolten, S., Rinas, U., & Schepers, T. (2018). Heparin: role in protein purification and substitution with animal-component free material. *Applied Biochemistry and Biotechnology*. <https://doi.org/10.1007/s00253-018-9263-3>

Poli, A., Anzelmo, G., & Nicolaus, B. (2010). Bacterial Exopolysaccharides from Extreme Marine Habitats: Production, Characterization and Biological Activities. *Marine Drugs* 2010, Vol. 8, Pages 1779-1802, 8(6), 1779-1802. <https://doi.org/10.3390/MD8061779>

Pronk, M., de Kreuk, M. K., de Bruin, B., Kamminga, P., Kleerebezem, R., & van Loosdrecht, M. C. M. (2015). Full scale performance of the aerobic granular sludge process for sewage treatment. *Water Research*, 84, 207-217. <https://doi.org/10.1016/j.watres.2015.07.011>

Raguenes, G., Pignet, P., Gauthier, G., Peres, A., Christen, R., Rougeaux, H., Barbier, G., & Guezennec, J. (1996). Description of a new polymer-secreting bacterium from a deep-sea hydrothermal vent, *Alteromonas macleodii* subsp. *fijiensis*, and preliminary characterization of the polymer. *Applied and Environmental Microbiology*, 62(1), 67-73. <https://doi.org/10.1128/AEM.62.1.67-73.1996>

Schäffer, C., & Messner, P. (2017). Emerging facets of prokaryotic glycosylation. *FEMS Microbiology Reviews*, 41(1), 49. <https://doi.org/10.1093/FEMSRE/FUW036>

Scott, J. E., & Dorling, J. (1965). Differential staining of acid glycosaminoglycans (mucopolysaccharides) by Alcian blue in salt solutions. *Histochemistry* 1965 5:3, 5(3), 221-233. <https://doi.org/10.1007/BF00306130>

Seeger, A., & Rinas, U. (1996). Two-step chromatographic procedure for purification of basic fibroblast growth factor from recombinant *Escherichia coli* and characterization of the equilibrium parameters of adsorption. *Journal of Chromatography A*, 746(1), 17-24. [https://doi.org/10.1016/0021-9673\(96\)00286-5](https://doi.org/10.1016/0021-9673(96)00286-5)

Seviour, T., Derlon, N., Dueholm, M. S., Flemming, H.-C., Girbal-Neuhauser, E., Horn, H., Kjelleberg, S., van Loosdrecht, M. C. M., Lotti, T., Malpei, M. F., Nerenberg, R., Neu, T. R., Paul, E., Yu, H., & Lin, Y. (2019). Extracellular polymeric substances of biofilms: Suffering from an identity crisis. *Water Research*, 151, 1-7. <https://doi.org/10.1016/j.watres.2018.11.020>

Sutherland, I. W. (1998). Novel and established applications of microbial polysaccharides. *Trends in Biotechnology*, 16(1), 41-46. [https://doi.org/10.1016/S0167-7799\(97\)01139-6](https://doi.org/10.1016/S0167-7799(97)01139-6)

Tomás-Martínez, S., Chen, L. M., Pabst, M., Weissbrodt, D. G., van Loosdrecht, M. C. M., & Lin, Y. (2022). Enrichment and application of extracellular nonulosonic acids containing polymers of *Accumulibacter*. *Applied Microbiology and Biotechnology*, 1-11.

Tomás-Martínez, S., Kleikamp, H. B. C., Neu, T. R., Pabst, M., Weissbrodt, D. G., van Loosdrecht, M. C. M., & Lin, Y. (2021). Production of nonulosonic acids in the extracellular polymeric substances of "Candidatus Accumulibacter phosphatis." *Applied Microbiology and Biotechnology*, 105(8), 3327-3338. <https://doi.org/10.1007/s00253-021-11249-3>

Urban, C. F., Ermert, D., Schmid, M., Abu-Abed, U., Goosmann, C., Nacken, W., Brinkmann, V.,

Jungblut, P. R., & Zychlinsky, A. (2009). Neutrophil Extracellular Traps Contain Calprotectin, a Cytosolic Protein Complex Involved in Host Defense against *Candida albicans*. *PLOS Pathogens*, 5(10), e1000639. <https://doi.org/10.1371/JOURNAL.PPAT.100639>

Varki, A., Cummings, R. D., Esko, J. D., Stanley, P., Hart, G. W., Aebi, M., Darvill, A. G., Kinoshita, T., Packer, N. H., Prestegard, J. H., Schnaar, R. L., & Seeberger, P. H. (2017a). Essentials of Glycobiology. Cold Spring Harbor (NY), 823.

Varki, A., Schnaar, R. L., & Schauer, R. (2017b). Sialic Acids and Other Nonulosonic Acids. <https://doi.org/10.1101/GLYCOBIOLOGY.3.E.015>

Vishniac, W., & Santer, M. (1957). The thiobacilli. *Bacteriological Reviews*, 21(3), 195–213. <https://doi.org/10.1128/BR.21.3.195-213.1957>

Wildhagen, K. C. A. A., García De Frutos, P., Reutelingsperger, C. P., Schrijver, R., Areésté, C., Areésté, A., Ortega-G'omez, A., Deckers, N. M., Coenraad Hemker, H., Soehnlein, O., & Nicolaes, G. A. F. (2014). Nonanticoagulant heparin prevents histone-mediated cytotoxicity in vitro and improves survival in sepsis. <https://doi.org/10.1182/blood-2013-2013-500000>

Xue, W., Zeng, Q., Lin, S., Zan, F., Hao, T., Lin, Y., van Loosdrecht, M. C. M., & Chen, G. (2019). Recovery of high-value and scarce resources from biological wastewater treatment: Sulfated polysaccharides. *Water Research*, 163, 114889.

Zamfir, A. D., Flangea, C., Sisu, E., Seidler, D. G., & Peter-Katalinić, J. (2011). Combining size-exclusion chromatography and fully automated chip-based nanoelectrospray quadrupole time-of-flight tandem mass spectrometry for structural analysis of chondroitin/dermatan sulfate in human decorin. *ELECTROPHORESIS*, 32(13), 1639–1646. <https://doi.org/10.1002/ELPS.201100094>

Zheng, C. H., & Levenston, M. E. (2015). Fact versus artifact: Avoiding erroneous estimates of sulfated glycosaminoglycan content using the dimethylmethylen blue colorimetric assay for tissue-engineered constructs. *European Cells and Materials*, 29, 224–236. <https://doi.org/10.22203/eCM.v029a17>

Zlatina, K., Lütteke, T., & Galuska, S. P. (2017). Individual impact of distinct polysialic acid chain lengths on the cytotoxicity of histone H1, H2A, H2B, H3 and H4. *Polymers*, 9(12), 1–13. <https://doi.org/10.3390/polym9120720>



# Alterations of glycan composition in aerobic granular sludge during the adaptation to seawater conditions

4

## Abstract

Bacteria can synthesize a diverse array of glycans, being found attached to proteins and lipids or as loosely associated polysaccharides to the cells. The major challenge in glycan analysis in environmental samples lies in developing high-throughput and comprehensive characterization methodologies to elucidate the structure and monitor the change of the glycan profile, especially in protein glycosylation. To this end, in the current research, the dynamic change of the glycan profile of a few extracellular polymeric substance (EPS) samples was investigated by high-throughput lectin microarray and mass spectrometry, as well as sialylation and sulfation analysis. Those EPS were extracted from aerobic granular sludge collected at different stages during its adaptation to the seawater condition. It was found that there were glycoproteins in all of the EPS samples. In response to the exposure to seawater, the amount of glycoproteins and their glycan diversity displayed an increase during adaptation, followed by a decrease once the granules reached a stable state of adaptation. Information generated sheds light on the approaches to identify and monitor the diversity and dynamic alteration of the glycan profile of the EPS in response to environmental stimuli.

## Published as:

Chen, L. M., Keisham, S., Tateno, H., Ede, J. van, Pronk, M., Loosdrecht, M. C. M. van, & Lin, Y. (2023). Alterations of Glycan Composition in Aerobic Granular Sludge during the Adaptation to Seawater Conditions. *ACS ES&T Water*. <https://doi.org/10.1021/ACSESTWATER.3C00625>

## 4.1 Introduction

Carbohydrates constitute the most structurally diverse class of natural products and can serve many functions in cells and organisms (Reid et al., 2012). Glycans refer to carbohydrate chains that can be free or attached to proteins or lipids to form simple or complex glycoconjugates (Reily et al., 2019). Glycans participate in almost every biological process (Bertozzi and Sasisekharan, 2009). In addition to forming important structural features, the glycans of glycoconjugates modulate or mediate a wide variety of functions, such as cell adhesion, recognition, receptor activation, or signal transduction in animal and plant cells (Herget et al., 2008).

Bacteria can synthesize a diverse array of glycans, being found attached to proteins and lipids, or as loosely associated polysaccharides to the cells (Reid et al., 2012). The precise role of these glycans in bacterial symbiosis and cell–cell and cell–environment interactions is just beginning to be understood. Most of bacterial glycans are located at the surface of cells, deposited in the extracellular space and attached to soluble signaling molecules (Reid et al., 2012). In this respect, when biofilm is formed, as the extracellular polymeric substances (EPS) are the components that form the matrix wherein the microorganisms are embedded, bacterial glycans are one of the important components of the EPS. However, EPS are frequently reported consisting of proteins (structural proteins and enzymes), polysaccharides, nucleic acids, and lipids, (Flemming and Wingender, 2010) which overlooks the possibility that proteins and polysaccharides and lipids and polysaccharides in EPS may present not only as separate components but also in various forms of glycoconjugates. Moreover, the frequently used EPS characterization methods (*e.g.*, colorimetric methods) only allow for characterization of the separate classes of molecules but provide little insight into the glycoconjugates.

At present, one of the proven effective methods for EPS glycoconjugate analysis is fluorescence lectin bar-coding (FLBC) (Neu and Kuhlicke, 2017). These lectins can bind to specific carbohydrate regions, allowing for the screening of glycoconjugates in a hydrated biofilm matrix. This method has been successfully applied to the analysis of a few different types of biomass, such as saline aerobic granular sludge, anaerobic granular sludge, anammox granular sludge, and “*Candidatus Accumulibacter phosphatis*” enrichment (Boleij et al., 2020; Gagliano et al., 2018; Tomás-Martínez et al., 2021). Glycans, with sugar residues including sialic acids, mannose, galactose, N-acetyl-galactosamine, and N-acetyl-glucosamine, were found in the EPS of those biomasses (Bourven et al., 2015; de Graaff et al., 2019). It is worth pointing out that information provided by this method only reflects the composition of the carbohydrates; it is still unclear whether these carbohydrates are attached to proteins, lipids, or simply as polysaccharides. Hence, to unravel the complete glycan

profile of the EPS in biofilms, it is significantly important to establish methodologies to identify glycoconjugates such as glycoproteins and glycolipids.

Protein glycosylation is the covalent attachment of single sugars or glycans to select residues of proteins. It is one of the common yet most complex post-translational modifications. Protein glycosylation has profound effects on protein function and stability (Eichler, 2019). Historically, glycosylation of proteins was used to be considered to occur exclusively in eukaryotes; only recently it is accepted that prokaryotes can also perform (complex) protein glycosylation (Messner, 2009). The glycosylation of prokaryotic proteins is far less studied, and most of the research focuses on specific pathogenic bacteria. Regarding a few studies on the glycoproteins in environmental samples, such as the glycoproteins in the EPS of anammox granular sludge, mass spectrometry was performed (Boleij et al., 2018). While this approach enables deciphering the structure of glycans derived from glycoproteins, it is not amenable to adaptation to a high- throughput platform (Hirabayashi, 2004). This brings a severe bottleneck in monitoring the diversity and dynamic alteration of the glycan profile. Especially, given that such diverse structures are important interfaces between bacteria and the environment. Thus, the major challenge in glycan research in the environmental field lies in developing high-throughput and comprehensive characterization methodologies to elucidate the structure and monitor the change of glycosylation.

To this end, in the current research, the dynamic change of the glycan profile of a few EPS samples was monitored by gas chromatography–mass spectrometry (GC-MS) and high- throughput lectin microarray as well as the sialylation and sulfation analysis. Those EPS samples were extracted from aerobic granular sludge collected at different stages during its adaptation to seawater conditions. The information generated sheds light on the approaches to identify and monitor the diversity and dynamic alteration of the glycan profile of the biomass in response to environmental stimuli.

## 4.2 Material and Methods

### 4.2.1 Reactor operation

Seawater-adapted aerobic granular sludge was cultivated in a 2.8 L bubble column (6.5 cm diameter) as a sequencing batch reactor (SBR) adapted from (de Graaff et al., 2019). The reactor was inoculated with aerobic granular sludge cultivated in a lab-scale reactor with glycerol as the carbon source under freshwater condition (Elahinik et al., 2022). The temperature was controlled at 20°C, and the pH was controlled at pH  $7.3 \pm 0.1$  by dosing 1.0 M NaOH or 1.0 M HCl. The DO was controlled at 2 mg of O<sub>2</sub>/mL (80% saturation). Reactor cycles consisted of 60 min of anaerobic feeding, 170 min of aeration, 5 min of settling, and 5 min of effluent withdrawal.

Artificial seawater was gradually introduced for 13 days until a concentration of 35 g/L was reached.

To investigate the glycan profile of the extracellular polymeric substances of aerobic granules during their adaptation to seawater, granules were collected at three different time slots: t0, t18, and t30. The sample at t0 refers to the inoculum. The sample at t18 was collected 18 days after the reactor started (5 days after the seawater concentration in the reactor achieved 35 g/L; the SRT in the reactor was not controlled). The sample at t30 was taken 30 days after the reactor start (the SRT in the reactor was controlled as 13.6 days), representing a relatively stable state of seawater-adapted granules.

The organic and ash fractions of the biomass were determined according to the standard methods after washing the granules three times with demi-water (APHA, 1998). For EPS extraction and characterization, the granules were lyophilized immediately and stored at room temperature.

4

#### 4.2.2 Microbial Community Analysis by Fluorescent In Situ Hybridization (FISH)

To investigate the microbial community, fluorescent in situ hybridization (FISH) was performed. The handling, fixation, and staining of samples were performed as described in Bassin et al. (2011). A mixture of EUB338, 13 EUB338-II, and EUB338-III probes were used to stain all of the bacteria (Amann et al., 1990; Daims et al., 1999). A mixture of PAO462, PAO651, and PAO846 probes (PAOmix) was used for visualizing polyphosphate accumulating organisms (PAOs) (Amann et al., 1990). A mixture of GAOQ431 and GAOQ989 probes (GAOmix) was used to target glycogen accumulating organisms (GAOs) (Crocetti et al., 2000). The samples were examined with a Zeiss Axioplan 2 epifluorescence microscope equipped with filter sets 26 (bp 575e625/FT645/bp 660e710), 20 (bp 546/12/FT560/bp 575e640), and 17 (bp 485/20/FT 510/bp 5515e565) for Cy5, Cy3, and fluos, respectively.

#### 4.2.3 EPS Characterization

##### Glycosyl composition analysis by TMS Method

Glycosyl composition analysis of the extracted EPS was performed at the Complex Carbohydrate Research Center (CCRC, University of Georgia) by combined GC/MS of the O-trimethylsilyl (TMS) derivatives of the mono- saccharide methyl glycosides produced from the sample by acidic methanolysis. These procedures were carried out as previously described in Santander et al. (2013). In brief, lyophilized EPS aliquots of 300 µg were added to separate tubes with 20 µg of inositol as the internal standard. Methyl glycosides were then prepared from the dry sample following the mild acid treatment by methanolysis in 1 M HCl in methanol at 80°C (16 h). The samples were re-N-acetylated with 10 drops of methanol, 5 drops of pyridine, and 5 drops of acetic anhydride and were kept at room temperature for 30 min (for

detection of amino sugars). The sample was then per-*o*-trimethylsilylated by treatment with Tri-Sil (Pierce) at 80°C (30 min). These procedures were carried out as described by Merkle & Poppe (1994). GC/MS analysis of the per-*o*-trimethylsilyl methyl glycosides was performed on an AT 7890A gas chromatograph interfaced to a 5975B MSD mass spectrometer, using a Supelco EC-1 fused silica capillary column (30 m × 0.25 mm ID) and the temperature gradient shown in Table 4.1.

Table 4.1. Temperature Program for GC-MS Analysis for the TMS Method

	rate (°C/min)	value (°C)	hold time (min)	run time (min)
initial		80	2	2
ramp 1	20	140	2	7
ramp 2	2	200	0	37
ramp 3	30	250	5	43.7

### Sulfated glycosaminoglycan assay

Detection and quantification of sulfated glycosaminoglycans (sulfated GAGs) in the extracted EPS were performed with the Blyscan sulfated glycosaminoglycan assay (Biocolor, Carrickfergus, UK), according to the manufacturer's instructions. Samples (2–5 mg) were digested with 1 mL of papain protein digestion solution at 65°C for 3h at 300 rpm (Sigma-Aldrich, Zwijndrecht, Netherlands). The supernatant was recovered after centrifugation at 10,000g for 10 min. 50 µL of sample was then added to 1 mL of 1,9-dimethyl-methylene blue (DMMB) dye reagent. Sulfated GAGs positive components bind and precipitate with the dye and are subsequently isolated and resolubilized. The concentration of sulfated GAGs was measured with a multimode plate reader at 656 nm (TECAN Infinite M200 PRO, Switzerland) as chondroitin sulfate equivalents. Lastly, the distribution of N-linked and O-linked sulfates in the samples was measured by performing nitrous acid cleavage according to the manufacturer's instructions prior to sulfated GAGs quantification.

### Nonulosonic Acid Analysis with Mass Spectroscopy

Detection of nonulosonic acids (Nulos) in the extracted EPS was done according to the approach described by Kleikamp et al. (2020). In short, lyophilized EPS fractions were hydrolyzed by 2M acetic acid for 2h at 80°C and dried with a Speed Vac concentrator. The released Nulos were labeled using DMB (1,2-diamino-4,5-methylenedioxybenzene dihydrochloride) for 2.5 h at 55°C and analyzed by reverse phase chromatography Orbitrap mass spectrometry (QE plus Orbitrap, ThermoFisher Scientific, Bleiswijk, Netherlands).

#### 4.2.4 Glycan Profiling of Glycoproteins by Lectin Microarray Analysis.

High-density lectin microarray was generated according to the method described (Tateno et al., 2011). 0.4 µg of EPS was labeled with Cy3-N-hydroxysuccinimide ester (GE Health-care), and excess Cy3 was removed with Sephadex G-25 desalting columns (GE Healthcare). Cy3-labeled proteins were diluted with probing buffer [25 mM tris-HCl (pH 7.5), 140 mM NaCl, 2.7 mM KCl, 1 mM CaCl<sub>2</sub>, 1 mM MnCl<sub>2</sub>, and 1% Triton X-100] to 0.5 µg/mL and were incubated with the lectin microarray at 20°C overnight. The lectin microarray was washed three times with probing buffer, and fluorescence images were captured using a Bio-Rex scan 200 evanescent-field-activated fluorescence scanner (Rexxam Co. Ltd, Kagawa, Japan).

The obtained signals were mean-normalized, and ANOVA test was performed using IBM SPSS Statistics 24.0 to identify lectins with significantly different intensities between the three samples. Heatmap of the lectins with significant intensities ( $p < 0.05$ ) was performed using the R package Pheatmap (version 1.0.12) on RStudio (version 4.2.2). Student's t test was performed using IBM SPSS for statistical analysis between EPSt18 and EPSt30 to obtain the t-value.

### 4.3 Results

#### 4.3.1 Reactor operation and Microbial Community in seawater-adapted aerobic granular sludge

An aerobic granular sludge reactor was inoculated with granular sludge from the other lab reactor (with glycerol as a carbon source (t0)). Acetate was used as a carbon source to enrich specifically for phosphate accumulating organisms (PAOs) (de Graaff et al., 2019). The salinity in the reactor was stepwise increased until 35 g/L of seawater was reached. After 7 days, complete acetate and phosphate removal were observed. Granular sludge samples were collected on the 18th and 30th days after the start of the reactor. The typical reactor profiles of t0, t18, and t30 show similar trends in acetate uptake and phosphate removal (Figure 4.1). During the anaerobic phase, acetate was taken up and a phosphate release was found to be up to 2.72 Pmmol/L. The reactor's biomass concentration was roughly constant at around 7 g VSS/L with a VSS/TSS of around 76%. The morphology of the granules is shown in Figure 4.1. No visual differences were observed among the three samples.

According to the FISH analysis, PAO was the dominant microorganism in the three granule samples (Figure 4.2). While the abundance of glycogen accumulating organisms (GAOs) was much lower than that of PAO. Comparatively, the abundance of GAO in granules collected at t18 (Figure 4.2A) seemed relatively higher than that in granules collected at t0 and t30 (Figure 4.2B, C). It was also observed that the size

#### 4. Alterations of glycan composition in aerobic granular sludge during the adaptation to seawater conditions

of the microcolony of PAO was much bigger in granules at t30 than in granules at t0 and t18.

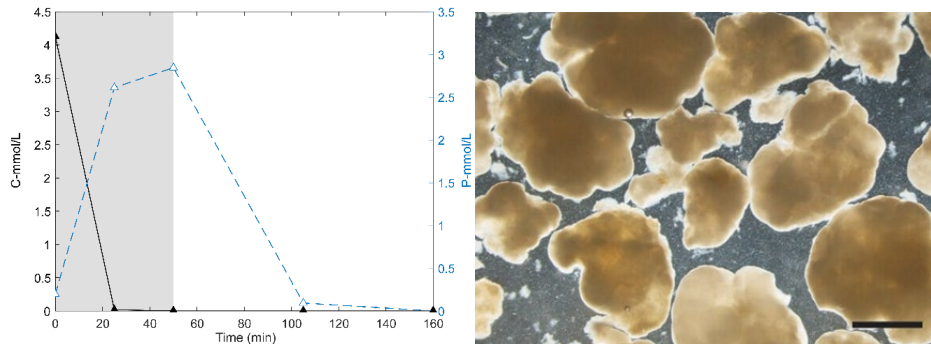


Figure 4.1. Left: reactor profile of a typical cycle of seawater-adapted aerobic granular sludge (t30). The uptake of the carbon source, acetate, is expressed in C-mmol/L indicated with black-filled triangles. The release and uptake of phosphate are indicated with blue open triangles. The anaerobic phase is indicated by the shaded area (50 min), followed by the aerobic phase (110 min). Right: the morphology of granules. No visual differences were observed among the three samples. The scale bar is 1 mm.

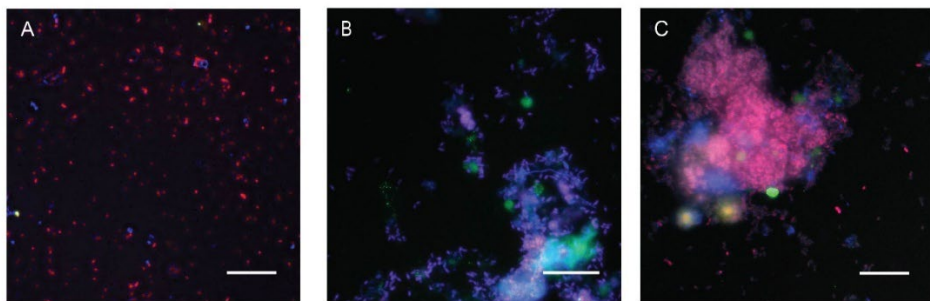


Figure 4.2. Fluorescence in situ hybridization (FISH) images of aerobic granular sludge (AGS) stained by EUB338 (Cy5/blue, eubacteria), PAO651 (A) or PAOmix (B and C, Cy3/red), and GAO (fluos/green). Magenta color is an overlap between eubacteria (blue) and PAOmix (red). Scale bar equals 20  $\mu$ m. A: inoculum (t0); B: granules 18 days after inoculation (t18); and C: granules 30 days after inoculation (t30).

#### 4.3.2 EPS Extraction and Characterization

The extracted EPS has the same yellow color as the aerobic granules. The yield of EPS at t0, t18, and t30 was  $308 \pm 117$ ,  $385 \pm 82$  mg/g, and  $640 \pm 42$  (VSS ratio), with VS/TS ratios of 69, 70, and 86%, respectively. Apparently, during the adaptation to seawater conditions, more EPS, which can be extracted with NaOH, was produced.

#### Glycosyl Composition

The glycosyl composition of the extracted EPS is listed in Table 4.2, and the GC-MS chromatogram is included in the Supplementary Materials (Figure S1-S3). The total carbohydrate amount increased from EPS<sub>t0</sub> to EPSt<sub>30</sub>. Glucose, rhamnose, mannose, fucose, and galactose were found to be the main components of all samples. The

relative molar ratio of each sugar monomer varied among samples, with glucose as the most abundant monomer. Xylose and N-acetyl glucosamine were also found in the seawater-cultured samples, while only the inoculum contained arabinose. Additionally, an unknown sugar was detected in all of the samples at about 29.3 min (marked by asterisk\* in GC spectrum in the Supplementary Materials Figure S1-S3). Thus, based on sugar composition, there is a clear difference between the inoculum and seawater-grown granular sludge EPS.

Table 4.2. Glycosyl Composition of the Extracted EPS (Relative Mole and Total Carbohydrate Percentage. Monomer Symbol Nomenclature is based on Varki et al. (2015)).

4

Glycosyl Residue (with symbol nomenclature)	EPS <sub>t0</sub>	EPS <sub>t18</sub>	EPS <sub>t30</sub>
Arabinose (Ara 	3.5	n.d.	n.d.
Rhamnose (Rha 	19.8	13.7	14.4
Fucose (Fuc 	2.8	1.9	1.4
Xylose (Xyl 	n.d.	1.0	0.9
Mannose (Man 	3.9	2.7	2.8
Galactose (Gal 	1.3	0.5	1.5
Glucose (Glc 	68.6	77.4	74.2
N-Acetylglucosamine (GlcNAc 	n.d.	2.8	4.8
Total carbohydrate (%EPS)	1.9	3.9	6.5

### **NulOs and Sulfated Glycosaminoglycan-like Polymers**

Glycoconjugate modifications with acidic groups such as sulfate (sulfation) and/or sialic acid (sialylation) on the glycans are common phenomena in the extracellular matrix of eukaryotes. Recently, these two glycoconjugate modifications (sulfation and sialylation) were found to be widely distributed in the EPS of granular sludge as well (Chen et al., 2023). In order to investigate the influence of seawater conditions on sulfation and sialylation, the same analysis was performed on the extracted EPS samples.

To identify which kinds of nonulosonic acids (NulOs, sialic acids is one type of nonulosonic acids) are present in the granules, mass spectrometry (MS) was applied. NulOs were detected in the form of N-acetyl neuraminic acid (NeuAc) and pseudaminic acid/legionaminic acid (Pse/Leg), which are also referred to as bacterial sialic acids in the literature. These two monomers have the same molecular weight and cannot be differentiated by MS). Hence, there are two different kinds of NulOs in all of the EPS samples. These NulOs could be part of glycoconjugates, including glycolipids, glycoproteins, and capsular polysaccharides.

The presence of sulfated GAGs was investigated by using the DMMB assay. The following sulfated GAGs, either still attached to the peptide/protein core or as free chains, can be assayed: chondroitin sulfates (4- and 6-sulfated), keratan sulfates (alkali sensitive and resistant forms), dermatan sulfate, and heparan sulfates (including heparins). The total content of sulfated GAGs measured in EPS<sub>t0</sub>, EPS<sub>t18</sub>, and EPS<sub>t30</sub>, was 20.3  $\pm$  0.3, 16.6  $\pm$  0.1, and 25.3  $\pm$  0.2 mg/g, respectively. It seemed that during adaptation to the seawater condition, the amount of these polymers in the EPS was increased. In addition, the percentage of N-sulfated GAGs in the respective EPS increased during adaptation, with the highest percentage in EPSt30 (Figure 4.3). In comparison to the aerobic granular sludge EPS reported by Chen et al. (2023), the total sulfated GAG content in the EPS of the seawater-adapted granules is much lower, mainly half of the reported amount. Likely, the differences in the operational conditions and microbial communities are the causes.

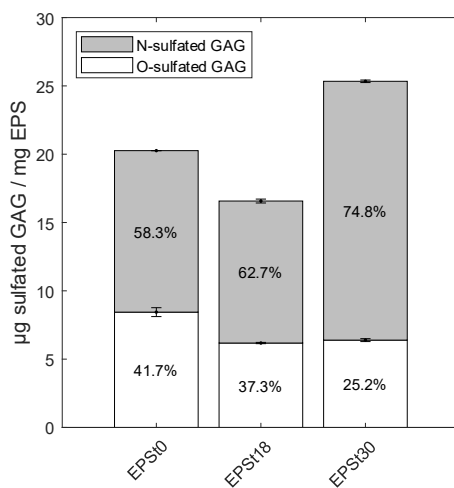


Figure 4.3. O- and N-sulfated glycosaminoglycan-like polymers (O- sulfated GAGs and N-sulfated GAGs) in the EPS extracted from aerobic granular sludge. EPSt0: EPS extracted from inoculum; EPSt18: EPS extracted from granules 18 days after the reactor start; EPSt30: EPS was extracted from granules 30 days after the reactor start.

### Lectin Microarray

To evaluate protein glycosylation and monitor the dynamic glycan profile of those glycoproteins, a lectin microarray has been used. It is based on the mechanism that lectins selectively bind with glycans by recognizing their specific patterns. It is worth noting that, in this analysis, proteins in the extracted EPS were fluorescently labeled with Cy3. If the labeled proteins are glycosylated and their distinct glycan structures match with the affinity of the lectins, they will bind with the lectins on the microarray and their fluorescent signal will be recorded by the evanescent-field fluorescence scanner. Thus, a strong fluorescent signal indicates the following: the bound proteins are glycoproteins; the glycan part of the bound protein has the same glycan profile pattern that the lectin can recognize, and the amount of this glycoprotein is high.

It was found that for all of the EPS samples, within the 97 lectins used in the lectin microarray, 65 gave a strong fluorescent binding signal. This clearly indicates that there are glycoproteins in all of the EPS samples since only glycoproteins can be detected by the microarray. In addition, from the specificity of the lectins, information on the glycan pattern can be obtained. The result of the lectin microarray showed that there were glycoproteins with N-linked glycosylation (*e.g.*, due to the binding of lectins TxLcl, rXCL, CCA, and rSRL) and O-linked glycosylation (*e.g.*, due to the binding of lectins HEA, MPA, VVA, and SBA). Those glycoproteins contained one or multiple glycans, such as sialic acids (with both  $\alpha$ 2-3 and  $\alpha$ 2-6 linkages), lactosamine and/or polylactosamine, mannose (including  $\alpha$ 1-3 and

$\alpha$ 1–6 linkages), fucose (including  $\alpha$ 1–2,  $\alpha$ 1–3, and  $\alpha$ 1–4 linkages), N-acetyl glucosamine, and galactose (with and without sulfation) (for details of the lectins, refer to the Supplementary Materials Figure S4). Interestingly, 55 lectins were found to be significantly different between the three EPS samples, indicating that the glycan profile of the glycoproteins is altered with the change of the environmental conditions (implied by the color change in Figure 4.4 from blue to red). If the two EPS extracted from seawater-adapted granules are compared, Figure 4.5 clearly shows that most of the glycan signals are increased in EPS<sub>t18</sub>, meaning that there are more glycosylated proteins in the EPS<sub>t18</sub>. In addition, as each lectin has its binding specificity, this also shows that the glycan profile of EPS<sub>t18</sub> has extremely strong diversity, while EPS<sub>t30</sub> has less glycan diversity. It suggests that, in response to exposure to seawater, the amount of glycoproteins and their glycan diversity first increases; once the granules reach a stable state of adaptation, both the amount of glycoproteins and their glycan diversity tend to decrease. Such a change may also be related to the shift of microbial community; as seen in Figure 4.2, at t<sub>18</sub>, the microbial community was more diverse with the presence of PAO, GAO, and other eubacteria; while at t<sub>30</sub>, PAO was fully dominating over GAO and other eubacteria.

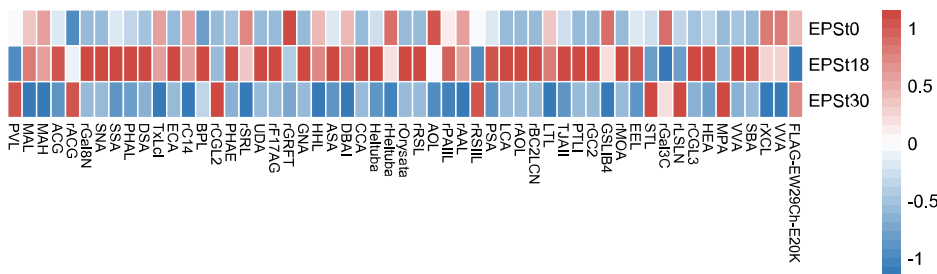
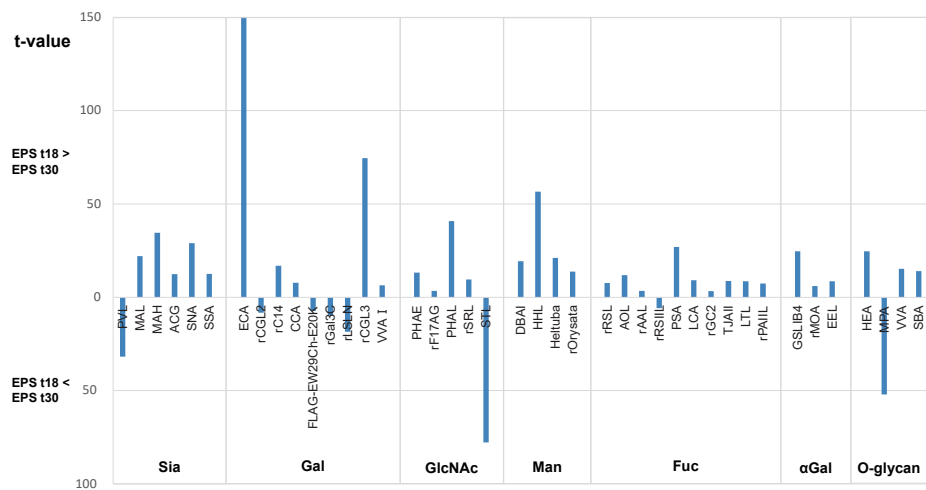


Figure 4.4. Lectin binding profiles of the extracellular polymeric substances extracted from aerobic granular sludge. EPSt0: EPS extracted from inoculum; EPSt18: EPS extracted from granules 18 days after the reactor start; EPSt30: EPS extracted from granules 30 days after the reactor start. The scale ranges from 1 to  $-1$ . Red: high intensity; blue: low intensity.



4

Figure 4.5. Comparison of the lectin binding profiles of the glycoproteins in the extracellular polymeric substances extracted from aerobic granular sludge. EPSt18: EPS extracted from granules 18 days after the reactor start; EPSt30: EPS extracted from granules 30 days after the reactor start. Abbreviations: Sia (sialic acid), Gal (galactose), GlcNAc (N-acetyl glucosamine), Man (mannose), Fuc (fucose),  $\alpha$ Gal (terminal  $\alpha$ -D-galactose), and O-glycan (O-linked glycoprotein).

## 4.4 Discussion

### 4.4.1 In response to the exposure to seawater, the glycan profile, especially that of the glycoproteins in the EPS of aerobic granular sludge, varied significantly

During the adaptation to seawater, EPS from aerobic granular sludge exhibited the following variation: there was more EPS, which can be extracted under alkaline conditions (with NaOH present). The yield of the EPS on day 30 was about 2 times that of the inoculum. This is in line with the reported finding that the adaptation of aerobic granular sludge to high saline conditions led to extra EPS production (Corsino et al., 2017). Within the EPS, the percentage of glycans detected by GC-MS was increased, as well. The amount of glycans was tripled on day 30. It is known that bacterial glycans can act as osmoprotection and desiccation protection factors against the salt (Varki et al., 2009). Producing a higher amount of glycans in the EPS might be used by the microorganisms as a strategy to protect themselves from harsh environmental stress factors such as the high salt content in seawater. Looking at the glycosyl composition of the glycans, during the adaptation to seawater condition, xylose and N-acetyl glucosamine appeared, while arabinose disappeared from the sugar monomers. This indicates that after being exposed to seawater, there is a significant change in glycan composition produced in the EPS. The role of these two sugar monomers against seawater conditions is unknown and needs further investigation. It is also noticed that, in the three EPS samples, the amount of glucose is extremely high in comparison to that of all of the other monomers. The possible explanation could be that there might be glucose-rich glycans, such as  $\beta$  glucan or lipopolysaccharides produced as part of the EPS (Singh and Bhardwaj, 2023). Further investigation is needed to understand the high glucose content. Within the glycans, besides free polysaccharides, there are glycoconjugates, such as glycoproteins and glycolipids. To further investigate the potential existence of glycoproteins and their glycan profile, lectin microarray analysis was performed. The existence of glycoproteins with diverse glycosylation patterns was observed for all EPS samples, strongly confirming that protein glycosylation is indeed common in aerobic granular sludge. Interestingly, there were more glycoproteins in EPS<sub>t18</sub> than EPS<sub>t0</sub> and EPS<sub>t30</sub>, and the glycosylation pattern of EPS<sub>t18</sub> is significantly diverse. This indicates that, in response to the environmental change, *i.e.*, exposure to the increased salt condition, one of the adaptation strategies of the microorganisms can be altering the glycosylation of proteins in quantity and diversity. Once the steady state of adaptation was reached, the diversity of protein glycosylation and the amount of glycoproteins reduced. In fact, similar phenomena were reported in anaerobic granular sludge: a significant shift in the glycoconjugate pattern in anaerobic granular sludge happened with increasing salinity (Gagliano et al., 2018). Therefore, it seems that not only the total glycome profile of the EPS but also the

glycan profile of glycoproteins are dynamic and sensitive to environmental stimuli such as salinity.

#### **4.4.2 It is important to investigate the glycan profile of glycoproteins in aerobic granular sludge**

The glycome is defined as the entire complement of glycan structures (including glycoproteins/glycolipids and free polysaccharides) produced by cells (Rudd et al., 2022). Unlike DNA replication, RNA transcription, or protein translation, glycan biosynthesis is not directed by a pre-existing template molecule (Broussard and Boyce, 2019). Instead, the glycome depends on the interplay among the glycan biosynthetic machinery, the available nucleotide sugars (serving as monosaccharide donors), and signals from the intracellular and extracellular environments. Thus, the glycome composition is dynamic and is influenced by both genetic and environmental factors (Flemming et al., 2022).

In granular sludge, the EPS is produced by the microorganisms and is involved in bacterial cells' interactions with their environment. As the extracellular environmental condition is one of the factors that influence the glycome, a change in the environmental condition must have its own reflection in the glycan profile. As demonstrated in the current research, the glycan profile, especially the glycoproteins in the EPS, is sensitive to environmental stimuli. Due to the fact that protein glycosylation is an important post-translational modification, small changes in the glycans of glycoproteins can have profound consequences for protein function (Broussard and Boyce, 2019). Such sensitivity and dynamic alteration of the glycan profile in the EPS may influence the chemical and physical structures and properties of the EPS and, furthermore, the stability of granular sludge. Further research is needed to find the correlation among the glycan profile dynamics, the property alteration of EPS, and the activities of the microbial community.

#### **4.4.3 Lectin microarray can be used as a high-throughput approach to monitor the diversity and dynamic change of the glycoproteins in the environmental sample.**

Given the profound impact of glycans on the function of glycoproteins, protein glycosylation might play an important role in the EPS of biofilm. However, protein glycosylation in the EPS remains largely uncharacterized, and the existence of glycoconjugates such as glycoproteins (and glycolipids) in the EPS was very recently reported and started getting attention (Flemming et al., 2022). On the other hand, the complexity of glycosylation poses an analytical challenge. Current methods for bacterial glycan analysis include MS, HPLC, and HPAEC-PAD. These methods require the release of glycans from a glycoprotein through enzymatic or chemical reactions. This makes an accurate assessment of glycosylation depend on a complete release of all of the glycans that are present in a glycoprotein. In this respect, a

significant investment of time and effort is needed, which becomes one of the bottlenecks for a high-throughput study of the diversity and dynamic change of the glycan profile. Recently, using a lectin microarray as a high-throughput approach has attracted great interest. Importantly, the lectin microarray directly measures glycan profiles on an intact protein without the need for enzymatic digestion or clipping glycans from the protein backbone. Such a platform is unique in increasing the possibility of full coverage of all glycan variants of glycoproteins (Tateno et al., 2007). In the current work, the application of the lectin microarray indeed confirmed the presence of glycoproteins and effectively monitored its alteration along the adaptation to the seawater condition. Additionally, the result of lectin microarray is in line with the result of other analyses performed: *i.e.*, sugar monomers such as mannose, fucose, galactose, and N-acetyl glucosamine were detected by the glycosyl composition analysis through GC-MS. The sialic acids captured by the MS and sulfated glycosaminoglycan-like polymers revealed by the DMMB assay were in line with the presence of sialic acids, lactosamine, and galactose with sulfation (*e.g.*, keratan sulfate) detected by the lectin microarray analysis. This suggests that the lectin microarray is a successful platform for glycan profiling of glycoproteins in microbial aggregates such as granular sludge. Despite the success, it is worth noting that as lectins are of diverse specificity, some have cross-reactivity with various glycans. It is relatively difficult to characterize a specific glycan using only one lectin. A second limitation is the lack of availability of lectins that recognize sugars unique to bacteria. Designing a bacteria (or biofilm)-specific lectin microarray is an interesting topic for future research.

#### 4.5 Conclusions

Protein glycosylation was identified in the extracellular polymeric substances (EPS) in aerobic granular sludge. In response to environmental stimuli such as exposure to seawater, the glycan profile, especially that of the glycoproteins, varied significantly: xylose and N-acetyl glucosamine appeared as sugar monomers in comparison to the inoculation. The amount of glycoproteins and their glycan diversity displayed an increase during adaptation, followed by a decrease once the granules reached a stable state of adaptation. Lectin microarray can be used as a high-throughput approach to monitor the diversity and dynamic change of glycans in the glycoproteins in the EPS of aerobic granular sludge.

#### Supplementary Materials

The Supplementary Materials of this chapter can be found at DOI [10.1021/acsestwater.3c00625](https://doi.org/10.1021/acsestwater.3c00625)

## References

Amann, R. I., Binder, B. J., Olson, R. J., Chisholm, S. W., Devereux, R., & Stahl, D. A. (1990). Combination of 16S rRNA-targeted oligonucleotide probes with flow cytometry for analyzing mixed microbial populations. *Applied and Environmental Microbiology*, 56(6), 1919–1925. <https://doi.org/10.1128/AEM.56.6.1919-1925.1990>

APHA. (1998). *Standard methods for the examination of water and wastewater* (20th ed.). American Public Health Association, American Water Works Association, Water Environment Federation, Washington, D.C., 1998.

Bassin, J. P., Pronk, M., Muyzer, G., Kleerebezem, R., Dezotti, M., & van Loosdrecht, M. C. M. (2011). Effect of elevated salt concentrations on the aerobic granular sludge process: Linking microbial activity with microbial community structure. *Applied and Environmental Microbiology*, 77(22), 7942–7953. <https://doi.org/10.1128/AEM.05016-11>

Bertozzi, C. R., & Sasisekharan, R. (2009). Glycomics. *Essentials of Glycobiology*. 2nd Edition.

Boleij, M., Kleikamp, H., Pabst, M., Neu, T. R., van Loosdrecht, M. C. M., & Lin, Y. (2020). Decorating the Anammox House: Sialic Acids and Sulfated Glycosaminoglycans in the Extracellular Polymeric Substances of Anammox Granular Sludge. *Environmental Science & Technology*, acs.est.9b07207. <https://doi.org/10.1021/acs.est.9b07207>

Boleij, M., Pabst, M., Neu, T. R., Van Loosdrecht, M. C. M., & Lin, Y. (2018). Identification of Glycoproteins Isolated from Extracellular Polymeric Substances of Full-Scale Anammox Granular Sludge. *Environmental Science and Technology*, 52(22), 13127–13135. <https://doi.org/10.1021/acs.est.8b03180>

Bourven, I., Bachellerie, G., Costa, G., & Guibaud, G. (2015). Evidence of glycoproteins and sulphated proteoglycan-like presence in extracellular polymeric substance from anaerobic granular sludge. *Environmental Technology (United Kingdom)*, 36(19), 2428–2435. <https://doi.org/10.1080/09593330.2015.1034186>

Broussard, A. C., & Boyce, M. (2019). Life is sweet: The cell biology of glycoconjugates. *Molecular Biology of the Cell*, 30(5), 525–529. <https://doi.org/10.1091/MBC.E18-04-0247>

Chen, L. M., de Bruin, S., Pronk, M., Sousa, D. Z., van Loosdrecht, M. C. M., & Lin, Y. (2023). Sialylation and Sulfation of Anionic Glycoconjugates Are Common in the Extracellular Polymeric Substances of Both Aerobic and Anaerobic Granular Sludges. *Environmental Science and Technology*, 57(35), 13217–13225. <https://doi.org/https://doi.org/10.1021/acse.est.2c09586>

Corsino, S. F., Capodici, M., Torregrossa, M., & Viviani, G. (2017). Physical properties and Extracellular Polymeric Substances pattern of aerobic granular sludge treating hypersaline wastewater. *Bioresource Technology*, 229, 152–159. <https://doi.org/10.1016/j.biortech.2017.01.024>

Crocetti, G. R., Hugenholtz, P., Bond, P. L., Schuler, A., Keller, J., Jenkins, D., & Blackall, L. L. (2000). Identification of polyphosphate-accumulating organisms and design of 16S rRNA-directed probes for their detection and quantitation. *Applied and Environmental Microbiology*, 66(3), 1175–1182. <https://doi.org/10.1128/AEM.66.3.1175-1182.2000>

Daims, H., Brühl, A., Amann, R., Schleifer, K. H., & Wagner, M. (1999). The Domain-specific Probe EUB338 is Insufficient for the Detection of all Bacteria: Development and Evaluation of a more Comprehensive Probe Set. *Systematic and Applied Microbiology*, 22(3), 434–444. [https://doi.org/10.1016/S0723-2020\(99\)80053-8](https://doi.org/10.1016/S0723-2020(99)80053-8)

de Graaff, D. R., Felz, S., Neu, T. R., Pronk, M., van Loosdrecht, M. C. M., & Lin, Y. (2019). Sialic acids in the extracellular polymeric substances of seawater-adapted aerobic granular sludge. *Water Research*, 343–351. <https://doi.org/10.1016/j.watres.2019.02.040>

Eichler, J. (2019). Protein glycosylation. *Current Biology*, 29(7), R229–R231. <https://doi.org/10.1016/j.cub.2019.01.003>

#### 4. Alterations of glycan composition in aerobic granular sludge during the adaptation to seawater conditions

Elahinik, A., Haarsma, M., Abbas, B., Pabst, M., Xevgenos, D., van Loosdrecht, M. C. M., & Pronk, M. (2022). Glycerol conversion by aerobic granular sludge. *Water Research*, 227, 119340. <https://doi.org/10.1016/J.WATRES.2022.119340>

Flemming, H. C., van Hullebusch, E. D., Neu, T. R., Nielsen, P. H., Seviour, T., Stoodley, P., Wingender, J., & Wuertz, S. (2022). The biofilm matrix: multitasking in a shared space. *Nature Reviews Microbiology* 2022 21:2, 21(2), 70–86. <https://doi.org/10.1038/S41579-022-00791-0>

Flemming, H. C., & Wingender, J. (2010). The biofilm matrix. In *Nature Reviews Microbiology* (Vol. 8, Issue 9, pp. 623–633). Nature Publishing Group. <https://doi.org/10.1038/nrmicro2415>

Gagliano, M. C., Neu, T. R., Kuhlicke, U., Sudmalis, D., Temmink, H., & Plugge, C. M. (2018). EPS glycoconjugate profiles shift as adaptive response in anaerobic microbial granulation at high salinity. *Frontiers in Microbiology*, 9(JUL), 1423. <https://doi.org/10.3389/fmicb.2018.01423>

Herget, S., Ranzinger, R., Maass, K., & Lieth, C. W. v. d. (2008). GlycoCT-a unifying sequence format for carbohydrates. *Carbohydrate Research*, 343(12), 2162–2171. <https://doi.org/10.1016/j.carres.2008.03.011>

Hirabayashi, J. (2004). Lectin-based structural glycomics: Glycoproteomics and glycan profiling. *Glycoconjugate Journal*, 21(1–2), 35–40. [https://doi.org/10.1023/B:GLYC.0000043745.18988.A1/METRICS](https://doi.org/10.1023/B:GLYC.0000043745.18988.A1)

Merkle, R. K., & Poppe, I. (1994). [1] Carbohydrate composition analysis of glycoconjugates by gas-liquid chromatography/mass spectrometry. *Methods in Enzymology*, 230, 1–15. [https://doi.org/10.1016/0076-6879\(94\)30003-8](https://doi.org/10.1016/0076-6879(94)30003-8)

Messner, P. (2009). Prokaryotic protein glycosylation is rapidly expanding from “curiosity” to “ubiquity.” *ChemBioChem*, 10(13), 2151–2154. <https://doi.org/10.1002/CBIC.200900388>

Neu, T., & Kuhlicke, U. (2017). Fluorescence Lectin Bar-Coding of Glycoconjugates in the Extracellular Matrix of Biofilm and Bioaggregate Forming Microorganisms. *Microorganisms*, 5(1), 5. <https://doi.org/10.3390/microorganisms5010005>

Reid, C. W., Reid, A. N., & Twine, S. M. (2012). *Bacterial glycomics: current research, technology, and applications*.

Reily, C., Stewart, T. J., Renfrow, M. B., & Novak, J. (2019). Glycosylation in health and disease. *Nature Reviews Nephrology*, 15(6), 346–366. <https://doi.org/10.1038/S41581-019-0129-4>

Rudd, P. M., Karlsson, N. G., Khoo, K.-H., Thaysen-Andersen, M., Wells, L., & Packer, N. H. (2022). Glycomics and Glycoproteomics. *Essentials of Glycobiology*. <https://doi.org/10.1101/GLYCOBIOLOGY.4E.51>

Santander, J., Martin, T., Loh, A., Pohlenz, C., Gatlin, D. M., & Curtiss, R. (2013). Mechanisms of intrinsic resistance to antimicrobial peptides of *Edwardsiella ictaluri* and its influence on fish gut inflammation and virulence. *Microbiology*, 159(Pt 7), 1471. <https://doi.org/10.1099/MIC.0.066639-0>

Singh, R. P., & Bhardwaj, A. (2023).  $\beta$ -glucans: a potential source for maintaining gut microbiota and the immune system. *Frontiers in Nutrition*, 10, 1143682. <https://doi.org/10.3389/FNUT.2023.1143682/XML>

Tateno, H., Toyota, M., Saito, S., Onuma, Y., Ito, Y., Hiemori, K., Fukumura, M., Matsushima, A., Nakanishi, M., Ohnuma, K., Akutsu, H., Umezawa, A., Horimoto, K., Hirabayashi, J., & Asashima, M. (2011). Glycome diagnosis of human induced pluripotent stem cells using lectin microarray. *Journal of Biological Chemistry*, 286(23), 20345–20353. <https://doi.org/10.1074/jbc.M111.231274>

Tateno, H., Uchiyama, N., Kuno, A., Togayachi, A., Sato, T., Narimatsu, H., & Hirabayashi, J. (2007). A novel strategy for mammalian cell surface glycome profiling using lectin microarray. *Glycobiology*, 17(10), 1138–1146. <https://doi.org/10.1093/GLYCOB/CWM084>

Tomás-Martínez, S., Kleikamp, H. B. C., Neu, T. R., Pabst, M., Weissbrodt, D. G., van Loosdrecht, M. C. M., & Lin, Y. (2021). Production of nonulosonic acids in the extracellular polymeric substances of “*Candidatus Accumulibacter phosphatis*.” *Applied Microbiology and Biotechnology*, 105(8),

3327–3338.  
<https://doi.org/10.1007/s00253-021-11249-3>

Varki, A., Cummings, R. D., Aebi, M., Packer, N. H., Seeberger, P. H., Esko, J. D., Stanley, P., Hart, G., Darvill, A., Kinoshita, T., Prestegard, J. J., Schnaar, R. L., Freeze, H. H., Marth, J. D., Bertozzi, C. R., Etzler, M. E., Frank, M., Vliegenthart, J. F. G., Lütteke, T., ... Kornfeld, S. (2015). Symbol nomenclature for graphical representations of glycans. *Glycobiology*, 25(12), 1323–1324. <https://doi.org/10.1093/GLYCOB/CWV091>

Varki, A., Cummings, R. D., Esko, J. D., Freeze, H. H., Stanley, P., Bertozzi, C. R., Hart, G. W., & Etzler, M. E. (2009). Essentials of Glycobiology. *Cold Spring Harbor (NY)*, 039, 2015–2017.



# Extracellular polymeric substances in aerobic granular sludge under increasing salinity conditions

5

## Abstract

The long-term effects of environmental conditions, such as seawater salinity, on the extracellular polymeric substances (EPS) of aerobic granular sludge (AGS) remain poorly understood. This study investigated EPS changes during a stepwise increase in salinity (0–4%), renewing over 90% of biomass at each condition. Stable granulation, complete anaerobic acetate uptake, and phosphate removal were maintained throughout. FT-IR of granules showed significant changes in glycans ( $1025\text{ cm}^{-1}$ ) and sialic acid ( $1730\text{ cm}^{-1}$ ), which were reflected in the EPS. Lectin microarray revealed that increasing salinity reduced glycan diversity in EPS glycoproteins, while increasing negatively charged groups, including sialic acids and sulfated groups. At 4% salinity, EPS negative charge increased by 19.8% compared to 0%. Microbial community composition shifted from a diverse mix (Dechloromonas; 23%, “*Candidatus Competibacter*”; 13%, “*Candidatus Accumulibacter*”; 28%) at 0% to a dominant (69% – 75%) unclassified *Accumulibacter clade I species* at 1 - 4% salinity. Metaproteomic analysis showed strong upregulation of genes of “*Ca. Accumulibacter*” involved in monosaccharide, lipopolysaccharide, and peptidoglycan biosynthesis from 3% - 4% salinity, indicating its adaptation to salinity stress. Dechloromonas and “*Ca. Competibacter*” represented a minor or a non-significant fraction of those proteins related to glycan synthesis across the salinities. Despite that no glycoprotein biosynthesis pathways were identified in the metaproteomic data, three putative glycoproteins produced by “*Ca. Accumulibacter*” were detected across all conditions. They were downregulated as the salinity increased. These findings highlight how “*Ca. Accumulibacter*” dynamically adapts its EPS, particularly glycoprotein glycans, in response to increasing salinity, offering new insights into EPS adaptation under environmental stress.

## Accepted as:

Chen, L.M., Keisham, S., Tateno, H., Kleine G.Y., van, Pronk, M., Loosdrecht, M.C.M. van, Pabst, M., Lin, Y.. **Extracellular polymeric substances in aerobic granular sludge under increasing salinity conditions.** *Water Research* (2026)

## 5.1 Introduction

Aerobic granular sludge (AGS) is a wastewater treatment process known for its robustness and efficiency (Pronk et al., 2015). With this technology, microorganisms grow in the form of compact granules where they are embedded in a self-produced matrix of extracellular polymeric substances (EPS) providing structural integrity and protection against various environmental factors. Among these factors, salinity has emerged as an important factor for the stability of AGS systems.

Salinity is one of the environmental factors increasingly affecting wastewater treatment systems, particularly in coastal cities. The daily usage of seawater for applications, such as flushing toilets, fire control, along with the discharge of high saline water from industrial wastewaters, can lead to the accumulation of high-salinity wastewater in treatment facilities, which can impact the sludge stability (Lefebvre and Moletta, 2006; Zhang et al., 2023). Despite several comprehensive studies on process performance, such as biological phosphate removal on seawater salinity (de Graaff et al., 2020), NaCl-induced salinity (Pronk et al., 2014; Wang et al., 2017; Welles et al., 2014) or alternating salinities (Hou et al., 2019), the understanding into corresponding changes in the EPS remain limited and contradictory. Some studies have reported that AGS cultivated under high saline conditions have shown to produce more EPS (Corsino et al., 2017) and proteins (Campo et al., 2018; Ou et al., 2018), whereas others have observed elevated polysaccharides content in the EPS at alternating salinities (Hou et al., 2019). While these studies provide some general insight into the adaptations in the EPS against saline conditions, it remains unclear which EPS components produced are being modified by the microorganisms during the adaptation. The EPS generally consists of polysaccharides, proteins, extracellular enzymes and diverse glycoconjugates, such as lipopolysaccharides and glycoproteins (Seviour et al., 2019). In particular, glycoproteins have recently gained more attention as an EPS component of AGS as they may play important structural and functional roles within the granule matrix (Chen et al., 2023b; de Graaff et al., 2019; Páez-Watson et al., 2024).

Protein glycosylation is one of the most common post-translational modifications found in nature and was long believed to be exclusive to eukaryotes (Schäffer and Messner, 2017). However, it is now recognized as widespread in bacteria and archaea, functioning in protein stabilization, cell motility and biofilm formation (Eichler and Koomey, 2017; Nothaft and Szymanski, 2010). While the understanding on the bacterial protein glycosylation pathways and functions are largely based on studies of pathogenic model species (*Campylobacter jejuni* and *Haemophilus influenzae*) (Eichler and Koomey, 2017), recent work has shown the presence and diversity of glycoproteins in environmental microbial communities.

For example, a dense array produced by two different of glycans were found on the surface-layer proteins of an anaerobic ammonium oxidizing bacterium, as identified from an enrichment culture (Pabst et al., 2022). In a microbial community enriched with "*Candidatus Accumulibacter*", glycans of glycoproteins in the EPS were found highly diverse (Páez-Watson et al., 2024). Interestingly, other studies have shown that the pathways and chemical composition of glycoproteins are altering against the change in the environment, *i.e.* two distinct protein N-glycosylation pathways in *Haloferax volcanii* are differentially regulated by salinity (Kaminski et al., 2013). A short-term exposure to the saline condition results in variation of the glycan composition of AGS glycoproteins (Chen et al., 2023b). Those findings imply that there is a strong correlation between protein glycosylation and the varying of salinity. However, what this correlation is, including why and how salinity affects protein glycosylation patterns remains unclear.

To investigate the relationship between salinity, charge and protein glycosylation regulation in aerobic granular sludge, granules were cultured under seawater conditions with stepwise increasing salinity from 0% to 4%. At each salinity, the EPS was extracted from the biomass and changes in glycoprotein composition were analyzed using lectin microarray. The charge density of the EPS was determined using conductometric titration. Metaproteomics was employed to assess the microbial community composition and changes, explore potential glycosylation pathways and identify putative glycoproteins. Finally, a discussion was included on potential of multi-omics approaches to study protein glycosylation in granular sludge.

## 5.2 Material and Methods

### 5.2.1 Reactor operation and monitoring the adaptation of granular sludge to the increasing seawater salinity

#### Reactor operation

A lab-scale bubble column with a working volume of 2.8 L (6.5 cm diameter) was operated as a sequencing batch reactor. The reactor was inoculated with 1:1 volume ratio of 600 mL sludge, consisting of activated sludge (Harnaschpolder, The Netherlands) and blended Nereda® sludge (Utrecht, the Netherlands). The temperature of the reactor was not directly controlled, but instead the room temperature was controlled at 20°C. The dissolved oxygen (DO) was controlled through a mixture of air and nitrogen at 0% (anaerobic) and 80% (aerobic phase). The pH was controlled at a pH  $7.3 \pm 0.1$  by dosing 1.0 M HCl or 1.0 M NaOH.

The salinity range (0 – 4%) was selected based on the typical concentrations of seawater (3.5%) intrusion in coastal wastewater systems resulting in brackish water (0.05 – 3%), such as in estuaries, and high-salinity streams from industrial

brine discharges (1 – 15%) (Lefebvre and Moletta, 2006) or high-saline seas (e.g. Red sea, 4%). The synthetic wastewater consisted of 1.2 L of demiwater or increasing concentrations of artificial seawater (final concentration of 1%, 2%, 3% and 4% w/v Instant Ocean®), 150 mL medium A and 150 mL medium B. Medium A contained 62.5 mM  $\text{NaCH}_3\text{COO}\cdot 3\text{H}_2\text{O}$ . Additional 3.6 mM  $\text{MgSO}_4\cdot 7\text{H}_2\text{O}$ , and 4.7 mM KCl was added to medium A when mixed with demi water.  $\text{MgSO}_4\cdot 7\text{H}_2\text{O}$  and KCl were removed from the medium when using artificial seawater. Medium B was composed of 41.13 mM of  $\text{NH}_4\text{Cl}$ , 0.34 mM of  $\text{K}_2\text{HPO}_4$ , 0.27 mM of  $\text{KH}_2\text{PO}_4$ , 0.07 mM of allylthiourea to suppress nitrification and 10 mL of trace elements solution (Vishniac and Santer, 1957), but 2.2 g/L of  $\text{ZnSO}_4\cdot 7\text{H}_2\text{O}$  was used instead of 22 g/L and 2.18 g/L of  $\text{Na}_2\text{MoO}_4\cdot 2\text{H}_2\text{O}$  instead of  $(\text{NH}_4)_6\text{Mo}_7\text{O}_{24}\cdot 4\text{H}_2\text{O}$ . The combination of medium A, B and the demi water or seawater, led to the final influent concentrations of 400 mg/L COD, 50 mg/L  $\text{NH}_4\text{-N}$ , and 12.2 mg/L  $\text{PO}_4\text{-P}$ . To monitor the reactor performance, samples were taken over the course of the cycle and filtered through a 0.22  $\mu\text{m}$  PVDF filter. Phosphate and ammonia were measured using a Thermo Fisher Gallery Discrete Analyzer (Thermos Fisher Scientific, Waltham, USA). Acetate was measured through high-performance liquid chromatography (Thermo Scientific Vanquish HPLC) at 50 °C (0.75 mL/min) with 1.5 mM phosphoric acid as eluent and Aminex HPC-87H column (Bio-Rad, California, USA).

During the start-up, the settling phase was gradually decreased from 20 min to 3 min by monitoring the time required for the bed to set. Once stable granulation was formed the settling time was set at 3 min. The following reactor cycles were, 5 min effluent withdrawal, 5 min  $\text{N}_2$  sparging, 5 min feeding with synthetic wastewater, 50 min anaerobic phase and 110 min of aerobic phase. Except for 4%, the anaerobic phase was 80 min and aerobic phase 160 min to ensure anaerobic acetate uptake and complete aerobic phosphate removal, respectively. The conductivity and the online profiles (DO, pH) were used to monitor the operation of the reactor. The volatile solids (VS) and ash fractions of the biomass were measured weekly of the granules and the effluent using the standard methods (APHA, 1998).

Stereo zoom pictures of the granules at the end of each salinity condition were taken with a stereo zoom microscope (M205 FA, Leica Microsystems, Germany) connected to the Eert Vision Auto Focus Microscope camera (Eert Vision, The Netherlands). The images were acquired with the Eert C304 software (V1.0, Eert Vision, The Netherlands).

The solid retention time (SRT) was controlled by manual sludge removal of the mixed liquid and recalculated each time based on the VS removed through sampling and effluent. During the start-up at fresh water condition (0% salinity), no sludge was removed for the first 52 days to allow the seed sludge to adapt to the new influent and reactor conditions. The overall SRT was maintained at  $14 \pm 1$  days over

the course of the experiment. The salinity was increased stepwise. At each salinity, the duration was at least 35 days, about 2.5 SRTs in order to detect differences in the sludge. At least 90% of the biomass was renewed before taking the samples for EPS extraction and metaproteomic analysis (Table 5.1).

For EPS analysis, the granules were taken at the end of the aerobic phase, rinsed with demi water to remove excess salt, lyophilized, and stored at room temperature. For the metaproteomic analysis, the granules were first potted and washed three times with PBS. The biomass pellets were lyophilized before analysis.

Table 5.1. Overview of the duration, average SRT and newly grown biomass per condition. The % of new biomass calculated was done by using the average SRT: % new biomass =  $1 - \exp(-t / \text{SRT})$ ), where t is the duration of the condition in days and SRT is the average SRT over that period.

% sea salt	Duration (days)	Average SRT	% new biomass calculated
0	118	13	99.3
1	35	13	93.7
2	42	14	95.0
3	36	14	92.9
4	35	15	90.2

### Functional group analysis with Fourier Transform – Infrared Spectroscopy

Biomass was taken throughout the experiment to monitor the general changes in the functional groups using Fourier transform-infrared spectroscopy (FT-IR). About 1 mL of granules were taken at the end of the aerobic phase and washed 3 times with 1 mL of demi water to remove the excess salt. The samples were immediately stored in the -80°C and lyophilized for further analysis.

The lyophilized sample was crushed into a powder and measured on a Spectrum 100 spectrometer (PerkinElmer, Shelton, CT). The spectra were recorded in attenuated reflectance (ATR) mode at room temperature over a wavenumber range of 600 – 4000 cm<sup>-1</sup> using 16 accumulations and a resolution of 1 cm<sup>-1</sup>. The spectra were analyzed in OriginPro® (OriginLab, US). Normalization was performed on MATLAB on the wavenumber 1535 cm<sup>-1</sup>, the amide II peak (Talari et al., 2016).

### Sialic acid lectin staining of aerobic granular sludge

At each salinity, 1 mL of granules were collected and put into Eppendorf tubes washed with Milli-Q water for three times. The supernatant was carefully removed by spinning down the biomass using a small tabletop centrifuge at low speed. After washing, the samples were covered with a 500 µL of the MAA lectin solution (0.1 mg/mL) and incubated for 20 min in the dark at room temperature. Then, the

samples were destained by carefully removing the unbound lectin by centrifuge at low speed. The supernatant was decanted, followed by adding 1 mL of tap water and carefully removed. The same washing steps were repeated three times. The destained sample was put on the glass slide, the cover slip was added on top of the biomass before imaging.

### 5.2.2 Monitoring the alteration of EPS properties in response to the increasing seawater salinity

#### EPS extraction and general analysis

About 350 mg of lyophilized granules (about 250 mg organic fraction, VS) were extracted in 25 mL 0.1 M NaOH (1% weight VS/volume) at 80°C for 30 min in duplicate. The extracted mixture was cooled under running tap water and centrifuged at 3180×*g* at 4°C for 20 min. The supernatant was dialysed overnight to remove the excess salts against demi water using dialysis tubing (3.5 kDa molecular cut-off).

The total solids fraction of the dialysed EPS was determined using overnight drying at 105°C, followed by burning at 550°C to determine the VS fraction (APHA, 1998). The extracted and dialysed EPS was stored overnight at 4°C. 100 mg equivalent of the total solids in volume was used for conductometric titration. The rest supernatant was frozen at -80°C, lyophilized and stored at room temperature for further EPS analysis.

The lyophilized EPS was analyzed by FT-IR as described earlier. The total protein content was determined by dissolving the lyophilized EPS in Milli-Q water to 1 mg/mL. The BCA protein assay was used following the manufacturer's instructions with bovine serum albumin as a standard (Pierce BCA protein assay Kit, Thermo Scientific). Protein absorbance was measured at 562 nm in triplicate using the multimode plate reader (TECAN Infinite M200 PRO, Männedorf, Switzerland).

#### The charge of EPS analyzed by conductometric titration

The conductometric titration was described in detail by Kleine et al. (2025). In short, one hundred mg equivalent of the total solids in the extracted EPS was diluted with demi water until a total volume of 50 mL. The solution was first set to pH 2 using 1 M HCl. The conductivity and pH curves were saved using LABVIEW 2014 SP1 (National Instruments). Afterwards, the solution was titrated to approximately pH 12 using a total of 1.5 ml 1 M NaOH with the set-up using a 765 dosimat (Metrohm, the Netherlands). During conductometric titration, pH and conductivity are measured simultaneously. As OH<sup>-</sup> is dozed, it first neutralizes excess H<sup>+</sup> and then deprotonates functional groups like COOH and NH3<sup>+</sup>. These reactions create plateaus in the pH and conductivity curves, which can be used to calculate the sample's charge density (mmoles NaOH/gVS).

### **Glycan profiling of glycoproteins by lectin microarray**

High-density lectin microarray was constructed according to the method described (Tateno et al., 2011) 0.4 µg protein eq. of lyophilized EPS was dissolved in 20 µL PBS-T and labeled with Cy3-N-hydroxysuccinimide ester (GE Health-care). Excess Cy3 was removed with Sephadex G-25 desalting columns (GE Healthcare) centrifuged at 1500 × g at 4°C for 2 min. Cy3-labeled proteins were diluted with probing buffer (25 mM tris-HCl (pH 7.5), 140 mM NaCl, 2.7 mM KCl, 1 mM CaCl<sub>2</sub>, 1 mM MnCl<sub>2</sub>, and 1% Triton X-100) to 0.5 µg/mL and were incubated with the lectin microarray at 20°C overnight. The lectin microarray was washed three times with probing buffer, and fluorescence images were captured using a Bio-Rex scan 200 evanescent-field-activated fluorescence scanner (Rexxam Co. Ltd., Kagawa, Japan). The samples were performed in technical duplicates on the duplicate EPS samples. The total fluorescence signal is normalized over each condition and visualized using Rstudio.

### **Detecting the glycan structure of the sialylated glycoproteins in the extracted EPS by combining lectin matrix prepacked column, enzymatic treatment and lectin microarray**

Because aerobic granules cultivated with 4% salinity displayed the strongest sialic acid lectin staining (Supplementary Materials Figure S1), the extracted EPS from the granules cultivated at this salinity was selected for the verification of the presence of sialic acid. The sialic acid-specific separopore®4B MAA lectin column (1ml) was used for the purification of macromolecules containing sialic acid in the above extracted EPS according to the procedure provided by glycoMatrix™ (Dublin, OH). The collected fraction was lyophilized for further analysis.

High-density lectin microarray was generated according to the method described above. 0.4 µg of the MAA lectin column-enriched fraction was labeled with Cy3-N-hydroxysuccinimide ester (GE Health-care), and excess Cy3 was removed with Sephadex G-25 desalting columns (GE Healthcare). 50 µL of Cy3-labelled sample was put into a separate tube and 0.5 µL of sialidase was added into the tube, mixed and incubated at 37°C for 1 hour (in parallel, the probing buffer was treated in the same way as the control). The above Cy3-labeled MAA lectin column-enriched fraction with and without sialidase treatment were diluted with probing buffer (25 mM tris-HCl (pH 7.5), 140mM NaCl, 2.7 mM KCl, 1 mM CaCl<sub>2</sub>, 1 mM MnCl<sub>2</sub>, and 1% Triton X-100) to 0.5 µg/mL and were incubated with the lectin microarray at 20°C overnight. Further preparations and data visualization of the lectin microarray were performed as described in section “Glycan profiling of glycoproteins by lectin microarray”.

### 5.2.3 Metaproteomic analysis

#### Protein extraction and digestion

The protein extraction was performed similar to Kleikamp et al. (2023). Hunderd fifty milligrams of acid washed glass beads (150–212  $\mu\text{m}$ ) with 170  $\mu\text{L}$  of both TEAB and B-PER buffer was added to approximately six mg of the collected lyophilized biomass. The samples were homogenized using the bead beater for 2.5 min with 3 min incubation ice and repeated for a total of 3 cycles. Freeze/thaw cycles were performed by freezing the samples at -80°C and thawing at 75°C with centrifugation (1000 rpm, 5 min) for a total of 3 cycles. The supernatant volume was collected in a LoBind Eppendorf tube after centrifugation (20 min, 4°C, 14000 rcf). Protein precipitation was performed by addition of TCA at a ratio of 1:4 to the supernatant, vortexed and incubated at 4°C for 30 min. The supernatant was removed after centrifugation (15 min, 4°C, 14000 rcf) and discarded. The protein pellets were washed with ice-cold acetone, spun down (3 min, 14000 rcf) and the acetone was discarded. The pellets were reconstituted in 50  $\mu\text{L}$  6 M urea. The samples were reduced using 8.5  $\mu\text{L}$  of 10 mM dithiothreitol (DTT) (60 min, 37°C, 300 rpm), followed by alkylation using 8.5  $\mu\text{L}$  of 20 mM iodoacetamide (IAA) by incubation for 60 min in the dark at room temperature. The samples were then diluted with 285  $\mu\text{L}$  of 100 mM ammonium bicarbonate to obtain a urea concentration of < 1 M. Finally, 10  $\mu\text{L}$  of 0.1  $\mu\text{g}/\mu\text{L}$  trypsin (Promega) was added to the samples and incubated overnight at 37°C. The obtained peptides were purified with a solid-phase extraction using Oasis HLB solid-phase extraction well plates (Waters) according to the protocol provided by the manufacturer. Purified peptide fractions were then dried in a SpeedVac concentrator and stored at -20°C until further preparations for the analysis.

#### Shotgun metaproteomic analysis

The shotgun proteomic analysis was performed as described previously Pabst et al. (2022), with changes as described in the following. An aliquot of each sample (corresponding to approx. 500 ng proteolytic digest) was analysed using a nano-liquid-chromatography system consisting of an EASY nano LC 1200 equipped with an Acclaim PepMap RSLC RP C18 reverse phase column (75 mm x 150 mm, 2 mm) coupled to a QE plus Orbitrap mass spectrometer (Thermo Scientific, Germany). Solvent A was H<sub>2</sub>O containing 0.1% formic acid, and solvent B consisted of 80% acetonitrile in H<sub>2</sub>O, containing 0.1% formic acid. The flow rate was maintained at 350 nL/min. The Orbitrap was operated in top 10 data dependent acquisition (DDA) mode, acquiring peptide signals from 385–1250 m/z, at 70K resolution in MS1 with an AGC target of 3e6 and max IT of 75 ms. The peptides were separated using a linear gradient from 5 to 25% B over 88 minutes, followed by a linear gradient to 55% B over 60 minutes. MS2 acquisition was performed at 17.5K resolution, with an AGC target of 2e5, and a max IT of 75

ms, using a NCE of 28. Unassigned, singly charged as well as >5 charged mass peaks were excluded.

### **Processing of metaproteomic raw data**

Mass spectrometric raw data were processed using PEAKS Studio X (Bioinformatics Solutions Inc., Canada) for database searching using the protein sequences identified from the contigs constructed from the whole metagenome sequencing data of the same samples including phage sequences, and the cRAP proteome (<https://www.thegpm.org/crap/>), allowing 20 ppm parent ion and 0.02 Da fragment mass error and up to 3 missed cleavages, oxidation/deamination as variable modifications and carbamidomethylation as fixed modification. Database search further used decoy fusion for estimation of false discovery rates (FDR) and subsequent filtering of peptide spectrum matches for 1% FDR, and 2 unique peptides per protein. Taxonomic classification of the identified proteins was performed using Diamond as described earlier (Kleikamp et al., 2023). Taxonomic composition was based on counting the number of matched peptides per taxonomic level (e.g. genus).

The annotation of protein functions was done using GhostKOALA to obtain KO numbers, and the R function keggGet (KEGG symbols). The number of detected peptides was normalized over the total abundance of each condition. The data was further processed in Rstudio; the protein abundances were normalized by Z-score normalization across the conditions and the library “pheatmap” was used for visualization. To determine the possible glycosylation sites, NetOGlyc 4.0.0.13 and NetNGlyc 1.0 were employed.

### **DNA extraction, sequencing and processing**

DNA extraction was performed using the DNeasy® UltraClean® Microbial Kit (Qiagen, Germany) for the AGS samples grown in 0%, 1% and 2% salinity. For AGS grown under 3% and 4% salinity, PowerSoil Pro Kit (Qiagen, Germany) was used due to the low-quality DNA obtained with the DNeasy® UltraClean® Microbial Kit. The extracted DNA was quantified with a Qubit fluorometer and the quality of the DNA was measured on the TapeStation System (Agilent, Santa Clara, CA). Shotgun sequencing was performed on an Illumina NovaSeqX or NovaSeq600 platform (Hogenomix, NL).

Processing of the raw sequencing data was performed by Hogenomix (Delft, NL). The quality of the sequenced raw reads was assessed by FastQC (version 0.11.7) with default parameters (Andrews, 2010) and visualized with MultiQC (version 1.19). Low-quality paired-end reads were trimmed and filtered by Fastp version 0.23.4 on the paired-end mode (Chen, 2023). Taxonomic classification of raw reads was performed to profile the microbiome from each sample using the standard

Kraken2 (version 2) database (uses all complete bacterial, archaeal, and viral genomes in NCBI Refseq database) complemented with a curated wastewater database (sludgeDB) with default tparameters (Wood et al., 2019). The taxonomic classification outcomes from Kraken2.0 were converted into abundance tables using the biom file converter tool and Pavian visualization tool (Breitwieser and Salzberg, 2020) to explore metagenomics classification datasets. To identify patterns in the microbiome, different types of ordination and statistical numerical methods were performed using the R software. The input data was the output of the taxonomic classification from Kraken2.0. Clean reads were assembled into contigs using MetaSPAdes (version 3.15.5) with default parameters (Nurk et al., 2017). Contigs resulting from the sequencing of only the iDNA pools of bioaggregates were binned with MetaBAT version 2.2.15 (Kang et al., 2019) to reconstruct metagenome-assembled genomes (MAGs or bins) on default parameters. The functional gene annotation process involved several steps. Firstly, Prokka version 1.14.5 was utilized to annotate the assembled sequences. This was executed in metagenomic mode, using the default databases and parameters as described by (Seemann, 2014). Subsequently, protein sequences were subjected to a two-step Diamond (version 2.1.8) blast search against the complete Uniprot database, encompassing Trembl and SwissProt (accessed the 10.09.2023). Initially, the search was conducted with default settings. Following this, a second search was performed using stringent parameters (e-value threshold of 0.0001, query coverage of 90%, and identity threshold of 90%). Upon identification of proteins through the Diamond blast searches, the headers of these proteins were replaced with the corresponding Prokka headers.

## 5.3 Results

### 5.3.1 Adaptation of granules towards increasing seawater salinity

The aerobic granular sludge reactor was started-up with freshwater based medium. After stable granulation was achieved, artificial seawater was used to prepare the medium. The salinity of the seawater (hereafter referred to as 'salinity') increased incrementally by 1 percentage point (1% w/v, equivalent to 10 g/L sea salt), reaching a final concentration of 4%. At each salinity condition, complete anaerobic acetate uptake and aerobic phosphate removal were observed. The entire biomass bed settled within 3 min. To ensure the long-term changes were captured, at each salinity, sampling of biomass was performed only after at least 90% of the biomass was renewed. The morphology of the granules across all the saline conditions (from 0-4%) is shown in Figure 5.1. The granules were compact with a smooth surface, and reached sizes between 0.5 – >3 mm.

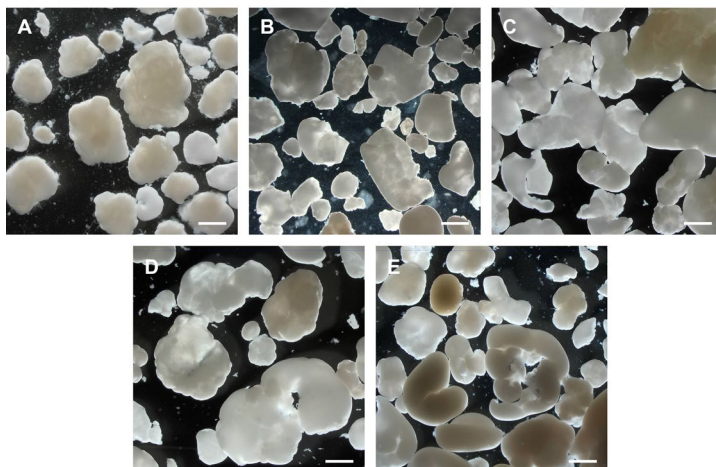


Figure 5.1. Stereo zoom microscope pictures of the AGS grown under 0% (A), 1% (B), 2% (C), 3% (D) and 4% (E). The scale bar indicates 1 mm.

Although the morphology of the granules was similar, there might be changes occurring in the functional groups of the biomass during the adaptation to the increasing salinity. To investigate this possibility, biomass was characterized by FTIR over the course of each salinity adaptation phase (Figure 5.2). The main differences between the samples were observed in the intensity of the bands at  $1025\text{ cm}^{-1}$  and  $1730\text{ cm}^{-1}$ , which were assigned to the -C-O-C bond in glycans (carbohydrates) and the  $\alpha$ -keto group of sialic acids (de Graaff et al., 2019; Talari et al., 2016). Notably, the variation tendency of these two bands were different: the absorbance intensity at  $1025\text{ cm}^{-1}$  was first increasing from 1% to 2% salinity, afterwards a slight decrease from 2% to 3%, followed by a sharp decrease at 4%, representing a parabolic-like shape. While the absorbance intensity at  $1730\text{ cm}^{-1}$

displayed the inverse trend, first a decrease from 1% to 2%, followed by a small increase from 2% to 3%, then a sharp increase at 4%. The band at  $1730\text{ cm}^{-1}$  was assigned to  $\alpha$ -keto group of sialic acids. To verify the presence of sialic acids in the granules, MAA lectin was employed to stain the granules. The MAA lectin binds sialic acids at the terminal sugar residue of glycan chains of glycoproteins (de Graaff et al., 2019). The signal of the lectin was weak for the 0% granules, while it became stronger with increasing salinity. The strongest signal was found for the 4% granules, indicated by a stronger red signal from the Cy5 labeled MAA lectin (Supplementary Materials Figure S1). Both the FTIR and lectin staining results indicated a change in glycan composition (including sialic acids) during the adaptation of AGS to each salinity condition, despite that the morphology of AGS remained highly similar.

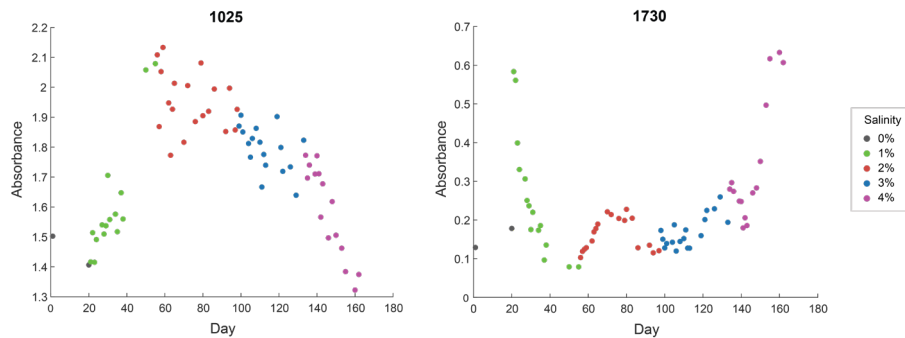


Figure 5.2. Absorption of the normalized FT-IR peaks  $1025\text{ cm}^{-1}$  (-C-O-C in carbohydrates) and  $1730\text{ cm}^{-1}$  ( $\alpha$ -keto acids of sialic acids) over the course of the increasing salinity.

### 5.3.2 General EPS characterization

To study whether the change in glycan composition is reflected in the EPS, the granules were collected at the end of each saline condition, and their EPS was extracted. As shown in Table 5.2, no significant differences were observed among the EPS yields. The protein content decreased by 5.9% from EPS<sub>0%</sub> to EPS<sub>1%</sub> and remained similar throughout the increasing salinity. When the functional groups of the EPS were examined by FT-IR, clear changes in the bands typical of carbohydrates were observed (Figure 5.3), *i.e.* the peak of 1120 cm<sup>-1</sup>, mostly representing C-O stretching of glycans (Talari et al., 2016), showed a strong peak at EPS<sub>0%</sub> but shifted towards a broader peak with increasing salinity. The intensity of the peak at 1025 cm<sup>-1</sup> (-C-O-C- bond in carbohydrates) increased relatively to 1120 cm<sup>-1</sup>. The peak 1730 cm<sup>-1</sup> ( $\alpha$ -keto group of sialic acids) appeared at EPS<sub>3%</sub> as a weak shoulder peak and became stronger at EPS<sub>4%</sub>. It seems that the glycans present in the EPS are altering in response to the increasing salinity, while there is a tendency for sialic acids to increase at higher salinity.

Table 5.2. Overview of the EPS yield and protein content. EPS yield (g VS EPS/VS granules). Protein content as determined by the BCA assay with BSA as a standard.

% salinity	Yield (g VS EPS /VS Granules)	%Protein content (mg BSA eq./ mg EPS)
0	54.7 ± 0.9%	42.7 ± 1.6%
1	55.6 ± 0.3%	36.6 ± 1.6%
2	60.5 ± 2.9%	36.5 ± 0.9%
3	59.4 ± 0.5%	38.2 ± 2.4%
4	54.2 ± 3.6%	39.1 ± 1.3%

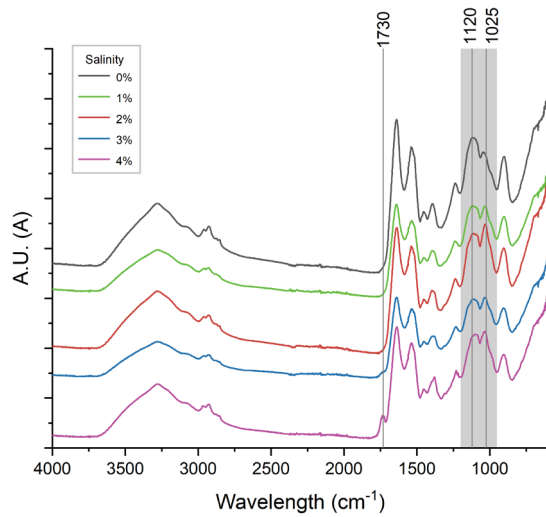


Figure 5.3. FT-IR spectrum of the extracted EPS of the AGS exposed to different salinities. The shaded area ( $1200 - 900 \text{ cm}^{-1}$ ) represent functional groups related to carbohydrates (Talari et al., 2016).

### 5.3.3 Comparative glycomics study

It is known that glycans include both free sugars (*e.g.* polysaccharides) and sugars attached to other molecules (*e.g.* sugars on glycoproteins and glycolipids) (Varki et al., 2017a). As protein glycosylation is one of the most abundant post-translational modifications, it impacts protein folding, stability and interactions (Nothaft and Szymanski, 2010). Glycoproteins in the EPS were specifically studied to understand their adaptation to salinity. To monitor the change of glycan-glycoprotein profile with salinity in the reactor, a lectin microarray was applied. Proteins were labeled with Cy3. If the proteins are glycosylated and the glycan profile matches the affinity of the lectins, a Cy3 signal will appear on the microarray. The intensity of the Cy3 signal reflects the relative abundance of glycoproteins, while the glycan patterns can be obtained from the specificity of lectins.

Among 96 lectins used, 90 gave a strong fluorescent binding signal across all EPS samples (Figure 5.4), implying the presence of glycoproteins. These glycoproteins carried both N-linked glycosylation (indicated by lectins TxLcl, rXCL, CCA, and rSRL) and O-linked glycosylation (indicated by lectins HEA, MPA, VVA, and SBA). Those glycoproteins contained one or multiple glycans, such as sialic acids, lactosamine and/or polylactosamine, mannose, fucose, *N*-acetyl glucosamine, and galactose (with/without sulfation).

Interestingly, among the 5 EPS samples, EPS<sub>0%</sub> showed the strongest binding for most lectins, indicating a higher glycan diversity (Figure 5.4, indicated by the higher number of red-coloured blocks). Upon increasing to 1% salinity, a large number of lectins showed decreased signal intensities, including those binding to Man, GlcNAc, Fuc,  $\beta$ GalNAc. As the salinity increased, the glycan diversity decreased, with the lowest glycan diversity for EPS<sub>4%</sub>. However, the specific glycan trends differed: signals representing O-linked glycosylation increased with salinity, while those from N-linked glycosylation decreased. Specifically, the signal of a few sialic acid binding lectins (PVL, MAL, MAH, rACG) also appeared to increase with salinity.

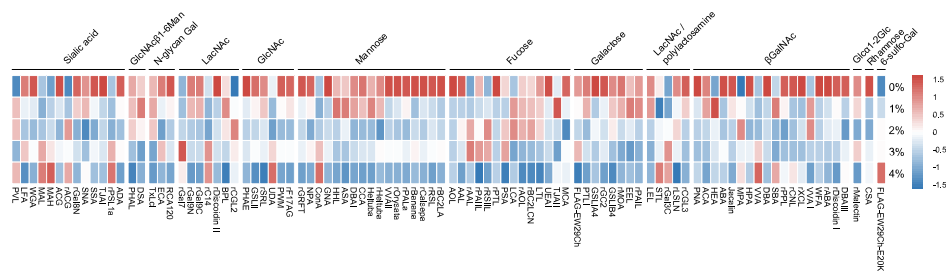


Figure 5.4. Lectin microarray profile of the EPS over salinities (rows) min-max normalized for each lectin (columns). Red indicates higher-than-average binding intensity, and blue indicates lower-than-average intensity for each lectin. The specific structure of each lectin is indicated in the Supplementary Materials (Table S1). GlcNAc, N-acetylgalucosamine; Man, mannose; Gal, galactose; LacNAc, N-acetyllactosamine.

To identify the most abundant glycan structures across EPS samples, the top 10 strongest signal of each EPS were visualized with their corresponding fluorescence intensity (Figure 5.5). Across all samples, the most prevalent glycans contained structures carrying O-linked glycosylation, sialic acid, 6-sulfo-Gal,  $\alpha$ 1-6 fucose and mannose. As salinity increased, charged glycan structures became the most prominent. The signal representing binding of 6-sulfo-Gal (FLAG-EW29Ch-E20K) increased with higher salinity, suggesting a higher production of sulfated glycoproteins. Moreover, lectins binding sialic acid (*e.g.* PVL and rACG) displayed strong signal at EPS<sub>4%</sub>, consistent with the FT-IR analysis and sialic acid staining of the granules. The sialic acid-containing glycoprotein from the EPS<sub>4%</sub> was further investigated by employing the MAA (MAL + MAH) lectin column for enrichment. The enriched glycoprotein contained sialic acids and GalNAc $\beta$ 1-4GlcNAc (also known as LacDiNAc) based on the lectin microarray analysis (Figure 5.5, indicated by the asterisk). After sialidase treatment, the signal of sialic acids lectins PVL and rACG significantly decreased by 7.5-fold and 1.5-fold, respectively (Supplementary Materials Figure S2), confirming both the presence of sialic acids, and the  $\alpha$ (2  $\rightarrow$  3) linkage between sialic acids and the penultimate sugar. As N-acetyl galactosamine is one possible penultimate sugar connected with sialic acids (de Graaff et al., 2019), there is a high probability that the structure Sia $\alpha$ 2-3GalNAc $\beta$ 1-4GlcNAc is present in the glycoprotein in EPS<sub>4%</sub>. Overall, the lectin microarray analysis provided a clear comparison among the glycan structure of glycoproteins in the extracted EPS, showing that with increasing salinity, although glycan diversity decreased, the charged groups (*e.g.* sialic acids, sulfates) and O-glycosylation became more prominent.

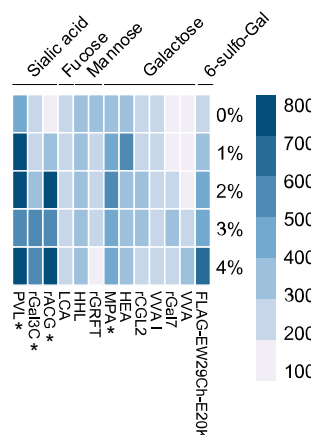


Figure 5.5. Lectin microarray profile of the EPS over salinities (rows) for the top 10 lectins in each condition (columns). The darker the color represents the intensity of the signal, showing direct comparison of absolute binding across conditions. The lectin labeled with asterisk indicate the glycan structure of the enriched glycoprotein fraction of EPS<sub>4%</sub> by MAA column (Supplementary Materials Figure S2).

### 5.3.4 Charge of the EPS

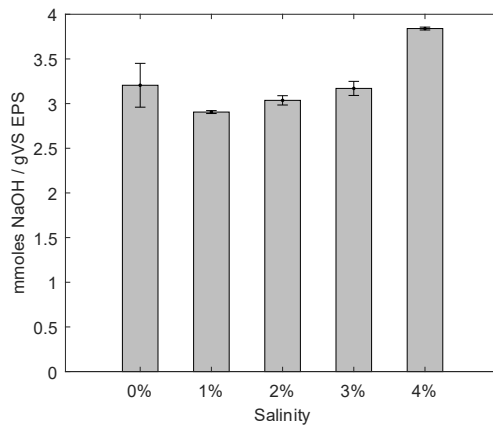


Figure 5.6. Charge density of the EPS at different salinity concentrations as determined by conductometric titrations.

As glycoproteins with charged groups (sialic acids, sulfate groups) appeared to increase as a response to higher salinity, they may influence the total charge of the EPS and thereby on the AGS. To investigate the charge density of the extracted EPS, conductometric titrations were employed. The charge density of the EPS is expressed as the moles of NaOH per gram VS EPS (Figure 5.6). It seems that increasing salinity from 0 to 3% hardly caused a change in the charge density. However, under 4% salinity, the negative charge density of EPS increased by 19.8%, reaching 3.84 mmoles NaOH / gVS, in comparison to EPS<sub>0%</sub>. Compared to EPS of 1-3% salinity, this was increased by 32.3%, 26.5% and 21.1%, respectively. Probably, the increased amount of sialic acids of the glycoproteins, as observed with lectin microarray (Figure 5.4) and lectin staining (Supplementary Materials Figure S1), is one of the contributing factors to the negative charge. These results indicate that EPS<sub>4%</sub> was the most negatively charged.

### 5.3.5 Comparative metaproteomic analysis for microbial community and glycoconjugate - related proteins

#### Microbial community

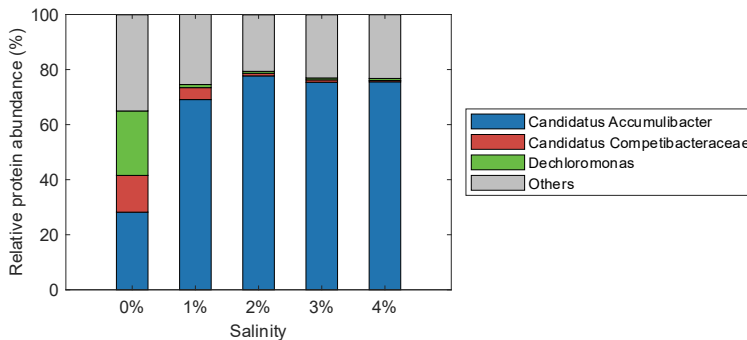


Figure 5.7. Microbial community composition based on the number of identified peptides (peptide spectrum matches) assigned to the genus-level.

The change in EPS properties, such as the charge and the glycan profile in glycoproteins, raised the question: is this alteration connected with the shift of microbial community composition? To answer this question, metaproteomics approach was applied. In metaproteomics, all proteins in the microbial communities are studied (Kleikamp et al., 2023; Kleiner, 2019), information obtained from these proteins can therefore not only be used to identify the composition of microbial communities, but also to search for glycan production pathways and extracellular proteins.

Based on the metaproteomic analysis, the AGS microbial community was populated with a large fraction of phosphate accumulating organisms (PAO), such as “*Candidatus Accumulibacter*” (“*Ca. Accumulibacter*”) (Figure 5.7). The abundance increased from 28% at 0% salinity to 69% at 1% salinity and remained constant at approximately 75% for the remainder of the salinities. Especially, based on the phylogenetic analysis of the PAO marker gene *ppk1* genes in the metagenome combined with the coverage depth data, it seems that one clade I Acumulibacter species (closely related to GCA032229525.1) was dominant throughout the 1 to 4% salinity reactor runs, reaching 64% - 90% of the total *ppk1* genes coverage depth counts (Supplementary Materials Figure S3). Other bacteria, specifically Dechloromonas and glycogen accumulating organism (GAO) “*Candidatus Competibacter*”, were only present under the freshwater condition. Thus, the microbial community was more diverse under freshwater condition, while increasing salinity led to a stable microbial community with the dominance of a single “*Ca. Accumulibacter*” species. In this respect, it is reasonable to assume that the dominant “*Ca. Accumulibacter*” species is likely the main producer of the alternated EPS glycans in response to the increasing salinity.

### Nucleotide sugars and glycoconjugates

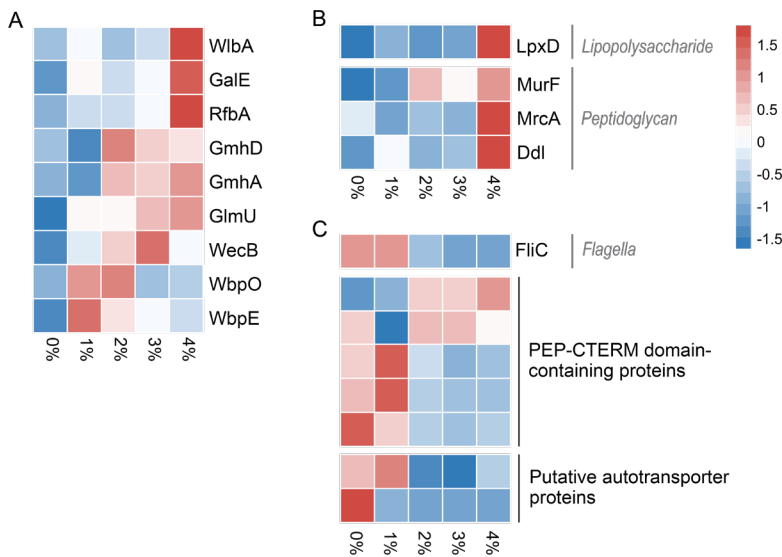


Figure 5.8. Comparative analysis of the proteins of “*Ca. Accumulibacter*” genus closely involved in the biosynthesis of nucleotide sugars (A) and glycoconjugates responding to salinity (B and C). The glycoconjugates are divided into proteins involved in pathways for the biosynthesis of lipopolysaccharides and peptidoglycans (B) and putative glycoproteins based on the KEGG database and database (NCBI / Uniprot) annotations (C). Proteins with no direct link to the production of glycans are excluded in this figure (*i.e.* proteins part of the glycolysis). Red indicates a higher-than-average protein abundance and blue indicates a lower-than-average protein abundance.

Regarding glycan synthesis, one of the prerequisite steps is activating the monosaccharide to a high-energy donor form called nucleotide sugar. These nucleotide sugars are monosaccharides linked to a mono-, di-, tri-nucleoside phosphates, such as uridine diphosphate (UDP), resulting in the activated sugar (van Ede et al., 2025; Li et al., 2017). Several enzymes such as kinases, epimerases, pyrophosphorylase, are involved in the formation of nucleotide sugars (Freeze and Elbein, 2022).

As “*Ca. Accumulibacter*”, an assumed EPS producer (He and Mcmahon, 2011; Martinez, 2023), remained strongly present across the increased salinity range (1 - 4%), the metaproteomic analysis was therefore focused on this organism, which contributed the majority proteins associated with glycan synthesis. Metaproteomic analysis revealed 7 enzymes involved in the biosynthesis of nucleotide sugars that were significantly upregulated at 4% salinity, indicating a higher production of these nucleotide sugars (Table 5.3, Figure 5.8A). Two enzymes were upregulated followed by a downregulation (Table 5.4, Figure 5.8A). Among these upregulated nucleotide sugars, dTDP-Glu, UDP-ManNAc, UDP-3-keto-glycero-β-D-manno-heptose are reported as important glycosylation precursors in

the synthesis of lipopolysaccharides. Only UDP-GlcNAc and UDP-Gal are essential precursors in various glycans, *i.e.* UDP-GlcNAc could be involved in protein glycosylation by O-GlcNAcylation, incorporated in cell wall structures, or used as a precursor for sialic acid synthesis (Chatham and Marchase, 2010; Han et al., 2019; Varki and Schauer, 2009). UDP-Gal could be incorporated as a residue in the glycoprotein glycan or used as a precursor for the synthesis of exopolysaccharides (Tytgat and Lebeer, 2014).

Table 5.3. Upregulated proteins identified involved in the biosynthesis of nucleotide sugars with reported roles in glycans of “*Ca. Accumulibacter*” across all salinity concentrations based on KEGG. Representative protein names are shown; in some cases, multiple orthologous proteins perform the same function and are mapped to the same KO number based on the KEGG database (Supplementary Materials Table S2)

Proteins upregulated	Enzyme activity	Nucleotide sugar donors	Reported glycoconjugate	Reference
<b>RfbA</b>	TDP-Glc pyrophosphorylase	dTDP-Glc	O-antigen of LPS	Samuel & Reeves (2003)
<b>WecB</b>	UDP-GlcNAc epimerase	UDP-ManNAc	O-antigen of LPS	Samuel & Reeves (2003)
<b>WlbA</b>	UDP-GlcNAcA dehydrogenase	UDP-3-keto-GlcNAcA	O-antigen of LPS	Thoden & Holden (2011)
<b>GmhA</b>	Sedoheptulose-7-phosphate isomerase	D-glycero- $\beta$ -D-manno-Heptose 7-phosphate	LPS (core and/or O-antigen), CP	Valvano et al. (2002)
<b>GmhD</b>	ADP-D-glycero- $\beta$ -D-manHep epimerase	ADP-L-glycero- $\beta$ -D-manno-heptose	LPS (core and/or O-antigen), CP	Valvano et al. (2002)
<b>GlmU</b>	GlcNAc-1P pyrophosphorylase	UDP-GlcNAc	Many glycans*	Tytgat & Lebeer (2014)
<b>GalE</b>	UDP-Glc epimerase	UDP-Gal	Many glycans*	Tytgat & Lebeer, 2014)

5

Table 5.4. Downregulated proteins identified involved in the biosynthesis of nucleotide sugars with reported roles in glycans of “*Ca. Accumulibacter*” across all salinity concentrations based on KEGG. Representative protein names are shown; in some cases, multiple orthologous proteins perform the same function and are mapped to the same KO number (Supplementary Materials Table S2).

Proteins downregulated	Enzyme activity	Sugar product	Reported function	Reference
<b>WbpO</b>	UDP-GlcNAc dehydrogenase	UDP-GalNAcA / UDP-GlcNAcA	Extracellular PS	Li et al. (2016)
<b>WbpE</b>	UDP-3-keto-GlcNAcA aminotransferase	UDP-GlcNAc3NA	O-antigen of LPS	Thoden & Holden (2011)

Thus, among the detected enzymes that are involved in the biosynthesis of nucleotide sugars precursors, those potentially lead to the synthesis of LPS were found strongly upregulated at higher salinity. This pointed to the production of more LPS as a response to increasing salinity. In fact, when the enzymes involved along the pathways of LPS and other cell wall glycans synthesis were searched in the metaproteomic results, a few enzymes were indeed found upregulated (Figure 5.8B), *i.e.* *LpxD*, which is responsible for catalyzing the third step in lipid A biosynthesis (Bertani and Ruiz, 2018), and three enzymes (*MurF*, *Ddl*, *MrcA*) related to peptidoglycan synthesis (*MurF* and *Ddl* are involved in the stepwise assembly of the peptide stem of peptidoglycan and *MrcA* is a peptidoglycan transferase that catalyzes one of the last steps in the biosynthesis of peptidoglycan (Barreteau et al., 2008). Unfortunately, enzymes directly related to known protein glycosylation pathways, such as the *en bloc* pathways (Li et al., 2017; Nothaft and Szymanski, 2010), were not detected.

### **Response of putative glycoproteins to the increasing salinity**

The lectin microarray analysis confirmed the presence of glycoproteins, while the enzymes related to known protein glycosylation pathways were hardly observed in the metaproteomic data. Therefore, potential glycosylated protein candidates were searched in the metaproteome based on the annotations in literature (Li et al., 2017; Nothaft and Szymanski, 2010; Olst et al., 2025; Tytgat and Lebeer, 2014) (Figure 5.8C). Several putative glycoproteins were identified in the metaproteome for “*Ca. Accumulibacter*”, including *FliC*, the flagellin filament of flagella, PEP-CTERM domain-containing proteins, and bacterial autotransporters. *FliC* was detected consistently but significantly downregulated at higher salinity. Among the five annotated PEP-CTERM proteins, three were downregulated and two upregulated. Two putative autotransporter proteins were detected and both showed a decrease in abundance with increasing salinity. Potential glycosylation sites reveal high % of potential O- and N-glycosylation for *FliC* (9.3%), followed by the bacterial autotransporter (6.5%, 1.8%, respective to Figure 5.8C) and PEP-CTERM proteins (1.0 – 2.0%) (Supplementary Materials Table S3). Apparently, most of these putative glycoproteins which were reported related to biofilm formation were downregulated. To summarize, the LPS and peptidoglycan biosynthesis appear to be upregulated with increasing salinity. Several putative glycoproteins were detected to be downregulated with increasing salinity.

## 5.4 Discussion

### 5.4.1 Adaptive response of extracellular polymeric substances of aerobic granular sludge on the increasing salinity

Previous works on saline AGS have shown contradictory responses in the EPS towards salinity; increased protein (Campo et al., 2018; Ou et al., 2018) and polysaccharide contents have been observed (Hou et al., 2019). However, in these cases it remains unclear whether the changes observed are due to gradual aging of the biomass or actual adaptation of the microorganisms in the EPS. Moreover, conventional EPS characterization metrics, such as the PN/PS ratio, are insufficient to fully characterize the changes within the EPS (Felz et al., 2019). To address these limitations, in this work it was ensured that at least 90% of the biomass was renewed prior to EPS analysis, thereby capturing microbial adaptations rather than aging effects. Importantly, EPS glycoconjugate characterization was performed in combination with metaproteomics, allowing us to connect the glycan specific modifications and charge density changes to a single "*Ca. Accumulibacter*" clade. This approach provides a more detailed understanding of EPS responses AGS under salinity stress.

The seawater salinity in a lab-scale aerobic granular sludge (AGS) reactor was stepwise increased, starting from freshwater condition (0% salinity), reaching up to 4% salinity with 1%pt. increments, to investigate the microbial and extracellular polymeric substances (EPS) adaptations. Initially, at 0% salinity, the microbial community was diverse, besides "*Ca. Accumulibacter*" (28%), there were *Dechloromonas* (23%) and "*Ca. Competibacter*" (13%) present. As the salinity increased to 1%, the community shifted to one dominant "*Ca. Accumulibacter*" species (69% – 75%) and remained similar until 4% salinity. Regarding the chemical composition of the granules, carbohydrate-related functional groups first increased by 0% and decreased when the salinity was increased. While sialic acid content followed the opposite trend. These shifts were reflected in the glycoproteins of the EPS: lectin microarray indicated a reduction in glycan diversity, along with an increase of charged groups such as sialic acids and sulfated groups. The overall negative charge of the total EPS was found to increase at higher salinity, corresponding to the increase of these charged groups. Thus, despite the stable granule morphology and dominance of a single species of "*Ca. Accumulibacter*" between 1% and 4% seawater salinity, significant changes in the EPS were observed. These findings indicated that the same microorganisms adjusted their EPS composition, as a response to increased salinity, particularly by modifying the glycoproteins with more negatively charged groups.

The increased negative charge in the EPS might be explained by the Derjaguin–Landau–Verwey–Overbeek (DLVO) theory of colloidal stability (Hermansson,

1999). According to this theory, when salinity increases, the range of the repulsive forces between the negatively charged functional groups decreases. This can cause unwanted aggregation of particles, such as proteins, leading to a loss in stability and/or function. To overcome this, microorganisms may produce EPS carrying more negatively charged groups, due to the fact that charged groups could facilitate electrostatic interactions or hydrogen bonding, creating a protein-water-salt hydration matrix. This leads to reduced protein aggregation and increased flexibility, so that the functions of proteins can still be maintained (Gunde-Cimerman et al., 2018; Howard et al., 2009; Zaccai et al., 1989). Microorganisms can adopt different strategies to enhance the negative charge of their proteins. Halophilic Archaea produce a highly acidic proteome when they are exposed to salinity (Gunde-Cimerman et al., 2018). Their proteins have a significant excess of negatively charged amino acids over amino acids with a positive charge. In the S-layer glycoprotein from the extreme halophile *Halobacterium halobium*, sulfated glucuronic acid residues are in the glycans of this glycoprotein, causing a drastic increase in surface charge density (Mengele & Sumper, 1992).

In the current research, another strategy for increased charges was highlighted: microorganisms in AGS produce/modify the glycoproteins with more sialic acids and sulfated groups to increase the negative charge of the proteins. Sulfated groups, the most charged glycan modification known to exist, are found along the glycan chain, whereas sialic acids, which are nine-carbon sugars, are typically found at the terminal ends of glycans (de Graaff et al., 2019; Mengele and Sumper, 1992; Varki et al., 2017b). Both modifications are reported to exhibit functions through their charge, such hydration (Varki et al., 2017), protein binding (Bedini et al., 2019) and gel-formation through  $\text{Ca}^{2+}$  mediated cross-links (Meldrum et al., 2018). Collectively, these functions may contribute to structural stabilization in the EPS matrix at increased salinities. Although in previous work it was found that sialic acids and sulfated groups are widely spread in granular sludge (Boleij et al., 2020; Chen et al., 2023a; Felz et al., 2019), this research demonstrates that decorating the glycans of glycoproteins with sialic acids and sulfated groups may represent an adaptive strategy of "*Ca. Accumulibacter*" under saline conditions. It supports the hypothesis from our earlier study (Chen et al., 2024) that AGS microorganisms actively produce more charged EPS as a response to increased salinity, maintaining protein function, granule integrity, and stability and thereby supporting the structural resilience of the granules under stress conditions.

#### **5.4.2 Exploring protein glycosylation pathways and the possible glycoprotein candidates through metaproteomics**

Metaproteomics enables the study of biosynthesis pathways by identifying specific enzymes (Kleiner, 2019). Despite the finding of both N- and O-linked glycoproteins

by lectin microarray, the enzymes involved in known glycosylation pathways have not been found at all, despite the potential reported earlier (Páez-Watson et al., 2024). Instead, enzymes related to LPS and peptidoglycans were found, with a clear upregulation tendency with salinity. This could be explained by a few reasons. Firstly, there is considerable overlap between glycosylation pathways, especially the LPS and glycoprotein glycan assembly pathways share diverse transferases and transporters (Hug and Feldman, 2011). Secondly, some nucleotide sugars may be shared by different glycoconjugate pathways. For example, UDP-GlcNAc is utilized in the synthesis of peptidoglycans, LPS and glycoproteins (Li et al., 2017). Moreover, some enzymes may have functions in different glycoconjugate biosynthesis pathways, *e.g.* glycosyltransferases, which catalyze the transfer of nucleotide sugar on a molecule, can sometimes participate in more than one pathway. In *Acinetobacter baumannii*, for example, the same glycosyltransferase participates in the synthesis of both glycoproteins and capsule polysaccharides (Lees-Miller et al., 2013). As glycan synthesis is non-template driven and complex, it is still challenging to find the exact protein glycosylation pathways by only searching for upregulated or downregulated enzymes in the metaproteome. Nevertheless, it is uncertain which pathways are responsible for the synthesis of the glycoprotein glycans in "*Ca. Accumulibacter*", but with the current evidence, it can be suggested that these pathways may share components with the LPS biosynthesis pathway (Hug and Feldman, 2011; Szymanski, 2022).

An alternative strategy is to screen for the known glycoproteins reported in the literature in the metaproteome. It revealed the presence of potential O-linked glycoprotein candidates: flagella, PEP-CTERM proteins, and bacterial autotransporters, which have been described to be involved in biofilm-related functions. While flagella are typically associated with initial surface attachment (Guttenplan and Kearns, 2013), they may also play a role in EPS matrix stabilization (Flemming and Wingender, 2010). Their detection in this study is notable, especially since they have not been observed for "*Ca. Accumulibacter*" before, despite the presence of the biosynthesis genes (Martín et al., 2006) and its expression on the metatranscriptome (Kondrotaite et al., 2025). This suggests a potential overlooked function of the flagella protein produced by "*Ca. Accumulibacter*". PEP-CTERM proteins, recently identified as an abundant protein in a "*Ca. Accumulibacter*" culture (Olst et al., 2025), are rich in amino acids serine (Ser), threonine (Thr) and asparagine (Asn). Ser and Thr are the amino acids most commonly glycosylated in O-glycosylation, while Asn is the most common site for N-glycosylation (Haft et al., 2006; Kelly et al., 2022). These proteins have been associated with floc formation in *Zoogloea* (Gao et al., 2018). Bacterial autotransporters, a class of outer membrane proteins, possess several functions, including bacterial adhesion and cell-to-cell aggregation (Tytgat and Lebeer, 2014; Wells et al., 2007). Although lectin

microarray indicated an increased signal of glycan motifs commonly associated with O-linked glycoproteins with increasing salinity, metaproteomic data demonstrated the downregulation of flagella, PEP-CTERM protein, and bacterial autotransporters. This discrepancy is likely a reflection of the following reasons: The knowledge of bacterial glycoproteins is limited and largely based on the pathogenic model organisms, such as *Campylobacter jejuni* (Li et al., 2017; Szymanski, 2022), leaving many glycoproteins undiscovered. Thus, the three proteins above are “a small piece of an iceberg” in the glycoproteins in AGS; their change cannot represent the change of the total O-linked glycoproteins shown by the lectin microarray. On the other hand, their downregulation at higher salinity seems logical. If higher salinity may already cause aggregation of particles due decreased electrostatic repulsion, as a counter reaction, microorganisms produce EPS carrying more negatively charged groups. It is not necessary to spend energy to produce those aggregation-related glycoproteins.

#### **5.4.3 Advancing the development of methodologies in the EPS research**

These findings have practical implications for both the operation of AGS systems and resource recovery. Despite maintaining the same granule morphology, the EPS is clearly adapted at the microscale. Those EPS adaptations in the glycoconjugates suggest that microbial community can maintain granule stability and performance under elevated salinity. These changes in the EPS charge and glycoproteins composition could serve as an indicator of microbial adaptation and guide operational adjustments, particularly under saline conditions. Besides, the EPS adaptations observed in this work highlight the need for more analytical approaches to gain better understanding of the EPS. With the rapid development of omics techniques, it is important to implement these tools in EPS research. It is known that bacteria can synthesize a diverse array of glycans, being attached to proteins and lipids, or as loosely associated polysaccharides to the cells. Through metagenomics, it is possible to identify the dominance of a single species of “*Ca. Accumulibacter*” in the microbial community. Glycomics, on the other hand, is the comprehensive study of glycans, it helps understand the role of glycans in bacterial cell-cell and cell-environment interactions (Rudd et al., 2022). Furthermore, metaproteomics is the study of all proteins in microbial communities (Kleiner, 2019). Information obtained can be used to identify the composition of microbial communities, the enzymes related to metabolic pathways, and the extracellular proteins. In the current research, the high-throughput lectin microarray enables monitoring changes in glycosylation patterns of glycoproteins under various salinity conditions. It also provides insights into glycosidic linkages and helps establish correlations between salinity and protein glycosylation in the EPS. Probably, these two omics tools, glycomics and metaproteomics (Pabst et al., 2022), need to be added to the

multidisciplinary roadmap for resolving the EPS composition and function proposed by Seviour et al. (2019) (Figure 5.9).

It is worth noting that, although both lectin microarray and metaproteomics revealed significant new insights in the EPS adaptation to the increasing salinities, a few challenges remain: For the lectin microarray, the limitations mainly lie in the structural epitopes that are recognized by the lectins and their commercial availability (Poole et al., 2018). No lectins reflecting bacterial-specific glycan structures are available. Limitations of metaproteomics, on the other hand, arise from protein functional annotations (Heyer et al., 2017; Kleikamp et al., 2023). The information obtained is limited to the known pathways. This makes it challenging to connect the metabolic pathways with the specific glycan output, especially in a diverse microbial community such as the granular sludge in this research. Additionally, many glycosylation-related enzymes function across multiple glycoconjugate pathways and thus may be overlooked during the analysis. Therefore, detailed structural characterization of glycoconjugates is essential for understanding their biosynthetic pathways and roles within the EPS (Szymanski, 2022).

#### MULTIDISCIPLINARY ROADMAP (SEVIOUR ET AL. 2019)

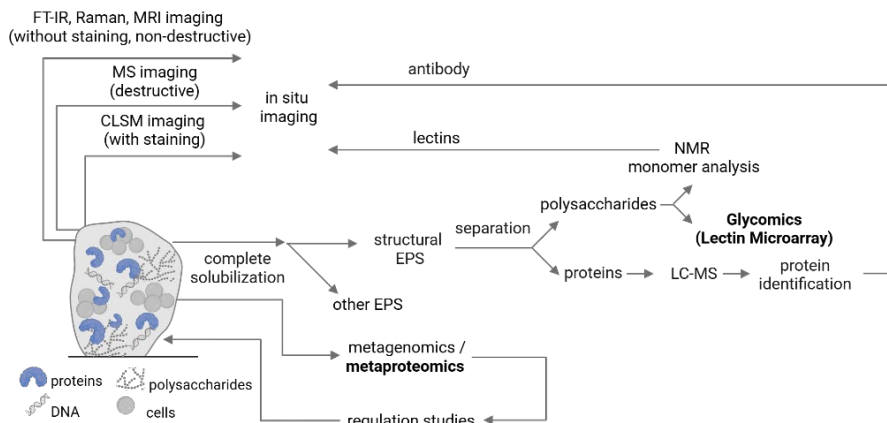


Figure 5.9. Multidisciplinary roadmap for resolving the EPS function and identity. Metaproteomic and lectin microarray are included, expanding the roadmap.

## 5.5 Conclusions

- Glycan diversity on glycoproteins decreases with increasing salinity, while the negatively charged groups, sialic acids and sulfated groups, increased.
- The increase in salinity resulted to a shift from a more diverse microbial community to a dominant community of "*Ca. Accumulibacter*".
- Increasing the negative charge in the EPS, specifically the glycoproteins, is an adaptive response towards increasing salinity by "*Ca. Accumulibacter*".
- Increased salinity induced upregulation of various glycoconjugates, including LPS and peptidoglycans.
- Flagella, bacterial autotransporters, and PEP-CTERM domain-containing proteins were identified in the AGS as putative glycoproteins using metaproteomics.

## Supplementary Materials

The Supplementary Materials of this chapter can be found at the TU Delft repository.

## References

Andrews, S. (2010). *FastQC: A quality control analysis tool for high throughput sequencing data.* <https://github.com/s-andrews/FastQC?tab=readme-ov-file#readme>

APHA. (1998). *Standard methods for the examination of water and wastewater* (20th ed.). American Public Health Association, American Water Works Association, Water Environment Federation, Washington, D.C., 1998.

Barreteau, H., Kovač, A., Boniface, A., Sova, M., Gobec, S., & Blanot, D. (2008). Cytoplasmic steps of peptidoglycan biosynthesis. *FEMS Microbiology Reviews*, 32(2), 168–207. [https://doi.org/10.1111/j.1574-6976.2008.00104.X](https://doi.org/10.1111/j.1574-6976.2008.00104.x)

Bedini, E., Corsaro, M. M., Fernández-Mayoralas, A., & Iadonisi, A. (2019). *Chondroitin, Dermatan, Heparan, and Keratan Sulfate: Structure and Functions*. 187–233. [https://doi.org/10.1007/978-3-030-12919-4\\_5](https://doi.org/10.1007/978-3-030-12919-4_5)

Bertani, B., & Ruiz, N. (2018). Function and Biogenesis of Lipopolysaccharides. *EcoSal Plus*, 8(1), 10.1128/ecosalplus.ESP-0001-2018. <https://doi.org/10.1128/ECOSALPLUS.ESP-0001-2018>

Boleij, M., Kleikamp, H., Pabst, M., Neu, T. R., van Loosdrecht, M. C. M., & Lin, Y. (2020). Decorating the Anammox House: Sialic Acids and Sulfated Glycosaminoglycans in the Extracellular Polymeric Substances of Anammox Granular Sludge. *Environmental Science & Technology*, acs.est.9b07207. <https://doi.org/10.1021/acs.est.9b07207>

Campo, R., Corsino, S. F., Torregrossa, M., & Di Bella, G. (2018). The role of extracellular polymeric substances on aerobic granulation with stepwise increase of salinity. *Separation and Purification Technology*, 195, 12–20. <https://doi.org/10.1016/j.seppur.2017.11.074>

Chatham, J. C., & Marchase, R. B. (2010). Protein O-GlcNAcylation: A critical regulator of the cellular response to stress. *Current Signal Transduction Therapy*, 5(1), 49. <https://doi.org/10.2174/157436210790226492>

Chen, L. M., Beck, P., van Ede, J., Pronk, M., van Loosdrecht, M. C. M., & Lin, Y. (2024). Anionic extracellular polymeric substances extracted from seawater-adapted aerobic granular sludge. *Applied Microbiology and Biotechnology*, 108(1), 144. <https://doi.org/10.1007/s00253-023-12954-x>

Chen, L. M., de Bruin, S., Pronk, M., Sousa, D. Z., van Loosdrecht, M. C. M., & Lin, Y. (2023a). Sialylation and Sulfation of Anionic Glycoconjugates Are Common in the Extracellular Polymeric Substances of Both Aerobic and Anaerobic Granular Sludges. *Environmental Science and Technology*, 57(35), 13217–13225. <https://doi.org/https://doi.org/10.1021/acs.est.2c09586>

Chen, L. M., Keisham, S., Tateno, H., Ede, J. van, Pronk, M., Loosdrecht, M. C. M. van, & Lin, Y. (2023b). Alterations of Glycan Composition in Aerobic Granular Sludge during the Adaptation to Seawater Conditions. *ACS ES&T Water*. <https://doi.org/10.1021/ACSESTWATER.3C00625>

Chen, S. (2023). Ultrafast one-pass FASTQ data preprocessing, quality control, and deduplication using fastp. *IMeta*, 2(2), e107. <https://doi.org/10.1002/IMT2.107>; JOURNAL L:JOURNAL:2770596X

Corsino, S. F., Capodici, M., Torregrossa, M., & Viviani, G. (2017). Physical properties and Extracellular Polymeric Substances pattern of aerobic granular sludge treating hypersaline wastewater. *Bioresource Technology*, 229, 152–159. <https://doi.org/10.1016/j.biortech.2017.01.024>

de Graaff, D. R., Felz, S., Neu, T. R., Pronk, M., van Loosdrecht, M. C. M., & Lin, Y. (2019). Sialic acids in the extracellular polymeric substances of seawater-adapted aerobic granular sludge. *Water Research*, 343–351. <https://doi.org/10.1016/j.watres.2019.02.040>

Eichler, J., & Koomey, M. (2017). Sweet New Roles for Protein Glycosylation in Prokaryotes. *Trends in Microbiology*, 25(8), 662–672. <https://doi.org/10.1016/j.tim.2017.03.001>

Felz, S., Vermeulen, P., van Loosdrecht, M. C. M., & Lin, Y. M. (2019). Chemical characterization

methods for the analysis of structural extracellular polymeric substances (EPS). *Water Research*, 157, 201–208. <https://doi.org/10.1016/j.watres.2019.03.068>

Flemming, H. C., & Wingender, J. (2010). The biofilm matrix. In *Nature Reviews Microbiology* (Vol. 8, Issue 9, pp. 623–633). Nature Publishing Group. <https://doi.org/10.1038/nrmicro2415>

Freeze, H. H., & Elbein, A. D. (2022). Glycosylation precursors. In *Essentials of Glycobiology [Internet]*. 4th edition. Cold Spring Harbor Laboratory Press.

Gao, N., Xia, M., Dai, J., Yu, D., An, W., Li, S., Liu, S., He, P., Zhang, L., Wu, Z., Bi, X., Chen, S., Haft, D. H., & Qiu, D. (2018). Both widespread PEP-CTERM proteins and exopolysaccharides are required for floc formation of Zoogloea resiniphila and other activated sludge bacteria. *Environmental Microbiology*, 20(5), 1677–1692. <https://doi.org/10.1111/1462-2920.14080>

Gunde-Cimerman, N., Plemenitaš, A., & Oren, A. (2018). Strategies of adaptation of microorganisms of the three domains of life to high salt concentrations. *FEMS Microbiology Reviews*, 42(3), 353–375. <https://doi.org/10.1093/femsre/fuy009>

Guttenplan, S. B., & Kearns, D. B. (2013). Regulation of flagellar motility during biofilm formation. *FEMS Microbiology Reviews*, 37(6), 849–871. <https://doi.org/10.1111/1574-6976.12018>

Haft, D. H., Paulsen, I. T., Ward, N., & Selengut, J. D. (2006). Exopolysaccharide-associated protein sorting in environmental organisms: The PEP-CTERM/SpsH system. Application of a novel phylogenetic profiling heuristic. *BMC Biology*, 4(1), 1–16. [https://doi.org/10.1186/1741-7007-4-29/TABLES/4](https://doi.org/10.1186/1741-7007-4-29)

Han, H., Song, B., Joon Song, M., & Yoon, S. (2019). Enhanced Nitrous Oxide Production in Denitrifying Dechloromonas aromatica Strain RCB Under Salt or Alkaline Stress Conditions. *Frontiers in Microbiology*, 10(JUN). <https://doi.org/10.3389/FMICB.2019.01203>

He, S., & McMahon, K. D. (2011). Microbiology of "Candidatus Accumulibacter" in activated sludge. In *Microbial Biotechnology* (Vol. 4, Issue 5, pp. 603–619). <https://doi.org/10.1111/j.1751-7915.2011.00248.x>

Hermansson, M. (1999). The DLVO theory in microbial adhesion. *Colloids and Surfaces B: Biointerfaces*, 14(1–4), 105–119. [https://doi.org/10.1016/S0927-7765\(99\)00029-6](https://doi.org/10.1016/S0927-7765(99)00029-6)

Heyer, R., Schallert, K., Zoun, R., Becher, B., Saake, G., & Benndorf, D. (2017). Challenges and perspectives of metaproteomic data analysis. *Journal of Biotechnology*, 261, 24–36. <https://doi.org/10.1016/j.jbiotec.2017.06.1201>

Howard, S. L., Jagannathan, A., Soo, E. C., Hui, J. P. M., Aubry, A. J., Ahmed, I., Karlyshev, A., Kelly, J. F., Jones, M. A., Stevens, M. P., Logan, S. M., & Wren, B. W. (2009). Campylobacter jejuni glycosylation island important in cell charge, legionaminic acid biosynthesis, and colonization of chickens. *Infection and Immunity*, 77(6), 2544–2556. [https://doi.org/10.1128/IAI.01425-08/ASSET/2C99F5B4-D3AB-409E-8DDA-545A901E7DBB/ASSETS/GRAPHIC/ZII0060979990007.jpeg](https://doi.org/10.1128/IAI.01425-08)

Hug, I., & Feldman, M. F. (2011). Analogies and homologies in lipopolysaccharide and glycoprotein biosynthesis in bacteria. *Glycobiology*, 21(2), 138–151. <https://doi.org/10.1093/GLYCOB/CWQ148>

Kaminski, L., Guan, Z., Yurist-Doutsch, S., & Eichler, J. (2013). Two Distinct N-Glycosylation Pathways Process the Haloferax volcanii S-Layer Glycoprotein upon Changes in Environmental Salinity. *MBio*, 4(6). <https://doi.org/10.1128/MBIO.00716-13>

Kang, D. D., Li, F., Kirton, E., Thomas, A., Egan, R., An, H., & Wang, Z. (2019). MetaBAT 2: An adaptive binning algorithm for robust and efficient genome reconstruction from metagenome assemblies. *PeerJ*, 2019(7), e7359. <https://doi.org/10.7717/PEERJ.7359/SUPP-3>

Kelly, J., Vinogradov, E., Robotham, A., Tessier, L., Logan, S. M., & Jarrell, K. F. (2022). Characterizing the N- and O-linked glycans of the PGF-CTERM sorting domain-containing S-layer protein of *Methanoculleus marisnigri*. *Glycobiology*, 32(7), 629–644. <https://doi.org/10.1093/GLYCOB/CWAC019>

Kleikamp, H. B. C., Grouzdev, D., Schaasberg, P., van Valderen, R., van der Zwaan, R., Wijgaart, R. van de, Lin, Y., Abbas, B., Pronk, M., van Loosdrecht, M. C. M., & Pabst, M. (2023). Metaproteomics, metagenomics and 16S rRNA sequencing provide different perspectives on the aerobic granular sludge microbiome. *Water Research*, 246, 120700. <https://doi.org/10.1016/J.WATRES.2023.120700>

Kleine, G. Y., Wilfert, P. K., & Picken, S. J. (2025). Quantifying Charge Density in Complex Biopolymer Systems via Conductometric Titration. *ACS Omega*. <https://doi.org/10.1021/AC SOMEAGA.5C07186>

Kleiner, M. (2019). Metaproteomics: Much More than Measuring Gene Expression in Microbial Communities. *MSystems*, 4(3). <https://doi.org/10.1128/MSYSTEMS.00115-19/ASSET/AD6943B7-5C75-4ABB-8897-F622F004750A/ASSETS/GRAPHIC/MSYSTEMS.00115-19-F0001.JPG>

Kondrotaite, Z., Petersen, J., Singleton, C., Peces, M., Petriglieri, F., Jensen, T. B. N., Sereika, M., Daugberg, A. O. H., Wagner, M., Dueholm, M. K. D., Nielsen, P. H., & Rodrigues, J. L. M. (2025). Ecophysiology and niche differentiation of three genera of polyphosphate-accumulating bacteria in a full-scale wastewater treatment plant. *MSystems*. <https://doi.org/10.1128/MSYSTEMS.00322-25>

Lees-Miller, R. G., Iwashkiw, J. A., Scott, N. E., Seper, A., Vinogradov, E., Schild, S., & Feldman, M. F. (2013). A common pathway for O-linked protein-glycosylation and synthesis of capsule in *Acinetobacter baumannii*. *Molecular Microbiology*, 89(5), 816–830. [https://doi.org/10.1111/MMI.12300/SUPPI\\_NFO](https://doi.org/10.1111/MMI.12300/SUPPI_NFO)

Lefebvre, O., & Moletta, R. (2006). Treatment of organic pollution in industrial saline wastewater: A literature review. *Water Research*, 40(20), 3671–3682. <https://doi.org/10.1016/J.WATRES.2006.08.027>

Li, H., Debowski, A. W., Liao, T., Tang, H., Nilsson, H. O., Marshall, B. J., Stubbs, K. A., & Benghezal, M. (2017). Understanding Protein Glycosylation Pathways in Bacteria. *Future Microbiology*, 12(1), 59–72. <https://doi.org/10.2217/FMB-2016-0166>

Li, Z., Hwang, S., & Bar-Peled, M. (2016). Discovery of a Unique Extracellular Polysaccharide in Members of the Pathogenic Bacillus That Can Co-form with Spores. *Journal of Biological Chemistry*, 291(36), 19051–19067. <https://doi.org/10.1074/JBC.M116.724708>

Martín, H. G., Ivanova, N., Kunin, V., Warnecke, F., Barry, K. W., McHardy, A. C., Yeates, C., He, S., Salamov, A. A., Szeto, E., Dalin, E., Putnam, N. H., Shapiro, H. J., Pangilinan, J. L., Rigoutsos, I., Kyriides, N. C., Blackall, L. L., McMahon, K. D., & Hugenholtz, P. (2006). Metagenomic analysis of two enhanced biological phosphorus removal (EBPR) sludge communities. *Nature Biotechnology*, 24(10), 1263–1269. <https://doi.org/10.1038/nbt1247>

Martinez, S. T. (2023). Extracellular Polymeric Substances of "Candidatus Accumulibacter": Composition, application and turnover. <https://doi.org/10.4233/UUID:88CE92A5-153E-47E4-BB21-999237161AB7>

Meldrum, O. W., Yakubov, G. E., Bonilla, M. R., Deshmukh, O., McGuckin, M. A., & Gidley, M. J. (2018). Mucin gel assembly is controlled by a collective action of non-mucin proteins, disulfide bridges,  $\text{Ca}^{2+}$ -mediated links, and hydrogen bonding. *Scientific Reports*, 8(1), 1–16. <https://doi.org/10.1038/s41598-018-24223-3>

Mengele, R., & Sumper, M. (1992). Drastic differences in glycosylation of related S-layer glycoproteins from moderate and extreme halophiles. *Journal of Biological Chemistry*, 267(12), 8182–8185. [https://doi.org/10.1016/S0021-9258\(18\)42424-6](https://doi.org/10.1016/S0021-9258(18)42424-6)

Nothaft, H., & Szymanski, C. M. (2010). Protein glycosylation in bacteria: sweeter than ever. *Nature Reviews Microbiology* 2010 8:11, 8(11), 765–778. <https://doi.org/10.1038/nrmicro2383>

Nurk, S., Meleshko, D., Korobeynikov, A., & Pevzner, P. A. (2017). MetaSPAdes: A new versatile metagenomic assembler. *Genome Research*, 27(5), 824–834. <https://doi.org/10.1101/GR.213959.116/-/DC1>

Olst, B. van, Eerden, S. A., Eštok, N. A., Roy, S., Abbas, B., Lin, Y., Loosdrecht, M. C. M. van, & Pabst, M. (2025). Metaproteomic Profiling of the Secretome of a Granule-forming Ca. Accumulibacter Enrichment.

## 5. Extracellular polymeric substances in aerobic granular sludge under increasing salinity conditions

PROTEOMICS, e202400189.  
<https://doi.org/10.1002/PMIC.202400189>

Ou, D., Li, W., Li, H., Wu, X., Li, C., Zhuge, Y., & Liu, Y. di. (2018). Enhancement of the removal and settling performance for aerobic granular sludge under hypersaline stress. *Chemosphere*, 212, 400–407. <https://doi.org/10.1016/J.CHEMOSPHERE.2018.08.096>

Pabst, M., Grouzdev, D. S., Lawson, C. E., Kleikamp, H. B. C., de Ram, C., Louwen, R., Lin, Y. M., Lücker, S., van Loosdrecht, M. C. M., & Laureni, M. (2022). A general approach to explore prokaryotic protein glycosylation reveals the unique surface layer modulation of an anammox bacterium. *The ISME Journal*, 16(2), 346–357. <https://doi.org/10.1038/S41396-021-01073-Y>

Páez-Watson, T., Tomás-Martínez, S., de Wit, R., Keisham, S., Tateno, H., van Loosdrecht, M. C. M., & Lin, Y. (2024). Sweet Secrets: Exploring Novel Glycans and Glycoconjugates in the Extracellular Polymeric Substances of "Candidatus Accumulibacter." *ACS ES and T Water*, 4(8), 3391–3399. [https://doi.org/10.1021/ACSESTWATER.4C00247/ASSET/IMAGES/LARGE/EW4C00247\\_0005.JPG](https://doi.org/10.1021/ACSESTWATER.4C00247/ASSET/IMAGES/LARGE/EW4C00247_0005.JPG)

Poole, J., Day, C. J., Von Itzstein, M., Paton, J. C., & Jennings, M. P. (2018). Glycointeractions in bacterial pathogenesis. *Nature Reviews Microbiology* 2018 16:7, 16(7), 440–452. <https://doi.org/10.1038/s41579-018-0007-2>

Pronk, M., de Kreuk, M. K., de Bruin, B., Kamminga, P., Kleerebezem, R., & van Loosdrecht, M. C. M. (2015). Full scale performance of the aerobic granular sludge process for sewage treatment. *Water Research*, 84, 207–217. <https://doi.org/10.1016/j.watres.2015.07.011>

Rudd, P. M., Karlsson, N. G., Khoo, K.-H., Thaysen-Andersen, M., Wells, L., & Packer, N. H. (2022). Glycomics and Glycoproteomics. *Essentials of Glycobiology*. <https://doi.org/10.1101/GLYCOBIOLOGY.4E.51>

Samuel, G., & Reeves, P. (2003). Biosynthesis of O-antigens: genes and pathways involved in nucleotide sugar precursor synthesis and O-antigen assembly. *Carbohydrate Research*, 338(23), 2503–2519.

<https://doi.org/10.1016/J.CARRES.2003.07.009>

Schäffer, C., & Messner, P. (2017). Emerging facets of prokaryotic glycosylation. *FEMS Microbiology Reviews*, 41(1), 49. <https://doi.org/10.1093/FEMSR/FUW036>

Seemann, T. (2014). Prokka: rapid prokaryotic genome annotation. *Bioinformatics*, 30(14), 2068–2069. <https://doi.org/10.1093/BIOINFORMATICS/BTU153>

Seviour, T., Derlon, N., Dueholm, M. S., Flemming, H.-C., Girbal-Neuhauser, E., Horn, H., Kjelleberg, S., van Loosdrecht, M. C. M., Lotti, T., Malpei, M. F., Nerenberg, R., Neu, T. R., Paul, E., Yu, H., & Lin, Y. (2019). Extracellular polymeric substances of biofilms: Suffering from an identity crisis. *Water Research*, 151, 1–7. <https://doi.org/10.1016/j.watres.2018.11.020>

Szymanski, C. M. (2022). Bacterial glycosylation, it's complicated. *Frontiers in Molecular Biosciences*, 9, 1015771. <https://doi.org/10.3389/FMOLB.2022.1015771/BIBTEX>

Talari, A. C. S., Martinez, M. A. G., Movasagh, Z., Rehman, S., & Rehman, I. U. (2016). Advances in Fourier transform infrared (FTIR) spectroscopy of biological tissues. <https://doi.org/10.1080/05704928.2016.1230863>, 52(5), 456–506. <https://doi.org/10.1080/05704928.2016.1230863>

Tateno, H., Toyota, M., Saito, S., Onuma, Y., Ito, Y., Hiemori, K., Fukumura, M., Matsushima, A., Nakanishi, M., Ohnuma, K., Akutsu, H., Umezawa, A., Horimoto, K., Hirabayashi, J., & Asashima, M. (2011). Glycome diagnosis of human induced pluripotent stem cells using lectin microarray. *Journal of Biological Chemistry*, 286(23), 20345–20353. <https://doi.org/10.1074/jbc.M111.231274>

Thoden, J. B., & Holden, H. M. (2011). Biochemical and structural Characterization of WlbA from *Bordetella pertussis* and *Chromobacterium violaceum*: Enzymes required for the biosynthesis of 2,3-diacetamido-2,3-dideoxy-d-mannuronic acid. *Biochemistry*, 50(9), 1483–1491. [https://doi.org/10.1021/BI101871F/ASSET/IMAGES/LARGE/BI-2010-01871F\\_0007.JPG](https://doi.org/10.1021/BI101871F/ASSET/IMAGES/LARGE/BI-2010-01871F_0007.JPG)

Tytgat, H. L. P., & Lebeer, S. (2014). The Sweet Tooth of Bacteria: Common Themes in Bacterial Glycoconjugates. *Microbiology and Molecular Biology Reviews: MMBR*, 78(3), 372. <https://doi.org/10.1128/MMBR.00007-14>

Valvano, M. A., Messner, P., & Kosma, P. (2002). Novel pathways for biosynthesis of nucleotide-activated glycero-manno-heptose precursors of bacterial glycoproteins and cell surface polysaccharides. *Microbiology*, 148(7), 1979–1989. <https://doi.org/10.1099/00221287-148-7-1979> CITE/REFWORKS

van Ede, J. M., Soic, D., & Pabst, M. (2025). Decoding Sugars: Mass Spectrometric Advances in the Analysis of the Sugar Alphabet. *Mass Spectrometry Reviews*, 1–52. <https://doi.org/10.1002/MAS.21927>; PAGE: STRING:ARTICLE/CHAPTER

Varki, A., & Schauer, R. (2009). Sialic Acids, chapter 14. *Essentials of Glycobiology*, 9, 1–19.

Varki, A., Cummings, R. D., Esko, J. D., Stanley, P., Hart, G. W., Aebi, M., Darvill, A. G., Kinoshita, T., Packer, N. H., Prestegard, J. H., Schnaar, R. L., & Seeberger, P. H. (2017a). Essentials of Glycobiology. *Cold Spring Harbor (NY)*, 823.

Varki, A., Schnaar, R. L., & Schauer, R. (2017b). *Sialic Acids and Other Nonulosonic Acids*. <https://doi.org/10.1101/GLYCOBIOLOGY.3.E.015>

Vishniac, W., & Santer, M. (1957). The thiobacilli. *Bacteriological Reviews*, 21(3), 195–213. <https://doi.org/10.1128/BR.21.3.195-213.1957>

Welles, L., Lopez-Vazquez, C. M., Hooijmans, C. M., van Loosdrecht, M. C. M., & Brdjanovic, D. (2014). Impact of salinity on the anaerobic metabolism of phosphate-accumulating organisms (PAO) and glycogen-accumulating organisms (GAO). *Applied Microbiology and Biotechnology*, 98(17), 7609–7622. <https://doi.org/10.1007/s00253-014-5778-4>

Wells, T. J., Tree, J. J., Ulett, G. C., & Schembri, M. A. (2007). Autotransporter proteins: novel targets at the bacterial cell surface. *FEMS Microbiology Letters*, 274(2), 163–172. <https://doi.org/10.1111/j.1574-6968.2007.00833.x>

Wood, D. E., Lu, J., & Langmead, B. (2019). Improved metagenomic analysis with Kraken



Identification of a surface protein  
in the extracellular polymeric  
substances of seawater-adapted  
aerobic granular sludge

6

## Abstract

Identifying structural proteins within the extracellular polymeric substances (EPS) will provide a better understanding of the stability of aerobic granular sludge and biofilms in general. In this work, an abundant surface protein was identified and localized in the extracellular matrix of seawater-adapted AGS. Granules with good phosphate removal were cultivated in a sequencing batch bubble column reactor with acetate as a carbon source dissolved in seawater. *“Candidatus Accumulibacter”* was observed as the most dominant community member through fluorescent *in-situ* hybridization. A surface protein of 74.5 kDa was identified in the EPS extract of the seawater-adapted AGS by SDS-PAGE and mass spectrometry. The surface protein was produced by an Accumulibacter species and showed homology to S-layer proteins. A type 1 secretion system was found adjacent to the gene encoding for the surface protein, suggesting a possible export system. Antibodies generated from a unique peptide of the surface protein confirmed the extracellular location of the surface protein. Microscopy observations with antibody staining showed the surface protein forms dense structures within the Accumulibacter microcolonies and larger fiber structures around the microcolonies. These observations highlight the importance of the protein for the structural properties of the granule. To detect more structural proteins in the EPS, optimization of the EPS extraction and *in situ* imaging validation methods are essential.

## Published as:

Chen, L. M., Hofstra, T., Langedijk, J., Andrei, S., Pabst, M., Pronk, M., van Loosdrecht, M. C. M., & Lin, Y. (2025). Identification of a surface protein in the extracellular polymeric substances of seawater-adapted aerobic granular sludge. *Water Research*, 124187. <https://doi.org/10.1016/J.WATRES.2025.124187>

## 6.1 Introduction

With the increasing global shortage of freshwater, the use of seawater has become an attractive solution for various applications, including fire control, road and toilet flushing in coastal cities (Zhang et al., 2023a, 2023b). Moreover, industries such as leather-, food-processing, and pharmaceutical industries, may discharge saline wastewater due to the processing (Lefebvre and Moletta, 2006; Zhao et al., 2020a). The saline wastewater will be discharged into wastewater treatment plants for further treatment.

Among all the treatment processes, aerobic granular sludge (AGS) technology has emerged as a promising technology to treat saline wastewaters (Bassin et al., 2011; de Graaff et al., 2020a; Zhao et al., 2020b), thanks to its reduction in area usage, lower energy costs and potential for resource recovery (Van Loosdrecht and Brdjanovic, 2014; Pronk et al., 2015). In the AGS process, granules with microorganisms embedded in a self-produced matrix of extracellular polymeric substances (EPS) are formed. The EPS keeps the stability of the granules and protects the microorganisms from harsh environmental conditions, such as salinity in the form of seawater or NaCl (Decho and Gutierrez, 2017). The stabilizing mechanism of EPS is still unknown, which is largely due to the uncharacterized nature of the EPS matrix (Seviour et al., 2019).

The EPS is composed of various components, such as polysaccharides, extracellular enzymes, and structural proteins. These components interact together to form a matrix supporting microbial growth under dynamic and stressful environments (Flemming and Wingender, 2010). Studies on AGS adapting to saline conditions have shown an increase in EPS, protein content, and hydrophobicity at higher salinities (Campo et al., 2018; Corsino et al., 2017; Ou et al., 2018). Notably, proteins make up to 40% of the extracted EPS and are found to play an important structural role in AGS stability (Felz et al., 2016; McSwain et al., 2005; Zhu et al., 2015). In addition, specific structural proteins have been linked to the stability of granular sludge. Amyloid proteins have been identified to play a structural role in AGS enriched with ammonia-oxidizing bacteria (Lin et al., 2018). Similarly, glycosylated S-layer proteins have been found to form a large fraction of the EPS in anammox granules acting as an adhesive and facilitating assembly with other community members (Boleij et al., 2018; Pabst et al., 2022; Wong et al., 2023). These reports highlight the importance of (structural) proteins in the EPS of granular sludge. However, no structural proteins have been identified in saline AGS to date.

Identification of EPS components involved in seawater AGS, especially (structural) proteins, will not only expand our database of important EPS components, but also allow a better understanding of the role that the EPS plays in maintaining the

stability of AGS. Insight into EPS composition and their interactions within the extracellular matrix may reveal their functions. Understanding of these functions and how they are regulated could generate knowledge on a better control of AGS process. Additionally, this may also open new opportunities and/or strategies for recovering EPS as a sustainable resource (Seviour et al., 2019). Therefore, the goal of this work was to identify the extracellular protein(s) in seawater-adapted AGS, visualize its distribution *in situ*, and understand its potential role in the granule. To this end, the extracellular proteins were extracted from AGS and an abundant protein was identified using mass spectrometry. *In situ* immunostaining was performed to localize the dominant protein.

## 6.2 Material and Methods

### 6.2.1 Reactor operation and microbial community analysis

#### Reactor operation

Aerobic granular sludge was cultivated in a 2.8 L bubble column (6.5 cm diameter) as a sequencing batch reactor (SBR) as adapted from (de Graaff et al., 2019). The seawater-adapted reactor was inoculated with 600 mL 1:1 volume ratio activated sludge from the wastewater treatment plant in Harnaschpolder the Netherlands and full-scale Nereda® sludge from Utrecht, the Netherlands. The temperature of the reactor was controlled by controlling the room temperature at 20°C. The pH was controlled at pH  $7.3 \pm 0.1$  by dosing either 1.0 M NaOH or 1.0 M HCl. The dissolved oxygen (DO) was controlled by a mixture of nitrogen gas and air at 0% and 80% (5.9 mg O<sub>2</sub>/L in seawater) in the anaerobic and aerobic phases, respectively.

Reactor cycles consisted of 5 min settling, 5 min effluent withdrawal, 5 min N<sub>2</sub> sparging, 5 min of feeding, 50 min N<sub>2</sub> gas sparging (anaerobic phase), and 110 min of aeration (aerobic phase). The average sludge retention time (SRT) was kept at 13  $\pm 1$  days by manual sludge removal for both reactors. Granules were samples for analysis at least 3 months of steady reactor performance in growth and phosphate removal for the first and second reactor, respectively.

The feed of 1.5 L per cycle consisted of 1.2 L artificial seawater (final concentration 30 g/L, Instant Ocean®), 150 mL of medium A and 150 mL of medium B. Medium A was composed of 62.5 mM of sodium acetate trihydrate. Medium B contained 41.13 mM of NH<sub>4</sub>Cl, 0.34 mM of K<sub>2</sub>HPO<sub>4</sub>, 0.27 mM of KH<sub>2</sub>PO<sub>4</sub>, 0.07 mM of allylthiourea and 10 mL/L of trace elements solution similar to Vishniac & Santer (1957), but using 2.2 g/L of ZnSO<sub>4</sub>·7H<sub>2</sub>O instead of 22 g/L and 2.18 g/L of Na<sub>2</sub>MoO<sub>4</sub>·2H<sub>2</sub>O instead of (NH<sub>4</sub>)<sub>6</sub>Mo<sub>7</sub>O<sub>24</sub>·4H<sub>2</sub>O. The combination of these feed streams led to influent concentrations of 400 mg/L COD, 50 mg/L NH<sub>4</sub>-N, and 12.2 mg/L PO<sub>4</sub>-P. To monitor the performance of the reactor, samples were taken at certain intervals and filtered through a 0.22  $\mu$ m PVDF filter. Acetate concentration was measured through high-

performance liquid chromatography, HPLC, (Thermo Scientific Vanquish HPLC) at 50°C (0.75 mL/min) with 1.5 mM phosphoric acid as eluent and Aminex HPC-87H (Bio-Rad, California, USA) as a column. Phosphate and ammonia concentrations were measured using a Thermo Fisher Gallery Discrete Analyzer (Thermo Fisher Scientific, Waltham, USA).

The organic and ash fractions of the biomass were determined according to the standard methods (APHA, 1998). Pictures of the granules were taken with a stereo zoom microscope (M205 FA, Leica Microsystems, Germany) connected to the Eert Vision Auto Focus Microscope camera (Eert Vision, The Netherlands), and the images were acquired with the Eert C304 software (V1.0, Eert Vision, The Netherlands). For protein extraction, the granules were rinsed with demi water to remove excess salt, lyophilized immediately, and stored at room temperature.

#### **Microbial community analysis by fluorescent in-situ hybridization (FISH)**

The granules were collected from the reactor at the end of the aerobic phase. The handling, fixation and staining of FISH samples were performed as described in (Bassin et al., 2011). The PAO651 probe was used for visualizing the polyphosphate accumulating organism (PAO), “*Candidatus Accumulibacter*” (Albertsen et al., 2016). The GAOmix (GAOQ431 and GAOQ989) was used for visualizing glycogen accumulating organisms (GAO) (Crocetti et al., 2000). EUBmix (EUB338, EUB338-II and EUB338- III) were used for staining all bacteria (Amann et al., 1990; Daims et al., 1999). Images were taken with a Zeiss Axio Imager M2 microscope equipped with the fluorescent light source X-Cite Xylis 720L. The image acquisition was performed with the Zeiss Axiocam 705 mono camera. The images were processed and exported in .tif format with the Zeiss microscopy software (ZEN version 3.3).

#### **6.2.2 Isolation and identification of the abundant EPS proteins**

##### **Protein extraction and gel-electrophoresis**

Optimization of the extraction method was first performed by varying the type of biomass (wet pellet, lyophilized granules), the concentration of lyophilized granules (3.2 – 12.8 mg/mL), temperature (5, 20, 60 and 80°C), chemical (NaCl, Na<sub>2</sub>CO<sub>3</sub>) and time (1, 6, and 24 hours) while assessing the intact protein bands on the SDS-PAGE. The optimal extraction condition was considered if the extraction method yielded the strongest protein bands on the SDS-PAGE. The optimal extraction method was found as follows: lyophilized granules of the first seawater-adapted reactor were crushed and extracted 0.5% w/v Na<sub>2</sub>CO<sub>3</sub> (Felz et al., 2016) at a concentration of 12.8 mg lyophilized biomass / mL. The extraction was performed overnight (approx. 15 hours) while stirring at 400 rpm at room temperature (20°C). After the extraction, the pellet was discarded by centrifuging at 14.000 ×g for 5 min at 5°C. The extracted proteins in the supernatant were denatured in dithiothreitol (12.5 mM) and NuPAGE LDS Sample Buffer 4x (Thermofischer Scientific) at 70°C for 10 min. 10 µL

of each sample was loaded on the NuPage ® Novex 4-12% Bis-Tris gels (Invitrogen). The Multicolor Broad Range Protein ladder (Thermofischer Scientific) was used as a molecular weight marker. The electrophoresis was performed for 35 min at 200V in NuPAGE MES SDS running buffer (Thermofischer Scientific). The gel was stained by either Coomassie Blue (Simply Blue, Invitrogen) or PAS staining (Pierce Glycoprotein Staining Kit), both following the manufacturer's instructions. The gels were visualized on a ChemiDoc MP Imaging System (Bio-Rad, Hercules, CA).

### **In-gel digestion**

Sample preparation and proteomics analysis of SDS-PAGE separated samples were performed as described in Pabst et al. (2022). SDS-PAGE analysis and in-gel digestion. To extract the peptides from the gel, the gel band was first cut out from the Coomassie-stained gel into smaller pieces and destained in destaining solution (100 mM NH<sub>4</sub>HCO<sub>3</sub> in 40% acetonitrile, ACN) for 15 min at room temperature. The destained gel pieces were incubated in the following solutions step-by-step as follows: 1) 200 µL 100% ACN for 10 minutes at room temperature for dehydration. 2) 200 µL 10 mM DTT in 100 mM NH<sub>4</sub>HCO<sub>3</sub> for 30 minutes at 56°C at 300 rpm for reduction of the cysteine residues. 3) Alkylation of the cysteine residues was performed by adding 200 µL of freshly prepared 55 mM iodoacetamide in 100 mM NH<sub>4</sub>HCO<sub>3</sub> for 30 min at room temperature in the dark. The alkylation solution was replaced by destaining solution for 5 minutes at room temperature. The gel pieces were dehydrated again as described above. The dehydrated gel pieces were rehydrated in 98 µL of 100 mM NH<sub>4</sub>HCO<sub>3</sub> and 2 µL digestion solution (Trypsin Sequencing Grade, Promega, 0.1 µg/µL in 1 mM HCl in LC-MS H<sub>2</sub>O). The sample was digested overnight (approx. 18 hours) at 37°C and 300 rpm. After the digestion, the solution was collected. The in-gel peptides were further extracted using 150 µL of peptide extraction solution (70% ACN with 5% formic acid, FA, in water) for 15 min at 37°C, collecting the solution. Then another extraction was followed using 100 µL solution of 10:90 ACN:water for incubated for 15 minutes at 37°C and collected. The extracted sample (approx. 450 µL) was subsequently dried in the SpeedVac concentrator (SPD1010-230, Thermo Scientific) at 45°C for approximately 2 hours. Finally, the sample was re-dissolved in 20 µL 3% ACN, 0.1% FA in H<sub>2</sub>O prior to injection into the mass spectrometer.

### **Shotgun proteomics and data processing**

The purified peptides were analyzed using a Q Exactive plus Hybrid Quadrupole-Orbitrap Mass Spectrometer (Thermo Scientific, Germany) connected online to an EASY-nLC 1200 system (Thermo Scientific, Germany). Chromatographic separation employed an Acclaim PepMap RSLC RP C18 separation column (50 µm x 150 mm, 2 µm) with solvents A (1% ACN, 0.1% FA) and B (80% ACN, 0.1% FA). A gradient from 5% to 35% B over 88 minutes, followed by a linear gradient up to 65% B over

another 30 minutes, was maintained at a constant flow rate of 350 nL/min. Approximately 4  $\mu$ L of the proteolytic digest each was injected. Electrospray ionization was performed in positive ionization mode, and MS1 analysis was executed at a resolution of 70 K, with an AGC target of 3.0E6 and a maximum IT of 75 ms. The top 10 signals were selected for fragmentation, using an isolation window of 2.5 m/z. HCD fragmentation was performed using an NCE of 28. For MS2 analysis, a resolution of 17.5 K, an AGC target of 2.0E5, and a maximum IT of 100 ms were employed.

Mass spectrometric raw data were database searched using PEAKS X (Bioinformatics Solutions Inc., Canada) and a database constructed from whole metagenome sequencing experiments of a “*Ca. Accumulibacter*” enrichment (Kleikamp et al., 2021), complemented with *Candidatus Accumulibacter* sequences obtained from UniprotKB, allowing for a 20 ppm parent ion and 0.02 m/z fragment ion mass error, 3 missed cleavages, carbamidomethylation as fixed and methionine oxidation and N/Q deamidation as variable modifications. Peptide spectrum matches were filtered for 1% false discovery rate and protein identifications with  $\geq$  2 unique peptides were considered significant. Analysis for the glycosylation was performed as described recently (Pabst et al., 2022).

## 6

### Homology search

The obtained protein sequence was identified using the BLAST tool on NCBI and Uniprot using the standard parameters. The protein query was searched against the non-redundant protein sequences (nr) database and UniprotKB reference proteomes + Swiss-Prot, for NCBI and Uniprot, respectively. The identified protein (WP\_313950548.1) was found in the CDS region (NZ\_JAVTWB010000028.1) in the nucleotide of the genome assembly ASM3222952v1.

#### 6.2.3 In situ visualization of the identified extracellular protein

##### Antibody generation

The selected two unique peptides (Supplementary Materials S2) of the identified protein was generated and immunized on rabbits by David's Biotechnology (Regensburg, Germany). The immunization schedule protocol followed 5 immunizations (Day 1, 14, 28, 42 and 56), where on Day 35 a test bleed was performed to monitor antibody titer development. The final bleed was performed on Day 63. Affinity purification was performed to obtain a specific polyclonal antibody fraction at a concentration of 0.68 mg/mL.

##### Immunoblotting

To determine the antibody specificity the purified antibody fraction was subjected to Western Blotting. After gel electrophoresis as described in section 6.2.2, the gel was transferred onto the Trans-Blot Turbo Mini PVDF membranes with a pore size

of 0.2  $\mu$ m (Bio-Rad, Hercules, CA). The proteins were transferred to the membrane at 25V for 15 min at room temperature using the Trans-Blot® Turbo Transfer system (Bio-Rad, Hercules, CA).

After blotting, 100 ng of the generated peptides were added on the membrane as a positive control. The blot was cut into strips and blocked at room temperature for 1 hour in blocking buffer consisting of 5% (w/v) skim milk powder in TBS-T (Tris 20 mM, NaCl 150 mM, pH 7.6, 0.1% (w/v) Tween-20). The membrane strips were washed in 5 mL TBS-T three times for 5 min. The primary antibody was diluted to 0.01 mg/mL in TBS-T and from there the optimal dilution of 1:500 (final concentration 20 ng/ $\mu$ L) was used to incubate the membrane overnight at 4°C. The optimal concentrations of primary antibody was determined by blotting using sequential concentrations of the primary antibody (1:500 – 1:15.000) and evaluating the blot intensity. The membrane was washed in six times 5 mL TBS-T for 5 min and incubated with 10.000-fold diluted Goat Ant-Rabbit IgG conjugated to horse radish peroxide (HRP) in TBS-T (final concentration 80 ng/mL) for 1 hour at room temperature. The membrane strips were washed in 5 mL TBS-T three times for 5 min. Afterwards, they were treated with 1 mL of HRP substrate (Immobilon® Crescendo Western HRP Substrate, Sigma-Aldrich) and visualized by chemiluminescence on the ChemiDoc MP Imaging System (Bio-Rad, Hercules, CA). Only one peptide was shown to be specific for the target protein, thus this was used for the subsequent immunostaining analysis. To confirm unspecific binding of the secondary antibody, a control was performed omitting the primary antibody (Supplementary Materials Figure S4)

### **Granule slicing**

Detailed methodology of granule slicing can be found Langedijk et al. (in preparation). Paraformaldehyde fixated granules were embedded in 5% (w/v) agarose dissolved in demi water. The sample was attached to the vibratome (700smz-2 Vibratome, Campden Instruments, England) using cyanoacrylate glue and covered with seawater (Instant Ocean 30 g/L). The granule was cut into 10  $\mu$ m slices at 0.5 mm/s and 50 Hz with a ceramic blade (Campden Instruments, England). The slices were collected on an Epredia™ SuperFrost™ Plus adhesion slides (Thermo Fisher Scientific, Waltham, MA) and dried to immobilize the slice to the slide.

### **Immunostaining**

To visualize the surface protein, immunostaining was performed on sliced and potted granules. The slides with either the slices or potted granules were dehydrated sequentially in 50%, 80%, and 96% (v/v) ethanol for 3 min each and air-dried. The immunostaining was followed similar to Wong et al. (2023). The optimal concentration of primary antibody (1:680) was determined after performing the immunostaining with different conditions. 5% BSA was used due to

the autofluorescence signal of the milk proteins in the same wavelength as the secondary antibody probe.

The slide was blocked overnight in a blocking buffer (5% w/v BSA in TBS-T) at 4°C with gentle shaking. The primary antibody was diluted to 1 µg/mL (1:680) in blocking buffer, 1 mL was added to cover the entire slide, and incubated for 1.5 h at room temperature with gentle shaking. The slide was washed in 20 mL of TBS-T three times for 5 min and air-dried. The secondary antibody, goat anti-rabbit IgG (H + L) – AlexaFluor488 (Thermo Fischer Scientific, Waltham, MA), was diluted 1:500 (final concentration 4 µg/mL) in blocking buffer and 250 µL was added on top of the slices and incubated for 1 h in a humidity chamber at room temperature in the dark. The slide was washed in 20 mL of TBS-T three times for 5 min and air-dried, followed by fixation with 4% paraformaldehyde for 10 min at room temperature. The fixed slide was rinsed with PBS followed by demi-water to remove the excess paraformaldehyde and salts. The fixed slide was dehydrated sequentially in 50%, 80%, and 96% (v/v) ethanol for 3 min each and air-dried followed by the FISH protocol as described in section 6.2.1, omitting the fluorescein (498/517 ex/em) probe. As a negative control, the primary antibody was omitted (Supplementary Materials S5). Images were taken with a Zeiss Axio Imager M2 microscope equipped with the fluorescent light source X-Cite Xylis 720L. The image acquisition was performed with the Zeiss Axiocam 705 mono camera. The images were processed and exported in .tif format with the Zeiss microscopy software (ZEN version 3.3).

## 6.3 Results

### 6.3.1 Reactor operation and Microbial Community Analysis by Fluorescent In Situ Hybridization (FISH)

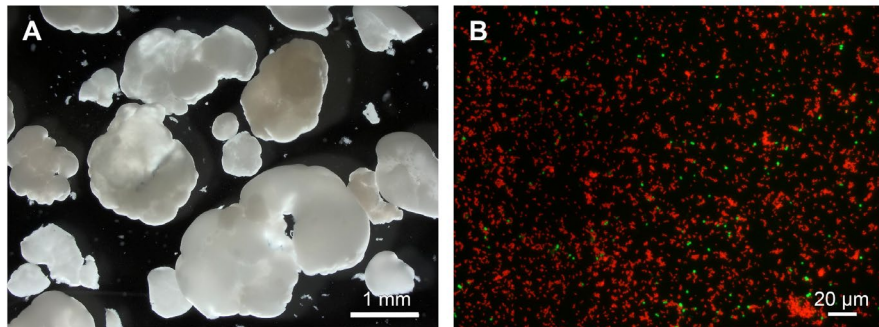
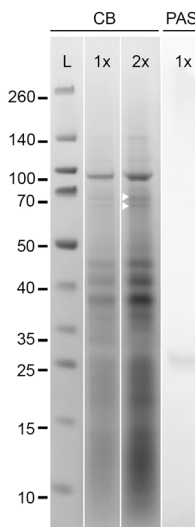


Figure 6.1. Stereozoom pictures of aerobic granular sludge grown under seawater conditions (A). Fluorescent in-situ hybridization (FISH) PAO651 in red and GAOmix in green of disintegrated seawater granular sludge (B).

The seawater-adapted AGS reactor showed good granule formation and enhanced phosphate removal performance. The granules had a size range of 0.5 – 3 mm in diameter (Figure 6.1A). The phosphate release and acetate uptake during a typical cycle corresponded to a P:C ratio of 0.40 P-mol / C-mol. Similar ratios were observed in other AGS studies with a dominant population of the phosphate accumulating organism (PAO) “*Candidatus Accumulibacter*” (“*Ca. Accumulibacter*”) (de Graaff et al., 2019; Weissbrodt et al., 2014; Welles et al., 2015). FISH analysis revealed a dominance of PAO “*Ca. Accumulibacter*” in the microbial community, whereas glycogen accumulating organisms (GAO) were observed in small quantities, less than 10% of the community (Figure 6.1B). Only trace amounts of other bacteria (positive stain for general eubacteria probe EUBmix) were observed (Supplementary Materials Figure S1). Overall, this shows that the microbial community in seawater-adapted AGS was dominant with “*Ca. Accumulibacter*”.

### 6.3.2 Identification of an abundant putative surface protein in seawater-adapted AGS

The proteins from the seawater AGS were extracted overnight in  $\text{Na}_2\text{CO}_3$  and characterized using SDS-PAGE. Following Coomassie Blue staining, a strong band was observed at an apparent molecular weight of 100 kDa (Figure 6.2, lane 1x), suggesting the presence of an abundant protein in the extract. This band was negatively stained by PAS (Figure 6.2), indicating it is not glycosylated. Right under this band, two weakly stained bands were shown at around 70 kDa (when a higher concentration of biomass was used in the extraction, these two bands were more apparent, Figure 6.2, lane 2x arrows). Furthermore, a range of smaller proteins was seen at the molecular weight lower than 50 kDa. Because the 100 kDa band was sharp and strong, it was taken as an indication that this protein is abundant in the granule. To further identify this protein, the Coomassie blue stained band was cut from the gel and digested into peptides for subsequent mass spectrometry analysis.



6

Figure 6.2. SDS-PAGE of proteins extracted from seawater-adapted granules. L: ladder 1x: granules concentration at 6.4 mg/mL and 2x: granules concentration at 12.8 mg/mL CB: Coomassie blue staining for all proteins (L, lane 1x, 2x). PAS: Periodic acid staining for glycoproteins. Left of the ladder are the molecular weights indicated as kDa. The small white arrows at the lane 2x indicate the two weakly stained bands at around 70 kDa.

### 6.3.3 Proteomic analysis revealed the presence of a surface protein

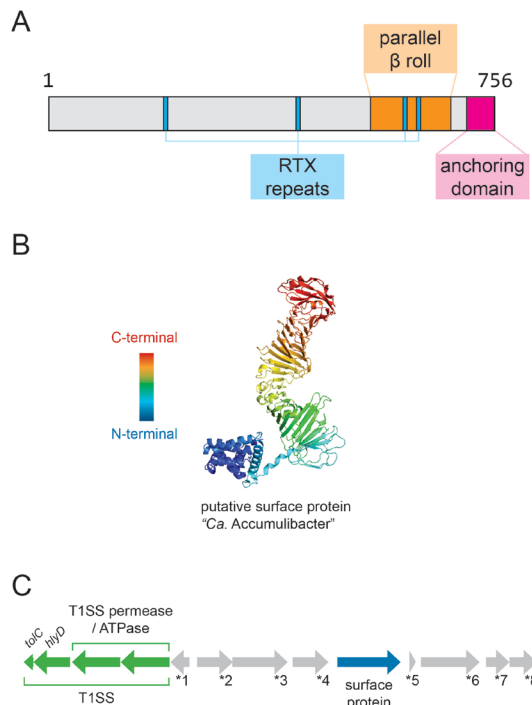


Figure 6.3. Proteomic analysis of the surface protein. A) The secondary structure showing the parallel beta roll (IPR011049) and the surface-anchoring domain (IPR048165) towards the C-terminal of the protein predicted by InterPro and the RTX repeats (IPR001343). B) The 3D protein structure predicted by AlphaFold3. The prediction template modelling score (pTM) was 0.81, indicating a high-quality prediction (Abramson et al., 2024). The blue to red gradient indicates the N-terminal to the C-terminal of the protein respectively. C) Annotated genes around the gene encoding for the surface protein in the coding sequence region (CDS). Type 1 secretion system (T1SS) (in green) consisting of the outer membrane protein TolC, membrane fusion protein HlyD, and the ABC transporters T1SS permease / ATPase. Other annotated proteins: \*1, hypothetical protein. \*2, FecR family protein. \*3, adenylate/guanylate cyclase domain-containing protein. \*4, hypothetical protein. \*5, DUF6447 family protein. \*6, methyltransferase type 11. \*7 ABC transporter permease. \*8, ABC transporter ATP-binding protein.

The protein observed at 100 kDa in the electrophoresis gel was identified by mass spectrometry as a protein containing 756 amino acids (full protein sequence is found in the Supplementary Materials Figure S2). 44.7% of the amino acids are hydrophobic of which alanine (17.7%) is found in the highest abundance. 35.2% of the amino acids are polar uncharged of which threonine (19.3%) is found in the highest abundance. The charged amino acids make up 9.8% of the total sequence. Notably, cysteine was not present in the protein sequence. The theoretical pI/Mw of this protein is 4.30 / 74.493 kDa according to the calculation by ExPASy.

Interestingly, when the full protein sequence was used as a query and BLAST against NCBI database, an exact sequence match was found to be a putative surface protein belonging to an unclassified *Accumulibacter* species (Table 6.1). Importantly, the conserved protein domain revealed that most of the amino acids (166-753) of this protein are arranged as  $\beta$ -sheets (with repeating  $\beta$ -strands), which has high similarity with the typical property of S-layer proteins (Bharat et al., 2017). Looking at the annotated proteins of other matches (2, 3 and 4 in Table 6.1), the E-value shows a good sequence homology, despite the low sequence identity. For the two proteins: beta strand-repeat containing protein and calcium-binding protein, they showed a match of 47.1% and 43.8% and E-values of 7E-133 and 1.8E-90, respectively. For the well-studied S-layer protein *rsaA* of *Caulobacter crescentus*, the match with our protein is only 30.5%, while the E-value is low (1.8E-41). This suggests that the identified protein may be involved in calcium binding and/or is similar to surface layer protein (S-layer protein).

To further understand the putative function of the surface protein, the protein domains were evaluated through InterPro, and its structure is predicted by AlphaFold3. A C-terminal parallel  $\beta$ -roll was found consisting of two RTX repeats and 13  $\beta$ -sheets (Figure 6.3A). The parallel  $\beta$  roll structure is suggested to play a role in conformational arrangements upon binding with  $\text{Ca}^{2+}$  extracellularly (Guo et al., 2019), matching with the homologs annotated with  $\text{Ca}^{2+}$  binding property found above. The protein was predicted by AlphaFold3 to consist of 35.2%  $\beta$ -sheets and 18.8%  $\alpha$ -helix (Figure 6.3B). At the N-terminal, 8  $\alpha$ -helix structures were found. Furthermore, the anchoring domain suggests that the protein may be anchored to the cell surface, thus the protein should be exported to the exterior by an export mechanism.

The protein was found to have four nonapeptide / RTX repeats, GGxGxDxUx, in the sequence (Figure 6.3A), which is commonly found in proteins exported by the type 1 secretion system (T1SS) (Spitz et al., 2019). No export signal peptide was detected while using SignalP 6.0 (Teufel et al., 2022). To determine whether *Accumulibacter* sp. carries the genes encoding for T1SS, the genome protein sequence match was first identified. The exact sequence match was found present in the metagenome-assembled genome (MAG) of the *Accumulibacter* sp. from a lab-scale reactor fed with glucose (Elahinik et al., 2023) and preliminary search of seawater AGS metagenomics dataset of this study revealed the presence of the surface protein as well (Chen et al., accepted). Four genes encoding for T1SS, together with the gene encoding for the surface protein, were found (Figure 6.3C); two genes were annotated as T1SS permease / ATPase, one gene for *HlyD* the membrane fusion protein, and *TolC* the outer membrane protein, making up the complete T1SS (Kim et al., 2016; Spitz et al., 2019). Overall, the abundant protein in the seawater-adapted

6. Identification of a surface protein in the extracellular polymeric substances of seawater-adapted aerobic granular sludge

---

AGS is a surface protein, likely exported extracellularly by T1SS, and may be involved in a structural role similar to S-layer proteins.

Table 6.1. BLASTp search of the surface protein in NCBI and Uniprot showing the hit (1) and the homology (2 - 4) of the putative surface protein with other proteins. The full BLASTp results from NCBI and Uniprot are found in the Supplemental Materials Table S2 and S3. Lower E-value indicates higher confidence that the similarity is not found by chance. E-values < 1E-25 indicate clear homology (Pearson, 2013).

	Description	Organism	E-value	%ID	Accession / Entry	Database
1	bluetail domain-containing putative surface protein	Accumulibacter sp.	0	100%	WP_313950548.1	NCBI
2	<b>beta strand repeat-containing protein</b>	Rhizobium oryzicola	7.00E-133	47.1%	WP_302078835.1	NCBI
3	<b>Calcium-binding protein</b>	Methylobacterium sp. Leaf99	1.80E-90	43.8%	A0A0Q4XER2	Uniprot
4	<b>S-layer protein rsaA</b>	Caulobacter crescentus	1.80E-41	30.5%	P35828	Uniprot

To conduct *in situ* visualization of the protein in the granules, immunostaining was applied. The specificity of the generated antibody was validated by immunoblotting (Figure 6.4). As expected, the antibody bound specifically to the protein at approximately 100 kDa, which is the same molecular weight as the band observed before with the Coomassie gel (Figure 6.4) The other bands that were present in the lower molecular weight range (< 45 kDa) with the Coomassie gel did not show any binding, indicating that the antibody is highly specific to the surface protein. Besides the 100 kDa band, the antibody was also found to interact strongly with a band at around 70 kDa, representing closely the theoretical molecular weight of 74 kDa. Although, shifts in apparent molecular weight can be caused by glycosylation (Scheller et al., 2021), the absent sugar staining and lack of glycosylation detected by the untargeted mass spectrometry approach suggest that the observed shift may instead result from different protein configurations, such as oligomerization and folding (Dunker and Rueckert, 1969).

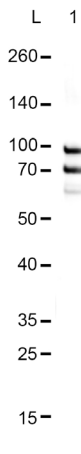


Figure 6.4. Immunoblot analysis of the antibody generated against the unique peptide of the surface protein. The ladder (L) in kDa and the 6.8 mg/mL Na<sub>2</sub>CO<sub>3</sub> extract from seawater (lane 1). A dot blot is presented on the bottom of the membrane of 100 ng of the unique peptide as a positive control.

### 6.3.4 Surface protein is found on the cell and in the extracellular matrix of seawater-adapted AGS

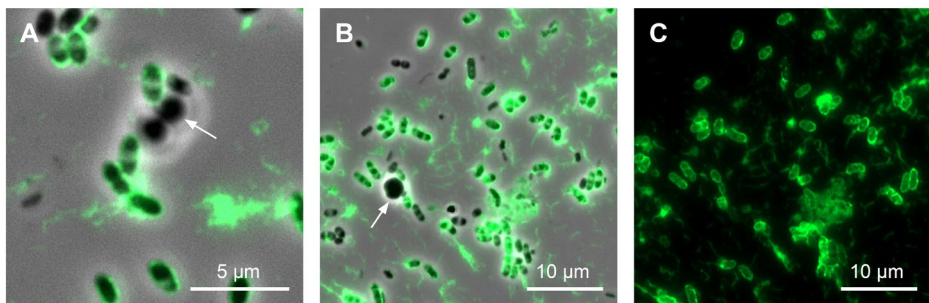


Figure 6.5. Immunofluorescence staining of pottered biomass of seawater AGS (A, B, C). The white arrows (A, B) indicate the GAO. Fluorescence staining of AlexaFluor-488 was overlayed with phase contrast pictures (A and B) and only the fluorescence staining is shown for C. The exposure of AlexFluor-488 was kept the same across all pictures, allowing comparison of the signal intensity between samples.

To visualize the location of the protein in the biomass, pottered biomass was used first. The antibody bound to the cell surface, showing a clear border around the rod-shaped bacteria (Figure 6.5). Judging from the shape and the FISH analysis before, this organism resembles "*Ca. Accumulibacter*". The antibody was confirmed to have specific binding, as other bacteria, *e.g.* larger cocci shaped likely resembling GAO, did not show any signal (Figure 6.5A, B arrow). Notably, about 1 µm long fibril-like structures were observed attached to the cells and in between the spaces of the cells (Figure 6.5), suggesting that the surface protein could be part of the extracellular matrix of the seawater-adapted AGS.

Granule slices were used to visualize the distribution of the surface protein in the granules (Figure 6.6). The surface protein was found to be distributed throughout the entire granule at different scales; around the microorganisms, within the microcolony, and in between the microcolonies. The surface protein was found around the "*Ca. Accumulibacter*" cells towards the loosely packed center of the granule (Figure 6.6C), confirming the previous proteomic analysis and staining on pottered biomass. The areas in between the cells were also stained, similar to a web-like structure (Figure 6.6C arrows). At the outer edge of the granule, the intensity of the surface protein signal was higher compared to the center (Figure 6.6A, B, D). The individual cells within the microcolony appeared densely packed with the surface protein forming a compact honeycomb-like structure surrounding the cells and filling the spaces between them (Figure 6.6B). This structure was consistently found across multiple granules. Lastly, a less common structure resembling large fiber strands with lengths >20 µm was also observed in between the microcolonies (Figure 6.6 F, E). The fibrous strands seemed to be present in the grooves of the granule where less "*Ca. Accumulibacter*" was observed (indicated by the lack of

overlap of the signals). To summarize, it was observed that the surface protein was located in the microcolonies, as well as in the extracellular matrix of the granules. Within the microcolonies, this protein was found around the outer membrane and in the space between the cells. It built up a dense honeycomb structure filling in the microcolony, while large fibers were located in between the microcolonies.

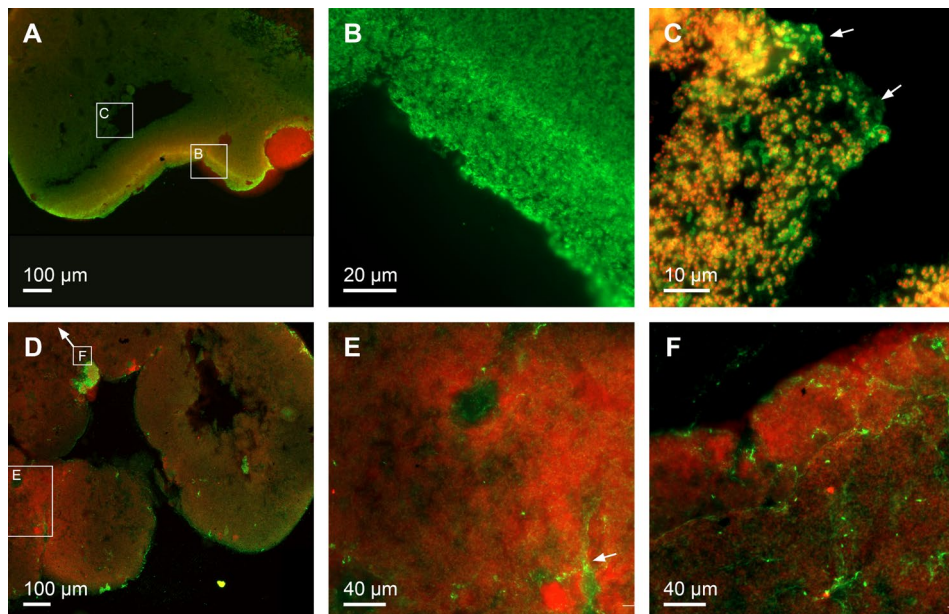


Figure 6.6. Immunofluorescence staining on sliced granules. The secondary antibody probe AlexaFluor-488 (green) was overlayed with the probe for PAO651 (red). Overlap of the red and green signal results in a yellow signal. For B, only the antibody probe is shown to show the structure. C shows the surface protein surrounding the PAO651 stained “*Ca. Accumulibacter*”, with the arrows indicating a web-like structure. A, B, and D show the dense honeycomb-like structure of the surface protein. E and F show the large fiber structure between the microcolonies, with the arrow in E indicate the fiber structure. A negative control without primary antibody confirmed the localized staining of the primary antibody and the autofluorescence (see Supplementary Materials Figure S5).

## 6.4 Discussion

### 6.4.1 An abundant surface protein in seawater-adapted AGS has similarities with previously identified S-layer RTX protein

Identifying the components in the EPS is important to understand the stability of aerobic granular sludge or biofilms in general. In the current study, an abundant protein in the seawater-grown AGS enriched with “*Ca. Accumulibacter*” was isolated and analyzed. It was revealed that this protein is a putative surface protein of *Accumulibacter* species. Especially, there are similarities with S-layer proteins. There is a low sequence similarity (30.5%) and a low E-value (1.80E-41) of the identified protein to the well-characterized S-layer protein of *Caulobacter crescentus* (Pearson, 2013). However, low homology is generally found on sequence level

between S-layer proteins (Pum and Sleytr, 2014). The identified RTX motifs in the sequence indicate that the surface protein may belong to the family of RTX proteins that are exported by the type 1 secretion system (Linhartová et al., 2010; Sleytr et al., 2014). The physicochemical properties of the surface protein match well with known S-layers as well as RTX proteins. The hydrophobic amino acids make up 44.7%, falling into the range of the S-layer proteins 40 – 60%. In addition, the acidic pI of 4.3 (typical range 3.2 – 4.9) and the lack of cysteine in the amino acid sequence are characteristic of RTX proteins (Linhartová et al., 2010). Also, the predicted secondary structure matches closely to other reported S-layer proteins (Sára and Sleytr, 2000); The proportion of  $\beta$ -sheets, 35.2%, is lower than the typical values of S-layer proteins of 40%  $\beta$ -sheets. Whereas, the  $\alpha$ -helix, 18.8%, falls in the expected range (10-20%). The  $\alpha$ -helix arrangement at the N-terminal is also typical for S-layer proteins. Therefore, based on the similarities, the identified abundant surface protein highly resembles an S-layer RTX protein.

“*Ca. Accumulibacter*” is a known EPS-forming organism and is mainly known for its phosphate removal activity in EBPR systems. Previous works on the EPS of “*Ca. Accumulibacter*” have mainly been focused on the glycoconjugates (Chen et al., 2024; Dueholm et al., 2023; Tomás-Martínez et al., 2021). In parallel, EPS proteins are another important component to be characterized. This study suggests that there might be an S-layer  $\text{Ca}^{2+}$  binding RTX protein produced by “*Ca. Accumulibacter*” present in the EPS. In fact, one study proposed before, that  $\text{Ca}^{2+}$ -binding RTX proteins produced by different Accumulibacter species may be part of the EPS (Martín et al., 2006). However, FISH analysis does not conclusively identify the specific Accumulibacter species in this study (Supplementary Materials Figure S6-S8) and BLAST analysis on the “*Ca. Accumulibacter*” taxa did not reveal clear homology on sequence level either (Supplementary Materials Table S3), as expected from the S-layer proteins (Pum and Sleytr, 2014). Thus, future research should focus on which species produce this surface protein to understand how widespread the protein is and the factors influencing its production. Moreover, future research should visualize potential crystalline lattices on the “*Ca. Accumulibacter*” cell surface using electron microscopy to confirm the presence of S-layer proteins and explore their assembly and functions (Sleytr et al., 2014).

#### 6.4.2 Function of the surface protein in the EPS of seawater-adapted AGS

The recovered surface protein has similarities with known S-layer protein. Immunostaining confirmed the location of the protein both on the cell surface and in the extracellular matrix. Similar to trehalose production and the alteration of EPS glycans (Chen et al., 2023b; de Graaff et al., 2020b), the production of the surface protein might be another response to the osmotic stress when exposed to seawater conditions in “*Ca. Accumulibacter*”-dominant AGS. It is reasonable to speculate that for the “*Ca. Accumulibacter*” cells, the surface protein might play a role in stabilizing

the membrane under high osmotic pressure similar to the S-layer protein in archaea, *Lactobacillus* and *Pseudoalteromonas* (Ali et al., 2020; Engelhardt, 2007; Palomino et al., 2016). In addition, the high  $\text{Ca}^{2+}$  concentration in seawater (9.6 mM in seawater vs. 0.26 mM in freshwater) may facilitate the folding of the RTX motifs with  $\text{Ca}^{2+}$  on the outer membrane and in the EPS (Bumba et al., 2016). As  $\text{Ca}^{2+}$  binding is one of the structural properties of the EPS (Felz et al., 2016), the surface protein might likely be a component of the structural EPS. Overall, the abundant surface protein of “*Ca. Accumulibacter*” can be a component of the structural EPS and may function as a scaffold to stabilize its membranes under seawater conditions.

Besides on the cell surface, it was also observed that the surface protein forms a honeycomb-like structure in the microcolonies and large fibers between the microcolonies in the extracellular matrix. As S-layer proteins are known to be shed from the cell, the interaction between the shed surface protein and other matrix components (e.g. metal ions, proteins, carbohydrates) may contribute to the formation of these types of structures (Ali et al., 2020; Kish et al., 2016; Wong et al., 2023). Future work employing high resolution microscopy (i.e. TEM, confocal microscopy) will provide more understanding of the role of the surface protein in aerobic granular sludge formation (Ali et al., 2020). Overall, this study suggests that surface proteins might not only play a role in stabilizing the cell membranes but also forming fibril structures that influence the mechanical properties of aerobic granular sludge.

6

It was worth noting that, S-layer proteins have been identified in the EPS of anammox granules and are thought to have a structural role within the EPS matrix (Boleij et al., 2018; Wong et al., 2023). Furthermore, one of the functions proposed in literature is their involvement in biofilm formation, e.g. S-layer proteins of *Tannerella forsythia* was up-regulated when grown as biofilms (Pham et al., 2010). Therefore, although there is no general function assigned to the S-layer proteins, it is reasonable to speculate that surface proteins (e.g. S-layer proteins) might be one of the structural proteins in granular sludge, or even in biofilm in general.

#### 6.4.3 Detection of structural proteins by *in-situ* imaging in biofilm

EPS plays an important role in maintaining biofilm stability (Flemming and Wingender, 2010). Identifying the EPS components will allow a better understanding of the EPS functionality. Proteins are one of the major components in the EPS. In order to identify the proteins that play a structural role in EPS, a multidisciplinary approach has been proposed involving separation, and identification combined with *in situ* imaging visualization (Seviour et al., 2019). However, the steps between protein identification and *in situ* imaging by using antibodies are not clearly defined. Moreover, with the fast development of analytical techniques, recent advances in the methodology should be taken into account.

Therefore, in the current research, this multidisciplinary approach was updated and expanded (Figure 6.7). The same general steps as proposed in the roadmap by (Seviour et al., 2019) were followed: an optimized EPS extraction on the biofilm, followed by protein separation on the SDS-PAGE and identification of the dominant protein by MS. Antibody generation with subsequent Western Blotting to evaluate specificity and finally, *in situ* imaging using immunostaining-FISH.

In practice, the following steps were identified as essential for the workflow: Optimization of the protein extraction and verification of antibodies through combined techniques. Protein extraction is a crucial step, obtaining sufficient amounts can be challenging (Boleij et al., 2019; Seviour et al., 2019). It is noted that complete solubilization of EPS can provide information regarding proteins; however, it may hinder the identification of structural proteins by compromising the clarity of the protein bands in SDS-PAGE. It is suggested in the current research that to identify proteins that play a structural role, prioritizing sufficient protein amounts to get clear bands in the SDS-PAGE is more important than achieving complete solubilization of the EPS, because it can simplify the subsequent MS analysis. Therefore, extraction conditions (*e.g* temperature, chemical, time) have to be optimized. Moreover, protein glycosylation can interfere with SDS-PAGE separation and MS analysis (Boleij et al., 2019; Chen et al., 2023a; Gagliano et al., 2018), therefore the presence of glycoproteins should be assessed and if present, deglycosylation should be performed if possible. Furthermore, to confirm the extracellular location of the EPS protein, *in situ* verification is required. Antibody staining, known for its high specificity, is commonly used for this purpose. Typically, knock-out organisms incapable of producing the target protein are used as a control (Griffiths and Lucocq, 2014). However, this approach is not feasible in microbial communities, due to its complexity and dynamic interactions between community members. Thus, combining antibody staining with microbial ecology techniques, such as immunostaining-FISH and proteomic analysis, is essential to identify the producer for proper validation.

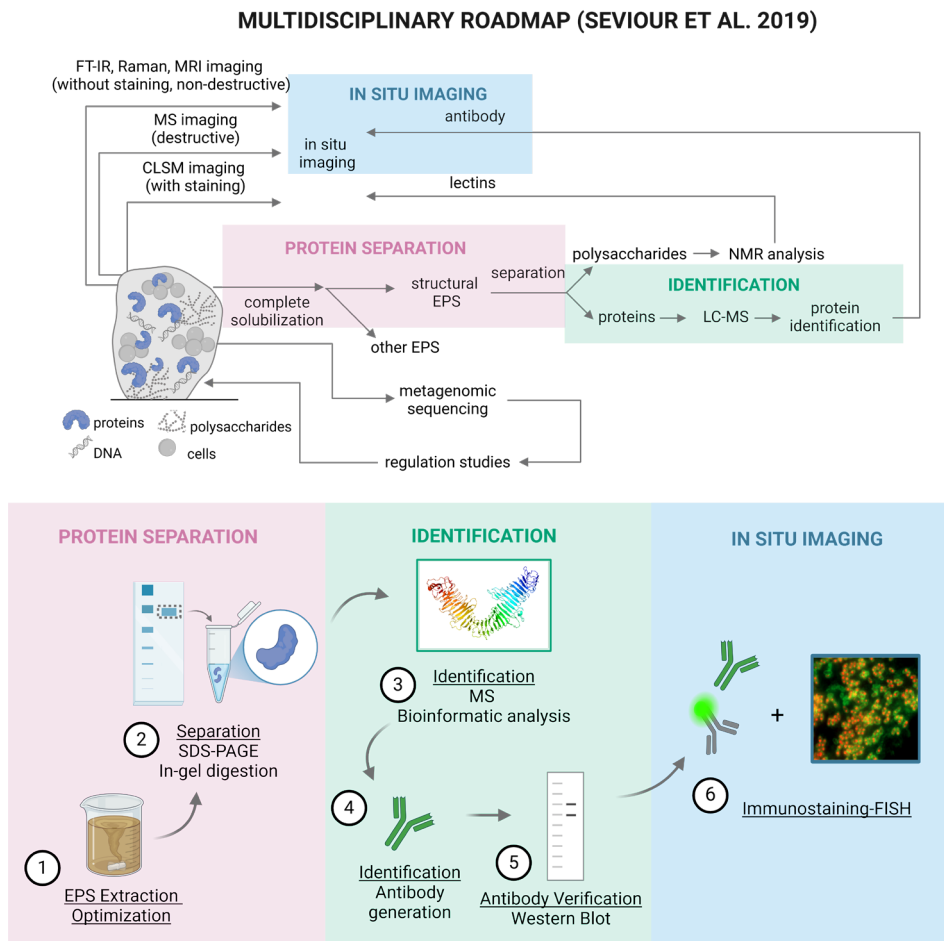


Figure 6.7. General workflow to identify structural proteins in EPS put in the context of the multidisciplinary roadmap proposed by (Seviour et al., 2019). The first step “complete solubilization” could be reconsidered into the optimization of EPS extraction. Microbial community analysis (FISH) should be considered in parallel to the roadmap linking with *in situ* imaging to identify the protein producer. Created in BioRender.

## 6.5 Conclusions

- Seawater-adapted AGS EPS contains an abundant surface protein produced by *“Ca. Accumulibacter”*.
- The surface protein resembles S-layer RTX proteins and is localized both on the cell surface of *“Ca. Accumulibacter”* and in the extracellular matrix of granular sludge as large macromolecular structures.
- Detection of structural proteins in mixed-species biofilms requires optimized extraction protocols and *in situ* imaging validation using a combination of immunostaining-FISH and proteomics.

## Supplementary Materials

The Supplementary Materials of this chapter can be found at DOI [10.1016/J.WATRES.2025.124187](https://doi.org/10.1016/J.WATRES.2025.124187)

## References

Abramson, J., Adler, J., Dunger, J., Evans, R., Green, T., Pritzl, A., Ronneberger, O., Willmore, L., Ballard, A. J., Bambrick, J., Bodenstein, S. W., Evans, D. A., Hung, C.-C., O'Neill, M., Reiman, D., Tunyasuvunakool, K., Wu, Z., Žemgulytė, A., Arvaniti, E., ... Jumper, J. M. (2024). Accurate structure prediction of biomolecular interactions with AlphaFold 3. *Nature*, 630(8016), 493–500. <https://doi.org/10.1038/s41586-024-07487-w>

Albertsen, M., McIlroy, S. J., Stokholm-Bjerregaard, M., Karst, S. M., & Nielsen, P. H. (2016). "Candidatus Propionivibrio aalborgensis": A Novel Glycogen Accumulating Organism Abundant in Full-Scale Enhanced Biological Phosphorus Removal Plants. *Frontiers in Microbiology*, 7(JUL), 1033. <https://doi.org/10.3389/FMICB.2016.01033>

Ali, S., Jenkins, B., Cheng, J., Lobb, B., Wei, X., Egan, S., Charles, T. C., McConkey, B. J., Austin, J., & Doxey, A. C. (2020). Slr4, a newly identified S-layer protein from marine Gammaproteobacteria, is a major biofilm matrix component. *Molecular Microbiology*, 114(6), 979–990. <https://doi.org/10.1111/MMI.14588>

Amann, R. I., Binder, B. J., Olson, R. J., Chisholm, S. W., Devereux, R., & Stahl, D. A. (1990). Combination of 16S rRNA-targeted oligonucleotide probes with flow cytometry for analyzing mixed microbial populations. *Applied and Environmental Microbiology*, 56(6), 1919–1925. <https://doi.org/10.1128/AEM.56.6.1919-1925.1990>

APHA. (1998). *Standard methods for the examination of water and wastewater* (20th ed.). American Public Health Association, American Water Works Association, Water Environment Federation, Washington, D.C., 1998.

Bassin, J. P., Pronk, M., Muyzer, G., Kleerebezem, R., Dezotti, M., & van Loosdrecht, M. C. M. (2011). Effect of elevated salt concentrations on the aerobic granular sludge process: Linking microbial activity with microbial community structure. *Applied and Environmental Microbiology*, 77(22), 7942–7953. <https://doi.org/10.1128/AEM.05016-11>

Bharat, T. A. M., Kureisaite-Ciziene, D., Hardy, G. G., Yu, E. W., Devant, J. M., Hagen, W. J. H., Brun, Y. V., Briggs, J. A. G., & Löwe, J. (2017). Structure of the hexagonal surface layer on Caulobacter crescentus cells. *Nature Microbiology*, 2, 759. <https://doi.org/10.1038/NMICROBIOL.2017.59>

Boleij, M., Pabst, M., Neu, T. R., Van Loosdrecht, M. C. M., & Lin, Y. (2018). Identification of Glycoproteins Isolated from Extracellular Polymeric Substances of Full-Scale Anammox Granular Sludge. *Environmental Science and Technology*, 52(22), 13127–13135. <https://doi.org/10.1021/acs.est.8b03180>

Boleij, M., Seviour, T., Wong, L. L., van Loosdrecht, M. C. M., & Lin, Y. (2019). Solubilization and characterization of extracellular proteins from anammox granular sludge. *Water Research*, 164, 114952. <https://doi.org/10.1016/j.watres.2019.114952>

Bumba, L., Masin, J., Macek, P., Wald, T., Motlova, L., Bibova, I., Klimova, N., Bednarova, L., Veverka, V., Kachala, M., Svergun, D. I., Barinka, C., & Sebo, P. (2016). Calcium-Driven Folding of RTX Domain  $\beta$ -Rolls Ratchets Translocation of RTX Proteins through Type I Secretion Ducts. *Molecular Cell*, 62(1), 47–62. <https://doi.org/10.1016/J.MOLCEL.2016.03.018>

Campo, R., Corsino, S. F., Torregrossa, M., & Di Bella, G. (2018). The role of extracellular polymeric substances on aerobic granulation with stepwise increase of salinity. *Separation and Purification Technology*, 195, 12–20. <https://doi.org/10.1016/j.seppur.2017.11.074>

Chen, L. M., Beck, P., van Ede, J., Pronk, M., van Loosdrecht, M. C. M., & Lin, Y. (2024). Anionic extracellular polymeric substances extracted from seawater-adapted aerobic granular sludge. *Applied Microbiology and Biotechnology* 2024 108:1, 108(1), 1–12. <https://doi.org/10.1007/S00253-023-12954-X>

Chen, L. M., de Bruin, S., Pronk, M., Sousa, D. Z., van Loosdrecht, M. C. M., & Lin, Y. (2023a). Sialylation and Sulfation of Anionic Glycoconjugates Are Common in the Extracellular Polymeric Substances of Both Aerobic and Anaerobic Granular Sludges.

## 6. Identification of a surface protein in the extracellular polymeric substances of seawater-adapted aerobic granular sludge

---

*Environmental Science and Technology*, 57(35), 13217–13225. <https://doi.org/https://doi.org/10.1021/acs.est.2c09586>

Chen, L. M., Keisham, S., Tateno, H., Ede, J. van, Pronk, M., Loosdrecht, M. C. M. van, & Lin, Y. (2023b). Alterations of Glycan Composition in Aerobic Granular Sludge during the Adaptation to Seawater Conditions. *ACS ES&T Water*. <https://doi.org/10.1021/ACSESTWATER.3C00625>

Corsino, S. F., Capodici, M., Torregrossa, M., & Viviani, G. (2017). Physical properties and Extracellular Polymeric Substances pattern of aerobic granular sludge treating hypersaline wastewater. *Bioresource Technology*, 229, 152–159. <https://doi.org/10.1016/j.biortech.2017.01.024>

Crocetti, G. R., Hugenholtz, P., Bond, P. L., Schuler, A., Keller, J., Jenkins, D., & Blackall, L. L. (2000). Identification of polyphosphate-accumulating organisms and design of 16S rRNA-directed probes for their detection and quantitation. *Applied and Environmental Microbiology*, 66(3), 1175–1182. <https://doi.org/10.1128/AEM.66.3.1175-1182.2000>

Daims, H., Brühl, A., Amann, R., Schleifer, K. H., & Wagner, M. (1999). The Domain-specific Probe EUB338 is Insufficient for the Detection of all Bacteria: Development and Evaluation of a more Comprehensive Probe Set. *Systematic and Applied Microbiology*, 22(3), 434–444. [https://doi.org/10.1016/S0723-2020\(99\)80053-8](https://doi.org/10.1016/S0723-2020(99)80053-8)

de Graaff, D. R., Felz, S., Neu, T. R., Pronk, M., van Loosdrecht, M. C. M., & Lin, Y. (2019). Sialic acids in the extracellular polymeric substances of seawater-adapted aerobic granular sludge. *Water Research*, 343–351. <https://doi.org/10.1016/j.watres.2019.02.040>

de Graaff, D. R., van Loosdrecht, M. C. M., & Pronk, M. (2020a). Biological phosphorus removal in seawater-adapted aerobic granular sludge. *Water Research*, 172, 115531. <https://doi.org/10.1016/j.watres.2020.115531>

de Graaff, D. R., van Loosdrecht, M. C. M., & Pronk, M. (2020b). Trehalose as an osmolyte in *Candidatus Accumulibacter phosphatis*. *Applied Microbiology and Biotechnology*, 2020 105:1, 105(1), 379–388. <https://doi.org/10.1007/S00253-020-10947-8>

Decho, A. W., & Gutierrez, T. (2017). Microbial extracellular polymeric substances (EPSs) in ocean systems. *Frontiers in Microbiology*, 8(MAY), 922. <https://doi.org/10.3389/fmicb.2017.00922>

Dueholm, M. K. D., Besteman, M., Zeuner, E. J., Riisgaard-Jensen, M., Nielsen, M. E., Vestergaard, S. Z., Heidelbach, S., Bekker, N. S., & Nielsen, P. H. (2023). Genetic potential for exopolysaccharide synthesis in activated sludge bacteria uncovered by genome-resolved metagenomics. *Water Research*, 229, 119485. <https://doi.org/10.1016/j.watres.2022.119485>

Dunker, A. K., & Rueckert, R. R. (1969). Observations on molecular weight determinations on polyacrylamide gel. *Journal of Biological Chemistry*, 244(18). [https://doi.org/10.1016/s0021-9258\(18\)94310-3](https://doi.org/10.1016/s0021-9258(18)94310-3)

Elahinik, A., Li, L., Pabst, M., Abbas, B., Xevgenos, D., van Loosdrecht, M. C. M., & Pronk, M. (2023). Aerobic granular sludge phosphate removal using glucose. *Water Research*, 247, 120776. <https://doi.org/10.1016/j.watres.2023.120776>

Engelhardt, H. (2007). Mechanism of osmoprotection by archaeal S-layers: A theoretical study. *Journal of Structural Biology*, 160(2), 190–199. <https://doi.org/10.1016/j.jsb.2007.08.004>

Felz, S., Al-Zuhairy, S., Aarstad, O. A., van Loosdrecht, M. C. M., & Lin, Y. M. (2016). Extraction of structural extracellular polymeric substances from aerobic granular sludge. *Journal of Visualized Experiments*, 2016(115), 54534. <https://doi.org/10.3791/54534>

Flemming, H. C., & Wingender, J. (2010). The biofilm matrix. In *Nature Reviews Microbiology* (Vol. 8, Issue 9, pp. 623–633). Nature Publishing Group. <https://doi.org/10.1038/nrmicro2415>

Gagliano, M. C., Neu, T. R., Kuhlicke, U., Sudmalis, D., Temmink, H., & Plugge, C. M. (2018). EPS glycoconjugate profiles shift as adaptive response in anaerobic microbial granulation at high salinity. *Frontiers in Microbiology*,

9(JUL), 1423.  
<https://doi.org/10.3389/fmicb.2018.01423> 1076.

Griffiths, G., & Lucocq, J. M. (2014). Antibodies for immunolabeling by light and electron microscopy: not for the faint hearted. *Histochemistry and Cell Biology*, 142(4), 347. <https://doi.org/10.1007/S00418-014-1263-5>

Guo, S., Vance, T. D. R., Stevens, C. A., Voets, I., & Davies, P. L. (2019). RTX Adhesins are Key Bacterial Surface Megaproteins in the Formation of Biofilms. *Trends in Microbiology*, 27(5), 453–467. <https://doi.org/10.1016/j.tim.2018.12.003>

Kim, J. S., Song, S., Lee, M., Lee, S., Lee, K., & Ha, N. C. (2016). Crystal Structure of a Soluble Fragment of the Membrane Fusion Protein HlyD in a Type i Secretion System of Gram-Negative Bacteria. *Structure*, 24(3), 477–485. <https://doi.org/10.1016/j.str.2015.12.012>

Kish, A., Miot, J., Lombard, C., Guignier, J. M., Bernard, S., Zirah, S., & Guyot, F. (2016). Preservation of Archaeal Surface Layer Structure During Mineralization. *Scientific Reports* 2016 6:1, 6(1), 1–10. <https://doi.org/10.1038/srep26152>

Kleikamp, H. B. C., Pronk, M., Tugui, C., Guedes da Silva, L., Abbas, B., Lin, Y. M., van Loosdrecht, M. C. M., & Pabst, M. (2021). Database-independent de novo metaproteomics of complex microbial communities. *Cell Systems*, 12(5), 375–383.e5. <https://doi.org/10.1016/j.cels.2021.04.003>

Lefebvre, O., & Moletta, R. (2006). Treatment of organic pollution in industrial saline wastewater: A literature review. In *Water Research* (Vol. 40, Issue 20, pp. 3671–3682). <https://doi.org/10.1016/j.watres.2006.08.027>

Lin, Y., Reino, C., Carrera, J., Pérez, J., & van Loosdrecht, M. C. M. (2018). Glycosylated amyloid-like proteins in the structural extracellular polymers of aerobic granular sludge enriched with ammonium-oxidizing bacteria. *MicrobiologyOpen*, 7(6), e00616. <https://doi.org/10.1002/mbo3.616>

Linhartová, I., Bumba, L., Mašn, J., Basler, M., Osička, R., Kamanová, J., Procházková, K., Adkins, I., Hejnová Holubová, J., Sadílková, L., Morová, J., & Šebo, P. (2010). RTX proteins: a highly diverse family secreted by a common mechanism. *Fems Microbiology Reviews*, 34(6), 6976.2010.00231.X 1076.

Martín, H. G., Ivanova, N., Kunin, V., Warnecke, F., Barry, K. W., McHardy, A. C., Yeates, C., He, S., Salamov, A. A., Szeto, E., Dalin, E., Putnam, N. H., Shapiro, H. J., Pangilinan, J. L., Rigoutsos, I., Kyripides, N. C., Blackall, L. L., McMahon, K. D., & Hugenholtz, P. (2006). Metagenomic analysis of two enhanced biological phosphorus removal (EBPR) sludge communities. *Nature Biotechnology*, 24(10), 1263–1269. <https://doi.org/10.1038/nbt1247>

McSwain, B. S., Irvine, R. L., Hausner, M., & Wilderer, P. A. (2005). Composition and distribution of extracellular polymeric substances in aerobic flocs and granular sludge. *Applied and Environmental Microbiology*, 71(2), 1051–1057. <https://doi.org/10.1128/AEM.71.2.1051-1057.2005>

Ou, D., Li, W., Li, H., Wu, X., Li, C., Zhuge, Y., & Liu, Y. di. (2018). Enhancement of the removal and settling performance for aerobic granular sludge under hypersaline stress. *Chemosphere*, 212, 400–407. <https://doi.org/10.1016/J.CHEMOSPHERE.2018.08.096>

Pabst, M., Grouzdev, D. S., Lawson, C. E., Kleikamp, H. B. C., de Ram, C., Louwen, R., Lin, Y. M., Lücker, S., van Loosdrecht, M. C. M., & Laureni, M. (2022). A general approach to explore prokaryotic protein glycosylation reveals the unique surface layer modulation of an anammox bacterium. *The ISME Journal*, 16(2), 346–357. <https://doi.org/10.1038/S41396-021-01073-Y>

Palomino, M. M., Waehner, P. M., Fina Martin, J., Ojeda, P., Malone, L., Sánchez Rivas, C., Prado Acosta, M., Allievi, M. C., & Ruzal, S. M. (2016). Influence of osmotic stress on the profile and gene expression of surface layer proteins in *Lactobacillus acidophilus* ATCC 4356. *Applied Microbiology and Biotechnology*, 100(19), 8475–8484. <https://doi.org/10.1007/S00253-016-7698-Y/FIGURES/4>

Pearson, W. R. (2013). An introduction to sequence similarity (“homology”) searching. *Current Protocols in Bioinformatics*, 0 3(SUPPL.42). <https://doi.org/10.1002/0471250953.bi0301s42>

## 6. Identification of a surface protein in the extracellular polymeric substances of seawater-adapted aerobic granular sludge

Pham, T. K., Roy, S., Noirel, J., Douglas, I., Wright, P. C., & Stafford, G. P. (2010). A quantitative proteomic analysis of biofilm adaptation by the periodontal pathogen *Tannerella forsythia*. *Proteomics*, 10(17), 3130–3141. <https://doi.org/10.1002/PMIC.200900448>; SUBPAGE:STRING:FULL

Pronk, M., de Kreuk, M. K., de Bruin, B., Kamminga, P., Kleerebezem, R., & van Loosdrecht, M. C. M. (2015). Full scale performance of the aerobic granular sludge process for sewage treatment. *Water Research*, 84, 207–217. <https://doi.org/10.1016/j.watres.2015.07.011>

Pum, D., & Sleytr, U. B. (2014). Reassembly of S-layer proteins. *Nanotechnology*, 25(31), 312001. <https://doi.org/10.1088/0957-4484/25/31/312001>

Sára, M., & Sleytr, U. B. (2000). S-Layer Proteins. *Journal of Bacteriology*, 182(4), 859. <https://doi.org/10.1128/JB.182.4.859-868.2000>

Scheller, C., Krebs, F., Wiesner, R., Wätzig, H., & Oltmann-Norden, I. (2021). A comparative study of CE-SDS, SDS-PAGE, and Simple Western—Precision, repeatability, and apparent molecular mass shifts by glycosylation. *ELECTROPHORESIS*, 42(14–15), 1521–1531. <https://doi.org/10.1002/ELPS.202100068>

Seviour, T., Derlon, N., Dueholm, M. S., Flemming, H.-C., Girbal-Neuhauser, E., Horn, H., Kjelleberg, S., van Loosdrecht, M. C. M., Lotti, T., Malpei, M. F., Nerenberg, R., Neu, T. R., Paul, E., Yu, H., & Lin, Y. (2019). Extracellular polymeric substances of biofilms: Suffering from an identity crisis. *Water Research*, 151, 1–7. <https://doi.org/10.1016/j.watres.2018.11.020>

Sleytr, U. B., Schuster, B., Egelseer, E. M., & Pum, D. (2014). S-layers: Principles and applications. *FEMS Microbiology Reviews*, 38(5), 823–864. <https://doi.org/10.1111/1574-6976.12063>

Spitz, O., Erenburg, I. N., Beer, T., Kanonenberg, K., Holland, I. B., & Schmitt, L. (2019). Type I Secretion Systems—One Mechanism for All? *Microbiology Spectrum*, 7(2). <https://doi.org/10.1128/MICROBIOLSPEC.PSIB-0003-2018/ASSET/9C2920A1-D783-4A4A-93C7-5819E4025BCB/ASSETS/GRAPHIC/PSIB-0003-2018-FIG3.GIF>

Teufel, F., Almagro Armenteros, J. J., Johansen, A. R., Gíslason, M. H., Pihl, S. I., Tsirigos, K. D., Winther, O., Brunak, S., von Heijne, G., & Nielsen, H. (2022). SignalP 6.0 predicts all five types of signal peptides using protein language models. *Nature Biotechnology*, 40(7), 1023–1025. <https://doi.org/10.1038/S41587-021-01156-3>

Tomás-Martínez, S., Kleikamp, H. B. C., Neu, T. R., Pabst, M., Weissbrodt, D. G., van Loosdrecht, M. C. M., & Lin, Y. (2021). Production of nonulosonic acids in the extracellular polymeric substances of “*Candidatus Accumulibacter phosphatis*.” *Applied Microbiology and Biotechnology*, 105(8), 3327–3338. <https://doi.org/10.1007/s00253-021-11249-3>

Van Loosdrecht, M. C. M., & Brdjanovic, D. (2014). Anticipating the next century of wastewater treatment. *Science*, 344(6191), 1452–1453. [https://doi.org/10.1126/SCIENCE.1255183/ASSET/4AFA3CFE-23CA-4751-8D4F-94D23DF70A18/ASSETS/GRAPHIC/344\\_1452\\_F2.JPG](https://doi.org/10.1126/SCIENCE.1255183/ASSET/4AFA3CFE-23CA-4751-8D4F-94D23DF70A18/ASSETS/GRAPHIC/344_1452_F2.JPG)

Weissbrodt, D. G., Shani, N., & Holliger, C. (2014). Linking bacterial population dynamics and nutrient removal in the granular sludge biofilm ecosystem engineered for wastewater treatment. *FEMS Microbiology Ecology*, 88(3), 579–595. <https://doi.org/10.1111/1574-6941.12326>

Welles, L., Tian, W. D., Saad, S., Abbas, B., Lopez-Vazquez, C. M., Hooijmans, C. M., van Loosdrecht, M. C. M., & Brdjanovic, D. (2015). *Accumulibacter* clades Type I and II performing kinetically different glycogen-accumulating organisms metabolisms for anaerobic substrate uptake. *Water Research*, 83, 354–366. <https://doi.org/10.1016/j.watres.2015.06.045>

Wong, L. L., Lu, Y., Ho, J. C. S., Mugunthan, S., Law, Y., Conway, P., Kjelleberg, S., & Seviour, T. (2023). Surface-layer protein is a public-good matrix exopolymer for microbial community organisation in environmental anammox biofilms. *The ISME Journal* 2023 17:6, 17(6), 803–812. <https://doi.org/10.1038/s41396-023-01388-y>

Zhang, Z., Liu, J., Xiao, C., & Chen, G. (2023a). Making waves: Enhancing sustainability and resilience in coastal cities through the

incorporation of seawater into urban metabolism. *Water Research*, 242, 120140.

Zhang, Z., Sato, Y., Dai, J., Chui, H. kwong, Daigger, G., Van Loosdrecht, M. C. M., & Chen, G. (2023b). Flushing toilets and cooling spaces with seawater improve water-energy securities and achieve carbon mitigations in coastal cities. *Environmental Science & Technology*, 57(12), 5068-5078.

Zhao, Y., Zhuang, X., Ahmad, S., Sung, S., & Ni, S. Q. (2020a). Biotreatment of high-salinity wastewater: current methods and future directions. In *World Journal of Microbiology and Biotechnology* (Vol. 36, Issue 3). <https://doi.org/10.1007/s11274-020-02815-4>

Zhao, Y., Zhuang, X., Ahmad, S., Sung, S., & Ni, S. Q. (2020b). Biotreatment of high-salinity wastewater: current methods and future directions. *World Journal of Microbiology and Biotechnology*, 36(3), 1-11. <https://doi.org/10.1007/S11274-020-02815-4/TABLES/2>

Zhu, L., Zhou, J., Lv, M., Yu, H., Zhao, H., & Xu, X. (2015). Specific component comparison of extracellular polymeric substances (EPS) in flocs and granular sludge using EEM and SDS-PAGE. *Chemosphere*, 121, 26-32. <https://doi.org/10.1016/J.CHEMOSPHERE.2014.10.053>







The chapters presented in this thesis deepened our understanding of the complex extracellular polymeric substances (EPS) matrix in biofilm, in particular AGS, with the focus on EPS components: glycoconjugates, such as glycoproteins, and structural proteins. Altogether, the chapters provided new insights into EPS components, the influence of seawater on the EPS composition and properties, with an extension to EPS application as a recovered resource. New research topics generated on the EPS research will be covered in this section and limitations of the current work are discussed.

## 7.1 Towards the identification of the EPS components

The deeper we investigate the composition of EPS, the more novel components are identified, highlighting both the complexity and unknowns. Notably, nonulosonic acids (NulOs) and sulfated groups, both contributing to the anionic property of glycoconjugates, were detected in the high molecular weight EPS fractions of both full-scale granular sludge systems (Chapter 2) and in seawater-adapted AGS (Chapter 3), indicating their consistent presence across granular sludge. Glycoproteins were identified as one glycoconjugate component carrying both NulOs and/or sulfated groups (Chapters 4 and 5).

Although many studies have demonstrated the presence of NulOs (Boleij et al., 2020; de Graaff et al., 2019; Kleikamp et al., 2020; Tomás-Martínez et al., 2021), their functional role remains largely hypothetical. To clarify their role, the structure of the associated glycoconjugates needs to be elucidated. Despite that it is speculated that a large part of NulOs is on the glycoproteins, it is still challenging to elucidate the exact structural formula of the sialylated glycoconjugate. The use of a sialic acid lectin column to purify the NulOs glycoprotein (Chapter 5) complemented by mass spectrometry (MS) (Pabst et al., 2022), is a promising method to resolve the structure of the glycoprotein(s) decorated with NulOs.

Further expanding on the NulOs glycoconjugates, recently, the LPS, known to also carry NulOs (Varki et al., 2017), has emerged as a hydrogel-forming component in the EPS of AGS (Li et al., 2025). Metaproteomic analysis under increasing seawater salinity revealed an upregulation of an LPS biosynthesis protein (Chapter 5), suggesting that the LPS production is responsive to environmental conditions and may interact dynamically with other EPS present in the matrix (Szczesny et al., 2018). To further characterize LPS, chemical structure determination through GC-MS for lipids (Chiu and Kuo, 2020) and NMR/MS for the glycan chains (Gimeno et al., 2020) present a logical next step.

Recently, metaproteomics has been applied to identify extracellular proteins in the EPS of granules. Various aggregate-forming proteins (Olst et al., 2025) and putative glycoproteins (Chapter 5) were found using this approach, revealing insights into

the identity and expression of the proteins. However, the limitation lies here in the function of the protein and how they are distributed within the EPS matrix. Commonly, *in-situ* approaches, such as antibody staining for proteins (Chapter 6) or lectin staining for carbohydrates (Seviour et al., 2019), are used to reveal the spatial distribution of the EPS component, but they are limited to a single target per lectin or antibody. Untargeted methods developed within the histological context could be an interesting complementary approach to explore, such as matrix-assisted laser desorption ionization (MALDI) imaging mass spectrometry (IMS) (Aichler and Walch, 2015). This would enable spatial mapping of multiple proteins simultaneously, providing a more comprehensive view of the protein distribution within the EPS.

## 7.2 Influence of environmental conditions on EPS

The influence of seawater salinity on the EPS properties was investigated for a short-term exposure (Chapter 4) and long-term stepwise exposure (Chapter 5). The results showed that glycoproteins became less diverse and more negatively charged with increasing salinity, suggesting a possible adaptive response of "*Ca. Accumulibacter*". This raised the question of whether such modifications are actively regulated through specific biosynthesis pathways. However, metaproteomics could not resolve this, due to limitations on functional protein annotations, and incomplete reference genomes (Heyer et al., 2017). To address these limitations, future work could employ long-read sequencing technologies, enabling the construction of high-quality metagenome assembled genomes (MAGs) and plasmids, which are not recovered with short-read sequencing (Agustinho et al., 2024). High-quality MAGs would provide a better genomic context, allowing for the identification of gene clusters potentially involved in EPS biosynthesis and modification. Interestingly, plasmids can carry genes encoding for glycoproteins (Benz and Schmidt, 1992) or glycosyltransferases (Fukao et al., 2019). Nonetheless, these approaches should be complementary to the structural analysis of the glycoproteins.

To further complement these findings, future studies could focus on linking the EPS components to functional roles, such as swelling and metal binding capacity. Combining fractionation methods followed by these functional studies may reveal connections that support their functions.

Notably, the same "*Ca. Accumulibacter*" species remained dominant throughout the increasing salinity (Chapter 5), allowing us to connect the observed increase in the charge of EPS with both the microbial producer and the environmental condition. To gain a broader understanding of EPS adaptation and function, it would be insightful to investigate how other environmental parameters, such as temperature,

affect the EPS composition in granules. Assigning specific functions to individual components of the EPS remains challenging, but environmental studies may show overlap in functionality or differences in EPS components that could underpin certain functional roles. These insights could help to reveal how specific EPS components contribute to granule stability or uncover novel functions.

### 7.3 Resource recovery of EPS and its applications

The growing interest in resource recovery of EPS from AGS has provided a drive to identify specific compounds or EPS properties suitable for diverse applications (Feng et al., 2021). In this thesis, the anionic EPS could bind with positively charged proteins that are of interest in both the medical and chemical fields (Chapter 3). Following up, an increased anionic charge was observed in the EPS under elevated seawater concentrations (Chapter 5), indicating that this could be a strategy to produce more negatively charged polymers for this application. To further explore this potential in medical applications, such as for sepsis treatment, besides chemical characterization, bioactivity tests would be required (Xue et al., 2019). For chemical applications, properties like swelling and degree of cross-linking are more relevant (Zagorodni, 2006).

In addition to anionic glycans, there are proteins identified in the EPS of AGS showing potential for high-value applications. One example is the surface protein produced by *“Ca. Accumulibacter”*, which shows strong similarities to S-layer proteins (Chapter 6). Known for their self-assembling and anti-fouling characteristics, S-layer proteins are promising candidates for nanobiotechnological applications such as drug delivery or the generation of nanostructured silica (Sleytr et al., 2014). Electron microscopy could be used to examine their assembly behavior in greater detail (Sleytr et al., 2014). Altogether, the identification of structural proteins and the anionic glycoconjugates highlights the diversity and technological promise of EPS-derived biomolecules.

Related but not directly part of the EPS work presented in this thesis, the waste side-streams of the Kaumera extraction process might be a valuable source for applications. Recently, a water-soluble fraction of Kaumera of Zutphen was found to have adhesive properties, exhibiting 1/3 of the strength of regular all-purpose glue as a proof-of-concept (Chen et al., 2024). Notably, this adhesive fraction closely resembles the acidic supernatant, which is currently discarded back into the wastewater treatment plants after the extraction, highlighting the possibility to valorize the side-streams in the EPS production process. However, further investigation is needed to determine whether this property can be found in Kaumera extracted from other wastewater treatment plants and the underlying

mechanism behind the adhesive property; ideally, the evaluation should follow the standardized testing protocols, such as the ASTM guidelines (Arias et al., 2021).

#### 7.4 Limitations of this work

A recurring limitation of the EPS research done in this thesis was the extraction, as it introduces irreversible modifications to the original structure. Most of the EPS extractions in this thesis have been performed similarly (0.1M NaOH, 80°C) (Chapters 2-5), except Chapter 6, where it was discovered that the NaOH extraction method degrades the proteins. In parallel, the yield obtained after acidic precipitation is also influenced by the extraction method. A small comparative test using NaOH and Na<sub>2</sub>CO<sub>3</sub> (each at 0.4 w/v%) on seawater-adapted AGS showed that the Na<sub>2</sub>CO<sub>3</sub> extraction yielded more EPS after acidic precipitation, suggesting a higher molecular weight and thus better gel-forming ability (Bou-Sarkis et al., 2022). Furthermore, the degree of destruction during the extraction of the original polymer is unknown. The extraction could destroy labile modifications, such as phosphorylation (Varki, 2017), that could be relevant for certain applications, such as flame retardancy (Kim et al., 2020). Therefore, extraction strategies must be optimized for the intended downstream application, whether it is for product development or for structural characterization.

Table 7.1. Yield for the seawater AGS EPS extraction in %VS EPS / VS AGS. Fractions after acidic precipitation with HCl to pH 2.2

	NaOH extraction	Na <sub>2</sub> CO <sub>3</sub> extraction
Supernatant	45	13
Pellet	5.0	12

Furthermore, the connection between the EPS of lab-scale and full-scale systems remains to be clarified. Previous work in the group has focused on characterization of the EPS of full-scale systems of AGS (Felz, 2019), anammox (Boleij, 2020), and anaerobic granular sludge (Bruin, 2024) or lab-scale systems with enrichments of “*Ca. Accumulibacter*” (Martinez, 2023). A comparison has been made, for example, in the work of Li et al. (2025) between the LPS of full-scale activated sludge and granular sludge. This work showed overlap in the composition of anionic glycoconjugates of full-scale EPS (Chapter 2) and lab-scale systems (Chapter 3). However, the other components identified in this work have not yet been studied in full-scale systems. Nonetheless, to translate insights obtained at lab-scale on functional EPS components into practice, systematic comparisons between lab-scale and full-scale AGS will be essential.

## References

Agustinho, D. P., Fu, Y., Menon, V. K., Metcalf, G. A., Treangen, T. J., & Sedlazeck, F. J. (2024). Unveiling microbial diversity: harnessing long-read sequencing technology. *Nature Methods*, 21(6), 954–966. <https://doi.org/10.1038/s41592-024-02262-1>

Aichler, M., & Walch, A. (2015). MALDI Imaging mass spectrometry: current frontiers and perspectives in pathology research and practice. *Laboratory Investigation*, 95(4), 422–431. <https://doi.org/10.1038/labinvest.2014.156>

Arias, A., González-Rodríguez, S., Vetroni Barros, M., Salvador, R., de Francisco, A. C., Moro Piekarski, C., & Moreira, M. T. (2021). Recent developments in bio-based adhesives from renewable natural resources. *Journal of Cleaner Production*, 314, 127892. <https://doi.org/10.1016/J.JCLEPRO.2021.127892>

Benz, I., & Schmidt, M. A. (1992). AIDA-I, the adhesin involved in diffuse adherence of the diarrhoeagenic *Escherichia coli* strain 2787 (O126:H27), is synthesized via a precursor molecule. *Molecular Microbiology*, 6(11), 1539–1546. <https://doi.org/10.1111/j.1365-2958.1992.tb00875.x>

Boleij, M. (2020). The anammox house: On the extracellular polymeric substances of anammox granular sludge. <https://doi.org/10.4233/UUID:18EBF770-FEB0-4835-BD0E-04173A346308>

Boleij, M., Kleikamp, H., Pabst, M., Neu, T. R., van Loosdrecht, M. C. M., & Lin, Y. (2020). Decorating the Anammox House: Sialic Acids and Sulfated Glycosaminoglycans in the Extracellular Polymeric Substances of Anammox Granular Sludge. *Environmental Science & Technology*, acs.est.9b07207. <https://doi.org/10.1021/acs.est.9b07207>

Bou-Sarkis, A., Pagliaccia, B., Ric, A., Derlon, N., Paul, E., Bessiere, Y., & Girbal-Neuhauser, E. (2022). Effects of alkaline solvents and heating temperatures on the solubilization and degradation of gel-forming Extracellular Polymeric Substances (EPS) extracted from aerobic granular sludge. *Biochemical Engineering Journal*, 185, 108500. <https://doi.org/10.1016/J.BEJ.2022.108500>

Bruin, S. de. (2024). Characterization and visualization of extracellular polymeric substances in anaerobic granular sludge. <https://doi.org/10.4233/UUID:6C67EDAB-6686-419C-BFD6-4AD57AB56AEE>

Chen, L. M., Erol, Ö., Choi, Y. H., Pronk, M., van Loosdrecht, M., & Lin, Y. (2024). The water-soluble fraction of extracellular polymeric substances from a resource recovery demonstration plant: characterization and potential application as an adhesive. *Frontiers in Microbiology*, 15, 1331120. <https://doi.org/10.3389/FMICB.2024.1331120/FULL>

Chiu, H. H., & Kuo, C. H. (2020). Gas chromatography-mass spectrometry-based analytical strategies for fatty acid analysis in biological samples. *Journal of Food and Drug Analysis*, 28(1), 60–73. <https://doi.org/10.1016/J.JFDA.2019.10.003>

de Graaff, D. R., Felz, S., Neu, T. R., Pronk, M., van Loosdrecht, M. C. M., & Lin, Y. (2019). Sialic acids in the extracellular polymeric substances of seawater-adapted aerobic granular sludge. *Water Research*, 343–351. <https://doi.org/10.1016/j.watres.2019.02.040>

Felz, S. (2019). *Structural Extracellular Polymeric Substances from Aerobic Granular Sludge*. <https://doi.org/10.4233/UUID:93E702D1-92B2-4025-AB57-6D2C141ED14D>

Feng, C., Lotti, T., Canziani, R., Lin, Y., Tagliabue, C., & Malpei, F. (2021). Extracellular biopolymers recovered as raw biomaterials from waste granular sludge and potential applications: A critical review. In *Science of the Total Environment* (Vol. 753, p. 142051). Elsevier B.V. <https://doi.org/10.1016/j.scitotenv.2020.142051>

Fukao, M., Zendo, T., Inoue, T., Nakayama, J., Suzuki, S., Fukaya, T., Yajima, N., & Sonomoto, K. (2019). Plasmid-encoded glycosyltransferase operon is responsible for exopolysaccharide production, cell aggregation, and bile resistance in a probiotic strain, *Lactobacillus brevis* KB290. *Journal of Bioscience and Bioengineering*, 128(4), 391–397. <https://doi.org/10.1016/J.JBIOSC.2019.04.008>

## 7. Outlook

Gimeno, A., Valverde, P., Ardá, A., & Jiménez-Barbero, J. (2020). Glycan structures and their interactions with proteins. A NMR view. *Current Opinion in Structural Biology*, 62, 22–30.  
<https://doi.org/10.1016/J.SBI.2019.11.004>

Heyer, R., Schallert, K., Zoun, R., Becher, B., Saake, G., & Benndorf, D. (2017). Challenges and perspectives of metaproteomic data analysis. *Journal of Biotechnology*, 261, 24–36.  
<https://doi.org/10.1016/J.JBIOTEC.2017.06.1201>

Kim, N. K., Mao, N., Lin, R., Bhattacharyya, D., van Loosdrecht, M. C. M., & Lin, Y. (2020). Flame retardant property of flax fabrics coated by extracellular polymeric substances recovered from both activated sludge and aerobic granular sludge. *Water Research*, 170, 115344.  
<https://doi.org/10.1016/J.WATRES.2019.11.5344>

Kleikamp, H. B. C., Lin, Y. M., McMillan, D. G. G., Geelhoed, J. S., Naus-Wiezer, S. N. H., Van Baarlen, P., Saha, C., Louwen, R., Sorokin, D. Y., Van Loosdrecht, M. C. M., & Pabst, M. (2020). Tackling the chemical diversity of microbial nonulosonic acids-a universal large-scale survey approach. In *Chemical Science* (Vol. 11, Issue 11, pp. 3074–3080). Royal Society of Chemistry.  
<https://doi.org/10.1039/c9sc06406k>

Li, J., Hao, X., van Loosdrecht, M. C. M., & Lin, Y. (2025). Understanding the ionic hydrogel-forming property of extracellular polymeric substances: Differences in lipopolysaccharides between flocculent and granular sludge. *Water Research*, 268, 122707.  
<https://doi.org/10.1016/J.WATRES.2024.12.2707>

Martinez, S. T. (2023). *Extracellular Polymeric Substances of "Candidatus Accumulibacter": Composition, application and turnover*.  
<https://doi.org/10.4233/UUID:88CE92A5-153E-47E4-BB21-999237161AB7>

Olst, B. van, Eerden, S. A., Eštok, N. A., Roy, S., Abbas, B., Lin, Y., Loosdrecht, M. C. M. van, & Pabst, M. (2025). Metaproteomic Profiling of the Secretome of a Granule-forming *Ca. Accumulibacter* Enrichment. *PROTEOMICS*, e202400189.  
<https://doi.org/10.1002/PMIC.202400189>

Pabst, M., Grouzdev, D. S., Lawson, C. E., Kleikamp, H. B. C., de Ram, C., Louwen, R., Lin, Y. M., Lücker, S., van Loosdrecht, M. C. M., &

Laureni, M. (2022). A general approach to explore prokaryotic protein glycosylation reveals the unique surface layer modulation of an anammox bacterium. *The ISME Journal*, 16(2), 346–357.  
<https://doi.org/10.1038/S41396-021-01073-Y>

Seviour, T., Derlon, N., Dueholm, M. S., Flemming, H.-C., Girbal-Neuhauser, E., Horn, H., Kjelleberg, S., van Loosdrecht, M. C. M., Lotti, T., Malpei, M. F., Nerenberg, R., Neu, T. R., Paul, E., Yu, H., & Lin, Y. (2019). Extracellular polymeric substances of biofilms: Suffering from an identity crisis. *Water Research*, 151, 1–7.  
<https://doi.org/10.1016/j.watres.2018.11.020>

Sleytr, U. B., Schuster, B., Egelseer, E. M., & Pum, D. (2014). S-layers: Principles and applications. *FEMS Microbiology Reviews*, 38(5), 823–864.  
<https://doi.org/10.1111/1574-6976.12063>

Szczesny, M., Beloin, C., & Ghigo, J. M. (2018). Increased osmolarity in biofilm triggers RcsB-dependent lipid a palmitoylation in *Escherichia coli*. *MBio*, 9(4).  
[https://doi.org/10.1128/MBIO.01415-18/SUPPL\\_FILE/MB0004184028ST1.PDF](https://doi.org/10.1128/MBIO.01415-18/SUPPL_FILE/MB0004184028ST1.PDF)

Tomás-Martínez, S., Kleikamp, H. B. C., Neu, T. R., Pabst, M., Weissbrodt, D. G., van Loosdrecht, M. C. M., & Lin, Y. (2021). Production of nonulosonic acids in the extracellular polymeric substances of "Candidatus Accumulibacter phosphatis." *Applied Microbiology and Biotechnology*, 105(8), 3327–3338.  
<https://doi.org/10.1007/s00253-021-11249-3>

Varki, A. (2017). Biological roles of glycans. *Glycobiology*, 27(1), 3–49.  
<https://doi.org/10.1093/GLYCOB/CWW086>

Varki, A., Schnaar, R. L., & Schauer, R. (2017). *Sialic Acids and Other Nonulosonic Acids*.  
<https://doi.org/10.1101/GLYCOBIOLOGY.3.E015>

Xue, W., Zeng, Q., Lin, S., Zan, F., Hao, T., Lin, Y., van Loosdrecht, M. C. M., & Chen, G. (2019). Recovery of high-value and scarce resources from biological wastewater treatment: Sulfated polysaccharides. *Water Research*, 163, 114889.

Zagorodni, A. A. (2006). *Ion exchange materials: properties and applications*. Elsevier.



## Acknowledgements

This thesis would not have been possible without the incredible support and encouragement of all the wonderful people I was surrounded by for the last 4 years.

First of all, thank you so much **Yuemei**, for giving me the opportunity to do pursue the PhD. Your sincerity, kindness and constant positivity have carried me through so many moments of doubt. I've always admired your talent for teaching and presenting, making complex topics feel simple and inviting. Your passion for the research and curiosity allowed me not only to be brave enough to explore more, but it really motivated me to go forward. You have encouraged me to think deeper and trust myself a little more each time. I'm truly grateful for the moments we spent side by side trying to understand each question we came across. Working with you never felt like work, it felt like learning together. Thank you for believing in me.

**Mario**, thank you for your endless curiosity about absolutely everything. Our countless meetings we would have where we would chat about the experiments first and somehow end up wandering to different conversations were always moments I genuinely looked forward to. Your analytical mindset and the gentle, thoughtful way you challenge ideas have pushed the research to a higher level and helped me to grow. Your openness and straightforwardness helped me to see things more clearly and pushed me to reflect on myself in ways I didn't expect.

Thank you, **Mark**, for showing me different angles during the PhD, you somehow exactly knew when I needed some extra steering in certain moments and provided new ideas. Of course, thank you so much for bringing the EBT group together. You always being the first to be there at Friday drinks is one of many things that brings the group as close as possible. Thank you so much for creating such an amazing working environment where I was able to express my thoughts freely, to make mistakes and learn from them.

To everyone who contributed to this thesis. **Martin**, thank you for your support. You contributed to almost every chapter of this thesis. You always found the time to help me with anything, whether it was for sialic acids or trying to precipitate the surface protein in the labs. **Gijs**, for your great support with the CT, that result was an important driver for chapter 5. **Siem**, thank you for the inspiring EPS discussions and your great help with the metagenomics dataset. Also thanks to **Hiroaki** and **Sunanda** for the lectin microarray analysis. Thank you to my lab-buddies, whom I spend so much time with executing our experiments through (fictional) tears and laughter: **Jelle**, for your brute honesty (seriously, I learned *a lot*), creative solutions to any problem and your incredible skills handling the microscope. **Sebastian**, for your kindness, bottomless knowledge in molecular biology and our endless conversations at the coffee table.

Thank you to my students, **Beck, Wessel, Robbert and Tessa**, whom I worked so closely with daily from the beginning till the end of your projects. Thank you for your persistence and motivation. The EPS research is not always easy, but thanks to your determination, we were able to uncover it together. You all single handedly contributed to a part of this thesis. Thank you for offering me new points of view and continuous challenges. I learned so much together with you.

A great thank you to the Kaumera team, **Anand, Claire, Eline, Herman, Mark S., Mathijs, Nouran, Leon, Philipp, René, Stephen, Suellen and Sofia** for your knowledge, your positive energies during the Kaumera meetings and ambition to learn more together. To the EPS-team, **Ji** for always being ready to help, your (very impressive) “easy to make” lunches and allowing me to organize your paronymph activities together with Stefan. **Bart** for your fun stories and your pragmatic character in anything you do.

A big thank you to **Anka, Apilena, Ben, Dita, Dirk, Gea, Jannie, Kawieta, Kevin, Laura, Marc, Miranda, Nayyar, Stef and Zita** for your great support in and outside the labs! Even though sometimes my problems were as easily solvable as pointing out the chemical that was right in front of my eyes (Zita) or me merely missing the ON button on the screen (Dirk, Kevin), you guys were always ready to help regardless.

Special thanks to my paronymphs. **Stefan**, we learned so much together. From having a shared paper together, to going to singing classes, and you now (hopefully) enjoying your paronymph tasks. I still remember the first time we worked together when our communication just didn't align at all (I can laugh about it now), yet we managed to publish it after days of locking ourselves up in room B2.300 and wrestling with the discussion section. Your calmness really taught me to trust that things will turn out fine in the end. Thank you for being such a significant part of my life the last 4 years. P.S. Sorry for always confusing you with my double negatives. I promise I won't never do it again. **Timmy**, I think you're genuinely one of the purest souls I've met. The way you connect with people is something I greatly admire, even if you need to overstep a language barrier (*if you know you know*). You somehow always manage to spark the most entertaining conversations at the lunch table. Honestly, life is short, and longer lunches really are the best. Thank you for always pointing out my lack of self-awareness when I mispronounce things. Without you, it would be easier for me to confuse people even more, besides the double negatives. P.S. Sorry for always confusing you by my Dutch-Chinese identity shuffle, please keep asking, there are daily updates. **Natalia**, my third unofficial paronymph and office buddy. Thank you for your positivity, our wonderful goofy moments and always being there to listen. Honestly, I don't think there is someone from EBT that I clicked with as fast as I did with you. From the moment you became my new office mate we instantly became good friends. Your endless energy to always be active,

whether it is padel, volleyball, or going to the gym together, has tricked me multiple times into thinking I could somehow keep up (I *absolutely could not*). But thank you for continuously believing in me. P.S. Sorry for my ever-growing mountain of papers between us. I am genuinely impressed you still managed to spot me across the desk by the end of the PhD.

And my office buddies. Thank you for the great conversations about all topics related to the PhD, life and other random stuff. **Sergio**, my master thesis supervisor turned office mate turned friend, thank you for your energy in the office, random dances, our matching outfits. You are the joyful distraction I miss the most when you are not around. Our trips to Berlin and Thailand were incredibly fun. Our *nail-salon* moment is one of my favorite memories with you. **David**, thank you for your inspiring endless focus, reality checks whenever I needed and your effortless jokes that always brightened my day. I'll never forget the endless looping of *Evanesce* that one week. **Puck**, thank you for always being there to give me hug when I need it the most, giving me advice on countless figures and always showing me perspective. **Linghang**, thank you for curiosity and for our endless discussions about research. Thank you, my next-door office friend, **Ali** for your down-to-earth energy, our refreshing afternoon walks and your pragmatic mindset in anything you do. Thank you for letting me drag you into my random activities I only discovered that week, whether it was golfing or snowboarding together. Our trip to the conference in Thailand was incredible and we made amazing memories there. I cherish each moment very much.

Thanks to all friends this PhD has brought me. **Angelos** for your open-hearted personality and your infectious laugh. **Alex**, for your love of food and coffee and goofy vibes (and inhuman strength). **Kiko**, for your curiosity and honesty, motivation in any challenge. Your jokes are a dangerous sport, but I appreciate them *100%*. **Matteo** for your infinite kindness and incredible humbleness. **Maxim** for your bright energy and passion in anything you do, whether it's research or pastas. **Nina** for your amazing help already since the internship times around the lab, your contagious *pepas* dances always brightened my day. **Rodoula** for our Tuesday yogalates sessions, always being up for coffee breaks and being our fashion-icon and influencer. **Mariana**, for your straight-up honesty and always being up for a good time, whether it is karaoke or movie nights. **Venda**, for your kindness, easy-going spirit and wonderful sense of humor. Your onigiris are the best.

To my fellow (ex)-EBTers for always bringing good times during lunches, EBT events, cakes, filming for defense videos, and fun and inspiring conversations around the labs and hallways, **Adarsh, Alba, Bea, Berdien, Chris, Christoff, Claudia, Cleo, Dimitry, Dinko, Edward, Emine, Gerben, Gijs, Gonçalo, Heike, Hugo, Ingrid, Ismail, Jelmer, Jelle, Jitske, João, Jules, Luz, Marit, Marta, Marte, Martijn, Michele, Ramon, Rebeca, Robbert, Sam, Samarpita, Sarah, Siem, Sirous, Sofia, Timo and Yubo**.

To all the BT'ers: **Angelique, Maarten, Hugo, Chiara, Alexandra, Georg, Koen, Marina**, who brought so much joy with each Friday drinks, parties, teaching duties and barbecues. And BT-committee: **Aster, Marieke, and Lars**, organizing the BT symposium was a great opportunity and holds forever a great memory to me! My bonus AE-PhD friends, **Andu, Andres, Esther, Teona** and **Sasha** for the incredible murder-mystery nights, dinner parties, Miami-sun mango-by-the-pool lounging and photoshoots.

Ik bedank ook mijn vrienden van de master, **Shannara**, en minor, **Elvis, Marcella, Hessel** voor alle gezellige “food adventures” en oneindige leuke momenten en verhalen die we met elkaar hebben mogen delen. Mijn “Compacte” vrienden, **Anne, Ayla, Dyantha, Jeannet, Karim, Loles, Roy en Simona**, en voor onze relaxte Compact-weekenden, wellness-dagen en gezellige activiteiten die mij altijd even alle stress deed vergeten. Mijn wintersport *gang*, **Sander, Daniël, Jos, en Sebas** voor alle legendarische momenten die we op grote hoogtes en ook onder de zeespiegel samen hebben mogen beleven. Mijn middelbare school meiden, **Mat en Sanne**, voor jullie ware zelf, tripjes vol slappe lachen en *girl dinners*. Jullie luisterend oor en eerlijke adviezen hebben mij altijd veel geholpen in momenten van twijfel. Dank jullie wel dat jullie er altijd voor mij zijn. Aan mijn beste vriendinnetje, **Rin**. Dankjewel dat je er altijd voor me bent geweest, van mijn diepste dalen tot mijn hoogtepunten in de afgelopen 12 (*ja, bizarre hé*) jaar. Ik ben zo onwijs dankbaar dat jij al die tijd naast mij hebt gestaan en mij bij elke stap die ik heb gemaakt hebt ondersteund. Je hebt me laten zien wat het betekent om onbevreesd te zijn, terwijl je altijd je blik strak op je einddoel houdt. Dankjewel dat je me hebt laten zien dat een beetje extra chaos in het leven helemaal oké is, en niets om bang voor te zijn.

Mijn familie en schoonfamilie **Mama, Papa, Ronald, Danny, Tonny, Angel, Anja, Simon, Ellen, Bert, Julin en Iwan**, bedankt voor jullie onvoorwaardelijke steun en liefde die jullie mij hebben gegeven. Bedankt voor het luisterend oor dat jullie mij hebben geboden. Jullie stonden altijd voor mij klaar, zonder aarzeling en zonder voorwaarden.

Tot slot, **Jan**, mijn nummer één cheerleader. Jij hebt altijd langs de zijlijnen gestaan en het hardst voor mij gejuicht. Altijd in mij geloofd, zelfs op de momenten dat ik dat zelf niet deed. Je hebt me zoveel zelfverzekerder gemaakt, je hebt altijd naar mijn verhalen geluisterd en mij gesteund waar ik dat het meest nodig had. Bedankt je al mijn kleine (en grote) successen samen met mij viert. Dankjewel voor alle keren dat je mij hebt geholpen met de figuren of teksten in dit proefschrift, door jou zijn ze aanzienlijk verbeterd. Ik geloof werkelijk dat jouw biotech-kennis de afgelopen jaren een best indrukwekkend niveau bereikt voor iemand met een aerospace achtergrond! Bedankt dat jij mijn veilige haven, mijn avontuur en mijn thuis in één bent.

## Curriculum Vitae

Le Min Chen was born on the 7<sup>th</sup> of September 1996 in Delft, the Netherlands. From a young age, she was already fascinated with nature and biology. Her interest in these fields developed during high school where she participated in the *Imagine* school competition, a science communication initiative in which students developed biotechnological solutions to societal challenges in developing countries. This experience led her to start the bachelor's program in Life Science and Technology in 2014 at Delft University of Technology and Leiden University. During her bachelor's studies, she worked on cloning and characterizing an aldolase enzyme, which sparked her interest in biotechnology.



After finishing her bachelor's degree, she continued with the Master in Life Science and Technology at Delft University of Technology. During that time, she learned more about the extracellular polymers during a lecture given by Yuemei at the course Microbial Community Engineering. In 2019, she started her master thesis project titled "*Nonulosonic acids in the extracellular polymeric substances of enriched "Candidatus Accumulibacter": Diversity and Function*".

In 2020, she joined Nestlé R&D in Lausanne Switzerland as a Research and Development Intern for a period of 7 months. She conducted research on various enzymes on bioplastic degradation. This experience broadened her perspective on sustainable polymer materials. Right after the internship, she came back to Delft to pursue her PhD within the Environmental Biotechnology section, focusing on what she left during her master project. The curiosity and challenges in the EPS research and combining multidisciplinary approaches has driven her to uncover more about the topic, resulting in this thesis.

Currently, she is continuing at the EBT section as a Postdoc, working on the characterization of sialoglycoproteins from extremophilic bacteria.

**Journal Articles**

**Chen, L. M.**, Keisham, S., Tateno, H., Kleine G.Y., van, Pronk, M., Loosdrecht, M.C.M. van, Pabst, M., Lin, Y.. Extracellular polymeric substances in aerobic granular sludge under increasing salinity conditions. *Water Research* (2026) - Accepted

**Chen, L. M.**, Hofstra, T., Langedijk, J., Andrei, S., Pabst, M., Pronk, M., van Loosdrecht, M. C. M., & Lin, Y. (2025). Identification of a surface protein in the extracellular polymeric substances of seawater-adapted aerobic granular sludge. *Water Research*, 124187. <https://doi.org/10.1016/J.WATRES.2025.124187>

**Chen, L. M.**, Erol, Ö., Choi, Y. H., Pronk, M., van Loosdrecht, M., & Lin, Y. (2024). The water-soluble fraction of extracellular polymeric substances from a resource recovery demonstration plant: characterization and potential application as an adhesive. *Frontiers in Microbiology*, 15, 1331120.

<https://doi.org/10.3389/FMICB.2024.1331120/FULL>

**Chen, L. M.**, Beck, P., van Ede, J., Pronk, M., van Loosdrecht, M. C. M., & Lin, Y. (2024). Anionic extracellular polymeric substances extracted from seawater-adapted aerobic granular sludge. *Applied Microbiology and Biotechnology*, 108(1), 144. <https://doi.org/10.1007/s00253-023-12954-x>

**Chen, L. M.**, Keisham, S., Tateno, H., Ede, J. van, Pronk, M., Loosdrecht, M. C. M. van, & Lin, Y. (2023). Alterations of Glycan Composition in Aerobic Granular Sludge during the Adaptation to Seawater Conditions. *ACS ES&T Water*. <https://doi.org/10.1021/ACSESTWATER.3C00625>

**Chen, L. M.**, de Bruin, S., Pronk, M., Sousa, D. Z., van Loosdrecht, M. C. M., & Lin, Y. (2023). Sialylation and Sulfation of Anionic Glycoconjugates Are Common in the Extracellular Polymeric Substances of Both Aerobic and Anaerobic Granular Sludges. *Environmental Science and Technology*, 57(35), 13217–13225. <https://doi.org/https://doi.org/10.1021/acs.est.2c09586>

Santos-Beneit, F., **Chen, L. M.**, Bordel, S., Frutos de la Flor, R., García-Depraect, O., Lebrero, R., Rodriguez-Vega, S., Muñoz, R., Börner, R. A., & Börner, T. (2023). Screening Enzymes That Can Depolymerize Commercial Biodegradable Polymers: Heterologous Expression of Fusarium solani Cutinase in Escherichia coli. *Microorganisms*, 11(2), 328. <https://doi.org/10.3390/MICROORGANISMS11020328/S1>

Tomás-Martínez, S., **Chen, L. M.**, Pabst, M., Weissbrodt, D. G., van Loosdrecht, M. C. M., & Lin, Y. (2022). Enrichment and application of extracellular nonulosonic acids containing polymers of Accumulibacter. *Applied Microbiology and Biotechnology*, 1–11.

Tomás-Martínez, S., **Chen, L. M.**, Neu, T. R., Weissbrodt, D. G., van Loosdrecht, M. C. M., & Lin, Y. (2022). Catabolism of sialic acids in an environmental microbial community. *FEMS Microbiology Ecology*, 98(5), 1–11.  
<https://doi.org/10.1093/FEMSEC/FIAC047>

Haridas, M., Bisterfeld, C., **Chen, L. M.**, Marsden, S. R., Tonin, F., Médici, R., Iribarren, A., Lewkowicz, E., Hagedoorn, P.-L., Hanefeld, U., & Abdelraheem, E. (2020). Discovery and Engineering of an Aldehyde Tolerant 2-deoxy-D-ribose 5-phosphate Aldolase (DERA) from *Pectobacterium atrosepticum*. *Catalysts*, 10(8), 883.  
<https://doi.org/10.3390/catal10080883>

### Book - Chapter

Wilfert, P. K., Loosdrecht, M. C. M. van, Posada, S. V., Picken, S. J., Chassagne, C., Lin, Y., Raja, A., Kleine, G. Y., Shajimon, A., **Chen, L. M.**, Bruin, S. de, Persiani, R. P., Diniz, B. C., Bahgat, T. M. S. M., Smit, M., Knaap, E. D. van der, & Pronk, M. (2024). *Kaumera Methods Manual: A comprehensive guide to lab extraction and characterization methods for extracellular polymeric substances (EPS)*. Delft University of Technology. <https://research.tudelft.nl/en/publications/kaumera-methods-manual-a-comprehensive-guide-to-lab-extraction-an/>

### Conference proceedings

MEWE-11, Atlanta, Georgia, USA (2025). A dominant surface protein in extracellular polymeric substances of seawater-adapted aerobic granular sludge. *Oral presentation - online*.

IWA Resource Recovery, Leeuwarden, Netherlands (2025). The water-soluble fraction of extracellular polymeric substances from a resource recovery demonstration plant. *Oral presentation*.

Scientific Spring Meeting KNVM & NVMM, Papendal, Netherlands (2024). Alterations of Glycan Composition in Aerobic Granular Sludge during the Adaptation to Seawater conditions. *Oral presentation*.

The Biofilm Matrix: Fundamental understanding and translational impact, SCELCE, Singapore (2024). Alteration of glycan composition in aerobic granular sludge during the adaptation to seawater conditions. *Oral presentation*.

Scientific Spring Meeting KNVM & NVMM, Papendal, Netherlands (2023). Extracellular polymeric substance from seawater-adapted aerobic granular sludge: enrichment of polyanionic fraction and exploration into its potential application for sepsis treatment. *Oral presentation*.

IWA Biofilms 2022, Phuket, Thailand (2022). Anionic extracellular polymeric substances: Enrichment and its potential application. *Oral presentation*

Biofilms10 Conference, Leipzig, Germany (2022). Polyanionic property of extracellular polymeric substances from seawater-adapted aerobic granular sludge and its potential application. *Poster presentation*.

